MASSEY UNIVERSITY

Behaviour of Emulsion Gels in the Human Mouth and Simulated Gastrointestinal Tract

A thesis presented in partial fulfillment of the requirements

for the degree of

Doctor of Philosophy in Food Technology

at Massey University, Manawatu, New Zealand.

Qing Guo

2015

Riddet Institute
FOOD | INNOVATION | HEALTH

Abstract

Food structure greatly impacts the digestion process of food in the human body. Food structure design is a potential strategy to modulate food digestion and develop foods with controlled nutrient digestion and release. This research aimed to understand the dynamic processes of digestion of whey protein emulsion gels from the mouth to the intestine. Therefore, a series of heat-set whey protein emulsion gels, the structure of which was designed by varying NaCl concentration (10, 25, 100 and 200 mM) and oil droplet size (1, 6 and 12 μm), were formed. Mechanical properties in linear viscoelastic region, large deformation and fracture region and microstructure of gels were evaluated. *In vivo* oral processing and *in vitro* oral-to-gastrointestinal digestion of whey protein emulsion gels with different structures were investigated with a focus on the effect of gel structure on the gel disintegration and lipid digestion.

Results showed that the gel strength increased with increasing NaCl concentration. At the micro-scale, the gel structure became from homogenous to porous with increasing NaCl concentration from 10 to 200 mM. The fragmentation degree of whey protein emulsion gels in the mouth showed a positive linear relationship with the gel strength (i.e. a higher gel strength, the greater gel fragmentation degree). During oral processing, the small oil droplets (~ 0.45 μm) incorporated in the protein matrix were stable without oil droplet release. During gastric digestion, the bolus of the gel containing 10 mM NaCl (soft gel) disintegrated much faster than that of the gel containing 200 mM NaCl (hard gel) in the human gastric simulator (HGS). The disintegration of the soft gel in the HGS was caused by both the abrasion and fragmentation while the abrasion was the predominant mechanism of the disintegration of the hard gel. The larger particle size of the soft gel bolus slowed down the emptying of gels from the HGS. With continued digestion, the emptying of both gels from the

HGS was accelerated by gel disintegration. The gel structure greatly influenced the gel disintegration at the micro-scale. The soft gel particles were gradually disrupted into individual oil droplets, with the protein matrix dissolving after gastric digestion for 4 hours while the hard gel particles still retained the oil droplets inside the protein matrix. The colloidal structure of emptied gastric digesta, which generated from original gel structure, still significantly impacted the digestion of whey protein emulsion gels in an *in vitro* intestinal model. In general, the colloidal structure of the emptied gastric digesta of the hard gel hindered the breakdown of gel particles and hydrolysis of oil droplets more effectively than that of the soft gel. The remaining structure within the hard gel particles limited the free motion of oil droplets, which led to a lower degree of coalescence and breakup of oil droplets. Interestingly, coalescence appeared to occur between neighboring oil droplets inside the emptied gastric digesta of the hard gel during intestinal digestion.

The structure of the gels containing 100 mM NaCl became from aggregated particle to emulsion-filled with increasing oil droplet size from 1 to 12 μm. The gel strength also decreased with the increase of droplet size. For the gels containing large oil droplets (6 and 12 μm), oil droplets were released from the protein matrix along with some coalescence during oral processing. During gastric digestion, a higher degree of coalescence of oil droplets occurred and coalesced oil droplets creamed to form a top oil layer. This slowed down the emptying of gels from the HGS. For the gels containing 1 μm oil droplets, most oil droplets still retained in the protein matrix during oral and gastric digestion with minimal instability of oil droplets. In addition, increasing interactions between oil droplets and protein matrix by decreasing oil droplet size hindered the protein hydrolysis.

Overall, this research provides an understanding of the way in which food

disintegrates in the human body and highlights the role of food structure on the digestion of food in the human body. These findings could assist in designing the functional new foods that deliver health benefits (e.g. lipid regulation, encapsulation and release of nutrients) and improving human health related to food digestion (e.g. dysphagia, dyspepsia).

Acknowledgement

When I look back the journey, I remember all the friends and family who have helped and supported me along this long but fulfilling road. It is a rewarding and exciting experience. I have felt their love, generosity, support and friendship in my heart.

First and foremost, I wish to express my sincere gratitude to my chief supervisor (Dr Aiqian Ye) and co-supervisors (Prof Harjinder Singh, Prof Douglas Dalgleish and Dr Mita Lad), for their continuous support, encouragement, insightful comments, hard questions and immense knowledge. Their guidance supported me throughout my study. I really appreciate that they have given me enormous freedom to do research independently. Their deep scientific insights often enlightened me when I was confronted with difficulties. Their dedication, enthusiasm, patentice, motivation and intellectual capacity and critical way of thinking and analyzing in academic areas have been a learning experience. I could not have asked for better role models. I could not be prouder of my academic roots and the dreams which they have given to me.

I wish to thank the Riddet Institute for providing me the financial assistance during my study and funding my project as well as providing travel grants to attend the international conferences. I would like to thank the Massey University Doctoral Completion Bursary for providing me financial assistance in the final stage of my PhD study.

I would like to thank Dr Maria Ferrua for her help in preparing the publication regarding to the gel disintegration in the model stomach. I am thankful to Prof John Bronlund for his constructive suggestions to my oral study. I would like to thank Dr Jianyu Chen for the training and guidance of the use of the confocal laser scanning microscopy. I am thankful to Dr Derek Haisman for demonstrating the human gastric

simulator. I would like to thank Prof Matt Golding to be my examiner of the PhD confirmation as well as his valuable advice and critical comments to my project. I am thankful to Prof Paul Moughan for his encouragement and motivation of my PhD journey. I would like to thank Dr Sophie Gallier, Dr Ashling Ellis, Dr Jaspreet Singh and Dr Simon Loveday for their academic discussions about my project.

I would like to thank Ms Janiene Gilliland, Mr. Chris Hall (Riddet Institute), Ms. Michelle Tamehana, Mr Warwick Johnson, Mr Steve Glasgow and Mr Gary Radford for being excellent lab managers, providing the lab induction, training of instruments, ordering of chemicals, technical help, safety advice and scientific advice. I would like to thank Dr Sylvia Chung and Mr Eli Gray-Stuart for their constructive advice for the application of human ethic approval for my oral study. I would like to thank Dr Peter Zhu, Ms Nok Sawatdeenaruenat, Ms Maggie Zou, Mr Trent Olson and Mr Jack Cui for their help in the lab. I am grateful to Ms Terri Palmer, Ms Ansley Te Hiwi, Ms Felicia Stibbards and Ms Yvonne Parkes for their administrative help and assistance. I would like to thank Mr Matt Levin and Mr Peter Jeffery for their timely help and services in information systems. I am also grateful to Mr Mark Ward, Ms Paula McCool, Ms Willi Twilight and Mr John Henley-King. I am grateful to all the human subjects who attended my oral study.

I would like to thank all the staff and research fellows at the Riddet Institute and the Institute of Food Nutrition and Human Health for their help in my PhD study. My special thanks go to my dear office mates: Dr Anant Dave, Mr Vikas Mittal, Mr Dave Poddar, Dr Jiahong Su, Ms Natascha Stroebinger, Ms Lakshmi Dave, Mr Shakti Singh and Mr Prateek Sharma for their company, support, encouragement, and academic discussion. I would like to thank all my friends in New Zealand and China for their encouragement and support.

And last, but not least, to my wife (Dongfang) and my beloved parents, who share my passion, depression, joy, pain, failure and success during this journey, thank you for your support, encouragement, listening and consoling. I cannot complete this manuscript without you.

Table of Contents

List of Figures

List of Tables

List of Symbols

G'	Shear storage modulus
$D_{4,3}$	Average volume-weighted diameter
$D_{3,2}$	Average surface-weighted diameter
pI	Isoelectric point

List of Abbreviations

α-La	α-lactalbumin
β-Lg	β-lactoglobulin
WPI	Whey protein isolate
Ig	Immunoglobulin
IgG	Immunoglobulin G
IF	Lactoferrin
SA	Serum albumin
BSA	Bovine serum albumin
TAG	Triglyceride
SDS	Sodium dodecyl sulfate
SGF	Simulated gastric fluid
SIF	Simulated intestinal fluid
HGS	Human gastric simulator

List of Peer-reviewed Publications

Guo, Q., Ye, A., Lad, M., Dalgleish, D., & Singh, H. (2013). The breakdown properties of heat-set whey protein emulsion gels in the human mouth. *Food Hydrocolloids*, 33(2), 215-224.

Guo, Q., Ye, A., Lad, M., Dalgleish, D., & Singh, H. (2014). Effect of gel structure on the gastric digestion of whey protein emulsion gels. *Soft matter*, 10(8), 1214-1223.

Guo, Q., Ye, A., Lad, M., Dalgleish, D., & Singh, H. (2014). Behaviour of whey protein emulsion gel during oral and gastric digestion: effect of droplet size. *Soft matter*, 10(23), 4173-4183.

Guo, Q., Ye, A., Lad, M., Ferrua, M., Dalgleish, D., & Singh, H. (2015). Disintegration Kinetics of Food Gels During Gastric Digestion and its Role on Gastric Emptying: an *in vitro* Analysis. *Food and Function*, 6(3), 756-764.

Guo, Q., Ye, A., Lad, M., Dalgleish, D., & Singh, H. (2015). Impact of colloidal structure of gastric digesta on in vitro intestinal digestion of whey protein emulsion gel (In preparation).

Chapter 1 Introduction

Lipids exist in almost all types of foods and present normally as emulsified oil droplets dispersed in continuous liquid or solid phase. Lipids can be end products in themselves or be part of a more complex food formulation (Singh et al., 2009). Lipids play an important role in providing flavor/texture/mouth-feel and carrying oil soluble nutrients/nutraceuticals. Lipids also are an important source of energy (Decker & McClements, 2007; Gu et al., 2009; Golding & Wooster, 2010). Meanwhile, extensive research from animal studies, controlled clinical trials, and epidemiologic or ecologic analyses provides strong evidence that dietary fats, especially saturated fats, trans fatty acids, and cholesterol, play a role in the development of obesity which has been linked to increased rates of heart disease, diabetes, certain cancers, gall bladder disease, osteoarthritis and other obesity related disorders (Bray & Popkin, 1998; Simopoulos, 1999; James et al., 2001). The increase in obesity and overweight can be broadly attributed to the overconsumption of calories. Reduced-energy intake is a widely-recommended, non-invasive treatment strategy for over-weight and obesity. However, it is difficult to control energy intake at a desired level of maintaining health for obese people because of the feelings of hunger and food cravings and easy access to cheap, palatable food (high in sugar and fat). Lipid regulation has become a big challenge to human health.

When a food product is consumed, it is exposed to a wide range of physical (e.g. mechanical shearing and temperature) and biochemical (e.g. dilution effect, pH, enzymes, bile salts, etc.) conditions as it passes through the mouth into the stomach and the intestines. Food is broken down into small particles in the mouth and stomach. The intestine is the main site for food digestion and absorption. Although food breakdown is a crucial part of the overall digestion and absorption processes in the human body, it is

still not fully understood, especially in the links between the structure of food and food breakdown in the gastrointestinal tract.

In the past decade, modulation of lipid digestion through the rational design of emulsion structures has received growing interests and made a significant progress (Maldonado-Valderrama et al., 2008; Singh et al., 2009; Chu et al., 2010; Golding et al., 2010; Singh & Ye, 2013). One of main mechanisms that is used to regulate lipid digestion is the manipulation of interfacial composition, which has been expected to alter the access of bile salts and digestive enzymes onto the emulsion surfaces. However, this effect via using different surfactants (non-ionic or ionic), building multi-layers or increasing crosslinking in adsorbed layers is not significant. In general, the stability of emulsions (coalescence, creaming and phase separation) within the gastrointestinal tract plays a more important role in determining the rate and extent of lipid digestion than the initial interfacial layer properties. Surprisingly, there have been limited reports on lipid digestion in solid food (a complex food system). Theoretically, tuning structural characteristics of food matrices may be a rational way to control lipid digestion through controlling difficulties of access of bile salts and enzymes to lipids.

Emulsion gel is a soft solid system containing dispersed oil droplets. The structure of an emulsion gel can be understood as a combination of the structure of matrix, size distribution of oil droplets, oil crystallinity and extent of oil droplet-matrix interactions. Whey proteins have an ability to aggregate and cross-link into three-dimensional solid-like networks (‘gel’) with desirable structural attributes (Phillips et al., 1994). Therefore, whey protein-stabilized oil-in-water emulsion gels represent such a model food in which its structure can be precisely designed. In practice, various foods can be categorized as these soft solid systems with a structure referred to as “emulsion gel”, such as set yoghurt, fresh cheese, gelatin, tofu, starch puddings, dairy desserts and

sausages. Whey protein emulsion gel is a realistic model food to investigate food breakdown in the human body and modulating lipid digestion through designing the structure of complex solid food.

Both human mastication and *in vitro* dynamic digestion model are used in my project to achieve and understanding of the process of food digestion. An important advantage of *in vitro* (over *in vivo*) experiments is that there are no ethical constraints, which often limit *in vivo* experiments. The aim of this project was to understand the dynamic changes of differently whey protein emulsion gels in physicochemical and biological aspects during eating and digestion, with a focus on effects of gel structure on lipid digestion in solid gel matrices. The purpose of this work was to develop a rational way to modulate lipid digestion.

The main objectives of this project were as follow:

1) To develop a series of whey protein stabilized oil-in-water emulsion gels with different structures by varying the structure of protein matrix and droplet size distribution followed by a systematic characterization of rheological/mechanical properties of gels.

2) To understand the breakdown properties of whey protein emulsion gels with varied protein matrix and droplet size in the human mouth.

3) To develop *in vitro* digestion method including *in vitro* oral processing, *in vitro* gastric digestion and *in vitro* intestinal digestion.

4) To understand subsequent behavior of whey protein emulsion gels with varied protein matrix and droplet size in a dynamic stomach model (human gastric simulator, HGS) after *in vitro* oral processing.

5) To model breakdown mechanics of whey protein emulsion gels in the HGS.

6) To explore the effect of colloidal structure of gastric digesta on the *in vitro* intestinal

digestion of whey protein emulsion gels.

These objectives were completed through 5 research chapters. *In vitro* digestion method was developed in Chapter 3. Breakdown properties of whey protein emulsion in the human mouth were determined in Chapter 4 and part of Chapter 7. Effect of characteristics of protein matrix on gastric digestion of whey protein emulsion gels was investigated in Chapter 5. Disintegration kinetics of whey protein emulsion gels and disintegration modeling during gastric digestion were described in Chapter 6. Effect of droplet size on gastric digestion of whey protein emulsion gels during gastric digestion was investigated in Chapter 7. Impact of colloidal structure of gastric digesta on intestinal digestion of whey protein emulsion gels was investigated in Chapter 8.

Chapter 2 Literature Review

This literature review covers the knowledge of emulsions, whey proteins, heat denaturation of whey proteins, mechanisms of protein gelation, protein stabilized-emulsion gels, and upper gastrointestinal tract as the background for PhD thesis. Food breakdown in the gastrointestinal tract, gastric emptying and lipid digestion are discussed and reviewed, with a focus on summarizing the effect of food characteristics on the digestion processes. This chapter is concluded with identifying the gaps between food structure and its role in food digestion in the gastrointestinal tract.

2.1 Emulsions

Emulsions are colloidal dispersions of liquid droplets in another immiscible and continuous liquid phase. The substance that makes up the droplets in an emulsion is called the dispersed or discontinuous phase, while the substance that constitutes of the surrounding liquid is called the continuous phase. A liquid that consists of oil droplets dispersed in water is called an oil-in-water emulsion (e.g. milk, salad dressings, cream etc). A liquid that is composed of water droplets dispersed in an oil phase is called a water-in-oil emulsion (e.g. margarine and butter) (McClements, 2005). Emulsions have two main types: (1) conventional emulsions, and (2) micro-emulsions. Conventional emulsions are thermodynamically unstable with a size range from 0.1 to 100 μm. Usually, their formation requires energy input and surfactants. The definition of microemulsions is from Danielsson & Lindman (1981) "*a microemulsion is a system of water, oil and an amphiphile which is a single optically isotropic and thermodynamically stable liquid solution*". Micro-emulsions have a size range from 5 to 100 nm and spontaneous formation occurs once the conditions are right (McClements,

2012). In this review, only conventional oil-in-water emulsions are considered unless otherwise specified.

2.1.1 Emulsion formation

When oil and water are placed in a container they tend to adopt their most thermodynamically stable state, which results in a layer of oil on top of a layer of water. To create an emulsion, it is necessary to supply energy in order to disrupt and intermingle the oil and water phases, which is usually achieved by mechanical agitation or sonication. To form an emulsion that is stable for a reasonable period of time (mesostable), one must prevent the droplets from merging together after they have been formed. The role of the emulsifier is as follows:

1. Decrease the interfacial tension between the oil and water phases, thereby reducing the amount of free energy required to deform and disrupt the droplets.
2. Form a protective coating around the droplets that prevents them from coalescing with each other.

Therefore, the size of the droplets produced during homogenization depends on a number of different characteristics of an emulsifier (e.g. the ratio of emulsifier to dispersed phase, the time required for the emulsifier to move from the bulk phase to the droplet surface, the extent to which the emulsifier reduces the interfacial tension, the adsorption efficiency of emulsifier, etc.) (McClements, 2005).

2.1.2 Emulsion stability

Due to the thermodynamic instability, almost all emulsions will breakdown into individual oil and water phases with time (Dalgleish, 1997; McClements & Decker, 2000; McClements, 2005). The most important mechanisms of physical instability are creaming, flocculation, coalescence, Ostwald ripening and phase inversion. In practice,

all these mechanisms act individually and can also influence one another (McClements, 2009).

2.1.2.1 Gravitational separation

In general, the droplets in an emulsion have a different density to that of the liquid that surrounds them. If the droplets have a lower density than the surrounding liquid they have a tendency to move upward, which is referred to as creaming. Conversely, if they have a higher density than the surrounding liquid they tend to move downward, which is referred to as sedimentation (Tadros & Vincent, 1983; McClements, 2005). In the case of oil-in-water emulsion, the rate at which an emulsion droplet creams in an ideal liquid is determined by the balance of gravitational force and frictional force. This can be explained by the 'Stokes' law equation:

$$v_{Stokes} = \frac{2gr^2(\rho_2 - \rho_1)}{9\eta_1} \cdots\cdots\cdots \text{Eqn 2-1}$$

Where, v_{Stokes}= velocity of creaming, r = emulsion droplet radius, ρ_2 and ρ_1 = densities of continuous and dispersed phases, respectively, η_1= shear viscosity of continuous phase and g is the acceleration due to gravity.

The creaming rate of particles in food emulsions is affected by many factors, such as hydrophobic interactions between droplets, Brownian motion, droplet fluidity, and droplet flocculation. (McClements, 2005).

2.1.2.2 Flocculation

Flocculation is the process whereby two or more droplets associate with each other without coalescence occurring (Tadros et al., 1983; McClements, 2009). The mechanism of flocculation can be attributed to droplet-droplet interactions. There is a model to describe droplet flocculation in colloidal dispersions containing monodisperse spherical particles. The flocculation can be explained by the following equation (Evans

& Wennerstrom, 1994):

$$\frac{dn_t}{dt} = -\frac{1}{2}FE \cdots\cdots\cdots\cdots \text{Eqn 2-2}$$

Where $\frac{dn_t}{dt}$ is the flocculation rate, n_t is the total number of particle per unit volume, t is the time, F is the collision frequency, and E is the collision efficiency. This equation indicates that the flocculation rate depends on two factors: the frequency of collisions between droplets and the fraction of collisions that leads to aggregation. The collision frequency (i.e. the total number of droplets encounter per time per unit volume of emulsion), is dependent on the Brownian motion and gravitational separation. If every encounter between droplets leads to aggregation, the emulsion will be totally unstable. To prevent aggregation of droplets, it is necessary to have a sufficiently high energy barrier to stop them coming too close. The collision efficiency can be explained by the height of energy barrier, which is determined by the nature of interfacial film and droplet-droplet interactions (i.e. electrostatic interactions, steric interactions, bridging interactions, hydrophobic interactions, depletion interactions, hydrodynamic interactions and covalent interactions) (McClements, 2005).

2.1.2.3 Coalescence

Coalescence is a process whereby two or more droplets are very close and merge together to form a single large droplet. An emulsion moving toward thermodynamically stable state is the principle mechanism of the coalescence because the emulsion system tries to decrease the contact area of two immiscible phases. Danov et al. (1993) proposed a mechanism of coalescence including four steps: (i) close approach of non-deformed droplets; (ii) formation and expansion of plane-parallel film; (iii) thinning of the film at almost constant radius; (iv) rupture of the film and fusion of the droplets into a larger droplet. When repulsive forces between droplets are strong (e.g. at large enough electrostatic repulsion), the deformation can become improbable and the droplets

behave as non-deformable charged spheres. Therefore, in general, emulsions are stable to coalescence because the droplets are covered by sufficient emulsifier (Dickinson & Stainsby, 1988). However, insufficient emulsifier, film stretching and film tearing can accelerate coalescence rate (van Aken, et al., 2003).

2.2 Whey proteins

Whey proteins are known to be the excellent emulsifiers because of its amphiphilic nature, which exhibit good surface activity by reducing surface tension and forming interfacial layer (Kinsella & Whitehead, 1989). Moreover, the aggregation and cross-linking of whey protein molecules into three-dimensional solid-like networks (gel‘) is one of the most important mechanisms for developing soft gel solids with desirable structures (Morr & Ha, 1993; Phillips et al., 1994). Major protein components of whey proteins are β-Lg, α-La, SA, Ig, and proteose-peptone fractions (Fox, 2003).

2.2.1 β-lactoglobulin

β-Lg is the most abundant whey protein in the milk of most mammals. β-Lg consists of a β-barrel of eight antiparallel β-strands (βA-βH) shaped into a flattened cone, an additional β-strand, βI, and one major and four short α-helices, and this secondary structure is predicted to comprise 15% α-helix, 50% β-sheet and 15-20% reverse turn (Creamer et al., 1983; Brownlow et al., 1997). β-Lg has a molecular weight of 18.4 kDa with a hydrodynamic radius of about 2 nm, and contains 162 amino acid residues, five of which are cysteine residues, including Cys-66, Cys-106, Cys-119, Cys-121, and Cys-160. Cys-66 and Cys-160 form a disulfide bond near the surface of the protein molecules, Cys-106 and Cys-119 form a disulfide bond inside, while Cys121 retains a free thiol group (Hambling et al., 1992; Brownlow et al., 1997; Qin et al.,

1998; Sawyer & Kontopidis, 2000). The quaternary structure of the protein varies among monomers, dimers or oligomers depending on the pH, temperature and ionic strength, with the dimer being the prevalent form under physiological conditions (McKenzie & Sawyer, 1967; Gottschalk et al., 2003). This variable state of association is likely to be the result of a delicate balance among hydrophobic, electrostatic and hydrogen bond interactions. Although β-Lg exists as a dimer at neutral pH, it dissociates into monomers at acidic pH while still retaining the native structure (Kuwata et al., 1998; Uhrínová et al., 2000; Sakurai & Goto, 2002). Because of its stability under acidic pH conditions, β-Lg is resistant to digestion in the stomach and is considered one of the allergens for human infant milk allergy (Peram et al., 2013).

2.2.2 α-lactalbumin

α-La is a 123-amino-acid, 14.2-kDa globular protein that is found in the milk of all mammals. α-La is made up of two domains: one largely contains helix (the α-domain) and the other has a significant content of β-sheets (the β-domain), which are connected by calcium binding loop. The β-sheet domain is composed of a series of loops, a small three-stranded anti-parallel β-pleated sheet (residues 41–44, 47–50, and 55–56) and a short 310 helix (h2: 77–80). The two domains are divided by a deep cleft. At the same time, the two domains are held together by the disulphide bridge between residues Cys73 and Cys91, forming the Ca^{2+} binding loop. Overall, the structures of α-La are stabilized by four disulphide bridges: Cys6–Cys120, Cys61–Cys77, Cys73–Cys91, and Cys28–Cys111 (Permyakov & Berliner, 2000; Brew, 2003).

2.2.3 BSA

BSA is approximately 583-residue protein and appears to function as a promiscuous transporter of hydrophobic molecules. It is one of the most abundant

proteins in plasma, ranging between 35 and 55 g/L (Schreiber & Urban, 1978). BSA is the main carrier in the blood for metabolites, hormones and drugs (Bujacz, 2012). BSA is built from three structurally similar domains with the distribution of 17 disulfide bridges and one cysteine that is not involved in the creation of a disulfide bridge. They are rare examples of proteins in which the domain divisions can be assigned to the middle of the secondary structure elements: long α-helices. Such a typical domain linkages are the result of gene triplication in the early stages of evolution. Each domain is composed of ten helices and can be further divided into two subdomains, A and B, containing six and four helices, respectively. The two subdomains are connected by a long loop. The conformational flexibility between the domains is based on helix bending, whereas loop flexibility is responsible for the change of orientations of the subdomains. The space between the domains and the subdomains is utilized to create binding pockets for various ligands (Bujacz, 2012).

2.3 Thermal denaturation of whey proteins

2.3.1 Molecular basis of protein interactions

The functionality of proteins is ultimately determined by the unique structures and the interactions of the protein (Bryant & McClements, 1998). Some of these molecular interactions govern the conformation and aggregation of proteins. The hydrophobic interactions play a key role in determining the conformation and interactions of protein molecules in solution (Israelachvili, 1992). The characteristics of the molecular interactions between protein molecules influenced by pH and ionic strength are summarized in Table 2-1.

Table 2-1 General characteristics of molecular interactions between protein molecules in solution [Adapted from (Bryant and McClements, 1998)].

Type of Force	Sign	Range	Strength	pH	Ionic strength
Hydrophobic	Attractive	Long	Strong	No	No
Electrostatic	Repulsive	Short to Long	Weak to Strong	Yes	Decreases
Hydrogen bonding	Attractive	Short	Weak	No	No
Hydration	Repulsive	Short	Strong	Yes	Yes
Van der Waals	Attractive	Short	Weak	No	No
Steric repulsion	Repulsive	Short	Strong	No	No
Disulfide bonds	Attractive	Short	Very Strong	Short	Yes

2.3.2 Heat-induced aggregation of β-Lg

At neutral pH, β-Lg exists primarily as a dimer. When heating up to approximate 70 ºC, the dimers will dissociate to monomers, followed by some critical changes in the conformation of the β-Lg monomer (Singh & Havea, 2003). These changes lead to the exposure of hydrophobic groups from within the interior to exterior of protein molecule (Iametti et al., 1995; Relkin, 1998), resulting in a reactive monomer which can propagate an aggregation reaction, and leading to the formation of non-native dimers, trimers, tetramers and larger aggregates. Although, the proteins that form these oligomers still have a large amount of secondary structure (i.e. α-helix and β-sheet), its structure is more mobile (Nicolai et al., 2011). This aggregation is irreversible and involves a combination of thiol-catalysed disulphide bond interchange and hydrophobic interactions (Singh et al., 2003).

Schokker et al. (1999) studied the early stages of the heat-induced aggregation

of β-Lg at neutral pH using size exclusion chromatography combined with multi-angle laser light scattering and gel electrophoresis. Upon heating, the amount of native β-Lg decreased, resulting in the formation of non-native monomers and various small aggregates with estimated molecular weights of ~ 31.5, 53 and 76.9 kDa, respectively. These molecular weight values corresponded to β-Lg dimer, trimer and tetramer, respectively. At low concentrations, the oligomers persisted at steady states, while at higher concentrations they associated into larger aggregates. Mehalebi et al. (2008b) studied the effect of different protein concentrations on the aggregation of β-Lg. The protein solutions were heated at 80 °C until steady state was reached and all proteins were denatured. With increased protein concentrations, the fraction of large aggregates increased until more than 95% had formed large aggregates. The hydrodynamic radius of the aggregates was independent on the protein concentration until the gel point concentration was reached. In addition, stable oligomers aggregated rapidly with increasing ionic strength or adjusting pH close to pI. The structure of stable aggregates of β-Lg at steady state depends on pH. Transmission electron microscopy shows small curved strands at pH 7.0, spheres at pH 5.8 and long rigid strands at pH 2 (Jung et al., 2008).

Pouzot et al. (2005) reported at all ionic strengths (3 – 200 mM) and at neutral pH, the β-Lg aggregates were formed by association of short curved strands with the length and diameter of 50 and 10 nm, respectively. At low ionic strength, the head to tail association of short curved strands constructed the larger aggregates. Upon increasing the salt concentration up to 200 mM, significantly denser clusters were formed randomly by short curved strands. The rate of aggregation of β-Lg was highly temperature dependent, but the structures of the aggregates did not depend on the heating temperature (Le Bon et al., 1999b; Le Bon et al., 1999a).

In conclusion, the effects of the pH, ionic strength, protein concentration and temperature on the aggregate structure are small compared to their effect on the gel structure on larger length scales (Mehalebi et al., 2008a).

2.3.3 Heat-induced aggregation of other whey proteins

In general, α-La undergoes a thermal unfolding at a lower temperature than β-Lg does. When pure α-La is heated under mild conditions (80 °C, pH 6.7), it does not form aggregates (Calvo et al., 1993; Hines & Foegeding, 1993). The lack of aggregate formation is explained by the lack of a free thiol group in α-La (Singh et al., 2003). When α-La is heated under more severe conditions (100 °C for 10-30 min), disulphide-linked polymers and modified monomers are formed, with a significant loss of disulphide bonds (Chaplin & Lyster, 1986). It was suggested that, as the disulphide bond was lost, a group similar to a thiol was formed simultaneously, which was probably responsible for the intermolecular disulphide interactions of α-La (Singh et al., 2003).

BSA is one of the most heat sensitive whey proteins, under a range of heating conditions at near neutral pH (deWit & Klarenbeek, 1984). A concentration of 4% (w/v) BSA is required for the formation of a self-supporting gel under 80 °C heating for 30 min in 100 mM sodium phosphate buffer (pH 6.8) (Matsudomi et al., 1993). Gezimati et al. (1996) suggested that BSA underwent thermal interactions in a similar way to that reported for β-Lg. Studies using native- and SDS-PAGE showed that BSA formed aggregates which were held together by hydrophobic interactions and thiol-disulphide bond interchange reactions at a higher temperature (Singh et al., 2003). The similarity should be expected on the basis that both BSA and β-Lg contain a free thiol group, Cys 34 for BSA and Cys 121 for β-Lg (Hambling et al., 1992).

2.3.4 Heat-induced aggregates of β-Lg, α-La and BSA in whey protein mixtures

Since whey proteins are a heterogeneous group of proteins, it is likely that the aggregation behaviour of any individual protein would be altered by the presence of other proteins (Havea et al., 2001). Using size exclusion chromatography and gel electrophoresis, it was shown that β-Lg could form soluble heat-induced complexes with α-La held together mainly by disulphide bonds at the early stage of heating (Dalgleish et al., 1997). The native α-La loses secondary structure more rapidly when heated in the presence of β-Lg compared with when it is heated alone. Hines et al. (1993) and Matsudomi et al. (1993) reported that the addition of β-Lg to BSA increased the rigidity of the resultant gels indicating a synergistic effect. It was also reported that BSA and α-La could interact to form soluble aggregates through thiol-disulphide interchange reactions during gel formation. Havea et al. (2001) reported the aggregation of whey proteins in whey protein concentrate (WPC) solutions. They found during initial stages of heating (75 °C), BSA molecules would begin to unfold and aggregate mainly via inter-molecular thiol-disulphide exchange and non-covalent interactions before β-Lg. The exposed thiol groups of BSA molecules or aggregates could also react with one of those of α-La via the thiol-disulphide interchange. During the later stages of thermal treatment, β-Lg was denatured and exposed a free thiol group which would react with other disulphide bonds of another β-Lg or α-La resulting in dimers, trimmers and polymers of β-Lg or α-La as well as mixed aggregates of the two proteins.

The structure of large aggregates formed at steady state in WPI at pH 7 was almost identical to those formed in pure β-Lg solutions. The dependence of hydrodynamic radius of aggregates on protein concentration is the same in WPI as in pure β-Lg if no salt is added and somewhat weaker than in pure β-Lg solutions (Nicolai et al., 2011).

2.4 Gelation of whey proteins

2.4.1 Heat-set whey protein gels

Schmidt (1981) and Aguilera (1995) propose a four-step procedure for heat-induced protein gelation:

1) the unfolding of native proteins (molten globule);

2) aggregation of unfolded molecules;

3) strand formation of aggregates; and

4) association of strands and network formation.

At neutral pH, native proteins are present as monomers and dimers. When heated, the dimers are dissociated into monomer and the protein structure is modified and become more mobile. Hidden hydrophobic groups and the free thiol group are exposed and interact with other molecules. When the concentration of oligomers (mainly dimers and trimers) exceeds a critical amount, oligomers associate into larger aggregates. With further increase above a critical gel concentration, a 3-D gel network is formed. The critical gel concentration decreases with increasing salt concentration and decreasing pH. In mixtures with α-La or in WPI aggregates, the similar structures are formed by co-aggregation of the different proteins (Nicolai et al., 2011).

The type of formed gel is determined by the strength of the electrostatic interactions (Pouzot et al., 2005; Mehalebi et al., 2008a). At relatively low salt levels (< 50 mM) or pHs which are distant from pI, most of the surface of the protein molecules is incapable of forming bonds with other proteins because of the residual electrostatic repulsion between them. Nevertheless, bonds may be formed between a non-polar patch on one protein and a non-polar patch on another due to the attractive hydrophobic interactions. The molecules are thought to aggregate in an ordered ‘head to tail’ on filament structure, suggesting that they became together at fixed sites on opposing ends

of the molecules. This type of gel is called fine-stranded gel.

On the other hand, at relatively high salt concentrations or pHs (> 50-100 mM) near pI, the electrostatic repulsion between the protein molecules is completely screened and, consequently, they can form bonds at any point on their surface (i.e. random aggregation). This leads to the formation of fairly large spherical aggregates. This type of gel is called particulate gel. At intermediate salt concentrations, a mixture of these two types of structure is formed. Ako et al. (2010) suggested that addition of NaCl and $CaCl_2$ led to heat-induced gels with the same overall structure, using light scattering and turbidimetry techniques.

Heat-induced gel formation results from the protein aggregation process. Denatured whey proteins aggregate irreversibly and eventually form a space-filling structure, i.e. a gel above a critical protein concentration (Verheul & Roefs, 1998). The mechanisms of heat-set gel formation have been elucidated. The heat-set gel network is usually composed of fine strands, the diameter of which is in the order of nanometers in size (Ikeda & Morris, 2002; Pouzot et al., 2005; Ako et al., 2009a). With decreasing intermolecular repulsion (obtained by shifting the pH toward the pI, or increasing the ionic strength, the gel networks become coarser), being composed of more particulate aggregates with the size in the micrometer range (Ikeda et al., 2002; Pouzot et al., 2004; Mehalebi et al., 2008a). These structural transitions are reflected in the macroscopic properties of gels. Fine-stranded gels are translucent or even transparent, and particulate gels are opaque and undergo syneresis. A fine-stranded gel formed at neutral pH is rubbery and deformable to a large strain with a small stress without fracturing. At acidic pH, intermolecular disulphide bonding is unlikely to occur, and the brittle nature of the gel is the signature of fine-stranded networks formed at acidic pH. Particulate gels normally fracture at a small strain, but the stress required to reach the strain is relatively

large (Ikeda & Foegeding, 1999a; Ikeda et al., 1999b).

2.4.2 Cold-set whey protein gels

Cold gelation involves two stages: (1) the preparation of a heat-denatured protein solution with steady protein aggregates; (2) the gelation induced by the addition of salts and a reduction in pH at low temperatures.

2.4.2.1 Salt-induced gels

Gelation of protein aggregates can be induced by sodium salt, calcium salt and other monovalent (K, Rb, Cs, etc.) and divalent (Ba, Fe, etc.) salts at room or lower temperature via screening the surface charges of proteins or protein aggregates (Kuhn & Foegeding, 1991; Bryant & McClements, 2000; Marangoni et al., 2000; Remondetto et al., 2004). The structure of cold-set gels is much more homogeneous than that of the corresponding heat-set gels formed by proteins at the same salt concentration and pH (Barbut & Foegeding, 1993; McClements & Keogh, 1995; Vardhanabhuti et al., 2001; Ako et al., 2010). Much higher concentrations of monovalent salts than divalent salts are needed to induce cold gelation of whey proteins (Barbut & Drake, 1997; Bryant et al., 2000; Marangoni et al., 2000; Ako et al., 2010). Both salts induce gelation by charge screening effects, but divalent salts also contribute to gel formation by the ion-bridging effect. Both gel strength and water holding capacity increase with the increase of protein concentration (Hongsprabhas & Barbut, 1997; Hongsprabhas et al., 1999; Marangoni et al., 2000). The rate of gelation increases strongly with increasing salt and protein concentrations (McClements et al., 1995; Bryant et al., 2000; Marangoni et al., 2000; W et al., 2005; Ako et al., 2010).

2.4.2.2. Acid-induced gels

Acidification can be used to induce gelation of pre-heated whey protein solution

by decreasing pH to isoelectronic point of whey proteins (Bryant et al., 1998). At the same conditions, the acid-induced whey protein gel is stronger than that induced by adding salts (Ju & Kilara, 1998a; Ju & Kilara, 1998b). The maximum gel strength reaches at pH ~5. The acidification rate plays a role in structural or molecular rearrangements during gel formation thereby impacting on gel properties. Gel strength increases with increasing acidification rate. The structure of acid-induced whey protein gel is not stable and the gel hardening has been observed (Alting et al., 2004; Rabiey & Britten, 2009). This is because of thiol-disulfide interchange reactions at pH > 3.9 which is supported by constant decrease of thiol groups during storage (Alting et al., 2004; Rabiey et al., 2009). Long β-Lg fibrils formed at pH 2.0 can also be used to induce cold gelation (Veerman et al., 2003). These fibrils are stable when the pH is raised to 7 or 8 and to cross-linking when $CaCl_2$ is added (Veerman et al., 2003).

2.5 Emulsion gels

The expression 'emulsion gel' is a convenient short-hand expression to denote a complex colloidal material that may exist as both an emulsion and a gel (Dickinson, 2012). There are two types of idealized emulsion gels: (1) emulsion-filled protein gel, where the solid-like rheological properties are determined predominantly by the network properties of the continuous matrix; (2) aggregated particle gel which is a particulate gel and its rheological properties are determined by the properties of the network of aggregated emulsion droplets (Dickinson, 2012). However, in practice, the emulsion gel is a mixture of these two types of gels as shown in Fig. 2-1.

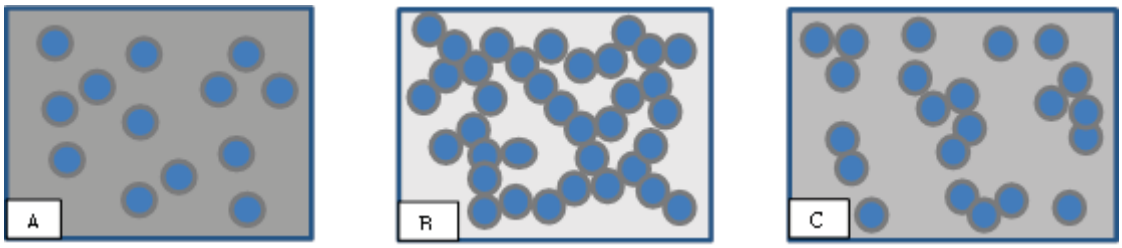

Figure 2-1 Schematic presentation of idealized emulsion-filled gel (A), protein-stabilized emulsion gel (B), and a mixture of both emulsion gels (C). The grey cycles filled with blue color represent the emulsified oil droplets. The grey color outside these filled cycles represents the protein matrix.

Protein stabilized oil-in-water emulsions are the main type of food emulsion gels which have drawn much attention in the last two decades (Dickinson, 2012). In practice, many foods have such a structure which is referred to as "emulsion gel" such as cheese, yoghurt, dairy desserts, tofu, sausages, etc. Whey protein emulsion gel appears to be a good food model representing those food products consumed daily. The feature of whey protein emulsion gel is that its structure can be designed accurately via manipulating properties of protein matrix, properties of oil phase and interactions between protein matrix and oil droplets.

2.5.1 Formation of protein emulsion gels

The first step is to prepare a liquid-like protein-stabilized oil-in-water emulsion. To achieve desirable structure, additional ingredients may be readily incorporated by mixing the fresh protein-stabilized emulsion with an aqueous solution of protein, surfactant or polysaccharide (Sala et al., 2009). A solid-like emulsion gel may be generated from a liquid-like emulsion by gelling the continuous phase (Fig. 2-1A) and/or aggregating the emulsion droplets (Fig. 2-1B). For a protein-stabilized emulsion kept at low or moderate oil content, the mechanism of transformation from liquid state to soft solid is similar to that of protein solution. The formation of 3-D emulsion gel network can be induced by heating ($T>T_{denature}$), salting (preheated protein-stabilized

emulsion), enzyme action (rennet and transglutaminase) and acidification (Dickinson, 2012). According to the temperature of gel formation, the protein emulsion gel can be categorized into two types: 1) heat-set emulsion gel and 2) cold-set emulsion gel.

Recently, there have been a number of studies conducted to understand the structural formation and physical properties of gelled whey protein emulsion gels (McClements et al., 1993; Dickinson & Yamamoto, 1996; Chen & Dickinson, 1998; Chen & Dickinson, 1999a; Dickinson & Chen, 1999; Sok Line et al., 2005; Boutin et al., 2007; Ye & Taylor, 2009). These studies suggest that emulsion droplets and the process of gel formation (for example, heating temperature, pH, ionic strength and enzyme action) strongly influence the structure and rheological properties of the emulsion gels. For example, the strength of heat-set whey protein emulsion gel increases with protein concentration and oil volume fraction (Chen et al., 1998). At a given oil content, the decrease of oil droplet size leads to the increase of the strength of whey protein emulsion gels (McClements et al., 1993; Dickinson et al., 1999; Ye et al., 2009). Increasing salt concentration (e.g. NaCl and $CaCl_2$) makes the structure of whey protein emulsion gel change from homogenous at the micro scale to porous in both heat-set and cold-set whey protein emulsion gels (Gwartney et al., 2004; Sok Line et al., 2005). A prior heating enhances the acid-induced gelation of a whey protein-stabilized emulsion (Ye et al., 2009). The enzyme transglutaminase can catalyze the formation of an isopeptide bond between lysine residues and glutaminyl residues. Due to the covalent character of the crosslinks, the transglutaminase-induced whey protein emulsion gel resembles a rubber-like materials (Dickinson et al., 1996). The shear storage modulus of transglutaminase-induced β-Lg emulsion gel is less frequency-dependent than that of equivalent heat-induced emulsion gels (Dickinson et al., 1996). This is because the heat-induced gelation is a consequence of the development of hydrophobic interactions

between protein molecules with partial reinforcement by sulfhydryl-disulfide interchange (Dickinson, 2012). Overall, the gel strength is determined by the magnitude of interactions (hydrogen bond, hydrophobic interaction, electrostatic interaction, covalent bond, etc.) between structural elements (protein matrix-protein matrix, protein matrix-oil droplet and oil droplet-oil droplet).

2.5.2 Active or inactive fillers

In the case of oil-in-water emulsion, the rheological properties of emulsion gels are dependent on the chemical nature of the interactions between filler particles and the surrounding matrix (Tolstoguzov & Braudo, 1983). According to the chemical nature of fillers, the filler particles can be described as either 'active' or 'inactive'. Active filler particles are mechanically connected to the gel matrix, thus contribute to the gel strength. Inactive filler particles in a composite material behave rather like small holes in the network leading to matrix connecting loosely and that the storage modulus decreases monotonically with the average particle concentration (Jampen et al. 2001). Dickinson and his co-authors (1998; 1999a; 1999b; 1999; 2000) reported much work on contrasting effects of active and inactive fillers on the elastic modulus of heat-set whey protein emulsion gels. They found that the interaction between protein matrix and oil droplets was a key factor determining the gel strength. The protein-coated oil droplets had strong cross-links with protein matrix through disulfide bonds, hydrophobic interactions and hydrogen bonds. These links could reinforce the connections of protein aggregates, thereby leading to an increase in gel strength. In contrast, the Tween-coated (small molecular weight surfactant) oil droplets almost had no crosslinking with protein matrix and so the gel strength decreases. However, if a surfactant that interacts strongly with the protein was added to the gel, this surfactant would have a positive effect on the elastic modulus.

Besides, they investigated the effect of oil volume fraction on storage modulus. As shown in the Fig. 2-2, the strength of gel with active fillers increased whereas that with inactive filler decreased dramatically with increasing oil volume fraction; this could be explained as the increase or decrease in the number of bonds between matrix and fillers per unit volume of the gel.

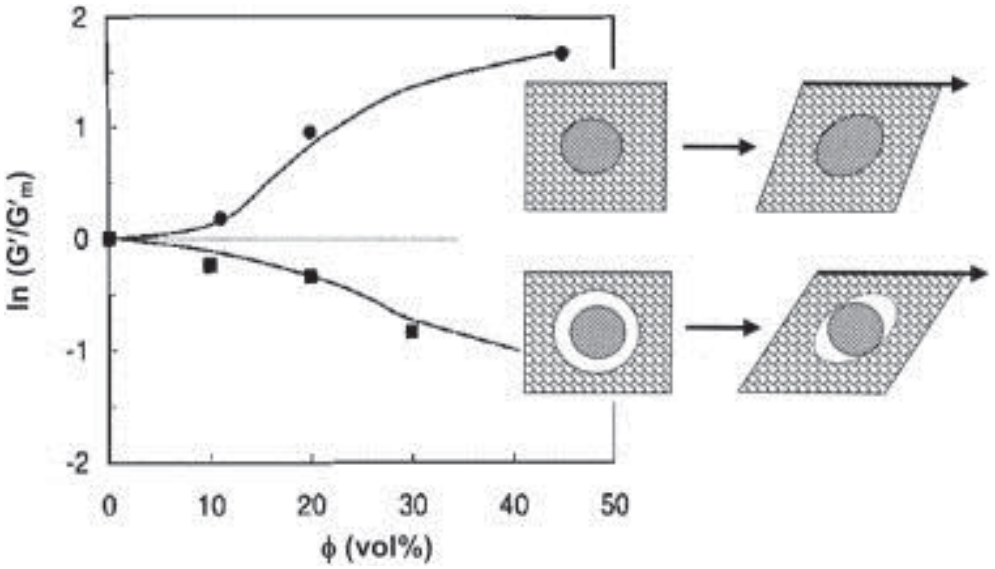

Figure 2-2 Contrasting effects of active and inactive fillers on storage of heat-set whey protein emulsion gels. The logarithm of G'/G_m', where G_m' is the modulus of the gel matrix, is plotted against the oil volume fraction ϕ. ● represents active filler and ■ represents inactive filler. Different effects of the applied shear stress on the active filler (upper diagram) and the inactive filler (lower diagram) are shown schematically (Dickinson et al. 2012).

On the other hand, the oil droplet size greatly impacts the physical properties of protein-stabilized emulsion gels, even as the active filler. With increasing oil droplet size, the gel strength decreases (Dickinson et al., 1999; Ye et al., 2009). It appears that the oil droplets (active fillers) can mediate gel strength reinforced by the interactions between oil droplets and surrounding matrix when the oil droplet size exceeds a certain value. At that time, the large oil droplets can act as the defects during gel compression (McClements et al., 1993).

2.6 Upper gastrointestinal tract

This section introduces the physiology of upper gastrointestinal tract including mouth, stomach and small intestine. Upper gastrointestinal tract is the main site for food digestion and absorption.

2.6.1 Mouth

2.6.1.1 Oral cavity

A schematic diagram of the anatomical structures of oral cavity is presented in Fig. 2-3. Although the general features and functionality of mouth would be same for all human beings, the oral individuality should never be underestimated. Factors such as gender, age, race, health status especially dental health will make oral individuality different.

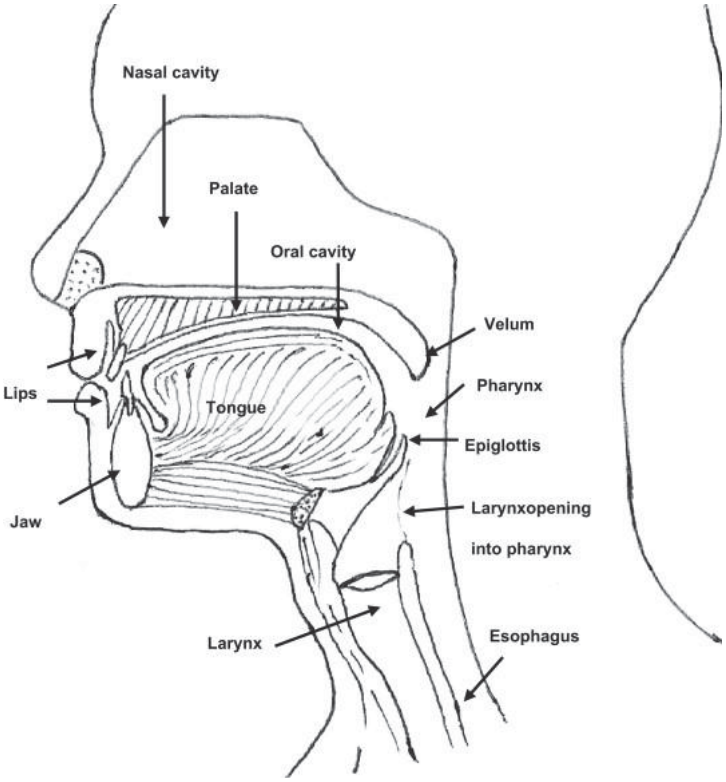

Figure 2-3 An anatomic diagram of oral organ (Chen, 2009).

2.6.1.2 Teeth

A healthy adult has 32 teeth, 16 in each jaw, including the incisors, the canine and the molars (Chen, 2009). As shown in Fig. 2-4, the front teeth are referred to as incisors and are used to take an initial bite of food pieces (cutting). The food is then broken up by the premolars which are located between the front incisors and the posterior molars (shearing and chewing). The maximum bite force that can be applied to the molars ranges from 500 to 700N (Wood & Williams, 1981).

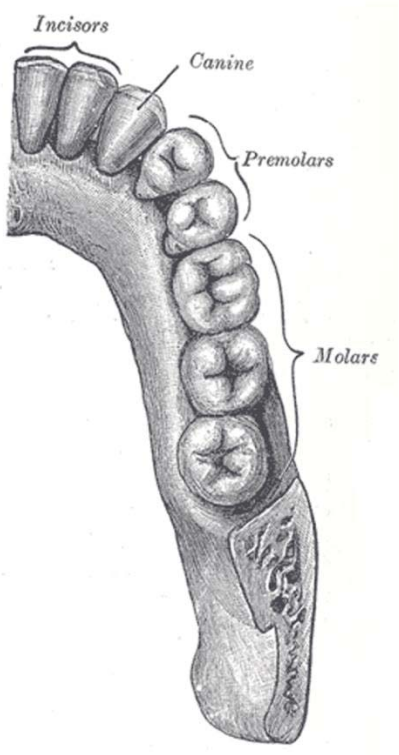

Figure 2-4 The teeth in human mouth (Xu & Bronlund, 2010).

2.6.1.3 Oral surfaces

The average total surface area of oral cavity is ~ 214.7 cm^2 which includes the surfaces of lips, cheeks, palate, tongue and teeth (Collins & Dawes, 1987). The oral surfaces are covered by a mucous layer, which mainly consists of mucins (0.5–5%) and

water (95%). The thickness of this layer is about 40 μm (Wolff & Kleinberg, 1998), which serves as a barrier against aggressive factors like pH and bacteria and as a lubricant protecting oral surfaces against shearing (van Aken et al., 2007). There are taste buds consisting of a cluster of taste receptor cells which are detected in the papillae of tongue (Bear et al., 2001). Four main types of papillae are distinguished in the tongue. The Papillae Circumvallata, Papillae Foliate and Papillae Fungiformis are found to have taste buds. The Papillae Filiformis do not contain taster buds. Their function is to provide the tongue surface a certain roughness needed for food processing. They are involved in the sense of touch on the surface of the tongue, and therefore play an important role in sensory perceptions of foods (Bear et al., 2001; van Aken et al., 2007).

2.6.1.4 Saliva

Saliva has an important role in lubrication, digestion of food and maintaining general oral health. It is a complex heterogeneous clear fluid consisting of water (99.5%), proteins (0.3%) and inorganic and trace substances (0.2%) (Humphrey & Williamson, 2001; van Nieuw Amerongen et al., 2004). Over 1050 proteins and peptides have been found in whole saliva, including proteins such as mucins, proline-rich glycoproteins, enzymes such as α-amylase, lingual lipase, and peptides such as cystatins, statherin, and histatins (van Aken et al., 2007). The inorganic fraction of saliva contains common electrolytes (sodium, potassium, chloride and bicarbonate) (van Aken et al., 2007). The pH of natural saliva ranges from 5.6 to 7.6 for healthy persons, an average value of 6.75 has been reported (Jenkins, 1978). Engelen et al. (2005) studied the flow rate of saliva using a panel with 266 subjects by chewing a piece of tasteless Parafilm. They found an average rate of 0.45±0.25 mL/min for unstimulated saliva flow and 1.25±0.67 mL/min for mechanically stimulated saliva flow. In practice, the flow rate of saliva is affected by the type of food and the time of day.

2.6.2 Stomach

2.6.2.1 Anatomy of stomach

As shown in Fig. 2-5, the stomach is a J-shaped enlargement of the gastrointestinal tract (Tortora & Derrickson, 2008). The stomach connects the oesophagus to the duodenum. The stomach is divided into four regions: the cardia, fundus, body and pylorus. The cardia surrounds the opening of the stomach. The rounded portion to the left of the cardia is the fundus. The large central portion of the stomach is called the body. The region of the stomach that connects to the duodenum is the pylorus; it has two parts: the pyloric antrum, which connects to the body of the stomach, and the pyloric canal, which leads into the duodenum. The pylorus communicates with the duodenum of the small intestine via the pyloric sphincter (valve). This valve regulates the passage of chyme from stomach to duodenum (Tortora et al., 2008). Fig. 2-6 presents a 3-D model to describe the size of the stomach after a typical meal (Ferrua & Singh, 2010). The width of the stomach is about 10 cm at its widest point; the greater curvature is about 30 cm long; the diameter of pyloric sphincter is about 1 cm or less (Ferrua et al., 2010). The stomach can expand to accommodate food up to a volume of about 4 L (Curtis & Barnes, 1994). The geometry of the stomach is affected by many factors, such as the position of body, the amount of type of meal and the digestion time (Liao et al., 2004; Schulze, 2006).

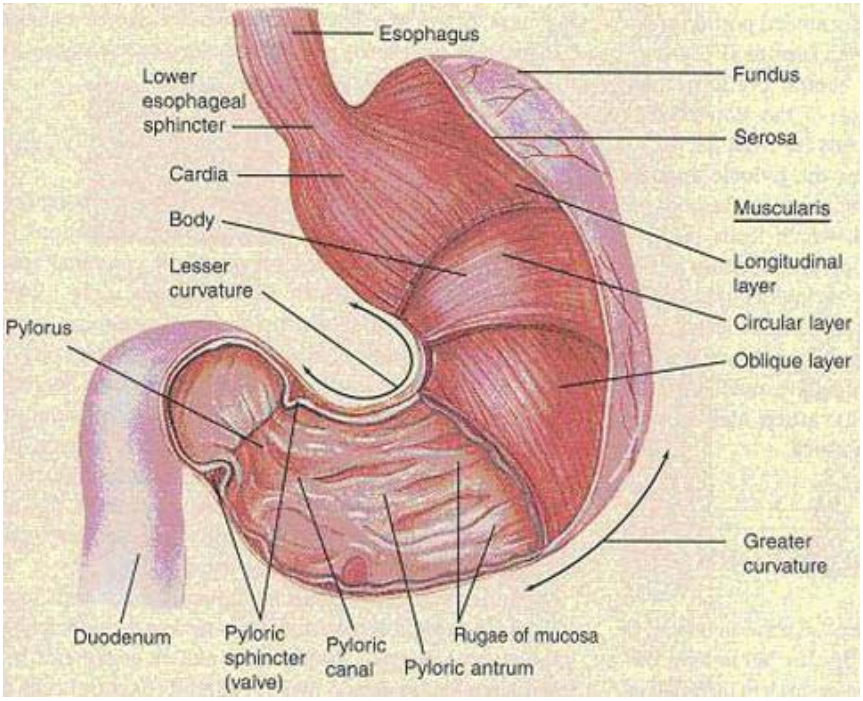

Figure 2-5 Anatomy of the stomach of man (Tortora et al., 2008).

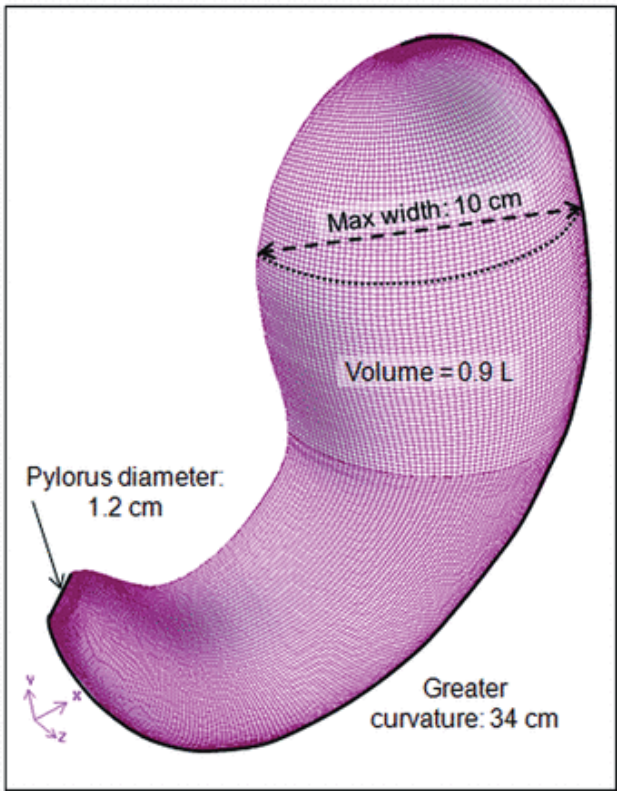

Figure 2-6 3-D model of the average human stomach (Ferrua et al., 2010).

2.6.2.2 Gastric motility and emptying

When food bolus enters into the stomach, the fundus and upper portion of the body relax and accommodate the food without significant increase in pressure. Several minutes after food enters the stomach, peristaltic movements of the stomach wall (known as antral contraction waves, ACWs) originated at the mid corpus (3 cycles min^{-1}) mix, shear and force food towards the pylorus (propulsion) (Marciani et al., 2001c; Ganong & Barrett, 2005; Ferrua et al., 2010). Indentations of these periodic ACWs deepen as they reach the pylorus. Small amounts of the gastric chyme (particle size <1-2 mm) are delivered into small intestine across pyloric sphincter when the ACWs move over the middle of antrum. When the antral contraction approaches the pylorus, the latter closes and the terminal antrum produces a mass contraction, which forcibly retro pulses antral contents (about 3mL/min) into the stomach (Bilecen et al., 2000; Schulze, 2006; Tortora et al., 2008; Malagelada & Azpiroz, 2010). The repeated grinding via a propulsion/retropulsion together with the functions of acids and enzymes reduces food into fine particles.

2.6.2.3 Gastric secretion

About 2.5 L of gastric juice is secreted daily by the cells of the gastric glands (Fig. 2-7). Pepsinogens, the inactive precursors of the pepsins, are secreted by the chief cells. Hydrochloric acid is secreted by parietal cells. Gastrin is produced mainly by G cells, the principal physiological action of which is the stimulation of gastric acid and pepsin secretions and the stimulation of the growth of the mucosa of gastrointestinal tract (Ganong et al., 2005). The pH of the stomach in fasting state is around 1.5 to 2.0 (Arora et al., 2005; Ibekwe et al., 2008; Ulleberg et al., 2011). Fordtran et al. (1973) studied the acid secretion of 6 healthy human subjects after eating a standard meal containing 5 ounces cooked steak, two pieces of toast with one teaspoon of butter and

360 mL water. The amount of acid needed to keep the pH of gastric content at 5.5 was determined. The authors found that the acid secretion rate rose from a basal value of 0.7 mmol/h to a peak of 31.8 mmol/h at 1.5 h and then diminished to 7.7 mmol/h at 4h. The average acid secretion rate was ~16.5 mmol/h during the 4h gastric digestion. Feldman et al. (1996) studied the acid secretion of 206 healthy human subjects stimulated by subcutaneous injection of 6 μg/kg pentagastin via aspiration method (collecting gastric juice from stomach). They found that the peak value of acid secretion of young and middle –aged groups was ~ 30 mmol/L and that of the elderly group (≥65 years old) was ~19 mmol/L. They thought that age was inversely correlated with acid secretion.

Feldman et al. (1996) also found that the peak pepsin output stimulated by administration of 6 μg/kg pentagastin was ~ 68100 U/60 min (6 μg/kg pentagastin reached maximal effect) in 186 young and middle-aged human subjects. It should be noted that the unit of pepsin activity mentioned in this chapter is Anson unit. The volume of gastric content is assumed to be constant 500 mL without emptying during 4 h digestion. The accumulative pepsin activity of 1 mL gastric content is 136, 272, 408, and 544 U/mL at the time of 1, 2, 3 and 4 h. Usually the pepsin output in the human stomach peaks (~ 180 - 420 mg/60min) during the first 60 min after eating liquid or solid foods and declines towards the basal level (~5 mg/60min) after 120 min (Malagelada et al., 1976; Malagelada et al., 1979). Kalantzi et al. (2006) studied the changes in pepsin concentration in the gastric content during 210 min gastric digestion in 20 healthy human subjects (16 males and 4 females) with an average age of 25 years. After intake of 500 ml of Ensure plus, the pepsin concentration increased from 0.26 mg mL^{-1} at 30 min to 0.58 mg mL^{-1} at 210 min. Øktedalen et al. (1988) found that pepsin concentration in human gastric juice was about 0.3 mg/mL in the fasted state. After serving a meal consisting of 62 g carbohydrate, 12 g protein and 21 g fat, pepsin

concentration in the gastric content decreased to about zero within 20 min and then gradually increased to 0.55 mg/mL at 180 min. Tang et al. (1959) lyophilized the pooled fresh human gastric juice from several human subjects , re-dispersed the gastric juice powder into water of pH 2 and determined the specific activity of pepsin. They found the pepsin activity was 843 U/mg protein. Ulleberg et al. (2011) determined the pepsin activity of pooled fresh human gastric juice from 18 human subjects which had a specific activity of 2220 U/mg.

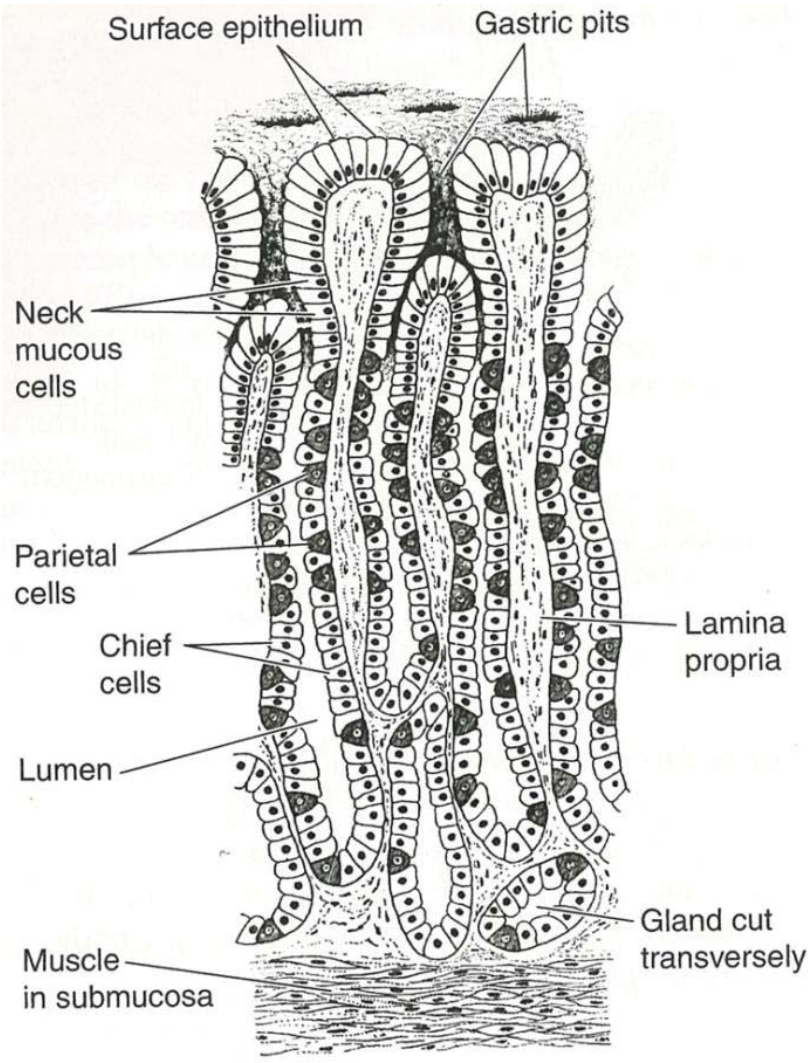

Figure 2-7 Glands in the mucosa of the body the human stomach (Ganong et al., 2005).

2.6.3 Small intestine

Small intestine is the place where the digestion is completed and the products of digestion are absorbed. The small intestine absorbs most of the fluid from dietary sources and gastrointestinal secretions (9 L) and allows only 1 - 2 L to pass into the colon (Ganong et al., 2005). The small intestine is composed of a duodenum, jejunum, and ileum (Fig. 2-8). The length of duodenum is 25 cm and that of jejunum and ileum is 260 cm, which are measured by intubation in living humans (Ahrens Jr et al., 1956). Throughout the length of the small intestine, the mucosa is covered by villi lined with enterocytes. The free surfaces of the enterocytes of the villi are divided into minute microvilli (Ganong et al., 2005). The villi and microvilli increase the surface area of inner intestine. Intestinal mobility is different from gastric motility. There are three types of motions of the small intestine: peristaltic waves, segmentation contractions and longitudinal contractions. Peristalsis, which is 8 – 12 cycles/min, propels the intestinal contents towards the colon. Segmentation contracts result from contractions of the circular muscle layer. They appear regularly along the small intestine and then disappear and are replaced by another set of contractions between the previous contractions (Ganong et al., 2005). The longitudinal contraction is a relatively prolonged contraction, which is mostly caused by the contraction and relaxation of the longitudinal muscle layer (Fullard et al., 2014). It is noted that the segmentation and longitudinal contractions slow the intestinal transit.

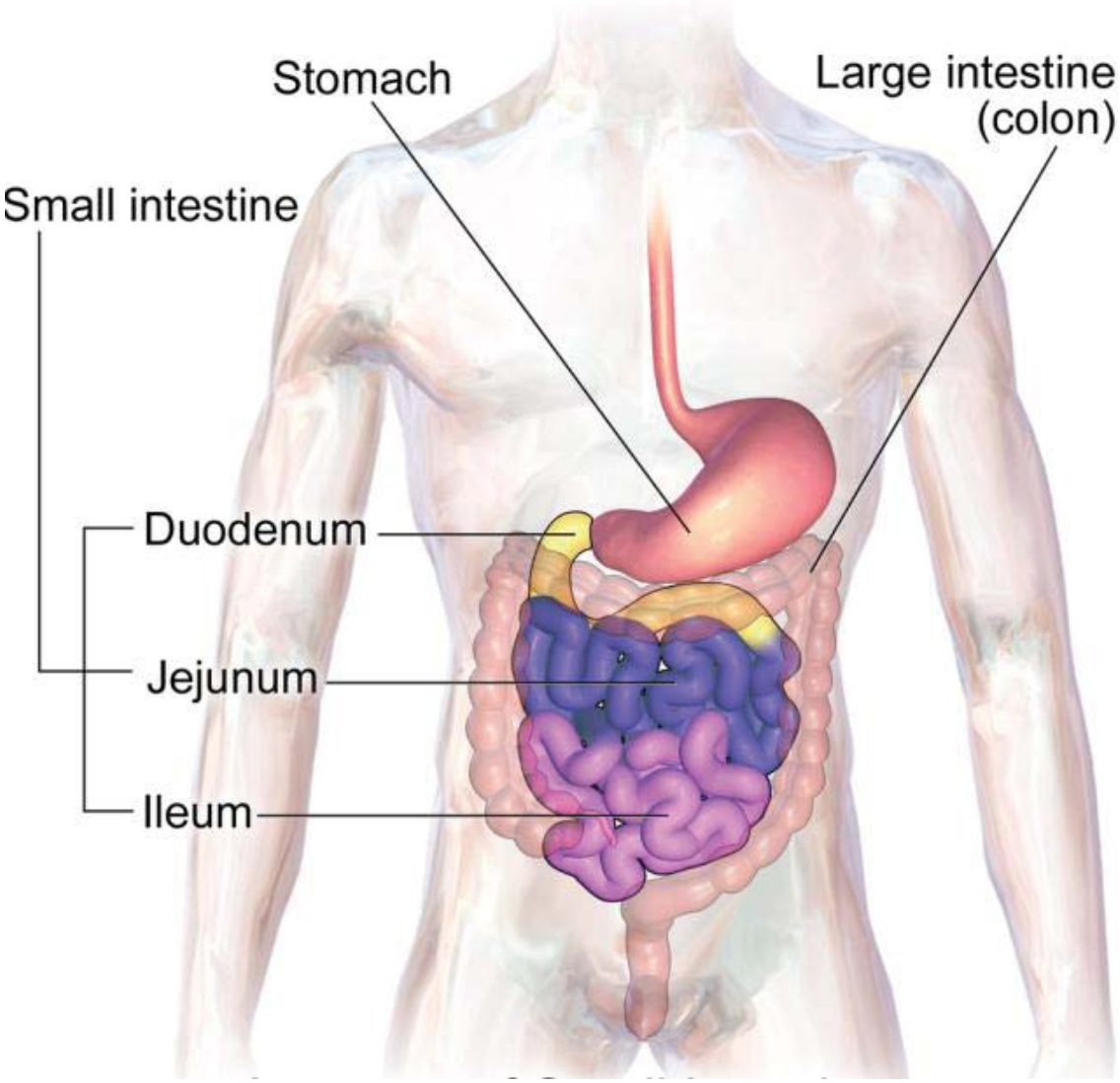

Figure 2-8 Anatomy of the small intestine (Wikipedian-contributors, 2014).

The pH of gastric chyme reaches ~ 6-7 in the duodenum due to mixing with pancreatic juice (pH 8), bile and intestinal juices (neutral or alkaline). When chyme reaches the jejunum, the pH is nearly neutral but rarely alkaline (Ganong et al., 2005). The principle enzymes in the pancreatic juice are presented in Table 2-2.

Table 2-2 Principles enzymes in pancreatic juice (Ganong et al., 2005).

Enzyme	Substrate	Catalytic function or products
Trypsin	Proteins or polypeptides	Cleave peptide bonds on carboxyl sides of basic amino acids
Chymotrypsin	Proteins or polypeptides	Cleave peptide bonds on carboxyl side of aromatic amino acids
Elastase	Elastin, some other proteins	Cleave bonds on carboxyl side of aliphatic amino acids
Carboxypeptidase A	Proteins or polypeptides	Cleave carboxyl terminal amino acids having aromatic or branched aliphatic side chains
Carboxypeptidase B	Proteins or polypeptides	Cleave carboxyl terminal amino acids that have basic side chains
Copliase	Fat droplets	Facilitates exposure of active site of pancreatic lipase
Pancreatic lipase	Triglycerides	Mono or di-glycerides, fatty acids
Bile salt-acid lipase	Cholesteryl esters	Cholesterol
Pancreatic α-amylase	Starch	Hydrolyzes 1:4 α linkages

Bile salts are important biological surfactant, which are produced by the liver and stored in gladder (Hofmann & Roda, 1984; Verde & Frenkel, 2010). Bile salts are biosynthesized from cholesterol. Bile salts are based on a tetracyclic steroid system that is rigid, slightly curved and hydrophobic (Madenci & Egelhaaf, 2010); 1 to 3 hydroxyl and one acidic group are attached to the hydrophobic system (Fig. 2-9A), which form

into a hydrophilic face (Fig. 2-9B). Bile salts differ in the number, position and spatial arrangement of the hydroxyl group and in the conjugated amino acids. The principle bile salts are cholate (50%), chenodeoxicholate (30%) and deoxicholate (15%) (Ganong et al., 2005; Maldonado-Valderrama et al., 2011).

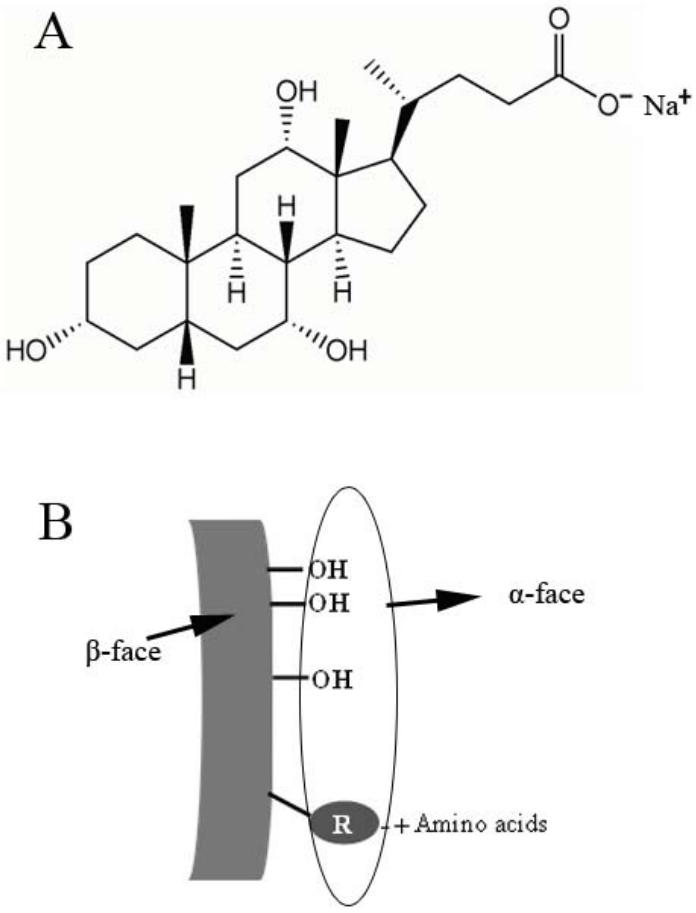

Figure 2-9 Cholate (A) and schematic representation of the amphiphilic structure of bile salts (B).

Due to the amphiphilic nature of bile salts, they self-assemble into various shapes of micelles or aggregates when in an aqueous environment above a critical micelle concentration (CMC) (Mukhopadhyay & Maitra, 2004; Madenci et al., 2010). CMC differs with the types of bile salts. Facial arrangement of hydrophilic and hydrophobic domains leads to the formation of small micelles and displays high CMC values (Madenci et al., 2010; Maldonado-Valderrama et al., 2011). The micelles can

collect lipolytic products in the hydrophobic cores, keep lipids in solution and deliver/transport them to surfaces of the intestinal epithelium, where they are absorbed (Fig. 2-10A and B). In the real digestion environment, the formation of micelles is much complex due to the action of phospholipids and monoglycerides.

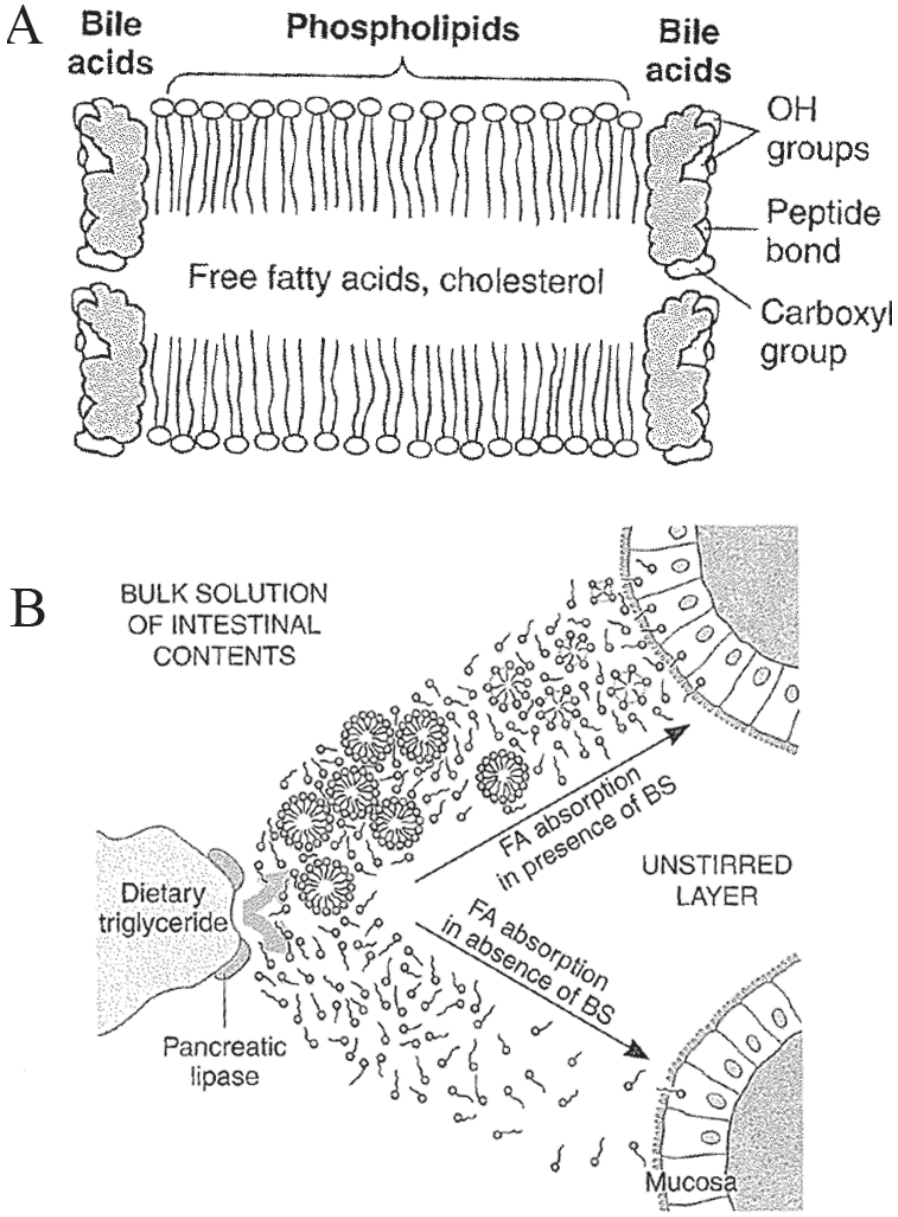

Figure 2-10 One disk-shaped bile salt-lipid mixed micelle (A) and lipid digestion and passage to intestine mucosa; the circular structures are bile salts micelles with lipolytic products in cores (B) (Ganong et al., 2005).

2.7 Disintegration of solid foods in the human body

2.7.1 Oral processing

Nearly all solid or semi-solid foods are subjected to the process of chewing in the oral cavity. The food particles are sufficiently broken up by each type of tooth, with the aid of the tongue and cheeks directing and keeping the food between molars for chewing (Chen, 2009; van Vliet et al., 2009; Xu & Bronlund, 2010). The forces applied on the teeth vary with different types of foods which are being chewed. The force applied to single tooth is also different from the total force between all the contacting teeth during chewing. On foods like biscuits, carrots and cooked meats, forces range from 70 to 150 N on any single tooth (Anderson, 1956), while forces on all the containing teeth range from 190 to 260 N (Gibbs et al., 1981).

From a physiological point of view, there are two main roles of chewing: to ensure fragmentation of food into particles small enough to be properly lubricated by saliva and form a cohesive bolus for swallowing (Hutchings & Lillford, 1988; Prinz & Lucas, 1995) and to have an enhanced release of flavor and aroma from food structure (van der Bilt, 2012). The result of chewing is mainly determined by oral factors (i.e. dental factors, jaw muscle activity, bite force, masticatory performance, saliva and swallowing of food) and the characteristics of the food (van der Bilt, 2012). The former is about the individuality of human beings which leads to variations of chewing. For example, the size of oral cavity varies dramatically from person to person (Chen, 2009); the large variation of biting force has been observed between different races, gender and individuals in the same ethnic groups (Paphangkorakit & Osborn, 1997; Bourne, 2002). The latter is the key factor influencing how a food is orally processed and sensually perceived (Jalabert-Malbos et al., 2007). Mastication is an early step in the process of size reduction to small molecules that can be absorbed into the bloodstream. It usually

reduces particle size by two or three orders of magnitude before passing to the stomach (Bourne, 2004).

Texture is the sensory and functional manifestation of the structural, mechanical and surface properties of foods detected through the senses of vision, hearing, touch and kinesthetics. This definition conveys four important concepts as follows: 1) texture is a sensory property and, thus, only the individual can perceive and describe it, 2) it is a multi-parameter attribute, 3) it derives from the structure of the food (molecular, microscopic or macroscopic), 4) it is detected by several senses, the most important ones being the senses of touch and pressure (Szczesniak, 1963; Bourne, 2002; Szczesniak, 2002). Though texture is sensory perceptions of human beings, it is finally determined by food structure (i.e. physical properties). Therefore, mechanical and tactile elements are often simultaneously investigated by various instruments and then correlation is established between sensory terms and mechanical/tactile properties. These rheological or mechanical assays may be classified as either empirical or fundamental. The benefit of using fundamental rheological methods (e.g. dynamic test, failure test, etc.) to evaluate the mechanical elements of texture is that they are linked to theories that explain molecular and microstructural mechanisms of texture. It is possible that mechanical properties measured up to and at fracture predict changes occurring during oral processing (Foegeding, 2007; Foegeding & Drake, 2007). In addition to these fundamental rheological methods, there is a very important empirical instrumental testing to imitate the first two bites of chewing which is called Texture Profile Analysis (TPA) (Szczesniak et al., 1963; Bourne, 1978). This procedure, as shown in Fig. 2-11, gives six or more different texture notes.

Fracturability is defined as the force at a significant break early in the first bite. The maximum force of the first bite is defined as hardness. The ratio of the positive

force areas under the first and second compressions (A2/A1) is defined as cohesiveness. The negative force area during the first decompression is adhesiveness. The distance the piece of food recovers its height between the first compression and the beginning of the second compression is defined as springiness. These parameters correlates highly with sensory ratings (Szczesniak et al., 1963; Kim et al., 1996; Drake et al., 1999; Breuil & Meullenet, 2001; Szczesniak, 2002; Di Monaco et al., 2008).

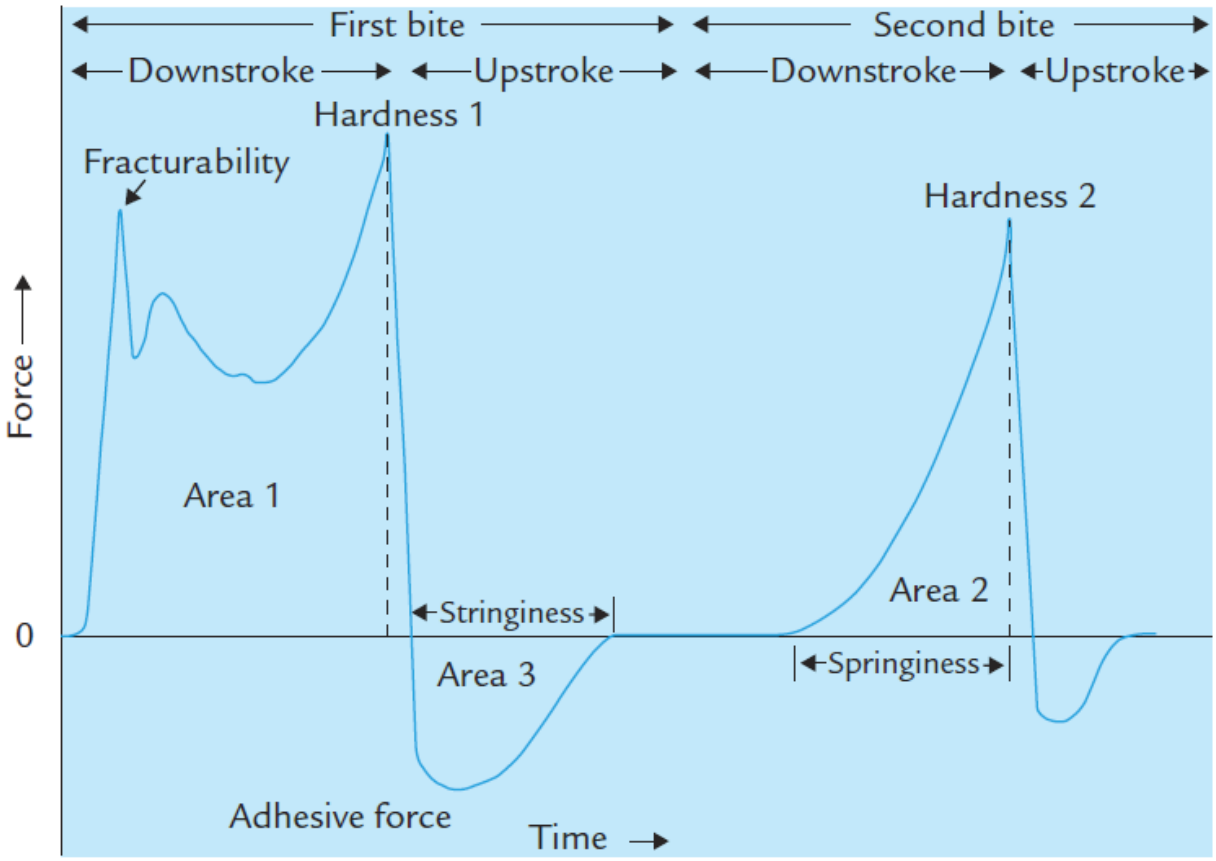

Figure 2-11 A generalized texture profile analysis curve obtained from the instron universal testing machine (Bourne, 2002).

The influence of food characteristics on the chewing process has been extensively studied. It is believed that the food structure is a key factor influencing the chewing behaviour of various foods (Chen, 2009). In general, a hard food would require more chewing cycles. For example, a mouthful of apple has shown to take 7 chewing

cycles to form the first bolus to swallow, while it has shown to take 16 and 19 chewing cycles to form a bolus to swallow a mouthful banana and cookie respectively (Hiiemae et al., 1996). Chen (2009) replotted the number of chewing cycles against the yield stress of different foods obtained from Engelen (2005) finding a perfect linear relationship between these two parameters, which strongly supports it. Jalabert-Malbos et al. (2007) also found harder foods such as carrots, peanuts and coconut required more chewing cycles than softer foods like egg white, gherkins and mushrooms. A clear relationship between food hardness and jaw muscle activity has been found in many studies. A harder food results in increased jaw muscle activity and longer burst duration of the muscle activity, regardless of food (Agrawal et al., 1998; Peyron et al., 2002; Foster et al., 2006; van der Bilt et al., 2007). Furthermore, the masticatory force was observed to increase from 100 to 150 N when the hardness of silicone rubber increased by a factor of 2 (Kohyama et al., 2004). In addition, the food characteristics also influence the jaw movement (Horio & Kawamura, 1989; Peyron et al., 2002).

Food type has a great effect on the degree of fragmentation of food. Jalabert-malbos et al. (2007) studied the fragmentation of ten natural foods upon chewing. The authors found that carrots had the highest number of chewing cycles, but the median particle size of bolus (D_{50}) was large. Peanuts and coconut had the similar chewing cycles, but the D_{50} of peanuts was half of that of coconut. Egg white had the smallest chewing cycles, but its D_{50} was not the lowest. These differences in degree of food fragmentation are mainly attributed to the food structure in these products. Peyron et al. (2004) drew similar conclusions when studying 6 natural foods (peanut, almond, pistachio, carrot, radish and cauliflower).

2.7.2 Food breakdown in the stomach

The stomach, which is a key organ in the human gastrointestinal tract, performs

four main functions: storing food, mixing food with gastric juice, reducing the size of food particles and emptying food (Davenport, 2010). Under mechanical and biochemical processing in the stomach, food bolus undergoes further disintegration into smaller pieces, which are then emptied into the duodenum. Mechanical properties of foods are responsible for resisting food breakdown in the human body (Lucas et al., 2002). The disintegration of solid foods in the human stomach is determined by the following factors:

2.7.2.1 Acid effect

HCl can hydrolyze the peptide linkages in proteins or peptides. The acid acts as a catalyst for the reaction between the amide and water. However, the reaction rate is very slow at 37 ºC because hydrogen ions are not able to easily access the peptide bonds due to the electrostatic and steric properties of the chain, as well as the nature of the amino acids forming each particular bond (Harris et al., 1956; Zhong et al., 2005). Synge et al. (1945) found that the half-period of various dipeptides (i.e. acid hydrolysis) in a mixture of equaled volumes of 10 N HCl and glacial acetic acid at 37 ºC ranged from 2.8 to 190 days. In the physiological conditions (pH 2, 37 ºC), the protein acid hydrolysis would be much lower. Compared with protein acid hydrolysis, starch acid hydrolysis is much faster (Hoover, 2000; Wang et al., 2003). Under mild acid conditions (2.2 N HCl, 35 ºC), the hydrolysis rates range from 7 to 29%/day according to the maize starch genotype (Gérard et al., 2002).

Mun et al. (2006) reported that at pH 1 and 35 ºC, native maize starch and pressure-cooked maize starch had 0.1 and 3.5% extent of hydrolysis after 6 h digestion, respectively. Pectin is the main component of plant cell wall which plays a role in protecting cell; some cell walls are difficult to break down by mechanical force thereby impacting the digestion of nutrients from plant sources. Pectin acid hydrolysis plays a

role in the non-enzymatic plant tissue softening during the gastric phase (Ilker & Szczesniak, 1990; Kong & Singh, 2009; Tydeman et al., 2010).

2.7.2.2 Ion effect

When food bolus enters into the stomach, the gastric juice begins to mix with the food. With the digestion, gastric juice gradually penetrates into the core of food particles from the surface. Food comes from various sources (e.g. animals, vegetables, etc.), and are mainly composed of proteins, lipids and carbohydrates. Proteins are charged molecules because of the presence of polar acidic amino acids (i.e. aspartic acid and glutamic acid), polar basic amino acids (i.e. lysine, arginine and histidine), carboxyl (-COOH) and hydroxyl (-OH) groups. By contrast, lipids are hydrophobic, except some, where the lipid has a charged –R group (e.g. phospholipid and sulfolipid). However, emulsified oil droplets form a major part of many processed food formulations (Singh & Sarkar, 2011), which may be charged based on the nature of emulsifiers. Carbohydrates are divided into four groups: monosaccharide, disaccharide, oligosaccharide and polysaccharide. In the monosaccharide, each carbon atom except carbonyl has one hydroxyl group (e.g. glucose, fructose and galactose). In the monosaccharide with carboxyl (charged), each carbon atom has one hydroxyl (e.g. glucuronic acid, galacturonic acid). Di, oligo or polysaccharides are composed of monosaccharides through glycosidic linkages. Starch is non-ionic polysaccharide. Alginic acid, pectin, xanthan gum, gum arabic, etc. are anionic polysaccharides. Very few food polysaccharides (e.g. chitosan) are cationic. Assuming a food particle containing 10% protein (negatively charged), 20% starch, 5% fat and 65 % water, the exchange of ions inside and outside food particle is represented by Fig. 2-12. The ions equilibrium between food particle and surroundings in the stomach resembles the Donnan membrane equilibrium (Donnan, 1924; Flory, 1953).

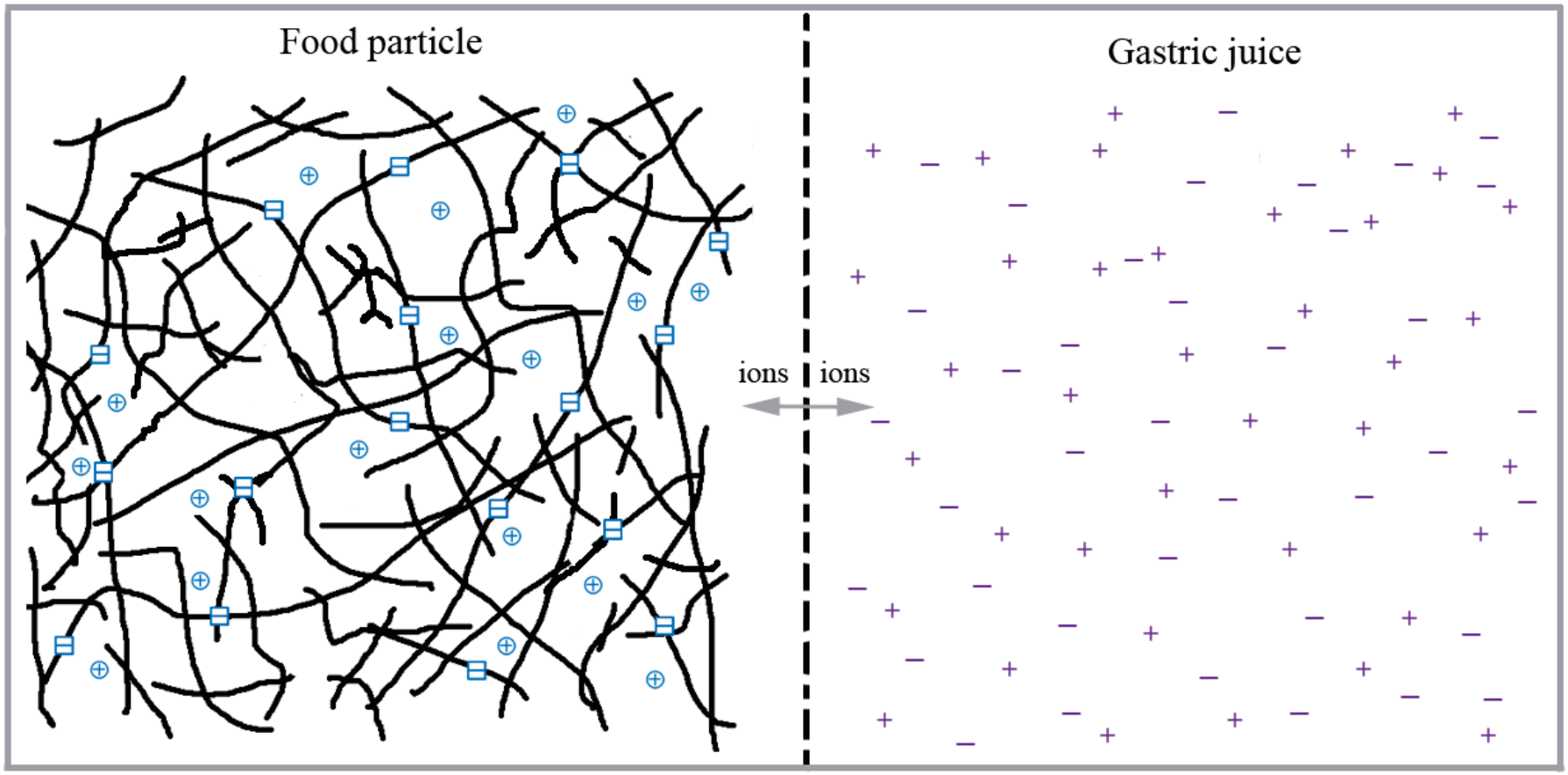

Figure 2-12 Diagram of ions equilibrium of a food particle in the stomach. ⊟, ⊕, +, and − represent fixed charges, counterions, mobile positive charges and mobile negative charges, respectively.

Due to ion concentration and electrical gradient, the mobile ions and counter-ions diffuse into and out of the food particle until an equilibrium is reached (Fig. 2-12). Food particles act as a semi-permeable membrane which prevents the fixed charged substituents from diffusing into the gastric juice. In equilibrium state, the concentration of mobile ions inside the food particle will always be higher than that outside because of the attracting power of the fixed charges. Usually it takes a relatively long time for equilibrium of ions inside and outside food particle. Vardhanabhuti et al. (2010) monitored the pH change of whey protein gel (15 wt % protein, 1.9 cm in diameter and 15.3 cm in length) by soaking the gel in acid solutions at room temperature. They reported that there was a sharp decrease in the pH of gel during the first 16 h and this pH decrease increased with acid concentration. Longer equilibrium time only slightly lowered the pH of gels. In the stomach, ion exchange between food particles and gastric juice is likely to be much faster because of mechanical shearing by the human antrum, enzymatic degradation and food fragmentation by oral processing (the average particle size of food bolus is usually lower than 4 mm). The diffusion of ions like Na^+, Cl^- and H^+ into the food particle greatly changes the physicochemical environment inside the food particles thereby influencing the breakdown of food particles in the stomach. Salts diffusing into the food particle shield the charges inside the particle, which may hinder the expansion or breakdown of the food particles. By contrast, H^+ diffusion results in the ionization of NH_2 to NH_3^+ (more charges and more electrostatic repulsion), leading to the relaxation of food network.

2.7.2.3 Swelling effect

According to Flory-Huggins theory, there are three contributions to the free Gibbs energy change of the system: network-solvent mixing, elastic retraction of network and the difference of mobile ion concentration inside and outside the network

when an ionic network is placed in a swelling agent (Flory, 1953; Quesada-Perez et al., 2011). The free Gibbs energy change is expressed as:

$$\Delta G = \Delta G_{mix} + \Delta G_{elastic} + \Delta G_{ion} \cdots\cdots\cdots\cdots \text{Eqn 2-3}$$

These three factors which cause the osmotic pressure inside and outside the network determine the swelling of the network (polymer). The food particle is an open system which can be regarded as a complex, ionized three-D polymer gel, composed mainly of proteins, polysaccharides and lipids. There have been many studies reporting the swelling of food particles during gastric digestion. Swelling of peanuts during *in vitro* gastric digestion was greatly affected by processing patterns (boiling, roasting and frying) with the highest swelling ratio of raw peanuts (Kong et al., 2013). Significant dilution (i.e. swelling) of vicious locust bean gum occurs during gastric digestion in the human body after 36 min (Marciani et al., 2001b). Time domain NMR relaxometry has been used to detect the swelling phenomenon occurring during *in vitro* gastric digestion, when the gastric fluid enters the meat matrix (Bordoni et al., 2014). Both *in vivo* and *in vitro* studies have shown a marked increase in carrot tissue swelling in a microscopy (Tydeman et al., 2010).

The swelling equilibrium of food particles in gastric juice during digestion greatly affects its mechanical properties. This instability can also be called mechanical instability at the phase transition. Tanaka et al. (1987) found that the crease appeared at the surface of polyacrylamide gels when the samples of gel were immersed into the water. At the beginning, the crease was fine, but the units of the crease coalesced with increasing time and eventually disappeared when the gel reached equilibrium. Through the experiment where the lowest layer of a gel was mechanically fixed to a rigid film and the top was free for swelling or expansion, the authors recognized the elastic origin of the mechanical instability. The reason for the formation of crease is the kinetic

process of the gel swelling, i.e. the outer surface is swollen first and that this layer is constrained by the inner surface that remains unswollen. This opposing behavior during gel swelling led to the formation of crease, which was also observed in other studies (Onuki, 1989; Tanaka et al., 1992; Tanaka & Sigehuzi, 1994). It is recognized that the penetration or diffusion of external solvent is a kinetic process from outer layer into inner layer. This is an indication of how gastric juice penetrates into the food particles. This gradual diffusion of gastric juice from outer layer into internal layer has been observed in various foods (peanut, carrot and locust bean gum) during both *in vivo* and *in vitro* gastric digestion using magnetic resonance imaging and others technique (Marciani et al., 2001b; Kong et al., 2009; Kong et al., 2013). The mechanical instability may favor the breakdown of food particles in the stomach, especially under mechanical shearing and enzymatic degradation which is the mechanism of softening of food particles during gastric digestion.

2.7.2.4 Enzyme effect

Pepsin is a charged macromolecule which prefers to cleave bonds adjacent to aromatic and hydrophobic amino acids (Ganong et al., 2005). The hydrolysis of proteins by pepsin is one of the most important contributors to the food disintegration in the stomach. According to Donnan law, pepsin can freely diffuse into the food particles in the stomach if the water channel inside the food particle is big enough for the diffusion of pepsin (Donnan, 1924). The diffusion of pepsin into the food particle may accelerate the disintegration of the food particles by disrupting its inner structure.

2.7.2.5 Gastric motility effect

The trituration occurs mostly in the antrum and pyloric region, where flow and shear forces are maximal.

In the human digestion tests, a 1.8 cm balloon was swallowed with meals (liquid or solid). It was exerted a cumulative forces of antral contraction of 6 N for emptying a liquid meal and 22 N for a solid meal over a 30 min period (Camilleri & Prather, 1994). Marciani et al. (2001a) found that agar gel beads (diameter: 1.27 cm) with low fracture strength (0.15-0.65 N) were broken down quickly in the human stomach whereas the beads with high fracture strength (> 0.65 N) were broken down into smaller particles much slowly; this study does not consider the effect of mastication on the breakdown of the agar gel beads (i.e. the beads were swallowed without mastication). Kamba et al. (2000) found that the mechanical destructive force from the human stomach was ~ 1.9 N when evaluating the crushing of a series of tablets (diameter: 7 mm and thickness: ~ 4 mm) with different crushing strength in the stomach.

2.7.2.6 Food structural effect

Food types and processing techniques are the main factors considered by researchers in the *in vitro* gastric digestion studies. These *in vitro* studies clearly show how food structure influences the gastric digestion of food, because there is only one variant in the system, i.e. food structure.

Recently, the effect of food structure on the disintegration of food during gastric digestion has received much attention. Both *in vitro* and *in vivo* studies have shown the structural effect of food on the disintegration of foods during gastric digestion. Mastication greatly changes the structure of solid food, which is swallowed as a form of bolus. The properties of bolus (e.g. the particle size distribution) play an important role in the gastric digestion of food. However, few studies consider the effect of oral processing on the gastric digestion of foods. Nevertheless, these studies about effect of original structure of food without oral processing on the disintegration of solid foods provide useful information for understanding food digestion in the human body. Kong

& Singh (2009) studied the disintegration of a variety of foods including ham, fried dough, carrot, beef jerky, almond and peanut in a stomach model, using the mass loss method. Their stomach model simulated the biochemical environment and antral shearing of the stomach. The rate of disintegration of the foods generally decreased with the increase of food hardness or toughness. For example, ham with very low hardness lost 50% weight within 5 min during gastric digestion whereas peanut with high hardness lost 50% weight using 715 min. A similar phenomenon, that different foods vary in disintegration rate during gastric digestion was also reported in other studies (Siegel et al., 1988). Processing of foods significantly affects their gastric digestion properties. Boiling, roasting and frying significantly change the structural properties of peanuts. The disintegration of peanuts represented by mass loss of food particles during gastric digestion varied with different processing methods. The time for loss of 50% weight was 10.7, 8.3, 6.7 and 3.6 hours for raw, boiled, roasted and fried peanuts, respectively (Kong et al., 2013). Furthermore, with the increase of boiling time, the disintegration rate of carrots in the stomach model increased because of the decreased food hardness.

Bornhorst & Singh (2013) examined the effect of the properties of bread bolus created by mechanical grinding and mixing with artificial saliva on the disintegration of bread bolus in the stomach model. It is believed that the original structure of various breads significantly influenced the disintegration of bread bolus in the stomach model via altering the water adsorption ability and cohesive force of bread bolus. In an *in vivo* study using six mini-pigs, the heated rennet milk protein gel was emptied significantly more slowly than the raw rennet milk protein gel with the similar composition, indicating the denser microstructure of heated rennet milk protein gel slowed down the gel disintegration (Barbé et al., 2013).

Mixing meals in the stomach is very important to food disintegration because the antrum is the main site for food trituration. There is an interesting report about the meal mixing in the stomach (Bornhorst et al., 2014). The pigs were fed with two equal-sized portions of meals which were labeled with different colors; the first portion was consumed first and subsequently the pigs were fed with the second portions. The rigid meals (raw almonds and brown rice) underwent a slower mixing process than the soft meals (roasted almonds and white rice). The authors believed that gastric emptying was a controlling factor to the mixing of meals that was more important than the type of food matrix and pre-processing prior to consumption. This was because the gastric emptying showed almost linear correlation to percent mixed meals. However, Urbain et al. (1989) found that the mixing of a meal with solid particles retained in fundus and antrum was fast, with an efficient mixing occurring during the lag phase of gastric emptying.

The food breakdown during gastric digestion at a macroscopic scale is discussed above, but the effect of food structure on the gastric digestion at a molecular level is another important area for understanding food digestion. Structural properties of protein aggregates or protein 3-D network determine the hydrolysis rate and peptide species generated in the gastric digestion. Heated whey proteins formed above pI (~ pH 4 - 5) are more susceptible to gastric digestion than those formed below isoelectric point probably because the unfolding and aggregation of whey proteins at near neural pH exposed more hydrophobic residue and accessible peptide bond for enzyme reaction (Zhang & Vardhanabhuti, 2014). The study of Nyemb et al. (2014) provides an evidence for how the food structure at a molecular level affects digestion. The authors prepared ovalbumin aggregates with different morphologies of linear (~ 33 nm), linear-branched (~ 16 nm), spherical (30 μm) and spherical agglomerated (80 μm) by heating at pH

9/ionic strength 0.03 M, 7/0.03 M, 7/0.3 M and 5/0.3 M, respectively. The results showed that linear aggregates hydrolyzed much faster than the spherical aggregates in the model stomach. Furthermore, the peptide bonds appeared to be specifically cleaved, depending on the morphology of the aggregates. Different surface area of aggregates and different cross-linked patterns of proteins during aggregate formation are likely to be the possible mechanisms.

The understanding of food breakdown in the stomach is crucial to maintaining the human health, and is also important when designing of new foods. However, there is a lack of knowledge of food disintegration in the human body because very few techniques can be used to monitor the change in physicochemical forms of foods in the human body. *In vitro* methods may help in exploring the disintegration mechanisms of solid food in the stomach, especially when the function of regular mechanical grinding of human antrum is simulated in an *in vitro* gastric model.

2.7.3 Gastric emptying

2.7.3.1 Pyloric sieving

Pyloric sphincter serves as a valve which only allows small solid particles and liquid to enter the duodenum during gastric emptying. The particle size distribution of chyme entering into duodenum is very important for food digestion and nutrient absorption in the intestine, because it determines the surface areas of the particles exposed to bile salts and pancreatin. James H. Meyer has done much pioneering work about the size of particles emptied from the stomach. In dog studies, after feeding a standard meal of beef steak, liver and water, the chyme was obtained through the duodenal cannula for particle size distribution. No solid particles exceeding 2 mm were emptied from the stomach; ~70% of solid particles emptied into the duodenum were smaller than 0.06 mm and ~97% were smaller than 1 mm (Meyer et al., 1979; Meyer et

al., 1985). In human studies, after feeding a meal of 60 g steak, 30 g ^{99m}Tc-chicken liver in 1 or 10 mm cubes, the rate at which aspiratable particles from proximal jejunum (< 1 mm) passed the aspiration tube was compared with the rate of gastric emptying of ^{99m}Tc particles by scintigraphic imaging. These two rates were almost similar, indicating almost all solid particles emptied from the stomach were smaller than 1 mm, which was similar to the gastric sieving of dogs (Meyer et al., 1981). The gastric emptying of solid meals shows a biphasic nature because of the pyloric sieving (Siegel et al., 1988).

2.7.3.2 Pyloric trituration

Food trituration in the stomach favors the gastric emptying because it decreases the meal particle size. During gastric digestion, disintegration kinetics of food bolus plays an important role in gastric emptying. However, there is little literature on the effect of disintegration kinetics of food on gastric emptying in either *in vivo* studies or *in vitro* studies. Meyer et al. (1985) fed dogs with a standard test meal of 99mTc-lablled liver, steak and water to which they added inert spheres of different sizes. With decrease of sphere size from 5 to 1 mm, the gastric emptying of spheres was promoted progressively. However, 0.015 mm spheres emptied no faster than 1 mm ones. This indicated the trituration no longer had a significant effect on the gastric emptying when the meal size decreased below 1 mm.

2.7.3.3 Meal particle size

Particle size of food entering into the stomach greatly impacts gastric emptying because of gastric sieving and rate-limited trituration of solid food in the stomach. In general, the greater particle size of food entering into the stomach leads to a lower rate of gastric emptying. Pera et al. (2002) studied the effect of mastication on gastric emptying and found that more chewing cycles of food led to a higher gastric emptying.

Urbain et al. (1989) provided another evidence on effect of meal particle size on gastric emptying. An egg meal was homogenized, or cut into 2.5 and 5 mm cubes respectively. Without chewing the meal, the human subjects swallowed the whole meal and the gastric emptying slowed down with increasing the meal particle size. The larger meal particle size still slows gastric emptying (Holt et al., 1982; Olausson et al., 2008).

2.7.3.4 Food composition

Gastric emptying is regulated by food composition (e.g. fat, protein and carbohydrates). Cecil et al. (1999) studied the gastric emptying of a high fat (cream) and high carbohydrate (maltodextrin) soup with the same meal volume and calorie in a group of the healthy human subjects. They found that the high-carbohydrate soup was emptied significantly faster than the high-fat soup. Some research reported that the duodenal action of the products of digestion of isocaloric amounts of fat, protein and carbohydrate had the equal effect on the slowing of gastric emptying (Calbet & MacLean, 1997). This means that fat is emptied slower than proteins and carbohydrate because fat has a calorie density of 9 kcal/g that is higher than 4 kcal/g of protein and carbohydrate. In addition, food components, like mono or di – saccharides and minerals, may result in the hyper-osmolality of chyme entering into duodenum, which suppresses gastric emptying (Shafer et al., 1985).

2.7.3.5 Food calorie content

Food calorie content is a factor independent of food composition influencing gastric emptying (Velchik et al., 1989). Increasing calorie content or calorie density leads to a slower gastric emptying which is attributed to the negative feedback mechanism mediated by the duodenal receptors (e.g. cholecystokinin release) (Moran & McHugh, 1982; Liddle et al., 1986). The gastric rate has a negatively linear relationship

to the meal calorie content (Hunt & Stubbs, 1975; Calbet et al., 1997). Generally the human stomach delivers ~ 150 kcal per hour or ~ 2.5 kcal per minute into the duodenum (Collins et al., 1983; Hunt et al., 1985). However, increasing meal calorie content and meal volume also increases the acceptance of energy by the intestine (Hunt et al., 1975; Brener et al., 1983).

2.7.3.6 Food density

The food components or particles with the density below and above 1 decrease gastric emptying. For example, the free oil or large oil droplets easily cream into the top layer of gastric contents in the stomach because of the low density (~0.92 g/mL) (Marciani et al., 2006; van Aken et al., 2011). Meyer et al. (1985) studied the emptying of nondigestible particles with the density below and above 1 g/mL in the dogs after feeding a standard meal. They found that decreasing density below 1 or increasing density above 1 g/mL reduced gastric emptying of particles (Meyer et al., 1985).

2.7.3.7 Food rheology

Rheological properties of foods are an important aspect for understanding the food digestion in the human body. Usually a food particle has combined properties of viscosity and elasticity. Liquid foods possess more viscous property whereas solid foods possess more elastic property. Liquid foods have less satiating effect than their solid equivalents with the similar compositions (Stull et al., 2008; Mattes & Campbell, 2009; Leidy et al., 2010). This may contribute to slowing gastric emptying.

Increasing viscosity of meals by adding different fibers may delay gastric emptying probably because the high viscosity increases the satiety (Di Lorenzo et al., 1985; French & Read, 1994; Leclère et al., 1994; Benini et al., 1995; Burton-Freeman, 2000; Marciani et al., 2001b; Darwiche et al., 2003; Zhu et al., 2013). By contrast, it has

been reported that increasing viscosity by adding digestible pectin to liquid meal accelerates gastric emptying; furthermore, the intake of pectin itself (pectin plus water) has no significant effect on gastric emptying compared with intake of water (Shimoyama et al., 2007). This indicates viscosity plays a role in gastric emptying via food itself.

The physicochemical forms of emptied chyme greatly impact the subsequent digestion in the small intestine. As described above, most studies of gastric emptying are conducted using *in vivo* methods. Therefore, the characterization of periodically emptied chyme is difficult because of ethic limitations. Based on the same reason, the knowledge of the effect of disintegration kinetics on the gastric emptying of foods is not clear. A dynamic gastric model may be a good alternative for bridging these gaps.

2.7.4 Food breakdown in the intestine

Food digestion is a dynamic and continued process. Chyme enters the duodenum where digestion continues. When food is fully digested, it is absorbed into the body. Carbohydrates, proteins and lipids are continued to be digested in the intestine by pancreatic amylase, trypsin and pancreatic lipase, respectively. Pancreatic juice diffusion (water, ions and enzymes), mechanical motility of the intestine and structural effects of food influence the breakdown of food in the intestine. Diffusion of enzymes into food particles causes further degradation of remaining food structure generated from gastric digestion (Snow & O'Dea, 1981; Benmoussa et al., 2006). Mechanical mobility of the intestine mixes the chyme and pancreatic juice (Ganong et al., 2005). Remaining food structure still affects food breakdown in the intestine. For example, although starch digestion begins in mouth, starch molecular structure determines the starch digestibility in the intestine. Amorphous starch (e.g. boiled hot potato) is digested rapidly within 20 min during *in vitro* intestinal digestion; amorphous/crystalline starch

(e.g. boiled millet) is digested slowly within 20 to 120 min during intestinal digestion; crystalline starch (e.g. raw potato starch) resists digestion (> 120 min) during intestinal digestion (Englyst et al., 1992; Faisant et al., 1995; Weurding et al., 2001; Hoover & Zhou, 2003). Compact and dense protein aggregates are digested slowly in gastric digestion and subsequent intestinal digestion compared to fine-stranded protein aggregates (Macierzanka et al., 2012; Nyemb et al., 2014). So far, the study about effect of remaining food structure on the intestinal digestion of food has been limited. Especially, the effect of interactions between different food components on food digestion in the intestine requires further investigation.

2.8 Modulation of lipid digestion

Dietary fat often comes from various sources like dairy products, meats and vegetables, which is one of the major nutrients for human-beings providing energy and delivering essential fatty acids and lipid soluble nutrients. Lipid absorption from small intestine is generally quite efficient, and only ~ 4% of the ingested fat escapes into the feces (Carey et al., 1983).

Each source of fat including vegetable oil, meat fat and milk fat is constituted by hundreds of different TAGs (Small, 1991). The general structure of TAG (triacylglycerides) is presented in Fig. 2-13. Usually the R groups are fatty acids (non-polar) or phosphoric acids.

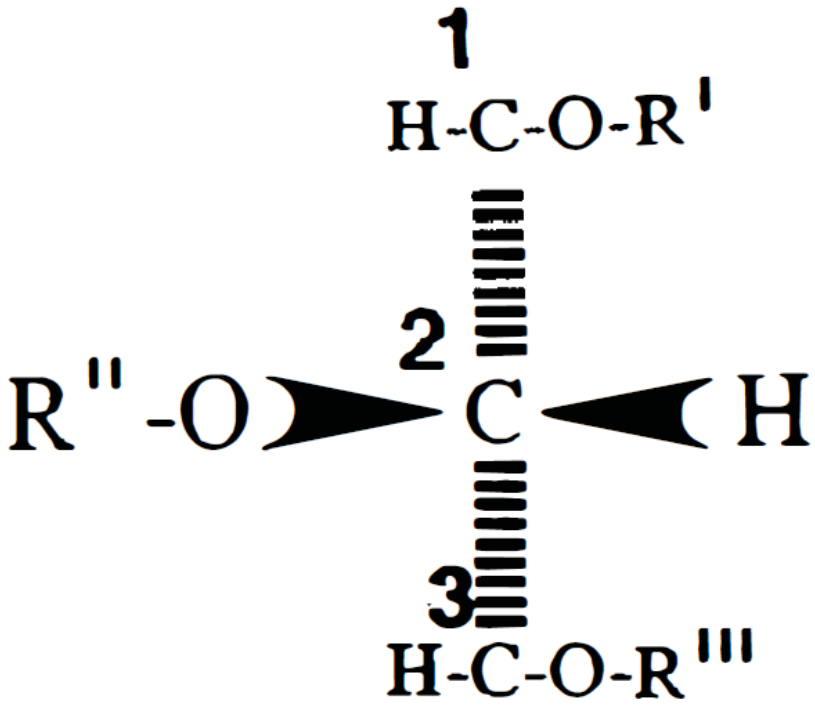

Figure 2-13 General structure of TAG (Small, 1991). The three R groups stand for different acyl groups. With the carbon in the 2-position in the plane of the page and the 1- and 3-carbons behind the plane of the page, if the –OH is drawn to the left then the top carbon becomes sn-1, the mid carbon becomes sn-2, and the bottom carbon becomes sn-3.

Melting of lipid from different sources (e.g. animal or vegetable origin) occurs over a wide temperature range because natural fats are complex mixture of TAGs as shown in Table 2-3. In addition, the long-chain saturated fatty acids (≥ 12 carbons) have quite high melting points; for example, the melting points for myristic, palmitic, and strearic acids are 54, 63, and 70 ºC respectively (Cistola et al., 1986).

Table 2-3 Composition and melting temperature of some natural lipids (Small, 1991).

Lipids	Melting temp. (ºC)	Major TAG's		
Soybean oil	-14	LLL	LLO	LLP
Corn oil	-14	LLL	LOL	LLP
Olive oil	-7	OOO	OOP	OLO
Palm oil	30-36	POP	POO	POL
Coconut oil	24-27	DDD	CDD	CDM
Butterfat	37-38	PPB	PPC	POP
Tallow (beef)	40	POO	POP	POS
Lard	46-49	SPO	OPL	OPO

Abbreviations used for acyl chains in the TAGs: B: C-4:0 (butyric), C=C-10:0 (capric), D=C-12:0 (dodecanoic), M=C-14:0 (myristic), P=C-16:0 (palmitic), S=C-18:0 (stearic), O=C-18:1 (oleic), and L=C-18:2 (linoleic).

The digestion of lipids is an interfacial process. In the mouth, stomach or intestine, free oil is emulsified by proteins, peptides, phosphoric salts, bile salts, polar lipids, monoglycerides and etc. Lipolysis in the intestine is a complex process. Pancreatic lipase which is one of the main enzymes catalyzes hydrolysis of sn-1 and sn-3 position of triglycerides. Lipase has to adsorb onto the surface of oil droplets to hydrolyze the triglycerides. Pancreatic lipase and co-lipase adsorb onto the surface of oil droplets by interacting with adsorbed bile salts (Fig. 2-14).

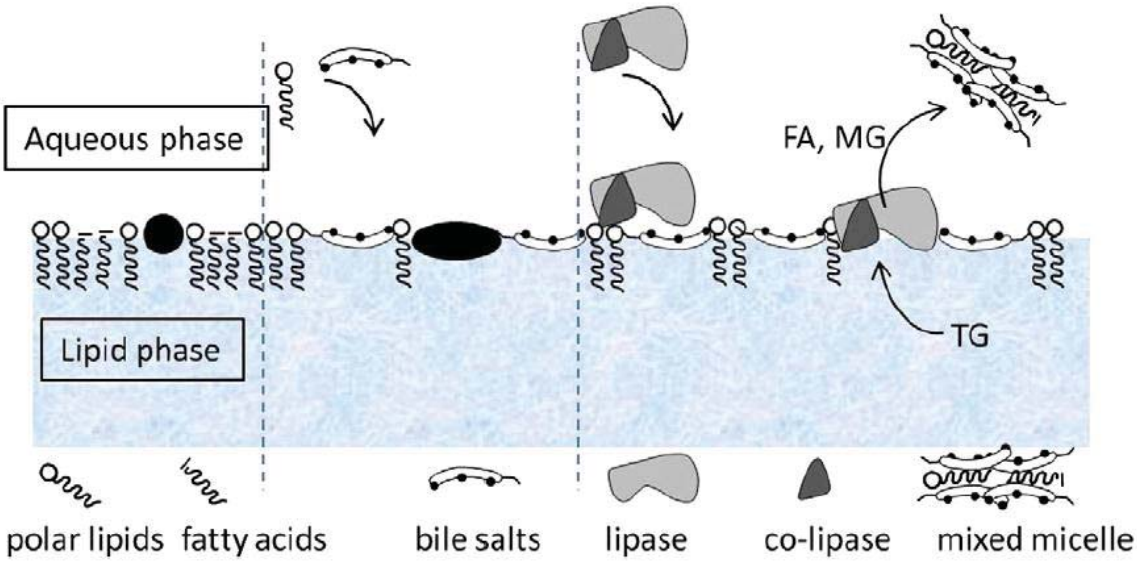

Figure 2-14 Mechanism of lipolysis in the intestine (Wilde, & Chu, 2011).

Lipolytic products can precipitate at the surface of undigested oil (e.g. fatty acids, diglycerides and monoglycerides), which inhibits pancreatic lipase accessing the surfaces of oil droplets (Reis et al., 2008a; Reis et al., 2008b; Devraj et al., 2013). The lipolytic products (i.e. fatty acids) are solubilized into forms of mixed micelles or vesicles by bile salts (Carey et al., 1983). It has been found that presence of bile salts in the digestion leads to a higher amount of free fatty acid release in emulsions prepared by different surfactants (Mun et al., 2007; Sarkar et al., 2010b).

However, the real situation of lipolysis of oil droplets is more complicated. During digestion, lipid undergoes several changes in phase due to the formation of self-assembled structures (e.g. emulsified microemulsions, and further dispersed micellar cubic, hexagonal and biocontinuous cubic structures). Monoglycerides as interface-active products of lipid digestion are known to form these structures in combination with oil and water (Qiu & Caffrey, 2000). During the lipid digestion, the simple oil droplets containing monoglycerides do not translate into complex mixtures of diglycerides, monoglycerides, fatty acids and other polar lipids. Mixing emulsions with

monoglycerides-based internally structured particles can lead to equilibration of the internal particle structure according to the composition, due to the entropy of mixing (Moitzi et al., 2007; Salonen et al., 2010; Salentinig et al., 2011). Salentinig et al. (2011) showed the transition from normal oil-in-water emulsions to internally self-assembled oil droplets or particles during *in vitro* digestion of lipids under simulated *in vivo* concentrations of bile salts juice, pancreatin porcine solution and pH as found in the human intestine. The final forms of oil droplets during the intestinal digestion are vesicles and mixed bile salts micelles. Bile salts increase the release rate of free fatty acids and favor the formation of soluble vesicles and mixed bile salts (Salentinig et al., 2011; Devraj et al., 2013). However, calcium enhances lipid digestion through the formation of insoluble calcium soaps with long chain fatty acids which cannot be solubilized by bile salts (Patton & Carey, 1981; Zangenberg et al., 2001; Devraj et al., 2013).

Recently, many studies have attempted to explore the role of interfacial properties (e.g. composition) in the ability of lipases to digest oil-in-water emulsions (Golding et al., 2010; Singh et al., 2013). The interfacial composition affects the lipid digestion probably by altering the access of bile salts and digestive enzymes onto the emulsion surfaces, thus changing the droplet size during the digestion (Sandra et al., 2008; Sarkar et al., 2010a; Golding et al., 2011; Malaki Nik et al., 2011; Pinheiro et al., 2013). However, this effect of interfacial composition on lipid digestion is not significant. Nik et al. (2011) reported that the soy protein-stabilized emulsions had more extensive lipid digestion than whey protein-stabilized emulsions. Pinheiro et al. (2013) reported that Tween 20-stabilized emulsions had a higher total free fatty acid release than SDS-stabilized emulsions. Sandra et al. (2008) reported that there was no significant difference in the rate and extent of *in vitro* lipid digestion of heated and

unheated emulsions stabilized by β-Lg, indicating the disulfide crosslinks of the interfacial proteins did not influence the lipolysis of the emulsions. In addition, Li et al. (2011) reported that the emulsions coated by complexes of β-Lg/chitosan, β-Lg/alginate, and β-Lg/alginate/chitosan did not show significant differences in the rate and extent of fatty acid release in an *in vitro* lipid digestion by pancreatic lipase compared with an emulsion coated by a β-Lg. Therefore, a rational design of layers coating oil droplets which could modulate lipid digestion requires further study.

2.9 Conclusions

Recently, structural changes of protein stabilized oil-in-water emulsions and milk in the gastrointestinal tract have been extensively investigated. Many mysteries have been figured out such as stability of oil droplets, the changes of interfacial properties and the role of bile salts during the digestion (Singh et al., 2009; Golding et al., 2010; Maldonado-Valderrama et al., 2011; Wilde et al., 2011; Singh et al., 2013). The lipid modulation is not easily achieved by designing interfacial layers of emulsions (Singh et al., 2013). A rational design of food structure which can modulate lipid digestion is desired.

As one of the main types of human diet, there are limited studies about the digestion of solid food in the human body or in a simulated gastrointestinal tract as well as behavior of oil droplets incorporated in solid matrix. The disintegration of solid food is a much more complex process than the liquid food. Usually, it would take a longer time to digest the solid food because it needs to be broken down into small particles. The process of disintegration of solid foods from the mouth to the intestine is important for understanding the relationship between food digestion and human health. This would bridge the gap of the relationship between food structure and food digestion in

the human body.

In addition, the food digestion in the human body is a consecutive process from the mouth to the intestine. It is difficult to examine how the food is broken down in the human body or animals because of the technical difficulties and ethic limitations. On the other hand, most *in vitro* studies only focus on one step of the whole digestion process (mouth, stomach or intestine), which can not provide the whole process of the food digestion. Therefore, the oral-gastrointestinal *in vitro* digestion studies are necessary.

Chapter 3 Materials and Methods

3.1 Materials

3.1.1 WPI

WPI 895 was purchased from Fonterra Co-operative Group (Auckland, New Zealand). The protein content is greater than 90% and the moisture content was less than 4.5% (Specification of WPI 895, Fonterra).

3.1.2 Soybean oil

Refined soybean oil was purchased from Davis Trading Company, Palmerston North, New Zealand. It contains tert-butylhydroquinone (TBHQ) and butylated hydroxyanisole (BHA) as anti-oxidants and polydimethylsiloxane (PDMS) as an antifoaming agent. Soybean oil was used without any further purification.

3.1.3 Chemicals

Milli-Q grade water (Milli-pore Corp., Bedford, MA, USA) was used for all experiments, except when making samples for the mastication studies, when food grade de-ionized water was used. Food grade de-ionized water was obtained from the Food Pilot Plant, Massey University, Palmerston North, New Zealand. Hydrochloric acid and sodium chloride were purchased from Merck Millipore (Darmstadt, Germany). Sodium bicarbonate was purchased from Avantor Performance Materials (Center valley, PA, USA). Sodium phosphate monobasic was purchased from Ajax Finechem Pty Limited (Sydney, Australia). Potassium chloride, potassium thiocyanate, sodium hydroxide, β-mercaptoethanal (β-ME), dithiothreitol (DTT), sodium dodecyl sulphate (SDS), Nile red (#71485), fast green FCF (#7252) dimethyl sulfoxide, and sodium azide were purchased from Sigma-Aldrich (St. Louis, MO, USA). The gel electrophoresis reagents were

obtained from Sigma-Aldrich (St. Louis, MO, USA). Precision plus protein unstained standards (#161-0363) were purchased from Bio-rad laboratories (Hercules, CA, USA). All chemicals were of analytical grade except the milli-Q and de-ionized water, hydrochloric acid and protein standards for gel electrophoresis.

3.1.4 Enzymes

Pepsin from porcine gastric mucosa (0.7 FIP U/mg) (#1071850100) was purchased from Merck Millipore (Darmstadt, Germany). Pancreatin (#P8096) (1 USP) was purchased from Sigma-Aldrich (St. Louis, MO, USA). Amano Lipase A from Aspergillus niger (≥ 12 000 U/g) (#534781) was purchased from Sigma-Aldrich (St. Louis, MO, USA). Bile extract from porcine (#B8631) (complex mixtures of bile acids and bile acid conjugates) was purchased from Sigma-Aldrich (St. Louis, MO, USA).

3.1.5 Artificial saliva

Artificial saliva (pH 6.8) contained 0.024 mol/L KCl, 0.002 mol/L KSCN, 0.008 mol/L NaH_2PO4, 0.004 mol/L Na_2SO_4, 0.005 mol/L NaCl, and 0.02 mol/L $NaHCO_3$. (Versantvoort et al., 2005). The pH was adjusted to 6.8 with 1 N HCl/NaOH.

3.1.6 Simulated gastric fluid (SGF)

SGF was prepared by adding 3.8 mL of 37% HCl and 8.775 g of NaCl to 500 mL of water and then making up to 1 L with Milli-Q water; 3 g of pepsin was added to this solution before use, with stirring for 30 min, and then the pH of the SGF was adjusted to 1.5 using 1 M HCl/NaOH (Kong & Singh, 2010). The SGF contained 3 g/L pepsin unless otherwise specified.

3.1.7 Simulated intestinal fluid (SIF)

SIF contained 150 mM/L NaCl, 8 mM/L KCl, 10 mM/L $CaCl_2$, 5 mg/L bile extract and 6.4 mg/L pancreatin (Sarkar et al., 2010a; Ye et al., 2013). The pH of SIF is

7.0.

3.2 Methods

3.2.1 Protein solution preparation

Proteins were prepared by adding 200 g WPI powder (small quantities were added each time) to 1400 g water and the dispersion was stirred for about 6 hours until completely dissolved at room temperature.

3.2.2 Emulsion preparation

Pre-emulsions containing 10 wt% WPI and 20 wt% soybean oil were prepared using a high-speed mechanical mixer (L5M, Silverson, Massachusetts, USA) at 9, 000 rpm for 3 minutes. The $D_{4,3}$ of the pre-emulsions was ~ 12 μm. These pre-emulsions were then homogenized using 4 passes through a two-stage valve homogenizer (APV 2000, Albertslund, Denmark) operated at different pressures for the first-stage and the second-stage (300/25, 100/10, 0/10 bars for the emulsions with the $D_{4,3}$ of ~ 0.45, 1 and 6 μm, respectively) (Ye et al., 2009). The stock emulsions, except food grade emulsions, contained 0.02% sodium azide and were stored at 4 °C until further use.

3.2.3 Emulsion gel preparation

The required quantities of solid NaCl were added to the emulsion solutions to give final concentrations of 10, 25, 100 or 200 mM (Ikeda et al., 2002; Pouzot et al., 2005; Mehalebi et al., 2008a; Ako et al., 2009). The solutions were gently stirred to allow the NaCl to completely dissolve. The emulsions were then put in sealed plastic cylindrical containers (inner diameter: 25 mm) and were heated in a water bath from 30 to 90 °C and held at 90 °C for 30 min. After heating, the gels were cooled at 4 °C refrigerator. Before each experiment, the gels were prepared freshly. The gels containing 10, 25, 100 and 200 mM NaCl were prepared using the emulsion with $D_{4,3}$ of ~ 0.45 μm

(Chapter 4). The gels containing 10 (soft gel) and 200 mM (hard gel) NaCl were prepared using the emulsion with $D_{4,3}$ of ~ 0.45 μm (Chapters 5-8). The gels containing 100 mM NaCl were prepared using the emulsion with $D_{4,3}$ of ~ 1, 6 and 12 μm, respectively (Chapter 7).

3.2.4 Small strain oscillatory rheology

The behaviour of polymer materials is usually discussed in terms of two particular types of ideal materials: the elastic solid and viscous liquid. The deformation of elastic solid (response to force) obeys Hooke's law-i.e. stress is proportional to strain. By contrast, the flow of a viscous liquid (i.e. response to force) obeys Newton's law of viscosity-i.e. stress is proportional to strain rate (Barnes, 2000). Natural materials display the intermediate range of properties (viscoelasticity) between an elastic solid and viscous liquid (Ward & Sweeney, 2012). Dynamic oscillatory testing is particularly suitable for testing linear viscoelasticity of polymer materials at sufficiently small deformations which do not affect material properties. The shear strain between times 0 and t is defined as $\gamma(0,t) = \int_0^t \dot{\gamma}\,(t)dt$ at linear viscoelasticity region. The shear strain and shear rate are given respectively by

$$\gamma(0,t) = \gamma^0 \sin \omega t \cdots\cdots\cdots\cdots \text{Eqn 3-1}$$

$$\dot{\gamma}\,(0,t) = \gamma^0 \omega \cos \omega t = \dot{\gamma}^{\,0} \cos \omega t \cdots\cdots\cdots \text{Eqn 3-2}$$

where γ^0 and $\dot{\gamma}^{\,0}$ are the amplitudes of the oscillatory shear strain and shear rate respectively and ω is the frequency of oscillation (Bird et al., 1987). Fig. 3-1 qualitatively presents the stress response to applied shear strain. Equation 3-1 can be re-written as:

$$\tau = -A(\omega)\gamma^0 \sin(\omega t + \delta) = -G'(\omega)\gamma^0 \sin \omega t - G''(\omega)\gamma^0 \cos \omega t \cdots\cdots\cdots \text{Eqn 3-3}$$

where ($0 \leq \delta \leq \frac{\pi}{2}$), τ is the shear stress, G' is shear storage modulus (stored in the material)

and $G''$is shear loss modulus (dissipated). G' of a purely elastic solid is equal to the constant shear modulus G, and G'' is zero. Then we can easily obtain:

$$A(\omega) = \sqrt{G'^2 + G''^2} = G^*, \tan\delta = \frac{G''}{G'} \cdots\cdots\cdots \text{Eqn 3-4}$$

where G^* is complex modulus (Bird et al., 1987).

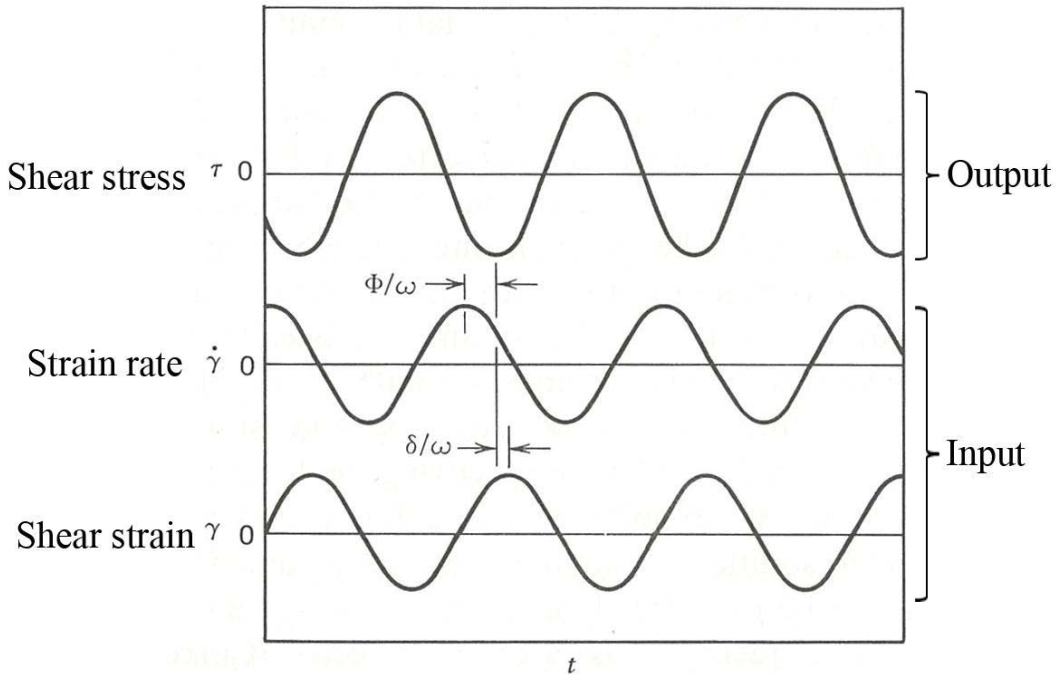

Figure 3-1 Oscillatory shear strain (γ), shear rate ($\dot{\gamma}$) and shear stress (τ). The shear strain, rate and stress oscillate with frequency ω. [Adapted from (Bird et al., 1987)].

A set of material functions (G' and G") are used to describe the elastic and viscous properties of materials respectively. The emulsion was carefully poured into the cup and covered with a thin layer of low-viscosity silicone oil to prevent evaporation. Heat-set gelation was induced *in situ* by (1) heating the sample at a constant rate of 3 °C/min from 30 to 90 °C, (2) holding at 90 °C for 30 min, (3) cooling at a rate of 1 °C/min from 90 to 30 °C, and (4) holding at 30 °C for 20 min. The shear storage and loss moduli were monitored as a function of time (s). All measurements were made in the linear viscoelastic region (0.5% strain) and at a constant frequency of 1 Hz. All experiments (both sample preparation and rheological measurements) were performed in triplicate.

3.2.5 Large deformation properties of gels

The properties of gels at large strains reflect the changes of structures during deformation (e.g. orientation or rearrangement of molecules in response to the deformation forces, breakage of gel structures, etc.) (Vincent, 2012). These properties can be related to the breakdown properties of gels in the mouth (Foegeding et al., 2011).

3.2.5.1 Compression test

The cylinder samples (20 mm in height and 25 mm in diameter) were compressed between two flat plates using a TA-XT2 texture analyser (TA instruments, Delaware, USA). Compression was performed up to a strain of 50%, with the test and post-test speed of 2 mm s^{-1} and automatic trigger force of 0.1 N. The 50% compression strain was chosen to avoid gel fracture. The force at the target strain was defined as the hardness of gels. The work to compress the gel to target strain (W_c) and recoverable work during decompression of the gel (W_d) were calculated from area under the force versus time curves. The recoverable energy (Re) was expressed as:

$$Re = \frac{W_d}{W_c} \cdots\cdots\cdots \text{Eqn 3-5}$$

The Young's modulus was calculated from the slope of the force-time curve in the linear region.

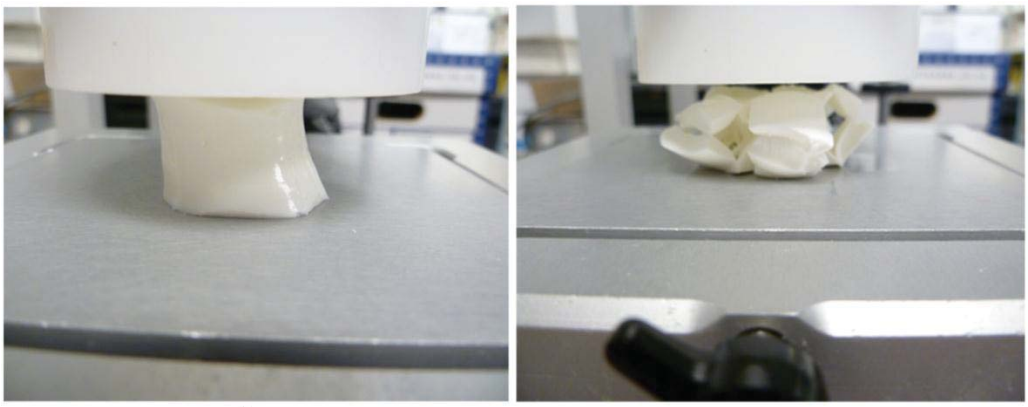

A B

Figure 3-2 Photographs of whey protein emulsion gels (A: 10 mM and B: 200 mM NaCl) during compression by the texture analyzer.

3.2.5.2 Cutting test

Another large deformation test was performed using the fracture wedge set where the angle of two wedges was 30°. The dimensions for the samples for this test were 16×16×25mm width, height and length, respectively. The cutting test was performed to a strain of 95% with the test speed of 2 mm s^{-1} and the trigger force set to 0.05 N. The fracture force and strain of gels were recorded. The toughness (energy for one unit new area crack) was estimated from the force-time curve according to methods of Agrawal et al. (1997) and Lucas & Pereira (1990). All tests were carried out at room temperature with at least 10 replicates.

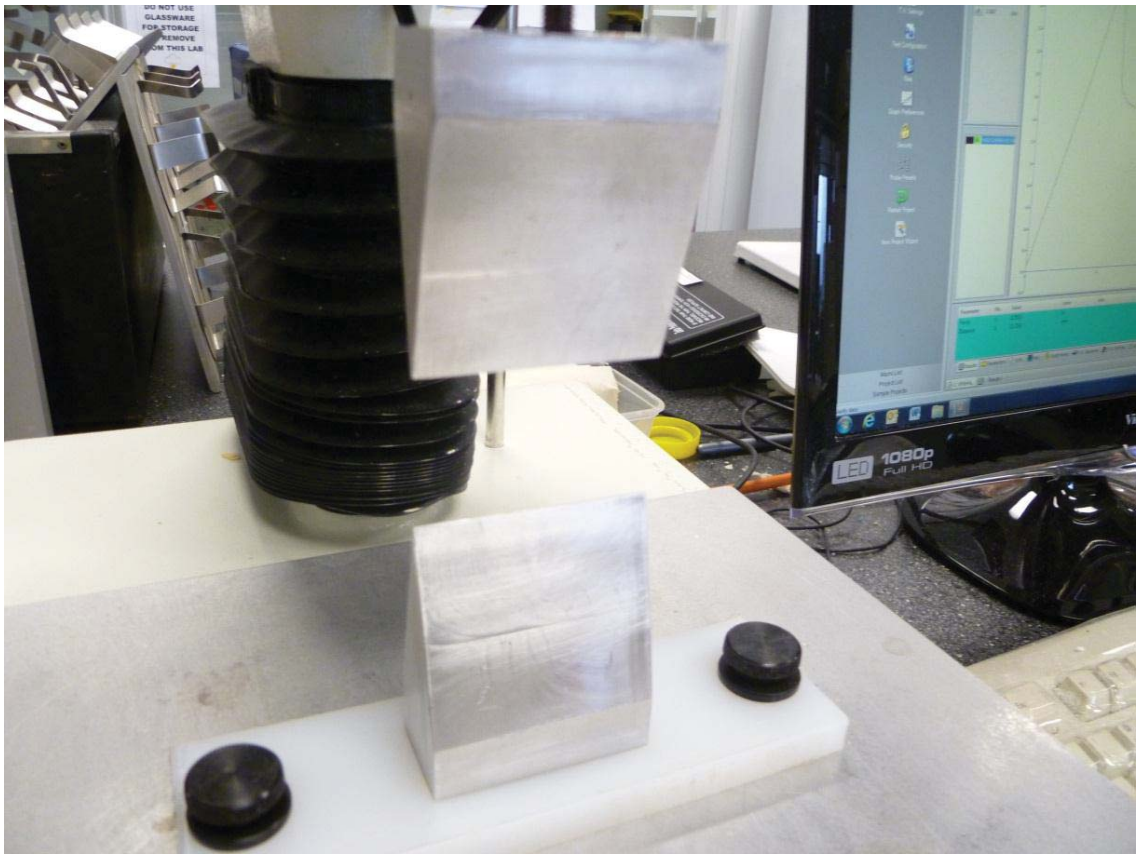

Figure 3-3 Image depicting the fracture wedge set geometry.

3.2.6 *In vivo* oral processing

3.2.6.1 Selection of panellists

The chewing study was approved by the Massey University Human Ethics

Committee: Southern A (Application 11/60). Eight subjects (4 males and 4 females) aged from 18-50 were selected for this study. Subject selection was based on strict dental criteria. Dental screening involves selecting only subjects with neutrocclusion, no significant tooth crowning, no obvious tooth decay, and a healthy periodontal condition; they have no functional disturbance of mastication evidenced by pain or clicking during chewing, and no other known oral or general health problems that could influence chewing; they are not smokers (Hutchings et al., 2011).

3.2.6.2 Mastication experimental procedure

Emulsion gels were prepared and stored in individual sample containers. Each container contained one sample of a single gel type (about 5 g). Subjects were given different containers randomly with an additional empty 60 ml plastic screw-cap container and 30 ml water per each sample. Pre-training was provided to the panellists to enable them to become familiar with the samples. Prior to chewing the gel samples, panellists were asked to rinse their mouth with water (3×30 ml). The panellists were given a sample and asked to chew the sample for as long as necessary and expectorate into the empty container provided before they felt the impulse to swallow. Once the panellist had expectorated the sample, they were asked to rinse their mouth with a further 30 ml of water and the debris was collected into another container. The chew duration and the number of chews for each sample were recorded.

Samples were collected from several sessions for analysing size distributions of fragments in masticated gel and mastication parameters, microstructure of bolus, oil droplet release from the protein matrix, and particle size distributions of oil droplets in the masticated gels.

3.2.7 *In vitro* oral processing

A grinder (MultiGrinder II EM0405, Sunbeam, Australia) was used to mimic oral breakdown and to prepare simulated gel boluses with similar size distributions to human gel boluses. The gels were cut into cylinders with the diameter of 25 mm and the height of 20 mm and then put vertically into the grinder. The gel containing 10 mM NaCl and ~ 0.45 μm oil droplets were ground for 1 s. The gel containing 200 mM NaCl and ~ 0.45 μm oil droplets was ground for 1 s, then the gel pieces were mixed and the samples were ground another 1 s. The gel containing 100 mM NaCl and ~ 12 μm oil droplets were ground for 1 s, whereas the gels containing 100 mM NaCl and ~1 or 6 μm droplets were ground for 1 s, then the gel pieces were mixed and ground for another 1 s. The grinding experiments were carried out at room temperature. Simulated boluses of the two types of gel were prepared by mixing 200 g of ground gel and 40 mL of artificial saliva (saliva secretion rate: ~ 0.2 mL/g) and warming at 37 °C for 2 min (Gavião et al., 2004).

3.2.8 Measurement of masticated gel or *in vitro* gel bolus

The wet sieving analysis was used to determine the size distributions of fragments within bolus.

Method 1 (Chapters 4, 5, 6 and 8)

The collected masticated gels (bolus and debris) or *in vitro* gel boluses were poured in a stack of sieves (mesh size: 0.038, 0.425, 0.85, 1.40, 2.00 and 3.15 mm). The sample retained in each sieve was washed in turn for at least 2 min using mild running water and washing bottle with gentle shaking. Any particles finer than 0.038 mm were discarded because of the difficulty of quantifying such small samples (< 5% of total particles). The fragments retained in each sieve were washed off the sieves and transferred to pre-weighed and pre-dried filter papers. The filter papers with gel

fragments were dried in an oven at 105 °C for 24 hours and then weighed. The weight of dry matter retained in each sieve was expressed as a percentage of the dry weight of collected samples in all sieves. The cumulative weight % of fragments passing each sieve was then calculated and the mean particle size distribution of each type of samples of every panelist was also determined (n = 2) and the median size was extracted from the curves.

Method 2 (Chapter 7)

The masticated gel (bolus and debris) from each subject was sieved by a stack of sieves (mesh size: 0.038, 0.425, 0.85, 1.40, 2.00 and 3.15 mm). It was difficult to collect and weigh the particles passing through the sieve of 0.0380 mm. Therefore, the weight of gel particles passing through the 0.038 mm sieve was estimated from the ratio of area of particles < 0.038 mm and particles > 0.038 mm in the particle size distributions measured by a Mastersizer 2000 (Malvern Instruments, Worcestershire, UK) of gel fragments passing through a sieve with the aperture of 0.85 mm (weight of gel particles > 0.038 mm known by sieving analysis). The weight of dry matter retained in each sieve and that smaller than 0.038 mm were expressed as a percentage of the whole dry weight.

The simulated gel bolus (200 g gel and 40 g artificial saliva) was sieved using a stack of sieves (0.425, 0.850, 1.40 and 2.00 mm). The dry weight of particle retained in each sieve was obtained. The dry weight of particles finer than 0.425 mm was calculated from the dry weight of the ingested gel minus the sum of the weights of dry matter retained in each sieve. The dry weights of particles (> 2.00, 1.40−2.00, 0.850−1.40, 0.425−0.850 and < 0.425 mm) were expressed as a percentage of the dry weight of the whole ingested gel.

The particle size distributions were expressed as the cumulative weight (%) of gel particles passing through a sieve as a function of the sieve mesh size and the median size was extracted from the curves.

3.2.9 Quantification of released oil droplets

Oil droplet release during *in vivo* and *in vitro* oral processing was measured by centrifugation. The masticated gels including gel bolus and debris from subjects or *in vitro* gel bolus (40 g as gel) were put in tubes and centrifuged at 2000 g for 20 min. After centrifugation, the tubes were frozen at -20 °C and the top oil layer was cut off. The oil phase was thawed and put back into a tube (diameter: 15 mm) before further centrifugation after which the height of oil layer was measured after centrifugation (4500 g); this gives the extent of oil droplet release.

3.2.10 *In vitro* gastric digestion

3.2.10.1 Human gastric simulator (HGS)

HGS was used for gastric digestion as shown in Fig. 3-4A which was designed by Kong & Singh (2010). The driving system of the HGS, consisting of 12 rollers, 4 belts, driving shafts, and pulley system, was installed to create peristaltic contractions on 4 sides of the latex stomach chamber. The rollers were bonded onto belts, which were distributed equally on four sides of the stomach. Each roller consisted of two side wheels of 9 mm length and 12 mm apart. Each belt (length: 81 cm) was spaced equally apart by 3 rollers. A pair of opposite rollers was placed 30 mm higher than the relative pair on the other side. The gap between two opposite rollers was 10 mm when they contracted. A stomach chamber (latex) was placed vertically inside the machine with a plastic tube connecting the chamber bottom to the outside for controlled emptying of gastric contents. A thin polyester mesh bag (pore size ~ 1 mm) was placed inside the

latex stomach chamber (Fig. 3-4B) to mimic human gastric sieving, which allows only particles of < ~ 1 mm to pass through to the duodenum in the human stomach (in this case, released at the bottom) (Meyer et al., 1976; Schulze, 2006). The simulated gel bolus (200 g mixed with 40 mL of artificial saliva) was placed in the HGS and left to equilibrate to 37 °C for 2 min. Before digestion, 70 mL of SGF containing pepsin was loaded to mimic the condition in which the stomach holds a certain amount of gastric juice during fasting. On account of the lag phase of solid foods, emptying was started after 30 min (Siegel et al., 1988; Urbain et al., 1989). Then, 45 mL gastric contents were removed from the bottom of the stomach manually every 15 min, equalling the gastric emptying rate of 3.0 mL/min (Kong et al., 2010). The contraction frequency was 3 times/min, simulating the actual stomach contraction. The temperature of the HGS was maintained at 37 °C by a heater and thermostat. The digestion time was 300 min. Figure 3-4C describes the process of grinding of solids in the HGS. In step 1, rollers descend and the gap between the opposite rollers becomes increasingly smaller. In step 2, the solid particles are disintegrated by the physical forces induced to the digesta by the contractive activity of the opposite roller as they approach the terminal region of the stomach chamber. In step 3, the contraction ends. During the emptying process, only particles small enough to go through the 1 mm mesh bag were emptied. To investigate the mechanical disintegration of the gels, experiments using SGF without the addition of pepsin were carried out.

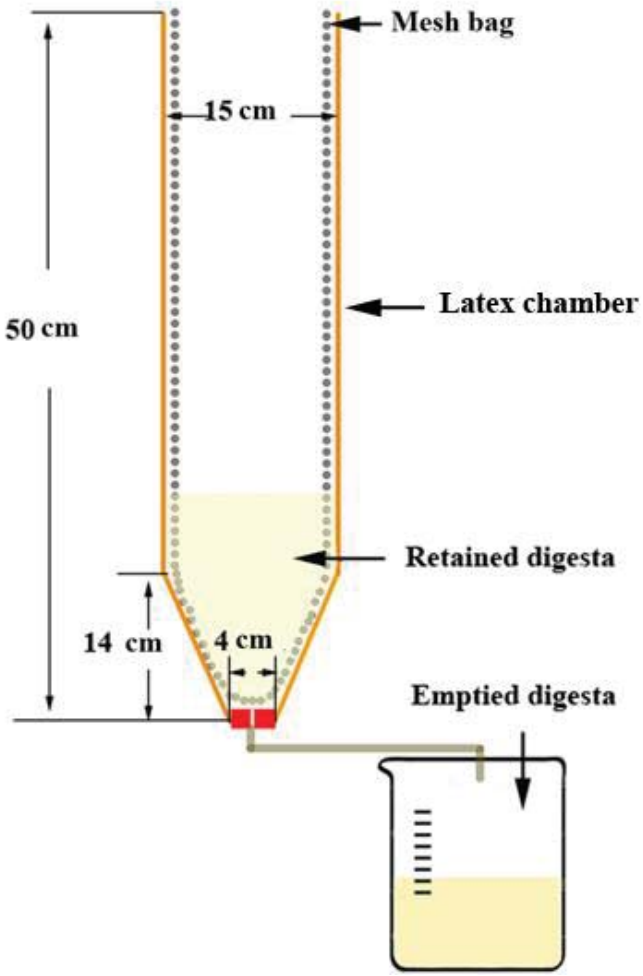

Figure 3-4 continued

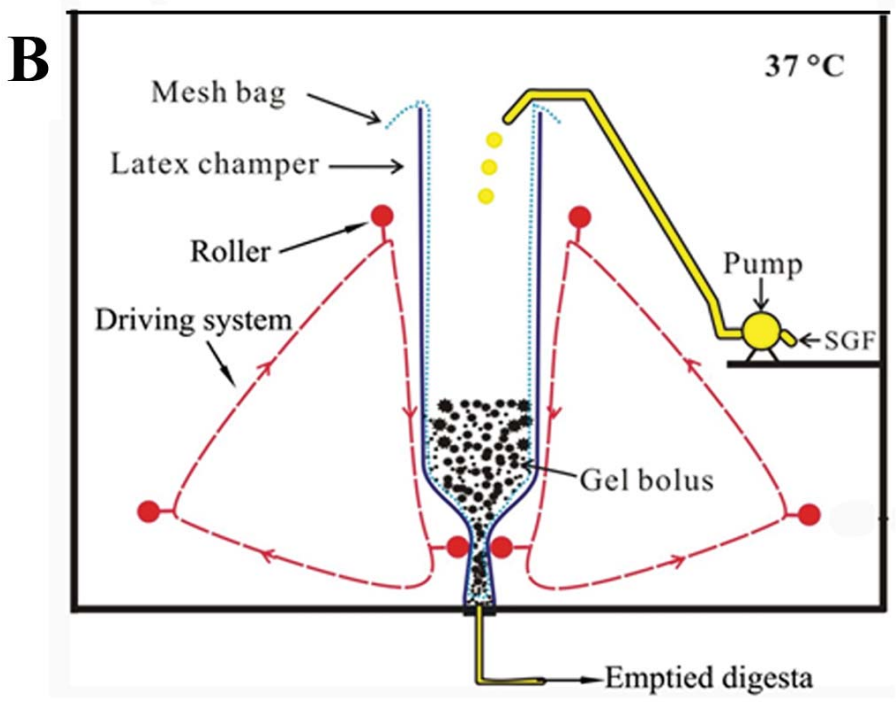

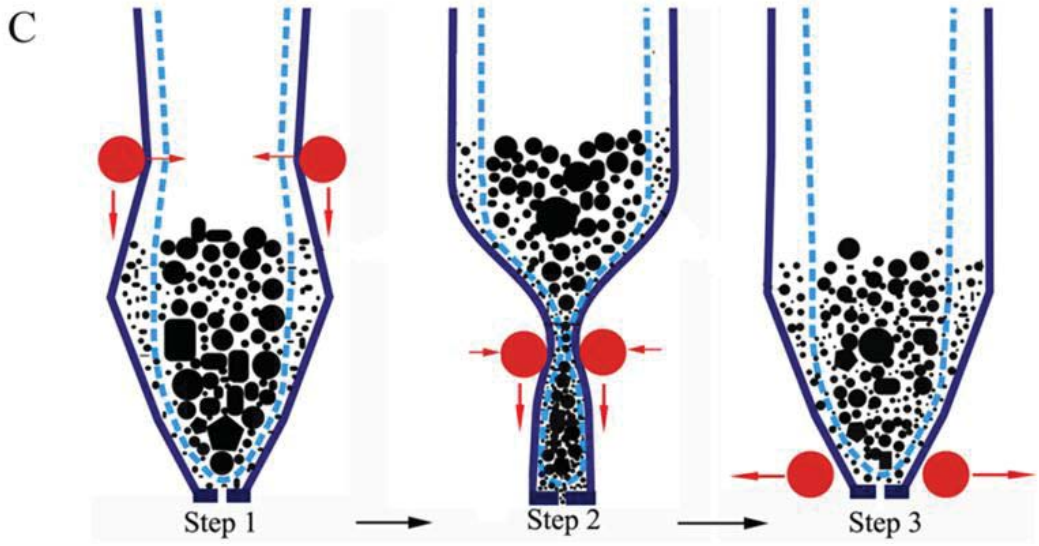

Figure 3-4 Image of an HGS and illustration of latex stomach chamber (A), (1) SGF; (2) plastic tubes for secretion; (3) pump; (4) latex chamber; (5) mesh bag; (6) roller; (7) belt; (8) pulley; (9) shaft; (10) angle gear; (11) Love-Joy joint; (12) fan heater for temperature control. Illustration of the human gastric simulator (B). The schematic diagram of grinding of solids in one sequence of contraction of the HGS (C).

3.2.10.2 Gel swelling

Gel sample (3 g and 5 mm thickness) was placed in 40 ml simulated gastric fluid (SGF) without added pepsin. Experiments were carried out at 37 °C. The gels were taken out of the solution after 1, 2, 3, 4, 5 and 20 h incubation respectively and excess water was removed by gently blotting with a tissue paper and the mass of the gel was recorded. Swelling ratio (SR) was calculated using the following expression:

$$SR= (W_t - W_0) / W_0, \quad \text{Eqn 3-6}$$

where W_t denotes the weight of the gel at time t and W_0 is the initial weight of the gel.1 Experiments were replicated 6 times.

3.2.10.3 Gastric emptying

Method 1 (Chapters 5 and 6):

The digesta, which were emptied at different digestion times, were dried in an oven for 24 h and the mass of dried digesta (X) was determined. In addition, a control experiment using 200 g of water as sample was done to calculate the dry matter of SGF retained in each digesta (Y). The actual dry weight of gel particles in the digesta emptied at different times was determined by subtracting Y from X. Then the solid content of the emptied digesta only, including gel particles, and the percentage of the gel bolus emptied out of the HGS after 300 min of digestion were calculated. The cumulative dry weight of the gel emptied out of the stomach at different times was calculated. The gastric retention percentage was calculated as:

$$y(t)=(W_0-W_t)/W_0, \quad \text{Eqn 3-7}$$

where y(t) is the fractional gel retention at time t, W_0 is the initial dry weight (g) of gel and W_t (g) is the cumulative dry weight of emptied gel at time t.

Method 2 (Chapter 7):

The digesta emptied at 45, 60, 75, 90, 105, ⋯, 285 and 300 min during the trial was dried in an oven for 24 h and the mass of each dried digesta (X) was weighed. Then the cumulative dry weight of solids emptied out of the HGS at different times was calculated. The gel retention, represented by the solid retention in the HGS was calculated as: $y(t)=(W_0-W_t)/W_0$, where y(t) is the fractional gel retention at time t, W_0 is the sum of dry weight (g) of solids (gel, salts and pepsin, 68.9 g) and W_t is the cumulative dry weight (g) of emptied digesta at time t.

Modelling emptying of gels from the HGS

The gel retention data were fitted into a power exponential model proposed by Siegel et al. (1988) to describe the biphasic nature (i.e. existence of lag phase) of the retention of solid meals in the human stomach:

$$y(t) = 1 - (1 - e^{-\kappa t})^{\beta}, \quad \cdots\cdots\cdots\cdots\cdots\cdots \text{Eqn 3-8}$$

where κ (1/min) is associated with the emptying rate. β is a shape parameter and a value of β>1 indicates an initial delay in emptying while a value of β <1 indicates an initial rapid emptying (Siegel et al., 1988). The time period of the lag phase (T_{lag}) was defined as the time during which the first 5 wt% of the initial mass of the gel bolus is emptied from the HGS. T_{half} was defined as the time of which 50 wt% of the initial mass of the gel bolus is emptied from the HGS (Tougas et al., 2000).

In addition, the digesta in the stomach after the 300 min digestion period was immediately put into a beaker to test whether an oil layer formed on the top.

3.2.10.4 pH measurement

The pH profile in the HGS was measured as follows. The initial pH in the HGS was defined as the pH of the simulated gel bolus mixture (200 g gel and 40 mL artificial saliva) and 70 mL SGF. With ingestion of SGF (2.5 mL/min) and gastric emptying (3

mL/min), the pH in the HGS at different times was represented by the pH of the emptied digesta, because the set-up (roller contraction) prevented easy access into the HGS. At 15 and 30 min, the digesta (6 mL) were returned to the HGS immediately after pH measurement, because gastric emptying started after 30 min.

3.2.10.5 Photos of emptied gastric digesta

Every emptied digesta was collected into the 50 mL plastic tubes, and immediately put into the boiling water for 5 min to inactivate the pepsin. Then the tubes were kept for 2 hours before an image was captured using a camera.

3.2.10.6 Measurement of gel disintegration

The particle size distributions of the combined digesta (i.e. the cumulative emptied digesta and the digesta retained in the HGS) at 0, 30, 60, 120, 180, 240 and 300 min were measured by the wet sieving analysis. The digesta were sieved by a stack of sieves (2.00, 1.40, 0.850 and 0.425 mm). The digesta retained in each sieve was washed carefully using running water. The particles retained in each sieve were washed off and transferred to pre-weighed and pre-dried filter papers. The dry weight of emptying particles smaller than 0.425 mm was calculated by subtracting the cumulative dry weight of particles retained in each sieve from the dry weight of initial gel (200 g gel). The dry weight of particles (> 2.00 mm, 1.40-2.00 mm, 0.850-1.40, 0.425-0.850 mm and < 0.425 mm) was expressed as a percentage of the dry weight of the initial gel. The cumulative particle size distributions of the digesta were calculated and the median size (D_{50}) was extracted from the curves.

The Weibull distribution function is widely used to describe the dissolution profiles of tablets during *in vitro* analysis.(Costa & Sousa Lobo, 2001; Dokoumetzidis et al., 2006; Papadopoulou et al., 2006). Although this is an empirical model, much *in vitro* experimental evidence for the successful use of the Weilbull function in drug/food

release has been provided (Papadopoulou et al., 2006; Kong & Singh, 2011). As part of this study, the Weibull distribution function was used to predict the progressive disintegration of gels in the HGS as given by the relative change of its D_{50} value:

$$F(t) = \frac{\Delta D_{50}}{D_{50}(0)} = \frac{D_{50}(0) - D_{50}(t)}{D_{50}(0)} = 1 - e^{-(\lambda t)^{\theta}}, \cdots\cdots\cdots\text{Eqn 3-9}$$

where $F(t)\geq 0, t\geq 0$ (digestion time), λ (> 0) defines the time scale (1/min) of the process which is associated with the disintegration rate (disintegration rate increases with λ), and θ (>0) is the shape parameter that characterizes the shape of curves (θ≤1: a parabola-like shaped curve whose slope decreases monotonically and θ>1: an S-shaped curve whose slope first increases and then decreases) (Langenbucher, 1972; Costa et al., 2001). θ≤1indicates an initially rapid decrease of D_{50} while a value of θ>1 indicates an initially delayed decrease. An equation for $D_{50}(t)$ is easily obtained:

$$D_{50}(t) = D_{50}(0)e^{-(\lambda t)^{\theta}} \cdots\cdots\cdots\text{Eqn 3-10}$$

T_{50} is defined as the time taken to decrease the initial median size of the gel bolus by 50% (i.e. $D_{50}(t = T_{50}) = \frac{D_{50}(0)}{2}$).

3.2.11 *In vitro* intestinal digestion

The gastric digesta emptied at 60 and 240 min of the soft and hard gels was used for *in vitro* intestinal digestion. The pH of gastric digesta (60 and 240 min) was adjusted to 7.0 using 1 M NaOH/$NaHCO_3$ immediately after emptying from the HGS. Then *in vitro* intestinal digestion was carried out. 20 mL gastric digesta was mixed with 40 mL SIF; calcium was mixed with digesta first and then mixed with SIF without added calcium to avoid the precipitation of calcium and bile salts. The mixture was put into a conical flask and incubated in a 37 ºC water bath with a constant shaking rate of 95 rev/min. The whole digestion lasted for 150 min.

3.2.12 Measurement of free fatty acid release

The pH of 20 mL gastric digesta emptied at 60 and 240 min was adjusted to 7.0 and then immediately mixed with 40 mL SIF. Then 40 mL mixture of digesta was immediately added into the cell of pH stat for testing fatty acid release. The test was run over 2.5 h using a pH-stat titration method with 0.05 M NaOH and an endpoint of pH 7.0. A blank titration without any pancreatin was carried out. The quantity of fatty acids liberated per mL intestinal digesta was calculated based on the following equation:

$$\frac{\mu mol_{fatty\ acid}}{ml_{reaction\ mixture}} = \frac{\left(volume_{NaOH\ for\ sample} - volume_{NaOH\ for\ blank}\right) \times C \times 1000}{volume_{reaction\ mixture}} \cdots\cdots \text{Eqn 3-11}$$

C is the molar concentration of the NaOH titrant (0.05 M).

The initial lipolysis rate ($\mu mol \cdot mL^{-1} \cdot min^{-1}$) was calculated as the free fatty acids release per 1 mL intestinal digesta per minute during the initial 2.5 min of reaction.

The quantity of fatty acids liberated per gram gel was calculated based on the following equation:

$$\frac{\mu mol_{fatty\ acid}}{g_{gel}} = \frac{\left(volume_{NaOH\ for\ sample} - volume_{NaOH\ for\ blank}\right) \times C \times 1000}{Weight_{gel}} \cdots\cdots\cdots \text{Eqn 3-12}$$

C is the molar concentration of the NaOH titrant (0.05 M).

3.2.13 Particle size characterization by laser diffraction

The principle of laser diffraction, also called static light scattering, is the detection of diffracted light. During the laser diffraction measurement, particles are passed through a focused laser beam. Smaller particles scatter light of a lower intensity to larger angles, while the larger particles scatter light of the relatively stronger intensity toward smaller angles (Desroches et al., 2005). The angular intensity of the scattered light is then measured by a series of photosensitive detectors.

A short wavelength blue light source (470 nm) is used in conjunction with forward and

backscatter detection for enhanced small particles sizing. This, combined with red-light measurements (632.8 nm) for larger particles sizing, provides superior sensitivity across a wide size range (0.02 to 2000 μm). The droplet size distribution, which gives the best statistical fit between the measurements of intensity versus scattering angle and those predicted by Mie theory, is then calculated. The droplet size distribution was reported as the Sauter-average diameter, $D_{3,2}$ (μm) and the volme-weighted average diameter $D_{4,3}$ (μm) respectively the expressions of which are given below:

$$D_{3,2} = \sum \frac{n_i d_i^3}{n_i d_i^2} \cdots\cdots\cdots\cdots\cdots \text{Eqn 3-13}$$

$$D_{4,3} = \sum \frac{n_i d_i^4}{n_i d_i^3} \cdots\cdots\cdots\cdots\cdots \text{Eqn 3-14}$$

where n_i is the number of particles with diameter of d_i.

Method 1 (particle size distribution of gastric digesta and intestinal digesta):

Particle size distributions of gastric digesta emptied through the mesh bag at 30, 60, 90, 120, 150, 180, 210, 240, 270 and 300 min were measured immediately by a Mastersizer (Malvern Instruments, Worcestershire, UK). The refractive index of the gastric digesta of the whey protein emulsion gel was set as 1.47 equaling to that of whey protein-stabilized emulsion (Ye et al., 2009) because it is difficult to define a refractive index of the gel particles (containing a high level of protein) digested for different times. The $D_{4,3}$ was reported for the particle size distributions. The method used to determine the particle size distribution of intestinal digesta was the same as that used for the gastric digesta. $D_{4,3}$ and $D_{3,2}$ were reported.

Method 2 (oil droplet size in the emulsion, gel and gels upon oral processing, gastric

digestion and intestinal digestion):

For measurements of the liquid emulsion, 2 mL emulsion was added to 10 mL SDS solution (5 wt%) and gently mixed for a few seconds before the particle size was measured. For measurements of the emulsion gel, 2 g gel was added to 20 ml solution containing SDS (5 wt %) and 2-mercaptoethanol (50 mM) and shaken overnight until totally dissolved. This treatment dissociates the protein network and liberates the fat droplets (2-mercaptoethanol reduces disulfide bonds and SDS disruptes non-covalent bonds). The adsorbed proteins in oil-in-water interface were replaced by SDS. For *in vivo* or *in vitro* gel bolus, SDS and 2-mercaptoethanol were added to the mixture of bolus and debris or *in vitro* gel bolus after oral processing. After the mixture was totally dispersed, the particle size was measured. For measurements of emptied gastric digesta, 5 mL of emptied digesta was mixed with 5 mL of 10% SDS solution and shaken for several seconds. Then, 30 mL water was added to each mixture, which was pH adjusted to 7.5 using 1M NaOH; 100 μL of 2-mercaptoethanol was then added to the mixture, which was shaken in a shaking water bath until the protein aggregates had dissolved totally. Finally, the particle size distributions of oil droplets within the emptied digesta were measured using large volume sample dispersion unit. For measurement of the intestinal digesta,1 mL intestinal digesta was mixed with 2 mL 5 wt% SDS solution. 50 mM 2-mercaptoethanol was then added. The mixture was shaken in a water bath until totally dissolved. The particle size distribution of the oil droplets was measured using an automated small volume sample dispersion unit (Hydro 2000S). The refractive index of oil droplet was 1.47 and that of water was 1.33. Each sample was measured three times at room temperature.

3.2.14 Zeta-potential

Zeta potential (ζ) is specific to a phenomenon (e.g., electrophoresis) which has

units of voltage. Zeta potential is a measure of fluid or particle flow (Kirby, 2010). Theoretically, Zeta potential is the electrokinetic potential in the interfacial electric double layer (EDL) at the location of the slipping plane inside of which the ions and particles or drops form a stable entity during electrophoresis (Fig. 3-5). Zeta potential is greatly affected by the electrolyte concentration and pH. The values of Zeta-potential of emulsion droplets were measured by Doppler velocimetry using a Malvern Zetasizer Nano ZS (ZEN 360) instrument (Malvern Instruments Ltd, Malvern, Worcestershire, UK). The velocity (U) at which emulsion droplets move in the applied electric filed is converted into a Zeta-potential by substituting the known variables in the Henry equation as follow:

$$U_E = \frac{2\varepsilon\zeta f(ka)}{3\eta} \cdots\cdots\cdots\cdots \text{Eqn 3-15}$$

where ε is dielectric constant of the medium, η is the viscosity of the medium and $f(ka)$ is the Henry function taken as 1.5.

Samples were diluted 500 times with background buffer (NaCl solution with different concentrations). The temperature of the electrophoresis cell was maintained at 25°C using a Peltier system. An individual Zeta-potential measurement was calculated from at least 10 readings from an individual sample. All measurements were triplicated.

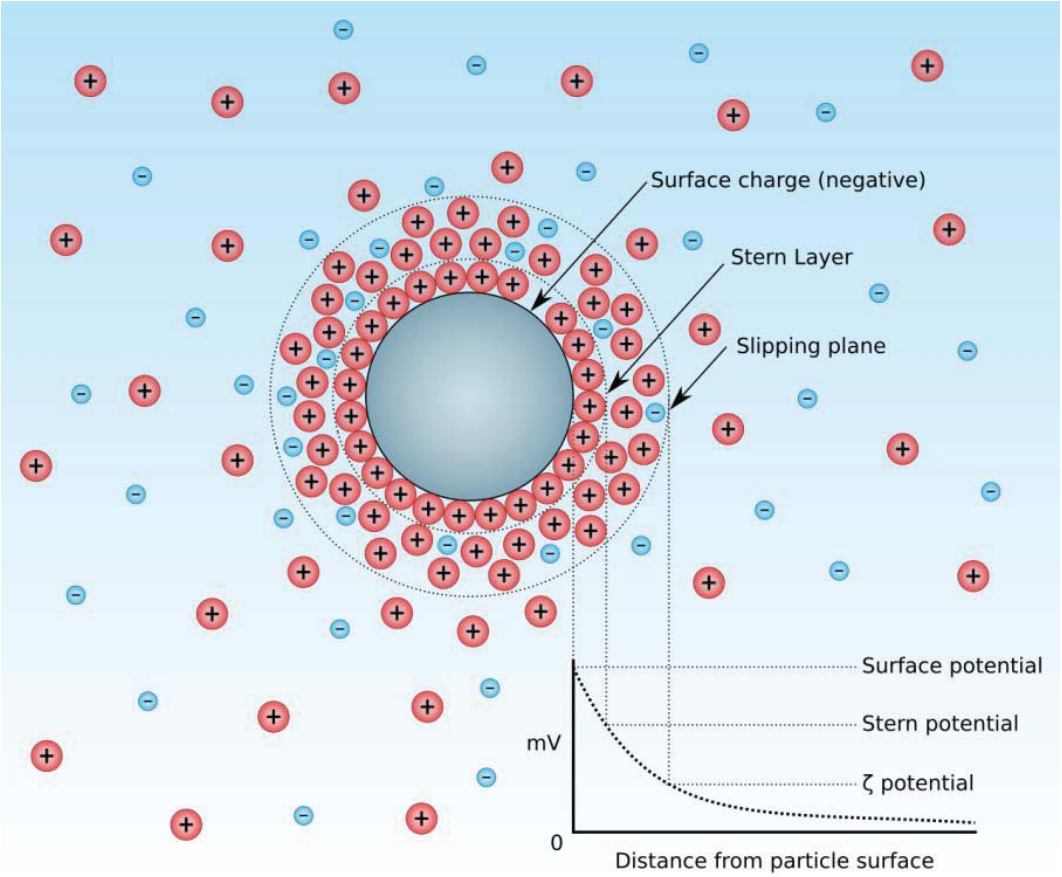

Figure 3-5 Schematic diagram of the zeta-potential of a particle. (Wikipedia contributors, 2014).

3.2.15 Tricine sodium dodecyl sulfate-polyacrylamide gel electrophoresis (SDS-PAGE)

Tricine SDS-PAGE under reducing conditions was used to characterize the proteins. With addition of SDS and β-mercaptoethanal, the secondary, tertiary and quaternary structures were destructed. The different proteins or peptides have a constant charge-mass ratio (1.4 g SDS/1 g protein) and keep the similar shape during electrophoresis (Smith, 1984). Therefore, the migration rate of proteins in gel electrophoresis is strictly determined by the molecular mass of proteins. I followed the methods described by Schägger & von Jagow (1987) and Dave et al. (2013) with some modifications.

3.2.15.1 Preparation of stock solutions

- 20% SDS

20 g SDS was added into 60 mL water. The mixture was stirred until completely dissolved. The mixture was transferred into a volumetric flask (100 mL) with water and made up to 100 mL. The solution was stored at room temperature.

- Acrylamide/bisacrylamide solution

48 g acrylamide and 1.5 g bisacrylamide were added into water and the mixture was stirred until completely dissolved. The mixture was transferred into a volumetric flask (100 mL) and made up to 100 mL with water. The solution was stored at 4 ºC in a dark color bottle up to 1 month.

- Gel buffer (3 M Tris, 0.3% SDS, pH 8.45)

363.342 g Tris and 0.3 mL 20% SDS solution were added into the 80 mL water. The pH of the mixture after complete dissolution was adjusted to 8.45 and then transferred into a 100 mL volumetric flask with water. The solution was stored at 4 ºC up to 1 month.

- Tricine sample buffer (0.2 M Tris, 40% glycerol, 2% SDS, pH 6.8)

20 mL glycerol, 10 mL gel buffer, 5 mL 20% SDS solution and 15 mL water were stirred. Then 20 mg Coomassie Brillant Blue was added into the mixture with stirring until completely dissolved. The solution was stored at room temperature and mixed with β-mercaptoethanal with a ratio of 19:1 (v:v) for reducing conditions.

- 10% Ammonium persulphate

100 mg Ammonium persulphate was added into 1 mL water. The mixture was stirred until completely dissolved. This solution is prepared before each electrophoresis.

- Running buffer (0.1 M Tris, O.1 M tricine, 0.1% SDS, pH 8.3)

12.11 g Tris, 17.92 g tricine and 5 mL 20% SDS were added into 800 mL water. After complete dissolution, the pH was adjusted to 8.3 and the mixture was made up to 1 L. The buffer was stored at 4 ºC.

- Anode buffer (0.2 M Tris, pH 8.9)

24.23 g Tris was added into 800 mL water. The mixture was stirred until completely dissolved and the pH was adjusted to 8.9. Then the mixture was made up to 1 L with water. The buffer was stored at 4 ºC up to 1 month.

- Cathode buffer (0.1 M Tris, 0.1 M tricine, 0.1% SDS, pH 8.25)

12.11 g Tris, 17.92 g tricine and 5 mL 20% SDS were added into 800 mL water. The mixture was stirred until completely dissolved. The mixture was made up to I L using water. The buffer was stored at 4 ºC up to 1 month.

- Staining solution

200 ml and 3 g Coomassie Brilliant Blue R were stirred for 20 min. The 100 mL acetic acid and 700 mL water were added. The solution was filtered twice through the filter paper and stored in a dark bottle at 4 ºC.

- Destaining solution

100 mL acetic acid, 100 mL isopropanol and 800 mL water were stirred for 5 min and stored in room temperature.

3.2.15.2 Gel preparation

- Resolving gel (16 %)

Placed plastic combs (15 wells) completely into the assembled gel cassettes. Marked the glass plates 1 cm below the comb teeth. This is the height to which the resolving gel is poured. 6.5 ml acrylamide/bisacrylamide solution, 6 mL gel buffer, 2g glycerol and water were stirred and degassed for 15 min. Before gel casting, 100 µL ammonium persulphate solution and 10 µL TEMED were added. The solution was

smoothly poured into the glass cassettes to the marked level. The isopropanol was immediately overlaid on the top of solution of resolving gels. The solution was allowed to polymerize at room temperature for 1 hour. The isopropanol was poured off and residual isopropanol was removed by filter paper.

- Stacking gel

1 mL acrylamide/bisacrylamide solution, 3 mL gel buffer and 8.3 mL water were stirred and degassed for 15 min. Before gel casting, 90 μL ammonium persulphate and 9 μL TEMED. The glass cassettes were filler the solution of stacking gel and the combs (15 wells) were placed into the cassettes completely. The solution of stacking gel was allowed to polymerize for 1 L.

3.2.15.3 Sample preparation

Samples (0.2 g) were treated with 1.8 mL of water and 2 mL of tricine sample buffer (0.2 M Tris-HCl buffer, pH 6.8, 40% glycerol, 2% SDS, 0.04% Coomassie Brilliant Blue G-250, β-mercaptoethanol (19:1, v:v)) and were heated in boiling water for 10 min.

3.2.15.4 Running of electrophoresis

The electrophoresis module was assembled firstly. The samples were centrifuged for 20 min at 4200 *g* after they had been cooled to room temperature, and a certain amount of subnatant with the same protein weight for each sample of digesta (different solid contents) was loaded on to tricine gels previously prepared on a Mini-PROTEAN II system (Bio-Rad Laboratories, Richmond, CA, USA). The electrode assemblies were placed in the Mini-PROTEAN Tetra tank. Anode buffer (lower buffer) and the cathode buffer (higher buffer) were added respectively. Voltage was set at 120 V constant. Run time was approximately 1.5 hours.

3.2.15.5 Staining and destaining

The gel was stained for 60 min using a Coomassie Brilliant Blue R-250 solution with gentle shaking. The gel was destained with a solution of 10% acetic acid and 10% isopropanol and scanned using a Molecular Imager Gel Doc XR system (Bio-Rad Laboratories).

Each well was loaded by the similar amount of solids in the emptied digesta in the presence of pepsin (chapter 5 and 7). Each well was loaded by the same amount of digesta in the absence pepsin (chapter 5).

3.2.16 Confocal laser scanning microscopy (CLSM)

CLSM is a breakthrough in the development of high-resolution optical microscopy. Principle of CLSM is presented in Fig. 3-6. A confocal microscopy uses point illumination combined with scanning technique which enhances the resolution of image. Laser only excites the parts of specimen very close to the focal plane, which greatly reduces out-of-focus fluorescence background (Huang et al., 2010). In addition, a narrow pinhole in front of the detector eliminates out-of-focus signal. Dyes of Nile red and fast green were dissolved in dimethyl sulfoxide and water respectively. 0.5 w/v % Nile red was used to stain for oil (Argon laser with an excitation line of 488 nm) while 1.0 w/v% fast green was used to stain for protein (He-Ne laser with an excitation at 633 nm). To enhance the image quality, the sequential scanning was used. A CLSM (Leica, Heidelberg, Germany) was used in this project.

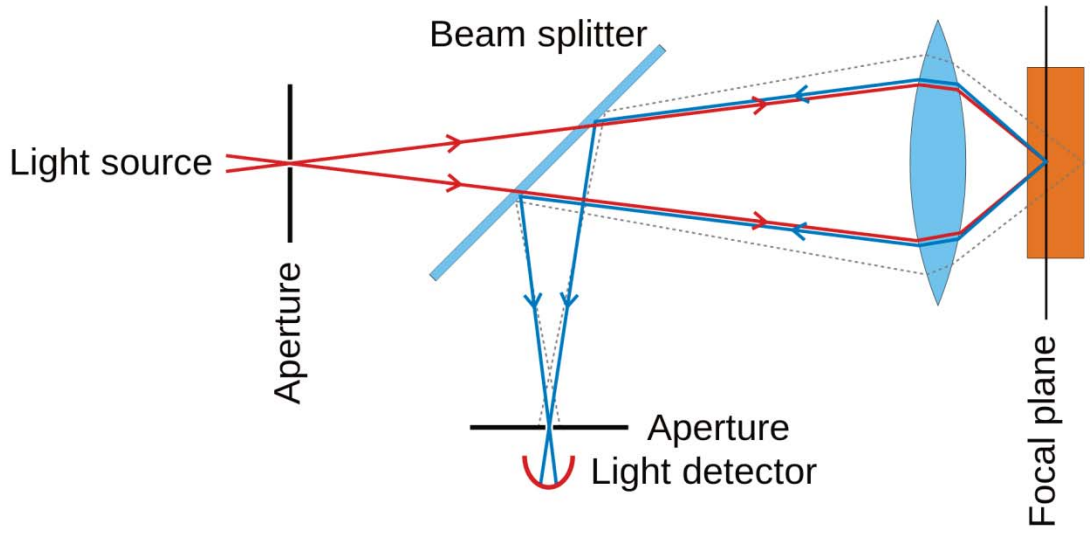

Figure 3-6 Principle of confocal laser scanning microscopy (Wikipedia contributors, 2015).

Method (Chapter 4):

A small quantity of the bolus was placed on a concave confocal microscope slide about 1.5 mm thick, mixed with 10 μl Nile Red and 10 μl Fast Green, stained for 20 min and then covered with a cover slip. The samples were observed using the × 10 len and ×100 oil immersion len. The procedure of detecting the microstructure of emulsion gel before mastication was the same with the exception of allowing the sample to stain for longer time.

Method (Chapter 5):

The pH of the emptied gastric digesta was adjusted to 7.0 using 1 M NaOH/NaHCO3. The digesta were then diluted three times using water. One drop of digesta was placed on a concave confocal microscope slide, mixed with 10 μL of Nile Red and 10 μL of Fast Green, stained for 15 min and then covered with a cover slip. . The samples were observed using the × 40 len and ×100 oil immersion len.

Method (Chapter 7):

The small pieces of original gels were stained for ~ 2 hours in the mixture of dyes (Nile red: Fast Green, 1:1). A small quantity of gel bolus or gastric digesta was placed on a concave confocal microscope slide immediately after the oral or gastric processing, mixed with 12 μL of Nile Red and 12 μL of Fast Green, stained within 15 min and then covered with a cover slip. The samples were observed using the × 10 len and ×100 oil immersion len.

Method (Chapter 8):

The microstructure of emptied gastric digesta (60 and 240 min) was observed using ×100 objective oil len as described in method for Chapter 7. Intestinal digesta was mixed with dyes (Nile red:Fast green, 1:1) immediately after taking out from the *in vitro* intestinal model and was observed with ×40 objective len and ×100 objective oil len.

3.3.17 Transmission light microscopy

CLSM (Leica, Heidelberg, Germany) was used to generate the transmission light (488 nm) which can pass through the specimens. After the light passed through the specimen, the image of the specimen goes through the objective lens and was captured with a photomultiplier tube.

3.3.18 Statistical analysis

The data were analyzed using one-way ANOVA. Means were compared by Duncan multiple-range test at $P < 0.05$ (using SPSS Statistics 21 software).

A Pearson correlation test was also performed to explore the correlation between median diameter (D_{50}) of particles within masticated gels and the fragmentation index of gels ($P < 0.05$).

The trials of gel disintegration and emptying of the gel bolus from the HGS were

performed in triplicate. The fitting of gel retention (y(t)vs.t), the kinetics of gel disintegration (D_{50} (t)vs.t) and relationship between the emptying from the HGS and gel disintegration (y(t) vs. (D_{50} (t))/(D_{50} (0)) by their empirical models was performed using non-linear regression in the SPSS Statistics 23 software. Estimates of parameters were obtained by the Levenberg-Marquardt method. The goodness of fit of models was assessed by the coefficient of determination (R^2). A significance test was conducted using one way analysis of variance in SPSS Statistics 23 software; differences between group means were analyzed by Duncan's multiple range test at a probability level of 0.05.

Chapter 4 Effect of Gel Characteristics on Breakdown Properties of Whey Protein Emulsion Gels in the Human Mouth[1]

4.1 Abstract

Differently structured whey protein emulsion gels were formed by heating and adding different concentrations of NaCl. The formation of gels was also monitored by a rheometer. The large deformation properties relevant to breakdown properties in the human mouth were measured by uniaxial compression test and fracture wedge set test using a texture analyzer. A panel of 8 subjects was used to examine the in-mouth behaviors of gels including mastication parameters, degree of fragmentation and oil droplet release. The results showed that with increased NaCl concentration the gel hardness was increased in general. The gels containing 10 or 25 and 100 or 200 mM NaCl were characterized as being soft and hard, respectively. These soft and hard gels had different breakdown patterns. Sensory experiments showed the soft gels with 10 mM NaCl needed a significantly lower number of chewing cycles (19.4±2.1) compared with gels containing higher NaCl. The values of median size of particles in masticated gels containing 10, 25, 100 and 200 mM NaCl were about 4.00, 2.85, 1.05 and 0.95 mm, respectively, which suggested that higher hardness led to a greater fragmentation degree in the mouth. Furthermore, the fragmentation degree of gel was highly correlated with the mechanical properties. In addition, there was no obvious coalescence of the oil droplets during oral processing and only very few oil droplets were released from protein matrix during mastication.

[1]Part of contents presented in this chapter has been published as a peer-reviewed paper: Guo, Q., Ye, A., Lad, M., Dalgleish, D., & Singh, H. (2013). The breakdown properties of heat-set whey protein emulsion gels in the human mouth. *Food Hydrocolloids, 33*(2), 215-224.

4.2 Introduction

When a food product is consumed, it is exposed to a wide range of physical (e.g. mechanical breakdown and temperature) and biochemical (e.g. dilution effect, pH, enzymes, salts, mucin, etc.) processes in the human mouth, especially for semi-solid or solid foods (Sarkar et al., 2009a; Foegeding et al., 2011). Within the human mouth, a bolus is formed from the mechanical (action of chewing) and biochemical (enzymes and proteins in the saliva) processing enabling safe swallowing of the food. Thus, oral processing leads to particle size reduction, and contributes to the taste and texture of foods (Foegeding et al., 2011). Mechanical breakdown (fragmentation) is the core part of oral processing (Chen, 2009).

The fragmentation degree of a food product is critically dependent on the nature (structural properties) of the food consumed (Agrawal et al., 1997; Lucas et al., 2002). In general, harder foods require more chewing cycles and masticatory force, and probably lead to a higher fragmentation degree during mastication (Chen, 2009). However, foods with the same hardness would probably have totally different fragmentation degrees, which demonstrate the importance of the original structures of the food on the fragmentation process (Peyron et al., 2004; Jalabert-Malbos et al., 2007). Agrawal et al (1997) and Lucas (2002) found the cracking of food in the mouth was highly correlated with mechanical property index: toughness (R) and Young's modulus (E). They first developed the food property indices including $(R/E)^{0.5}$, $(RE)^{0.5}$ and R to reflect the fragmentation degree for different foods. However, there are obvious limitations in their study, i.e. they did not consider the effect of saliva and temperature on mastication and the rate of breakdown of food was obtained only after one chew. Therefore, further work is needed on understanding the relationship between

the true rate of breakdown of food in the human mouth and mechanical properties of foods.

Whey protein emulsion gels have a simple composition and can mimic a real food emulsion. Whey protein emulsion gels provide a systematic way to precisely manipulate the structures and allow systemic investigation of structural factors affecting the breakdown of food materials during oral processing. Therefore, the aim of this work was to explore the effect of different gel structures, induced by NaCl, on the physical/mechanical properties of heat-set whey protein emulsion gels and their breakdown properties in the human mouth. The relationship between physical/mechanical properties and breakdown properties was also explored.

4.3 Results

4.3.1 Droplet size and zeta-potential of oil droplets

The particle size distribution of whey protein oil-in-water emulsion is presented in Fig. 4-1A. With increasing NaCl concentration, the droplet size distribution showed no changes. However, the zeta-potential values of the droplets decreased significantly with increasing NaCl concentration (Fig. 4-1B) because of the shieling effect of surface charges of oil droplets by ions of Na^+ and Cl^-. This is consistent with the previous study (Kulmyrzaev & Schubert, 2004).

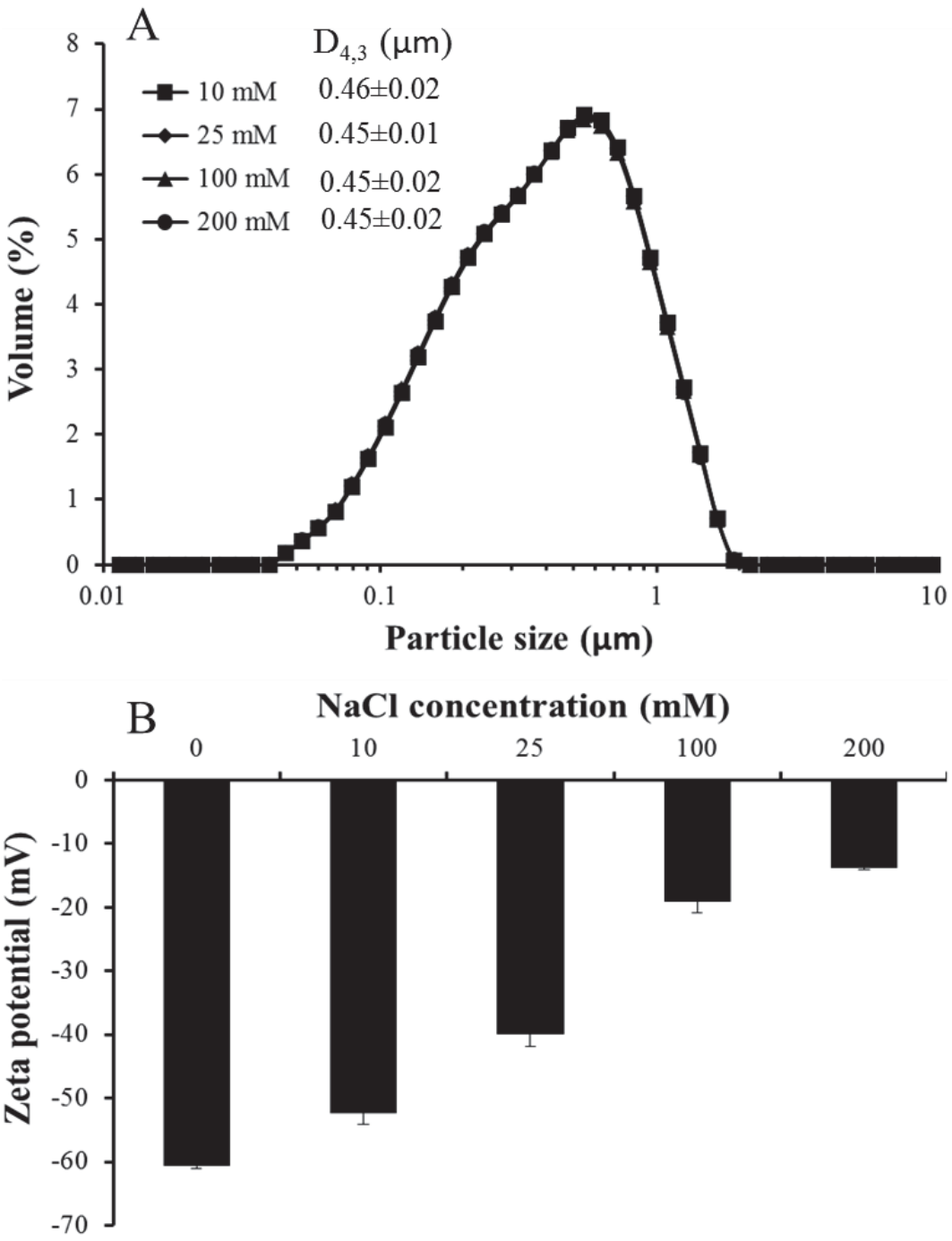

Figure 4-1 Particle size and zeta-potential of whey protein stabilized oil-in-water emulsions containing different NaCl concentrations.

4.3.2 Emulsion gel formation

The original whey protein emulsion gels with different NaCl concentrations are presented in the Fig. 4-2. All gels were opaque and self-standing. Fig. 4-3 shows the

changes in linear viscoelastic properties during the formation of whey protein emulsion gels with varying NaCl levels. The varying magnitude of these results indicates the differences in intermolecular bonding and microstructure. The gels containing 10, 25, 100 and 200 mM NaCl were called gels A, B, C and D, respectively. The final storage moduli of gels A, B, C and D were 7.3 ± 1.8, 23.0 ± 0.3, 107.0 ± 5.2 and 91.0 ± 1.1 kPa, respectively. The gelling points for gels A, B, C and D (i.e. the temperature where G' = G") was 85.0 ± 1.3, 84.2 ± 0.1, 79.0 ± 0.3 and 73.2 ± 1.4 °C, respectively. These results suggested that the increase in ionic strength caused a gradual decrease in the gelling temperature of whey protein emulsions, and a marked increase in storage modulus up to 100 mM added NaCl. However, the final storage modulus of the gel containing 200 mM NaCl was significantly lower than that with 100 mM, which is consistent with the rheological properties of heat-set whey protein gels with different NaCl concentration reported by Ikeda et al. (1999b).

Confocal microscopy images (Fig 4-4) revealed that oil droplets (red) were quite evenly distributed in emulsion gels A-D. These images also appeared to show possible flocculation of oil droplets within the protein matrix. Emulsion gels A-C appeared to have a continuous protein network (green) on a micro-scale. By contrast, emulsion gel D did not show a compact protein network but rather a network containing pores.

The particle size distributions of oil droplets incorporated into the gelled emulsions, measured using the Mastersizer, are also presented in Fig. 4-4. The oil droplet size distributions within the four gels were essentially the same, confirming that no coalescence of droplets occurred during the preparation of the gels. This is consistent with the study of Hunt & Dalgleish (1995).

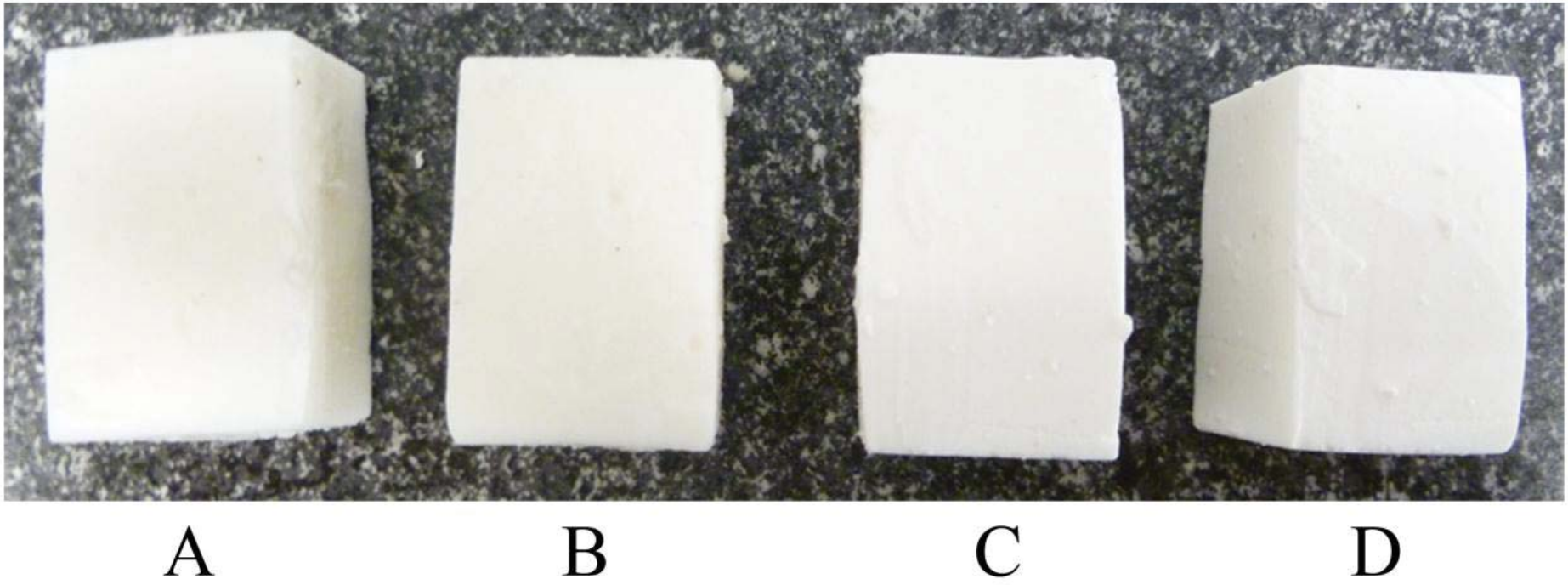

Figure 4-2 Typical photographs of original whey protein emulsion gels containing 10 (A), 25 (B), 100 (C) and 200 mM (D) NaCl.

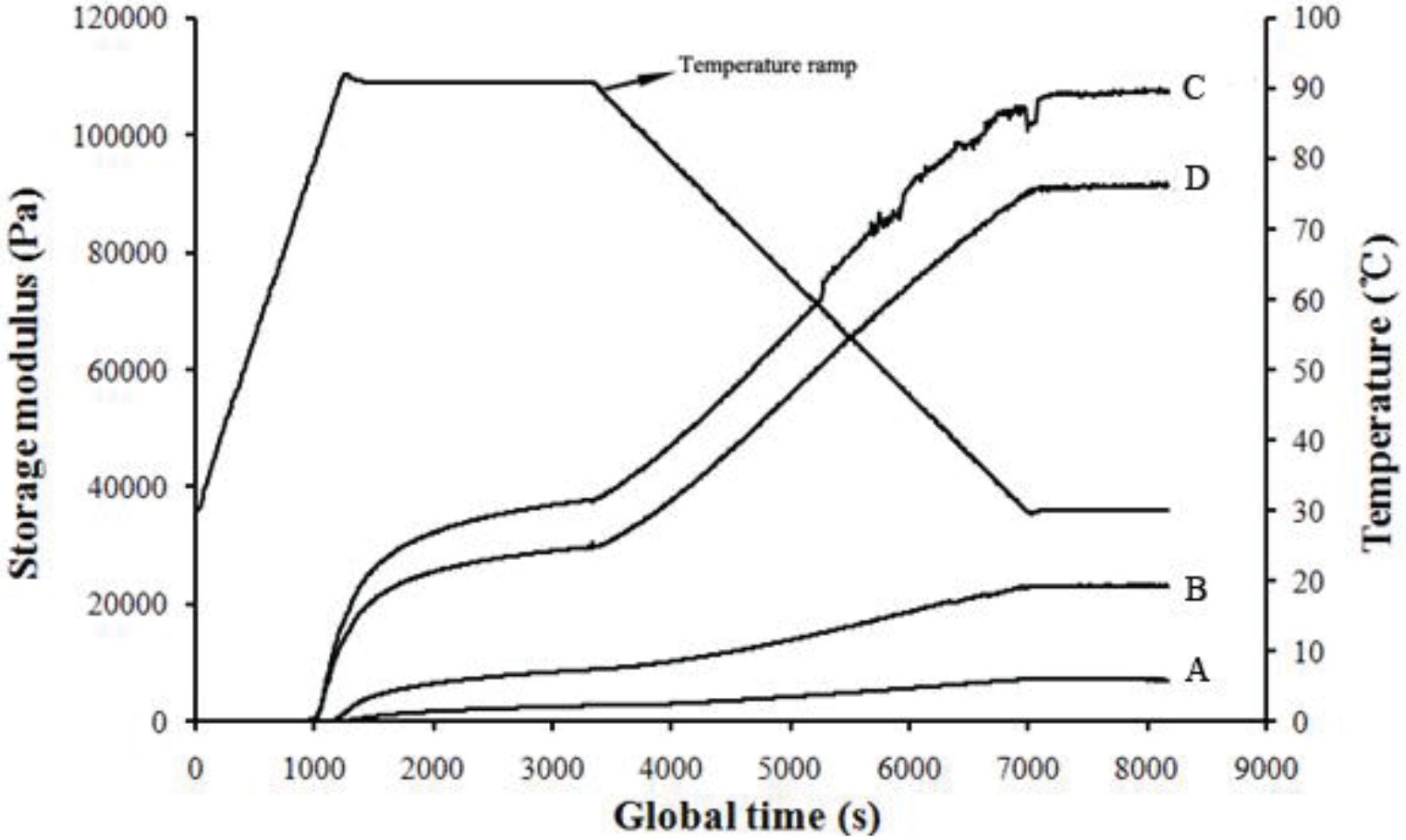

Figure 4-3 Development of viscoelastic properties of whey protein emulsion gels containing 10 (A), 25 (B), 100 (C) and 200 (D) mM NaCl.

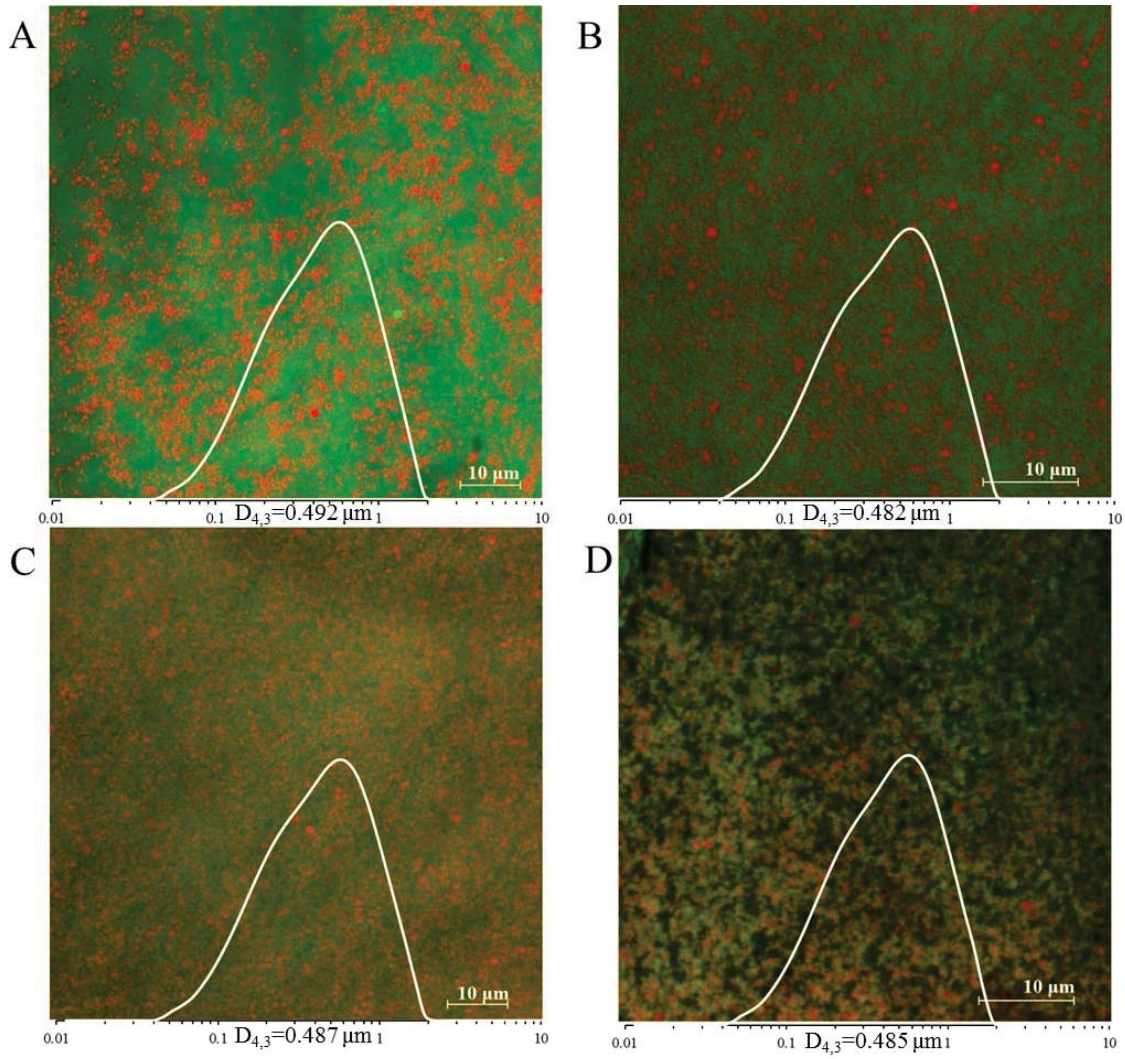

Figure 4-4 Confocal micrographs of whey protein emulsion gels containing 10 (A), 25 (B), 100 (C) and 200 (D) mM NaCl and particle size distributions of oil droplets within gels. Red represents oil and green represents protein.

4.3.3 Mechanical properties of the gels

4.3.3.1 Large deformation properties before fracture

Large deformation properties were obtained from the compression tests using plate-plate geometry in a texture analyser at 50% strain. As shown in Table 4-1, the hardness of the gel generally increased with increasing NaCl concentration, but increasing NaCl concentration from 100 to 200 mM led to a significant decrease in the hardness, which was in accordance with the result of small-strain rheological

measurements. The Young's modulus showed a similar trend. The recoverable energy decreased significantly with increasing NaCl concentration, indicating changes in the gel structure.

Table 4-1 Mechanical properties (large deformation) of whey protein emulsion gels.

Gel type	Hardness (N)	Young's modulus (Pa)	Recoverable energy (J/m^2)
A	19.2±0.6*	19.7±2.6*	47.7±0.5****
B	56.5±1.3**	60.5±15.1**	45.1±0.6***
C	77.8±0.4****	256.3±13.9****	35.7±1.4**
D	69.9±0.3***	228.8±8.5***	30.8±0.4*

Values with different superscripts (* to ****) are significantly different ($P< 0.05$) within the same groups. A, B, C and D represent the gels containg 10, 25, 100 and 200 mM NaCl respectively.

4.3.3.2 Fracture properties

The fracture tests were carried out using the texture analyser with a fracture wedge set. As illustrated in Table 4-2, with increased NaCl concentration, the fracture force which can be considered as the hardness at fracture point, and toughness, increased markedly. The fracture strains of gels A and D were higher than those of gels B and C. In order to see the differences in the breakdown pattern after the fracture point of gels with different structures, the force versus time curves were normalized by their fracture force and fracture time (Fig 4-5). The slopes of the normalized curves indicate the crack propagation speed within gels (Çakir et al., 2012). The slopes of

curves for the gels containing 100 and 200 mM NaCl were relatively high indicating the gels fractured at the fracture point. The slope of the curve of gel with 25 mM NaCl was intermediate while that of gel with 10 mM NaCl was low indicating the fracture propagation of these two gels was slow after fracture.

Table 4-2 Fracture properties of whey protein emulsion gels.

Gel type	Fracture force (N)	Fracture strain (%)	Toughness (J/m^2)
A	3.9±0.3*	63.1±1.9**	102.9±2.6*
B	7.0±0.1**	51.9±3.1*	146.5±12.6**
C	12.9±1.4***	55.6±5.0*	226.6±24.1***
D	17.2±1.9****	68.1±5.0***	327.6±39.6****

Values with different superscripts (* to ****) are significantly different ($P< 0.05$) within the same groups. A, B, C and D represent the gels containing 10, 25, 100 and 200 mM NaCl respectively.

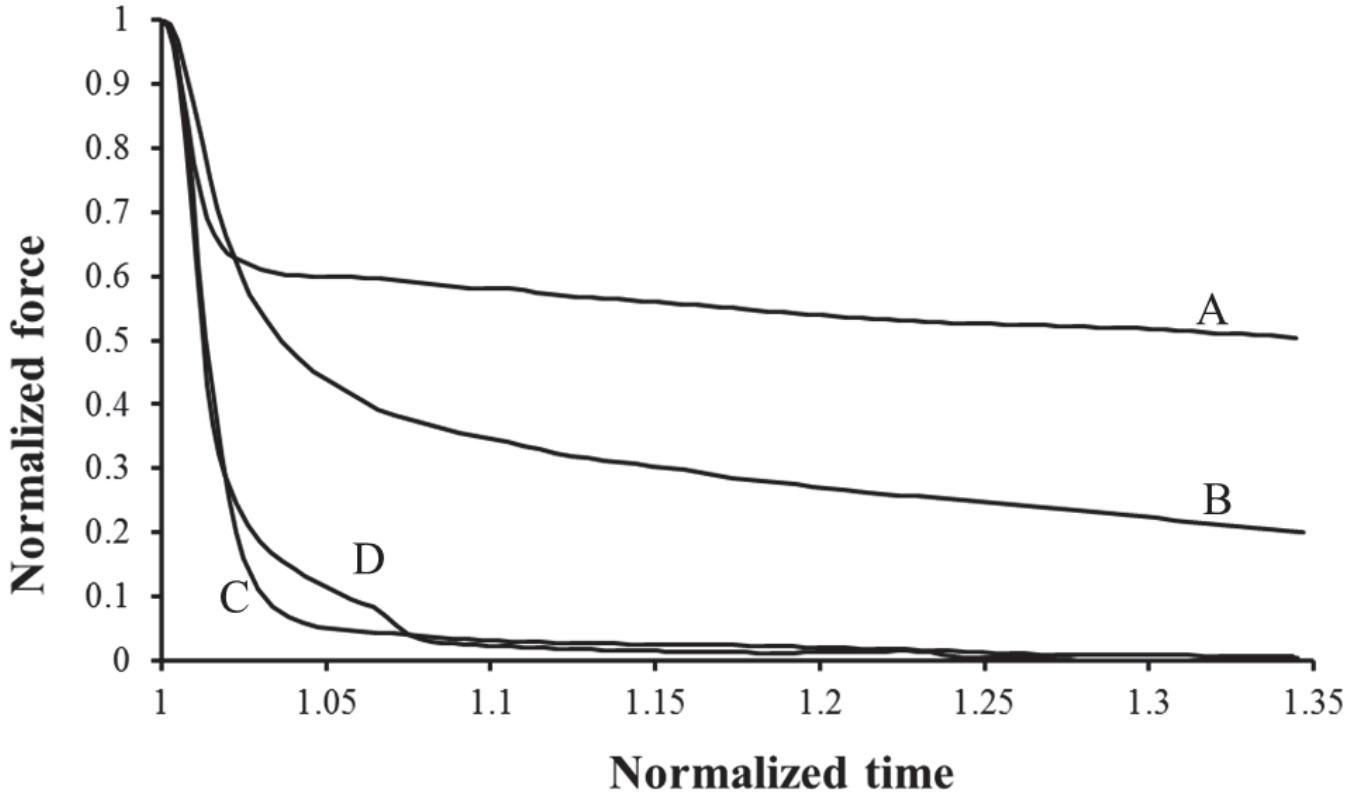

Figure 4-5 Normalized force versus normalized time curves after fracture point of whey protein emulsion gels. A, B, C and D represent the gels containing 10, 25, 100 and 200 mM NaCl, respectively.

4.3.4 In-mouth behaviour

4.3.4.1 Mastication parameters

The comparison between the mastication parameters of different gels is presented in Table 4-3. The results showed the number of chewing cycles of gel A was significantly lower than that of gels B, C and D ($P<0.05$) while the chew duration and chew frequency of four gels were very similar with no significant difference ($P>0.05$).

Table 4-3 Mastication parameters of whey protein emulsion gels.

Gel type	Number of chews	Chew duration (s)	Chew frequency (1/s)
A	19.4±2.1*	11.6±2.8*	1.75±0.33*
B	24.3±4.3**	13.0±3.3*	1.93±0.31*
C	24.8±4.8**	13.6±2.7*	1.83±0.20*
D	23.7±3.8**	13.5±2.7*	1.78±0.14*

Values with different superscripts (* to **) are significantly different ($P< 0.05$) within the same groups. A, B, C and D represent the gels containing 10, 25, 100 and 200 mM NaCl respectively.

4.3.4.2 Analysis of masticated gel

Example images of boluses of gels A, B, C and D are illustrated in Fig. 4-6. The boluses of gels A and B appeared to be very wet and the fragments within them had slippery and smooth surfaces. In contrast, the boluses of gels C and D looked very dry. Masticated gels upon collection were sieved and typical sample fragments remaining in each sieve are shown in Fig. 4-7. It can be seen that a larger quantity of larger fragments (i.e. larger than 2 mm) was retained in gels A and B whereas gels C and D retained a greater portion in sieves between 0.850-0.0380 mm. This result

suggested that a 'soft' gel produced a greater quantity of larger fragments than a 'hard' gel. The fragments collected were used to determine particle size distributions. The results expressed as the cumulative percentage of dry particle mass passing each sieve are presented in Fig. 4-8. The percentages of the particles larger than 3.15 mm (not passing this sieve) for gels A and B were about 60% and 44% while those for gels C and D were around 7% and 10%; By contrast, the percentages of particles smaller than 0.425 mm of gels A and B were below 5% while those of gels C and D were higher than 20%. The average data obtained from 8 subjects quantitatively supported the qualitative data in Fig 4-7. The particle size distribution curves of hard gels were near to the Rosin–Rammle distribution whereas the shapes of curves of soft gels were nearly linear, which is consistent with the studies of Jalabert-Malbos et al. (2007) and Hutchings et al. (2011) on natural foods. The approximate median size D_{50} (4.00, 2.85, 1.05 and 0.95 mm), corresponding to theoretical sieve which can pass 50% of weight, was extracted from curves of gels A, B, C and D. It should be noted that the total dry sample mass recovered on sieves, expressed as a percentage of the dry matter ingested was quite high (90.0 ± 7.5%, 86.1 ± 5.5%, 79.2 ± 5.6% and 80.3 ± 3.3% for gels A, B, C and D, respectively)

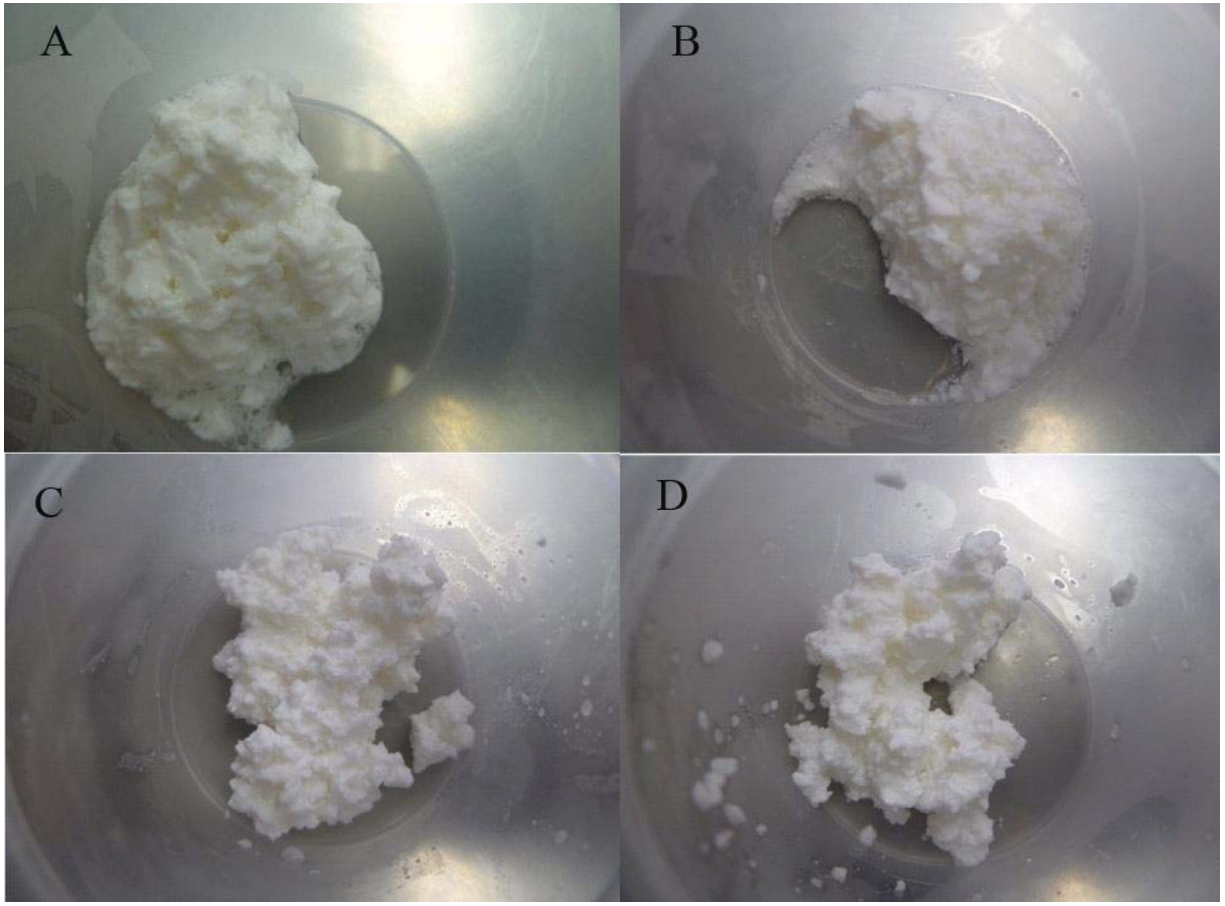

Figure 4-6 Typical image of whey protein emulsion gel boluses (A: 10, B: 25, C: 100 and D: 200 mM NaCl)

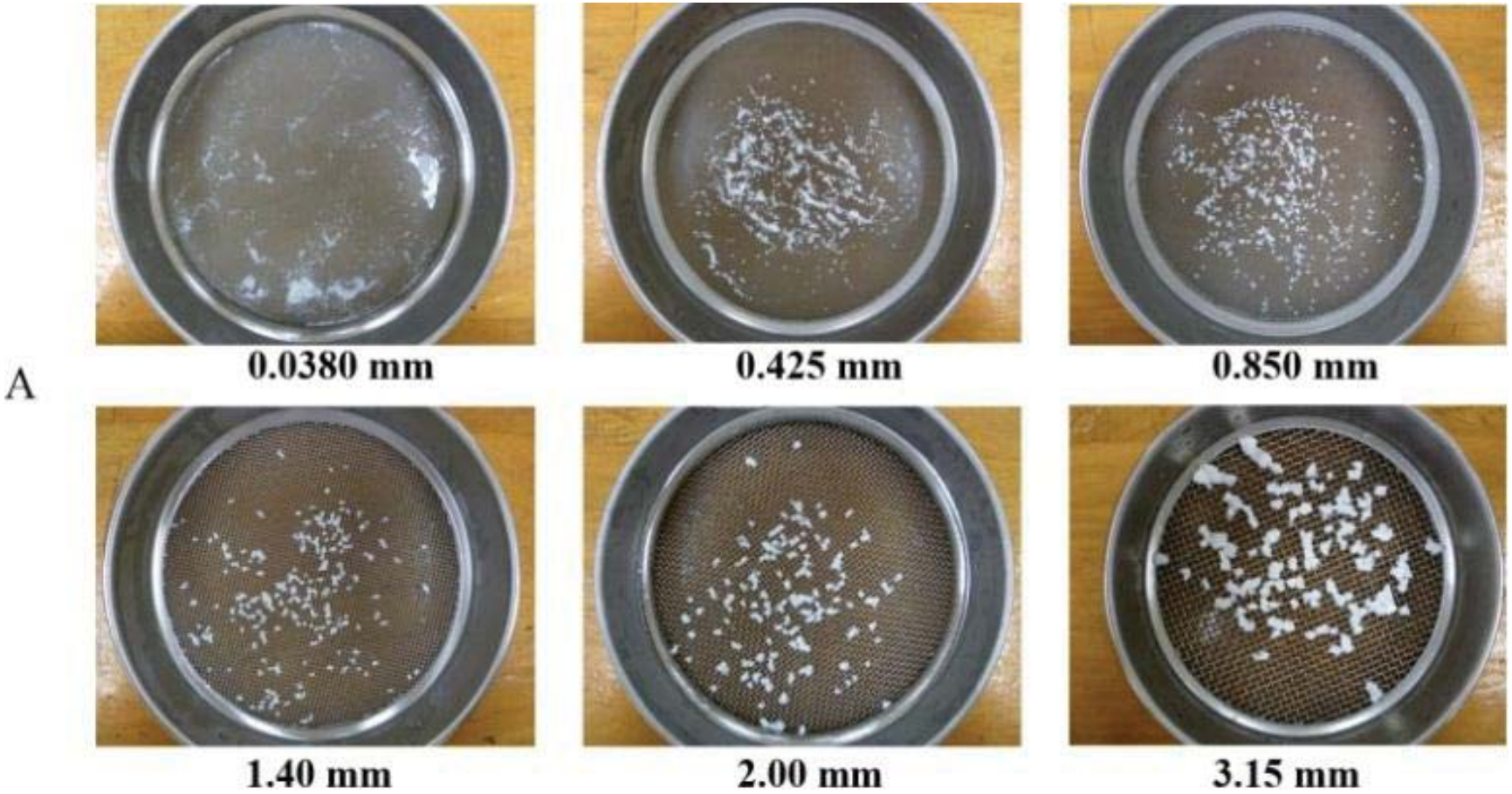

Figure 4-7 continued

B

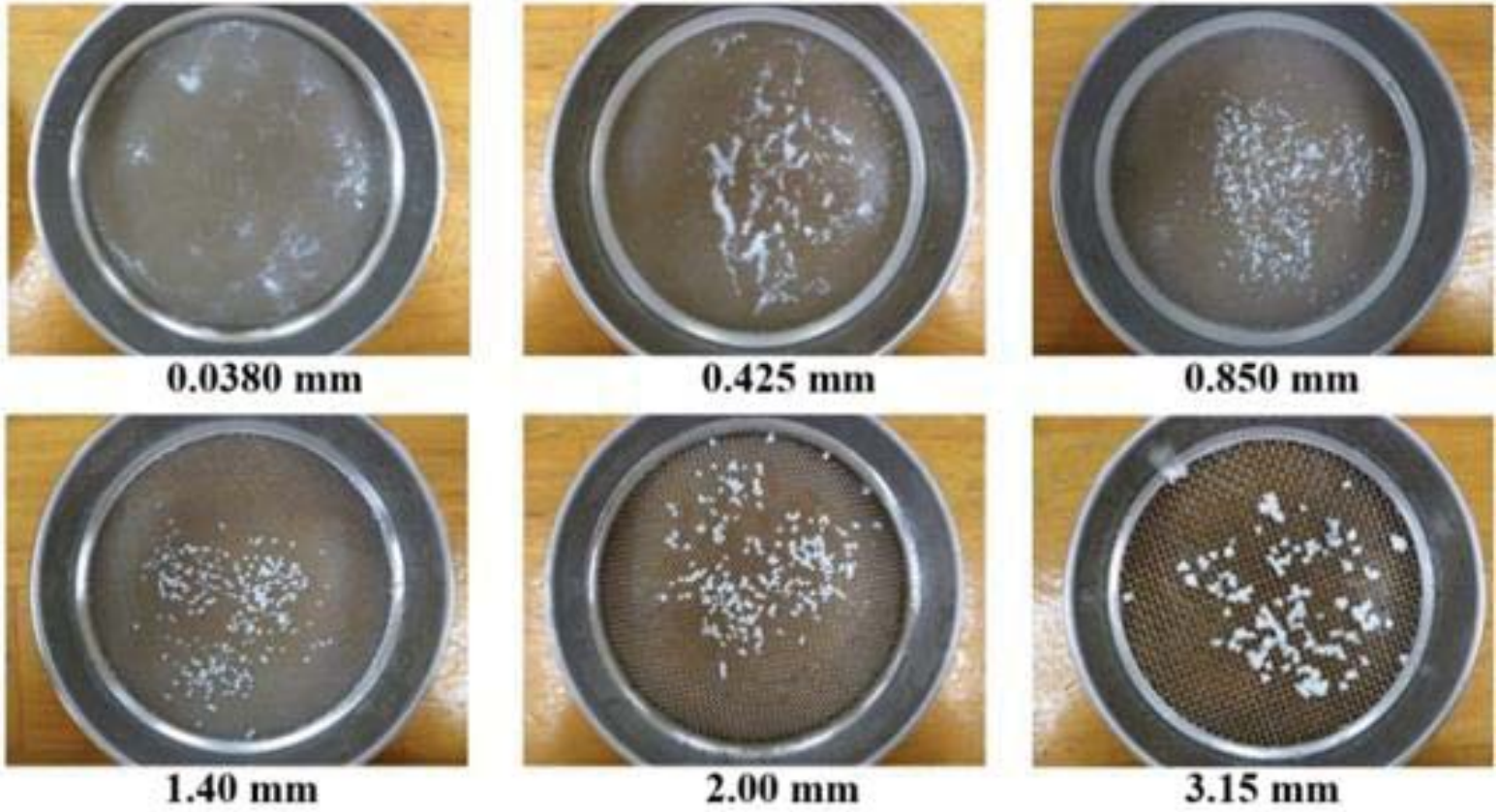

Figure 4-7 continued

C

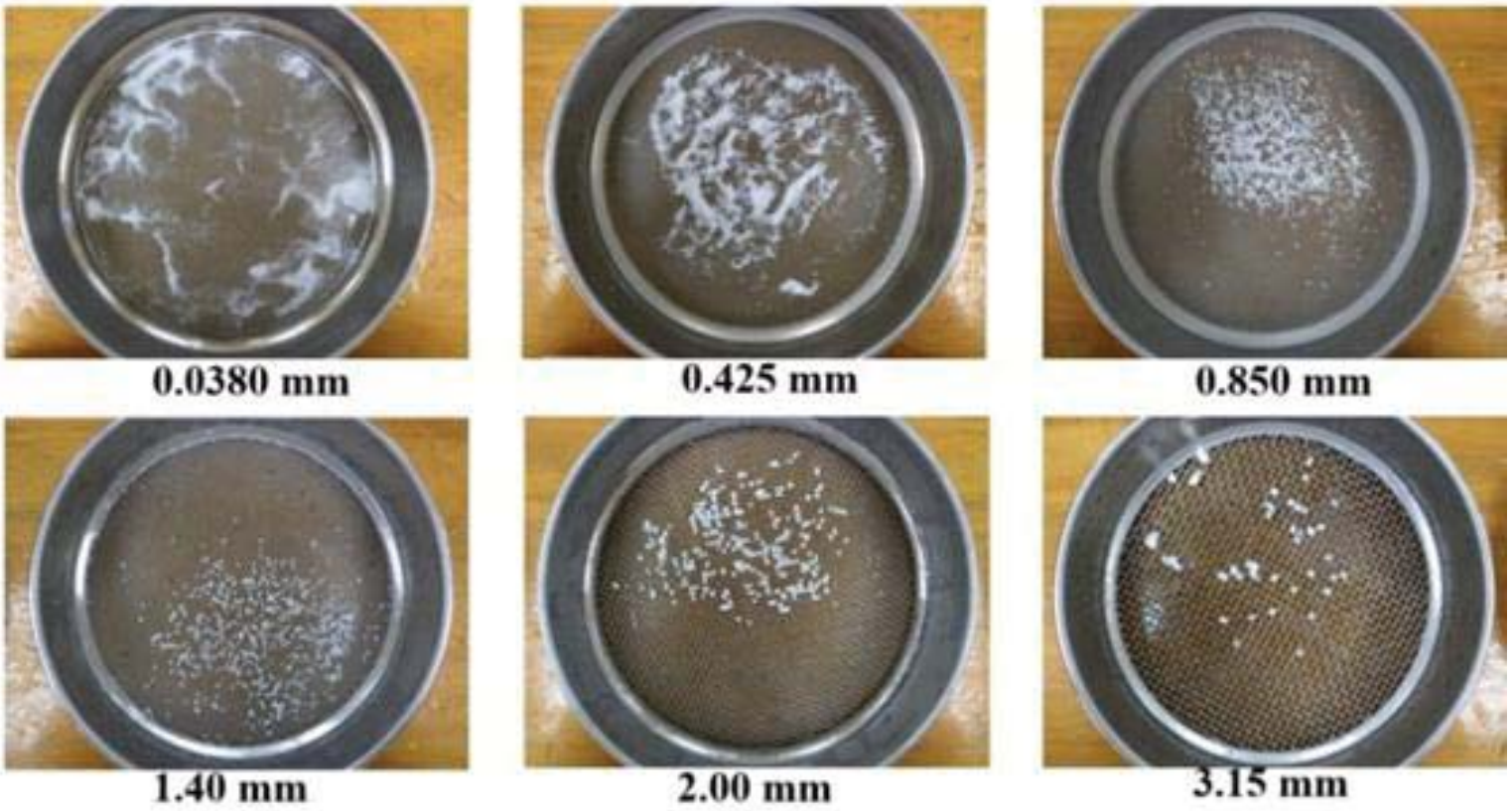

Figure 4-7 continued

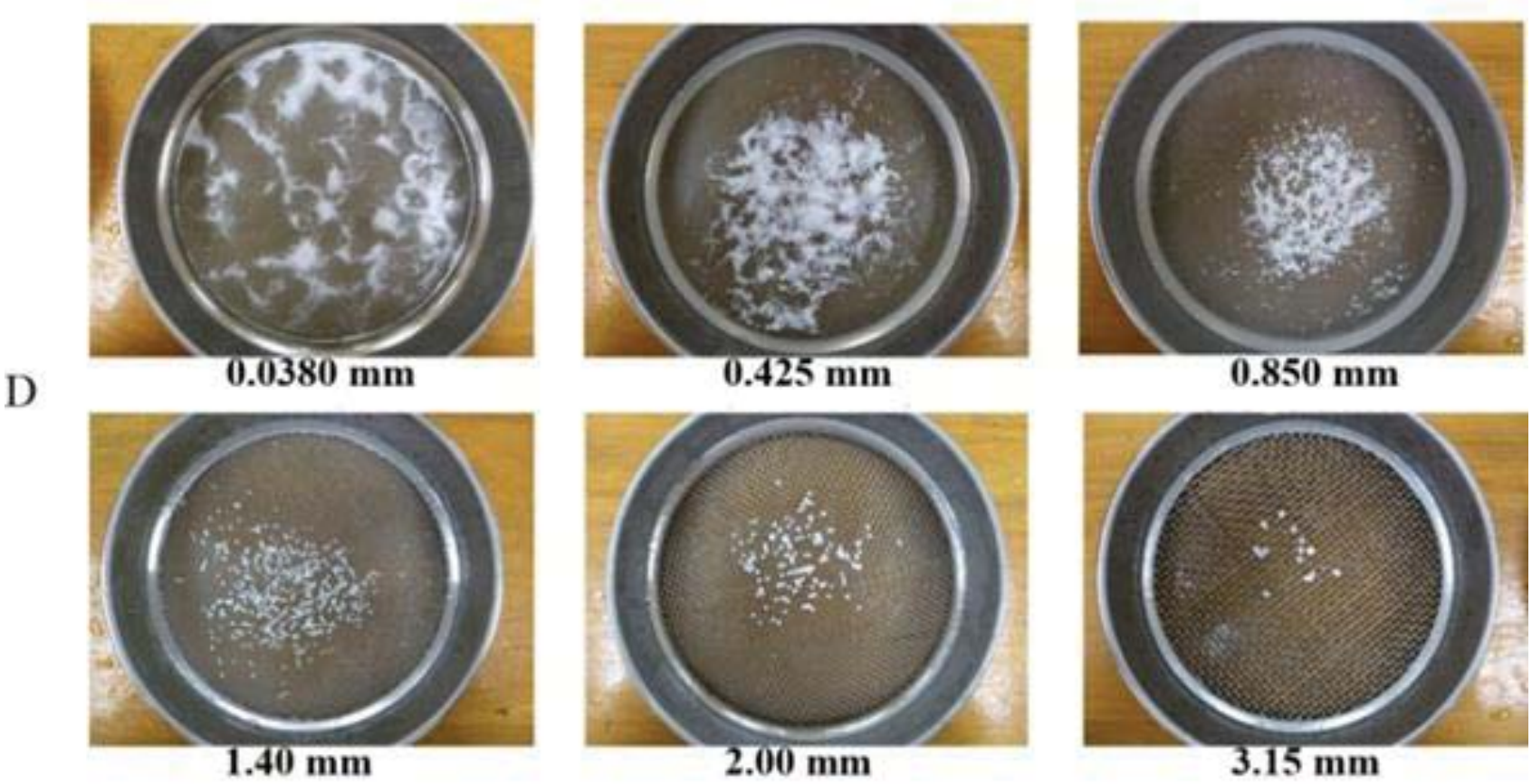

Figure 4-7 Typical image of particles within each masticated whey protein emulsion gel (A: 10, B: 25, C: 100 and D: 200 mM NaCl) retained in each sieve (0.038, 0.425, 0.85, 1.4, 2 and 3.15 mm, respectively) after washing.

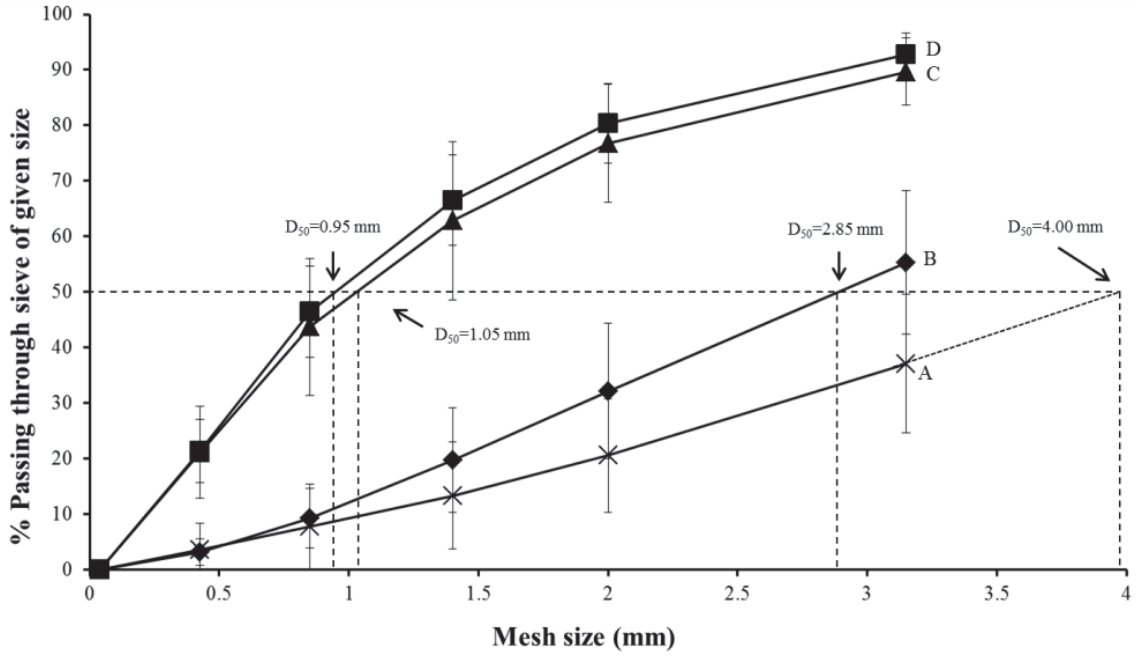

Figure 4-8 Average particle size distributions of fragments of whey protein emulsion gels upon chewing obtained from 8 human subjects. The symbols (×, ♦, ▲ and ■) represent whey protein emulsion gels containing 10, 25, 100 and 200 mM NaCl, respectively.

4.3.4.3 Oil droplet release

Confocal microscopy images (Fig. 4-9) for masticated gels show fragments of varying size and shape. Most of oil droplets appeared to have been retained in the fragments of the protein network with some released oil droplets. And the particle size distributions of oil droplets in gels after mastication were not different from those before mastication (Figs. 4-4 and 9), indicating that no coalescence occurred during mastication. Further support for the low oil droplets released from within the protein matrix of the masticated samples could be seen in the images of centrifuged boluses (Fig. 4-10), where very little oil had come to the surface of centrifuged sample

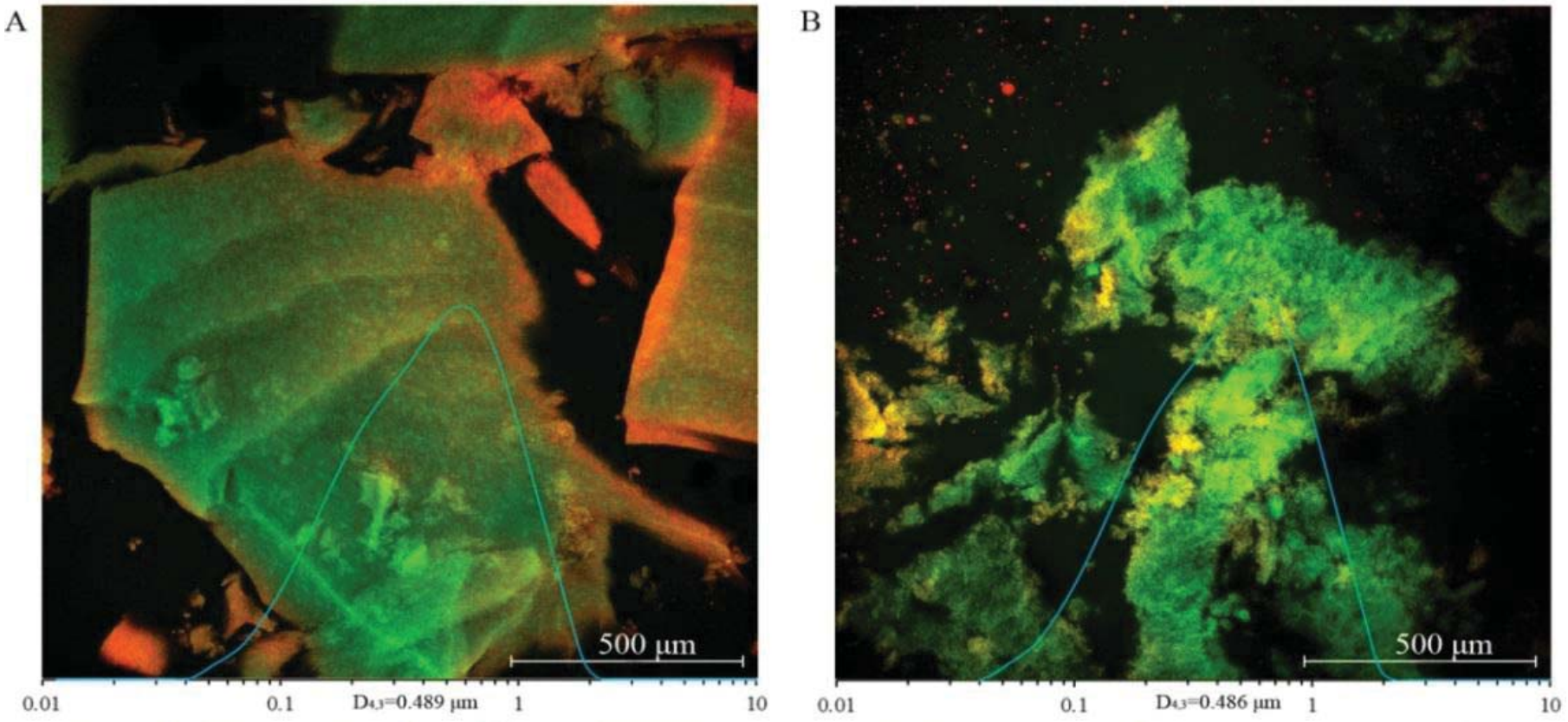

Figure 4-9 continued

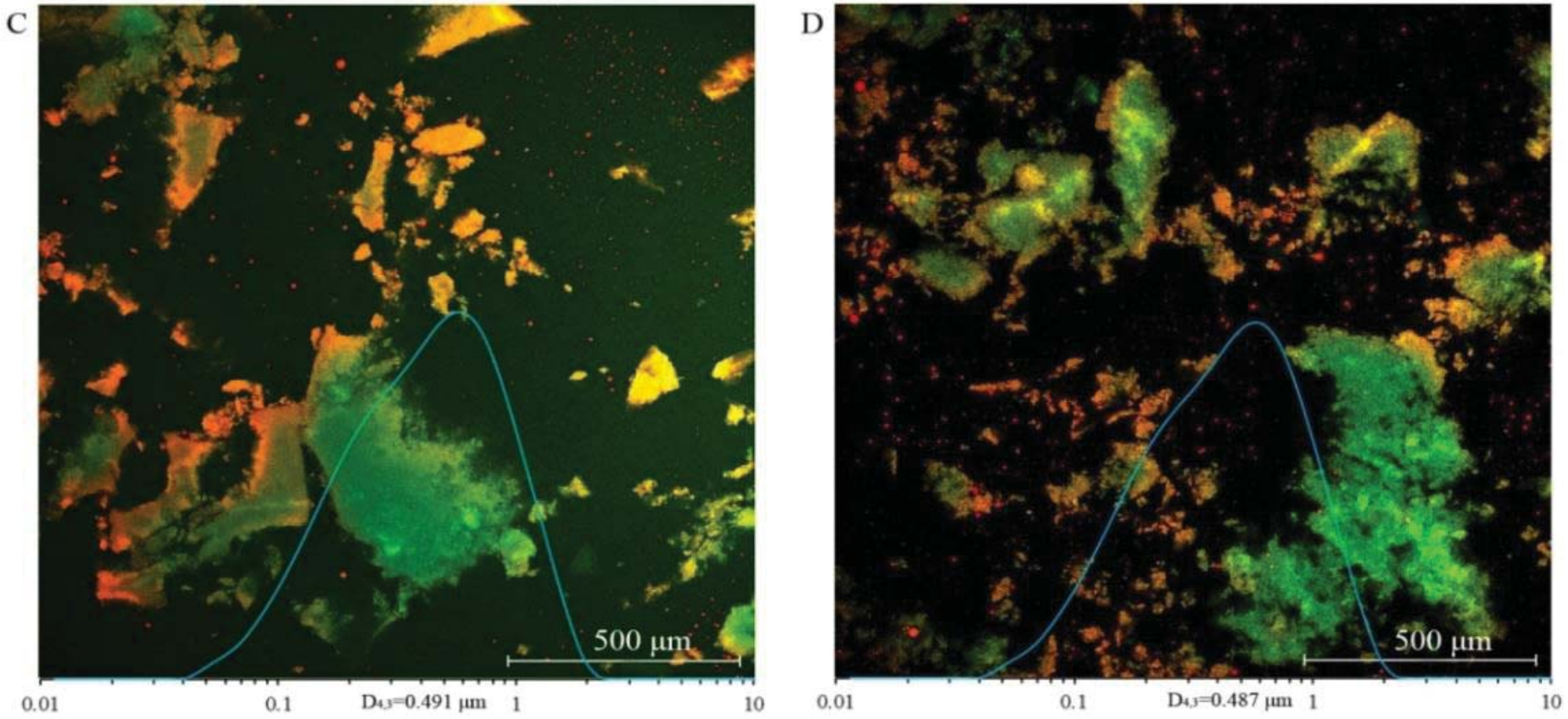

Figure 4-9 CLSM of boluses of whey protein emulsion gels containing 10 (A), 25 (B), 100 (C) and 200 (D) mM NaCl and particle size distributions of oil droplets within masticated gels. Colour in red represents the oil and green the protein.

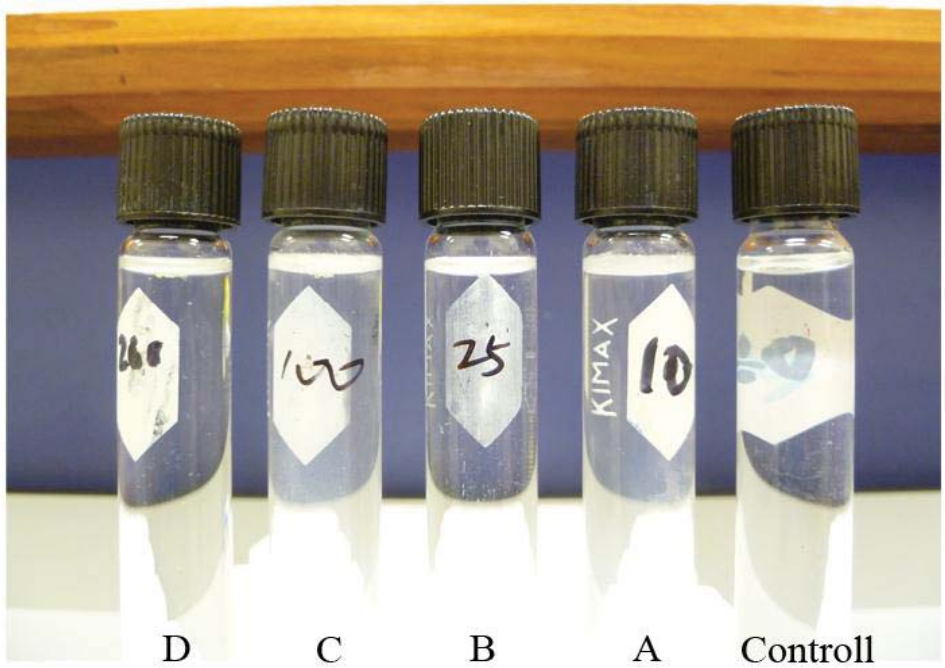

Figure 4-10 Oil droplet release measured by centrifugation.

4.3.5 Correlation between physical/mechanical properties and degree of gel fragmentation

The correlations between D_{50} of masticated gels and food property indices are presented in Fig 4-11. The fragmentation degree of gels was represented by D_{50} (the higher fragmentation degree is, the lower D_{50} is). The hardness measured by uniaxial compression test did not give a significant linear correlation with d_{50} of masticated gels ($P > 0.05$) (data not shown). By contrast, D_{50} had a significant negative linear correlation ($r = -0.959$, $P = 0.041$) with fracture force measured by the fracture wedge set (Fig 4-11a).

Fig 4-11b shows that the d_{50} of masticated gels had a significant positively linear correlation with $(R/E)^{0.5}$ ($r = 0.955$, $P = 0.045$). Fig 4-11c shows that D_{50} had a significant negatively linear correlation with $(RE)^{0.5}$ ($r = -0.986$, $P = 0.014$). By contrast, the D_{50} of masticated gels did not have a very significant linear correlation with R ($P = 0.087$) as shown in Fig 4-11d.

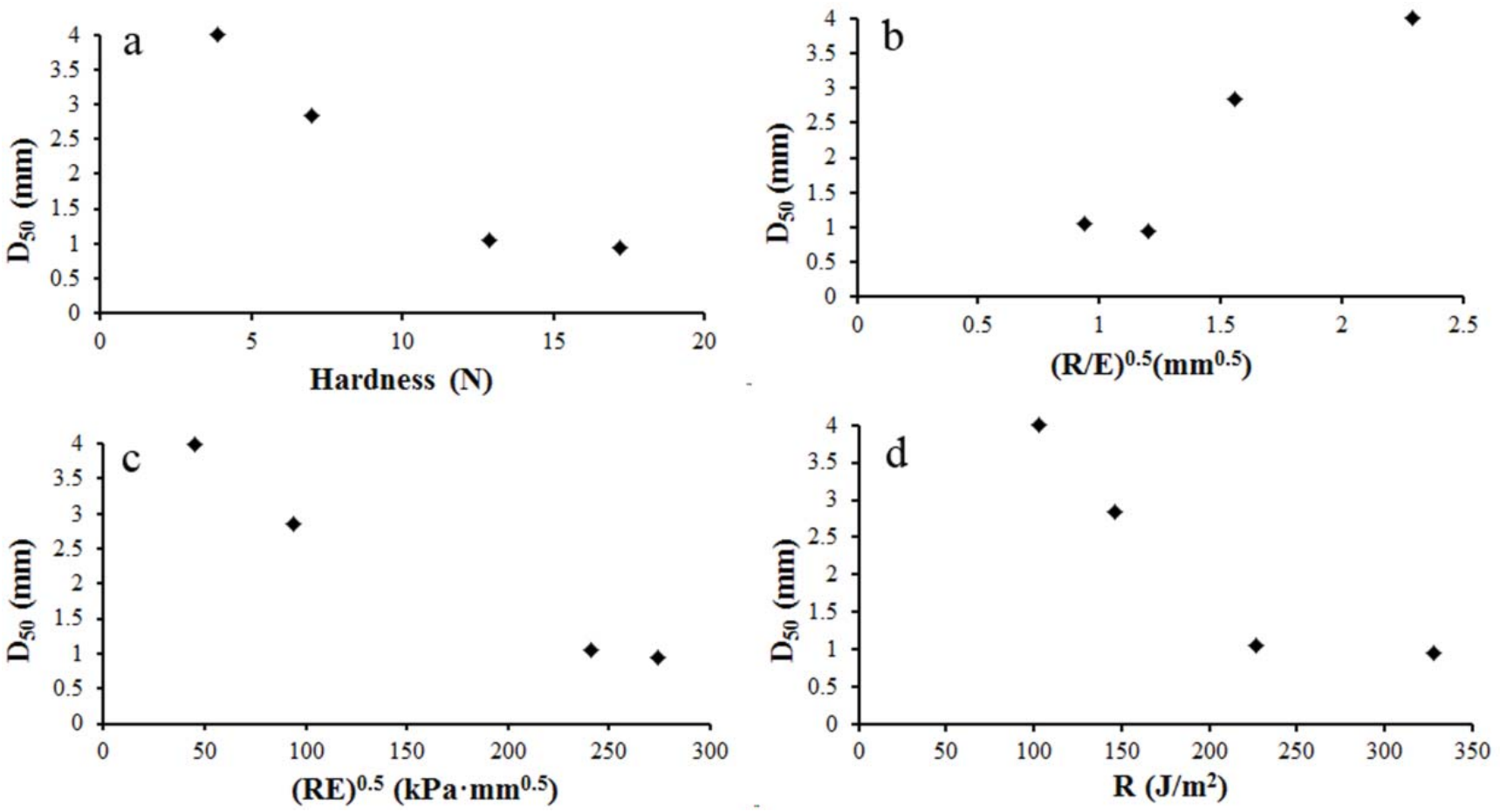

Figure 4-11 Correlation between physical/mechanical properties and fragmentation degree of whey protein emulsion gels. (a), represents the hardness measured by the fracture wedge set; (b), represents the mechanical property index $(R/E)^{0.5}$; (c), represents the mechanical property index $(ER)^{0.5}$; (d), represents toughness (R).

4.4 Discussion

Gel texture has been claimed to have a large influence on the number of chewing cycles. Foster et al. (2006) have demonstrated that both harder elastic and plastic model foods need more chewing cycles. The hardness of a gel can be described more accurately by linear viscoelasticity, large deformation properties before fracture and fracture properties (Çakir et al., 2012). In the gels used in this study, the gel strength or hardness was increased with NaCl concentration and the gels containing 10/25 and 100/200 mM NaCl could be characterized as soft and hard gels, respectively. As shown in Table 4-3, although the gel containing 10 mM NaCl required significantly fewer chews than the others, the gels containing 25, 100 and 200 mM NaCl showed no significant difference in the number of chewing cycles.

Liquid release may be another important factor influencing the number of chewing cycles (Pereira et al., 2006; van der Bilt et al., 2007). For gels containing 100 and 200 mM NaCl, some fluids released from the gels during compression by the texture analyzer which could be attributed to the phase separation (syneresis) during the gel formation. Minimal liquid released from gels containing 10 and 25 mM NaCl. However, a significant increase in the number of chewing cycles was observed in the gel containing 25 mM NaCl compared with that containing 10 mM NaCl and therefore it appears that hardness rather than liquid release is the key factor influencing the number of chewing cycles in these two gels. The fact that the number of chewing cycles does not increase in the much harder gels made with 100 and 200 mM NaCl suggests that liquid release may play an increasingly important role in the number of chewing cycles of gels. In addition, salt release might impact the chewing behaviour of the gels containing 100 and 200 mM NaCl which have a higher salt level than saliva because

sodium release is negatively correlated with the number of chewing cycles per minute (Neyraud et al., 2003; Pionnier et al., 2004).

The number of chewing cycles and retention time in the mouth of the four gels had no relation with the degree of breakdown of the gels (Table 4-2 and Figs. 4-7 and 8), which implied mastication parameters were not important factors influencing the fragmentation of gels during bolus formation. Salt perception might also influence the breakdown of heat-set whey protein emulsion gels containing high NaCl containing 100 and 200 mM according to a study of Pionnier et al. (2004). They found that high saltiness could be related to low rate of breakdown of model cheeses. However, the gel hardness generally increased with increasing NaCl concentration in the present study, and increased hardness of heat-set whey protein emulsion gels led to a higher degree of fragmentation, which is consistent with the report of Peyron et al. (2004) and Jalabert-Malbos et al. (2007) on natural foods with different hardness. Especially, the fragmentation degree of four gels had a high linear correlation with the fracture force. As a result, gel structure is the key factor determining the breakdown of gels in the human mouth. The harder gel that had a higher fragmentation degree can be explained by two mechanisms: 1, mastication strategy and 2, gel breakdown pattern.

A masticatory sequence is the whole set of movements from ingestion to swallowing which includes: stage I transport, processing, stage II transport and pharyngeal swallow (Lund, 1991; Hiiemae & Palmer, 1999). Stage I transport includes food intake, compressing food against the hard palate and tongue, and transporting food to the occlusal surface of the molar teeth (Hiiemae et al., 1999; Okada et al., 2007). During stage I transport, the texture of ingested food is recognized by intra-oral compression and 10–12% strain during the tongue-palate compression was suggested to be the critical point of gelatin and agar gels for deciding mastication strategy for size

reduction (Arai & Yamada, 1993; Okada et al., 2007; Ishihara et al., 2012). Arai & Yamada (1993) used 40 subjects to observe their mastication from crushing to swallowing using gelatin and agar gels. They found that there were two types of mastication strategies and that the strategy altered from mainly compressing with tongue and hard palate (strategy 1) to mainly grinding with the molars (strategy 2) as the hardness and rupture stress of the model samples increased. The threshold of hardness for strategy alteration was about 1.33×10^4 Pa for gelatin gel. The hardness of the heat-set whey protein emulsion gel containing 10 mM NaCl at a strain of 12% was about 0.5×10^4 Pa, which implied the breakdown may be manipulated by the tongue-hard palate compression. Rupture stress is another important factor influencing the mastication strategy. The results of the fracture wedge set showed that the fracture force of gel containing 10 mM NaCl was relatively low. As a result, this gel can be easily fragmented to smaller pieces by incisors or canines. Therefore, it is inferred that the breakdown of gel containing 10 mM NaCl may be mainly manipulated by both the shearing of incisors or canines and compression with tongue and hard palate. The gel with 10 mM NaCl that was fragmented mainly into large pieces during chewing strongly supported this inference (Figs. 4-7 and 8). By contrast, the values of hardness of gels containing 25, 100 and 200 mM NaCl at 12% strain were higher than 1.33×10^4 Pa and their fracture forces, especially those of gels containing 100 and 200 mM NaCl, were quite high. Therefore, these gels probably were processed mainly by the grinding of molars thereby leading to a high percentage of small particles during chewing (Figs. 4-7 and 8). Moreover, literature has shown harder food needs higher chewing force and chewing activity (Kohyama et al., 2004; Foster et al., 2006; van der Bilt et al., 2007). Therefore, the gel masticated by strategy 1 is considered to have greater median size than that masticated through strategy 2.

Another important factor influencing the degree of breakdown of the whey protein emulsion gels is determined by the gel breakdown pattern. Gels containing 10 and 25 mM NaCl had a highly homogeneous microstructure (Fig. 4-4) and were soft; at 100 mM NaCl, the gel microstructure began to become hard and inhomogeneous (Fig. 4-4) due to the decrease of electrostatic repulsion (Fig. 4-1) although this feature cannot be observed clearly in confocal images (Pouzot et al., 2005); at 200 mM NaCl, the gel had a micro-phase separated structure with large pores (Fig. 4-4). The whey protein emulsion gels with homogeneous microstructure had a low fragmentation degree while the gels with inhomogeneous microstructure had a high fragmentation degree, which is in agreement with the report of Gwartney et al. (2004). According to the model of van Vliet et al. (1993), the energy applied to deform a material (W) can be elastically stored (We), dissipated either by vicious flow of the material (Wv) or by friction process between structural elements (Wc) or used to cause fracture (Wf):

$$W = We + Wv + Wc + Wf \cdots\cdots\cdots\cdots\cdots \text{Eqn 4-1}$$

To cause fast fracture, the stress at the tip of a crack should be higher than the cohesive stresses between the structural elements and the elastically stored energy released during crack growth should be higher than the amount of energy to cause crack growth. The storage modulus of hard gels containing 100 and 200 mM NaCl was much higher than that of soft gels containing 10 and 25 mM (Fig. 4-3) while the recoverable energy of hard gels (representing elastically stored energy) was a little lower than that of soft gels. Moreover, the energy consumed in growing a crack of per unit area (toughness) of hard gels was only a little higher that of soft gels (Table 4-2). This suggested that during deformation the hard gel could store high energy to cause the fast free-running crack and the crack growth was fast. In contrast, soft gels could not store enough energy to cause a fast crack. In addition, the slopes of normalized force–time curves of hard gels

after fracture point were much higher than those of soft gels (Fig. 4-5), which also suggested that hard gels broke down fast and soft gels broke slowly. The former probably caused the formation of more small particles during mastication. Overall it is suggested that the gel structure was the key factor determining the fragmentation degree of heat-set whey protein emulsion gels.

According to the work of Lucas et al. (2002), there are three patterns of crack start and growth of food particles during chewing: 1, a crack starts and grows remote from cusps as a result of bending against a three- (more) point cuspal support; 2, a crack is adjacent to a cusp and runs straight and rapidly through the food particle; 3, a crack is adjacent to a cusp and the arrested crack can only be continued by displacement of the cusp into the particle. The first and third crack propagation can be represented by $(R/E)^{0.5}$, which is limited by the displacement of food particles. The second can be represented by $(RE)^{0.5}$ which is limited by the stress imparted on the food particle. The authors also suggested different criteria of oral fragmentation for different foods, namely $(R/E)^{0.5}$ for thick block food, $(RE)^{0.5}$ for food requiring high stress to fracture or toughness (R) for very thin food. In the results (Fig. 11b), $(R/E)^{0.5}$ had a significant positive linear correlation with the D_{50} of masticated heat-set whey protein emulsion gels, i.e., a negative linear correlation between degree of fragmentation and $(R/E)^{0.5}$, which is in agreement with the report of Agrawal et al. (1997). This implied $(R/E)^{0.5}$ is a valid criterion for estimating the fragmentation degree of differently structured heat-set whey protein emulsion gels during chewing. However, a better linear correlation (negative) was found between D_{50} and $(RE)^{0.5}$, i.e., a positively linear correlation between degree of fragmentation and $(RE)^{0.5}$. Therefore, both $(R/E)^{0.5}$ and $(RE)^{0.5}$ can be used as criteria of fragmentation, which implies that the fragmentation (crack

propagation) of the whey protein emulsion gels is complicated and the combined mechanical property of R and E was indeed highly correlated with fragmentation of gels.

Finally, there was a very small proportion of oil droplets released from the gel matrix, which is in accordance with the work of Sala et al. (2007). This suggested the small oil droplets within the gels were firmly bound to the gel matrix even under strong mechanical processing and the solid 3-dimensional protein network surrounding the oil droplets also provided a good protection against mechanical release from the gel matrix.

4.5 Conclusions

This study improved an understanding of the breakdown behavior of heat-set whey protein emulsion gels with different textures in the human mouth and its relationship with the physical/mechanical properties. The gel structure which determined physical/mechanical properties was the key factor influencing oral fragmentation of heat-set whey protein emulsion gels. From linear viscoelasticity, large deformation properties before fracture and fracture properties, whey protein emulsion gels were characterized as two types: hard gel (100 and 200 mM) with inhomogeneous microstructure and soft gel (10 and 25 mM NaCl) with homogeneous microstructure. The hard gels had a fast free-running crack pattern and a high fragmentation degree while soft gels had a slow crack propagation pattern and a low fragmentation degree. And the fragmentation was highly linearly correlated with the fracture force. Furthermore, $(R/E)^{0.5}$ and $(RE)^{0.5}$ which are the mechanical property indices representing food cracking in the human mouth were found to be good criterion for estimating fragmentation degree of heat-set whey protein emulsion gels. In addition, the oral processing had minimal impact on such small oil droplets within differently structured heat-set whey protein emulsion gels.

Chapter 5 Effect of Structure of Protein Matrix on Gastric Digestion of Whey Protein Emulsion Gels[2]

5.1 Abstract

This study aimed to characterize and determine the physicochemical characteristics of the gastric digesta. Using thermal treatment at 90 °C, whey protein emulsion gels with different structures and gel strengths were formed by varying the ionic strength. Simulated boluses of soft (containing 10 mM NaCl) and hard (200 mM NaCl) gels, which had similar particle sizes to those of human subjects, were created for gastric digestion. For both gels, it took 4-5 hours to decrease the pH of gastric contents in the HGS to ~ 2. The boluses of both gels gradually disintegrated into particles of size ~ 10 μm. With further digestion, the protein matrix of the soft gel particles dissolved, the proteins were disrupted mainly by proteolysis and large quantities of oil droplets were released. In contrast, for the hard gel particles, all proteins were hydrolysed after 240 min but the breakdown of the particles was slow and no oil droplets were released after 300 min. The differences in the breakdown of soft and hard gels in the HGS were attributed to the structures of the emulsion gel, which resulted in different sets of peptides after digestion. Coalescence of the oil droplets was observed only for the soft gel. Experiments carried out using a lower pepsin level showed similar phenomenon, although the gel digestion or disintegration was slower, indicating a higher pepsin level promotes the gel digestion or disintegration.

[2]Part of contents presented in this chapter has been published as a peer-reviewed paper: Guo, Q., Ye, A., Lad, M., Dalgleish, D., & Singh, H. (2014). Effect of gel structure on the gastric digestion of whey protein emulsion gels. *Soft Matter, 10*(8), 1214-1223.

5.2 Introduction

To better design foods for the future, there needs to be an understanding of the way in which they break down in the human body (Norton et al., 2007). This understanding could assist in developing new foods that provide fat regulation, release of macronutrients, encapsulation and targeted release (Norton et al., 2007; Golding et al., 2010). One means of achieving an understanding of the process of food digestion in the stomach is to develop effective *in vitro* gastric models that simulate the gastric environment (Kong & Singh, 2008; Chen et al., 2011; Hur et al., 2011; Guerra et al., 2012). An important advantage of *in vitro* (over *in vivo*) experiments is that there are no ethical constraints, which often limit *in vivo* experiments. However, although *in vitro* methods are thought to be more flexible, accurate and reproducible than *in vivo* methods, it is still impossible to simulate the overall physiological conditions of *in vivo* digestion in a single *in vitro* model (Guerra et al., 2012).

The behaviour of whey protein oil-in-water emulsions in simulated gastric environments has recently received much attention (Singh et al., 2013). Whey protein emulsion solutions have been shown to undergo extensive flocculation and creaming in a dynamic gastric model with gradual acidification (Helbig et al., 2012; Shani-Levi et al., 2013). β-Lactoglobulin oil-in-water emulsion droplets (0.8 wt% protein and 20 wt% oil in the final emulsion) coalesced after 1 h of digestion in a gastric model (pH 2, 3.2 g pepsin/L), which was attributed to pepsinolysis of the interfacial layer (Sarkar et al., 2009b). The adsorption of whey proteins at the oil–water interface affects their conformational structure and their susceptibility to peptic hydrolysis. As will be shown below, adsorbed β-lactoglobulin was hydrolysed into small peptides whereas the resistance of α-lactalbumin to pepsin increased on adsorption at the interface. Meanwhile, exchanges between adsorbed and non-adsorbed whey proteins are likely to

occur at the oil−water interface (i.e. hydrolysis of the proteins adsorbed at the interface can induce further adsorption and hydrolysis of the proteins from the aqueous phase) (Malaki Nik et al., 2010). In addition, the stability of whey protein oil-in-water emulsions during gastric digestion depends mainly on the original protein concentration (Malaki Nik et al., 2010; Malaki Nik et al., 2011).

In this chapter, two whey protein emulsion gels containing 10 or 200 mM NaCl, representing 'soft' and 'hard' food types respectively, were chosen. The gel containing 10 mM NaCl was homogeneous on the micron length scale whereas that containing 200 mM NaCl was heterogeneous. The first objective was to mechanically prepare a simulated gel bolus that had a similar degree of fragmentation to the gel bolus of human subjects. The HGS was employed to mimic human gastric digestion. The physicochemical characteristics of the emptied gastric digesta were investigated, with a focus on the effect of the gel structure on the digestion and disintegration of emulsion gels in the simulated gastric environment. In addition, the effect of pepsin level during gastric digestion was also investigated.

5.3 Results

Before investigating the effect of gastric digestion on whey protein emulsion gels, the swelling ability of the gels was investigated.

5.3.1 Gel swelling in the gastric environment

Gel swelling ratio, measured in the SGF without the addition of pepsin, is illustrated in Fig. 5-1. With 5 hours of soaking in the SGF containing no pepsin, the gel swelling ratio increased to ~ 10.5 and 3.0 % for the soft and hard gels, respectively. With further soaking (20 hours), the swelling ratio of the soft gel increased to ~ 16.6 %

while that of the hard gel showed no significant change. This indicates that the soft gel had a higher water holding capacity probably because of its soft gel properties (i.e. high strain for fracture and low gel strength). These mechanical properties of the soft gel allow the gel to reach equilibrium between elastic forces of the gel and swelling forces at a large swelling ratio.

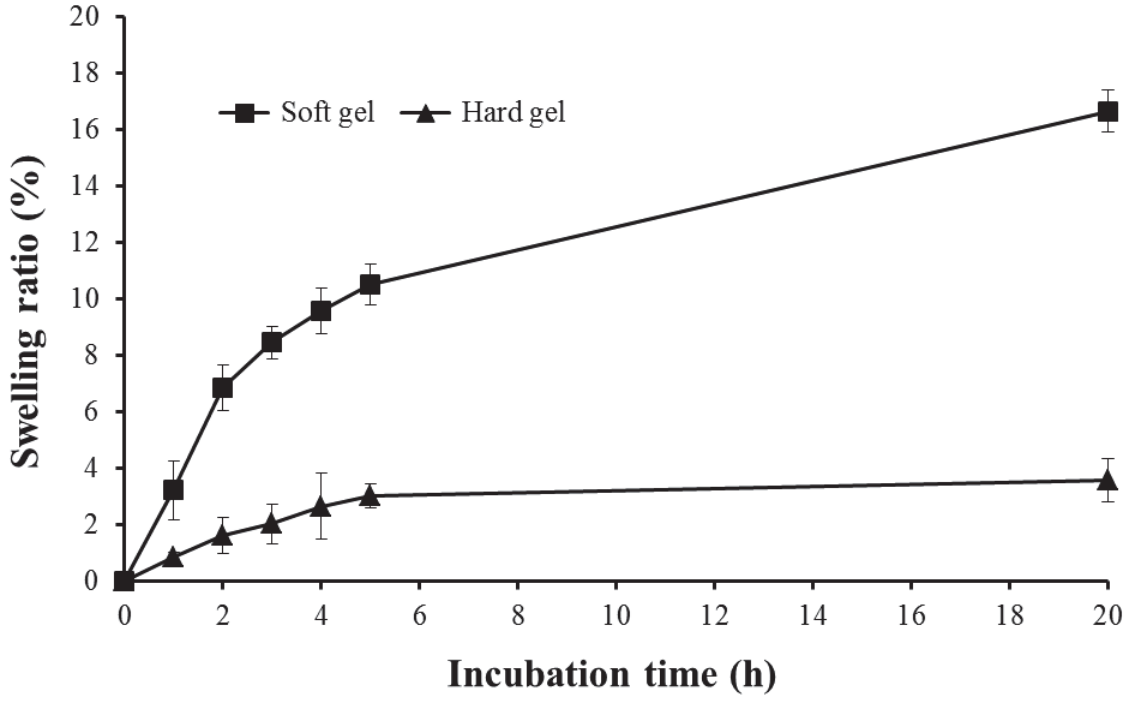

Figure 5-1 Swelling kinetics of whey protein emulsion gels in the SGF.

5.3.2 pH profiles in the HGS

The initial pHs in the stomach after ingestion (i.e. the pH of the mixture of simulated gel bolus and 70 mL of SGF) was ~ 5.55 and 5.70 for the soft and hard gels respectively. With the gradual addition of SGF (2.5 mL/min), the pH in the stomach (represented by the pH of the emptied digesta) gradually decreased, as shown in Fig. 5-2. In the absence of pepsin, the pH decreased to ~1.72 over 300 min for both soft and hard gels. In the presence of pepsin, the pH decreased to ~ 1.94 after 300 min for both soft and hard gels, i.e. the pH decreased slightly more slowly with added pepsin. The

pH profile trends were similar for both soft and hard gels, suggesting that the gel structure had no significant effect on the pH change in the stomach. There are no data available for *in vivo* digestion of whey protein emulsion gels, but our data for pH decrease are comparable with those measured *in vivo* for American meals (Simonian et al., 2005) or milk-based meal (Kalantzi et al., 2006).

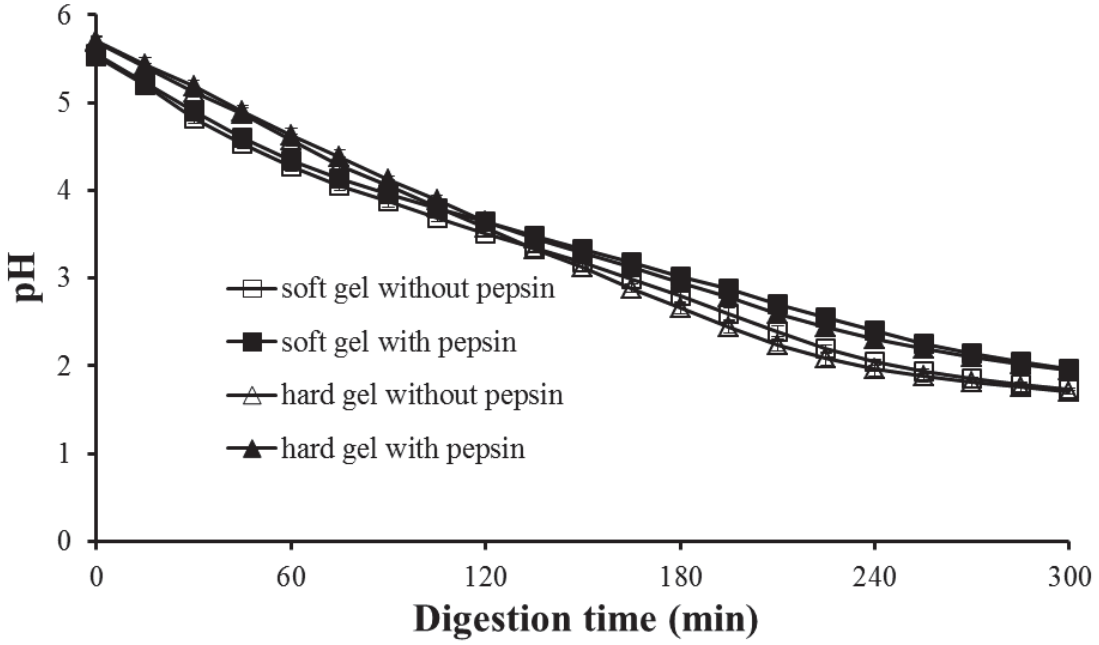

Figure 5-2 pH change during *in vitro* digestion of whey protein emulsion gels in the HGS.

5.3.3 Physicochemical characteristics of emptied gastric digesta

5.3.3.1 Image of emptied gastric digesta

Fig. 5-3 clearly shows the changes of the emptied gastric digesta of the soft gel during gastric digestion in the presence of pepsin. At 60 min, the particles appeared to sediment with appearance of supernatant in the top after 2 hours storage. With the digestion of the gel, the digesta appeared to be a mixture of particles at 120 min. With further digestion, small particles creamed to the top while large particles sedimented to the bottom at 180 min. At 240 and 300 min, most particles appeared to cream to the top, which can be explained by the decrease of density of gel particles. Soybean oil density

is about 0.92 g/mL. Oil phase accounts for 66.7% of the dry weight of whey protein emulsion gel while protein accounts for 33.3%. With the digestion, the protein matrix of gel particles was hydrolysed and dissolved. The gel particles creamed to the top layer because the density of gel particles decreased below 1. The hard gel also showed a similar trend.

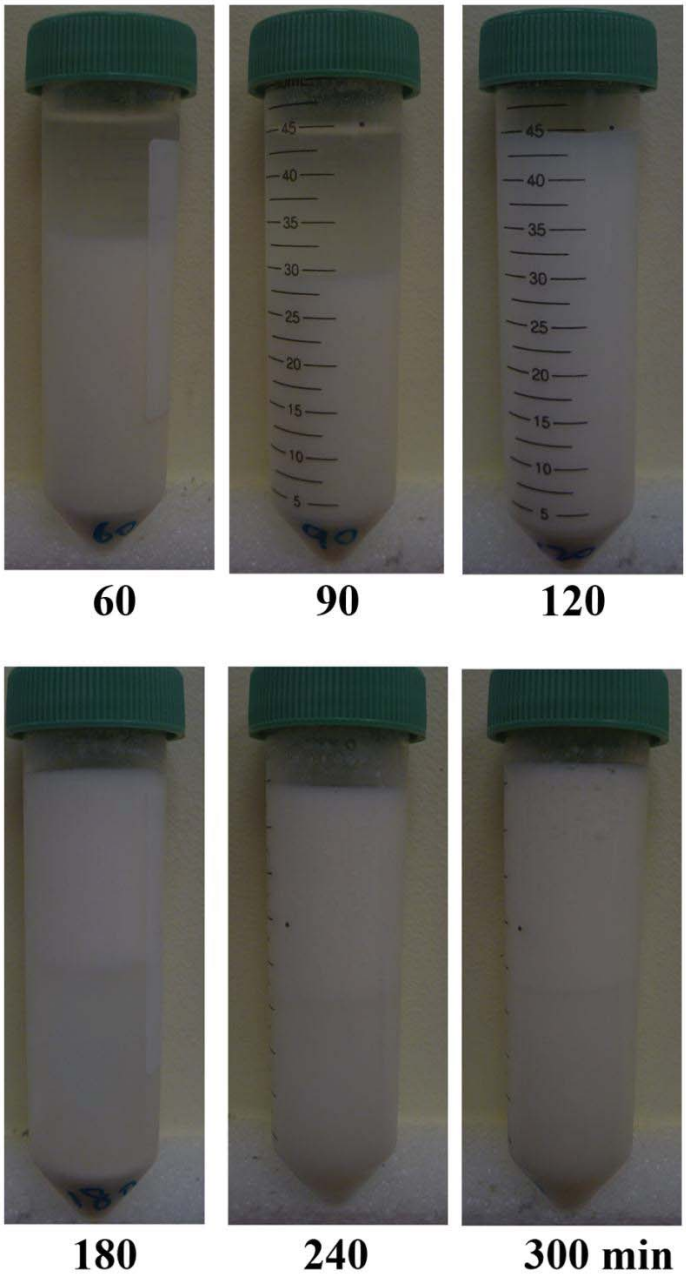

Figure 5-3 Typical images of emptied gastric digesta of whey protein emulsion gels during gastric digestion in the presence of pepsin.

5.3.3.2 Solid content of emptied digesta

The profiles of the solid content of the emptied digesta as a function of time are presented in Fig. 5-4. Without the addition of pepsin, the solid contents decreased with increasing digestion time for both soft and hard gels, with the solid content being higher for the hard gel than for the soft gel because of the smaller particle size of the gel bolus. With added pepsin, the solid contents of the emptied digesta of both gels were higher than those without pepsin because of pepsinolysis of the protein matrix. The solid content of the emptied digesta decreased with time during the first 180 min for both gels. However, the solid content of the emptied digesta of the soft gel increased significantly beyond 180 min, which was attributed to hydrolysis of the protein matrix at low pH (< 3). In contrast, the solid content of the emptied digesta of the hard gel showed no significant change after 180 min, implying that the effect of pepsin digestion was greater for the soft gel.

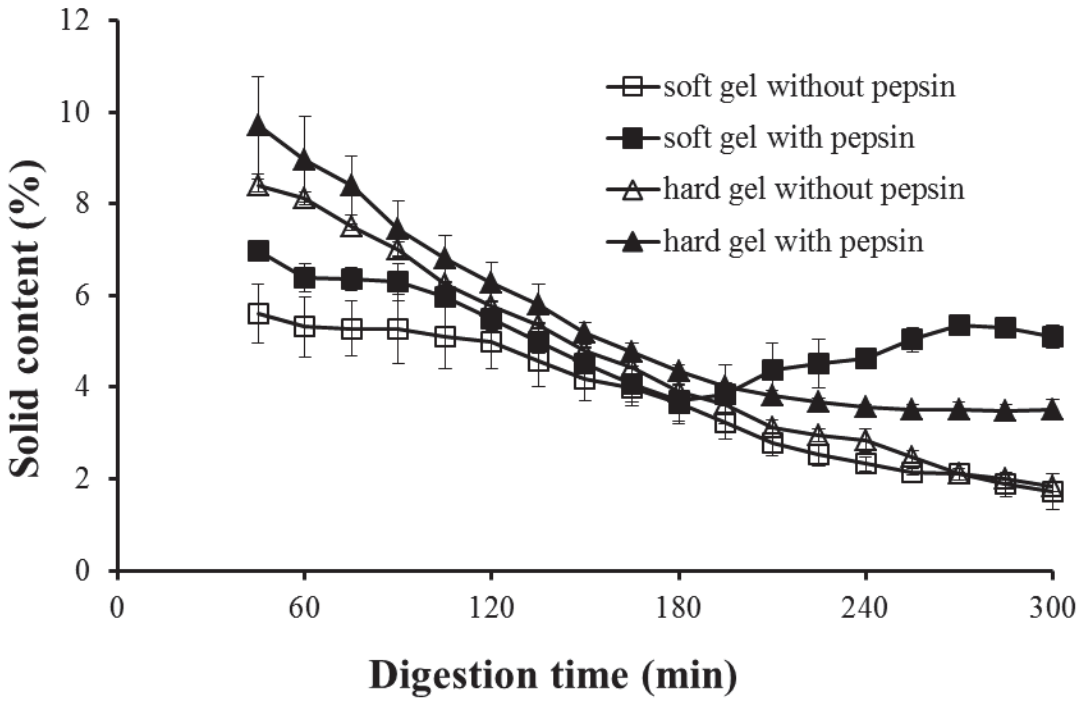

Figure 5-4 Solid content of emptied digesta as a function of time.

5.3.3.3 Particle size distributions of emptied digesta

Evolution of particle size of emptied gastric digesta with digestion time is important to understand the whole process of food digestion. The $D_{4,3}$ of particles within the emptied digesta are presented in Fig. 5-5. Without the addition of pepsin, the $D_{4,3}$ for the soft gel particles increased significantly during the first 120 min but showed almost no change with further increase in the digestion time. The $D_{4,3}$ for the hard gel particles increased slightly throughout the 300 min of digestion. Overall, with the addition of pepsin, the $D_{4,3}$ values for both the soft gel particles and the hard gel particles were lower than those obtained without the addition of pepsin. For the soft gel, the $D_{4,3}$ increased significantly during the first 150 min of digestion and then decreased sharply. For the hard gel, the $D_{4,3}$ showed no significant change during the first 210 min of digestion and then decreased markedly from 210 to 300 min.

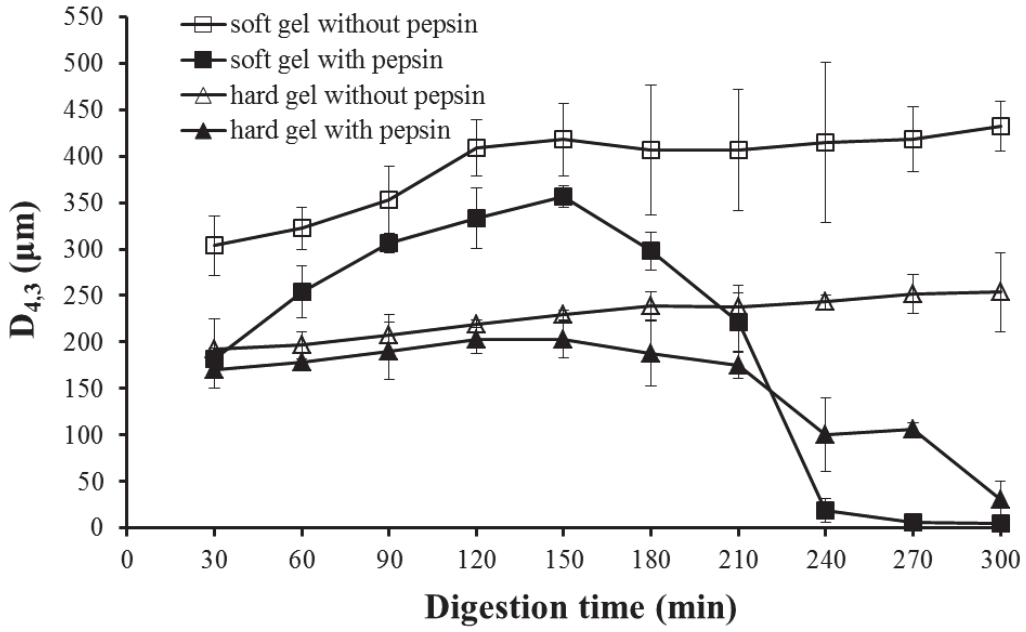

Figure 5-5 Volume-weighted average diameter ($D_{4,3}$) of emptied digesta as a function of time.

Particle size distributions of the emptied digesta with or without the addition of pepsin are presented in Fig 5-6. Without added pepsin, Figs. 5-6A1 and B1show that the

particle sizes for both soft gels and hard gels were between ~ 2 and 2000 μm, with two peaks (one at ~ 100 μm and the second at ~ 1000 μm). The peak at 1000 μm was much higher than that at ~ 100 μm for the soft gel whereas the peak at 1000 μm was much lower than that at 100 μm for the hard gel. For the soft gel, the areas of the peaks at 100 and 1000 μm decreased and increased markedly respectively during the first 120 min of digestion and then changed little with further digestion. For the hard gel, the overall particle size distribution showed no obvious change. For both soft gels and hard gels, the peak at 100 μm did not move towards a smaller size with an increase in the digestion time.

In the presence of pepsin, the simulated gel bolus disintegrated further (Figs. 5-6A2 and B2). For the soft gel, from 30 to 150 min of digestion, the area of the peak at 100 μm gradually decreased and a new peak appeared at ~ 10 μm whereas the area of the peak at 1000 μm gradually increased to a maximum value. From 150 to 210 min, the area of the peak at 1000 μm gradually decreased, the peak at 100 μm disappeared, the area of the peak at 10 μm gradually increased to a maximum value and a new peak appeared at ~ 0.45 μm. Beyond 240 min, the peak at 1000 μm almost disappeared, the volume of the peak at 10 μm decreased and the area of the peak at 0.45 μm gradually increased, indicating that the large particles were being totally broken down and that most of the oil droplets were being released from the protein matrix. For the hard gel, the area of the peak at 1000 μm increased slightly during the first 150 min of digestion and then decreased. The peak at 100 μm gradually moved to 10 μm, with the area of the peak at 10 μm increased sharply after 210 min, with its shift towards a smaller size being very slow after 210 min. After 300 min of digestion, the emptied digesta consisted mainly of ~10 μm particles, with some particles between 100 and 1000 μm and no peak at 0.45 μm, in contrast to the observations on the soft gel.

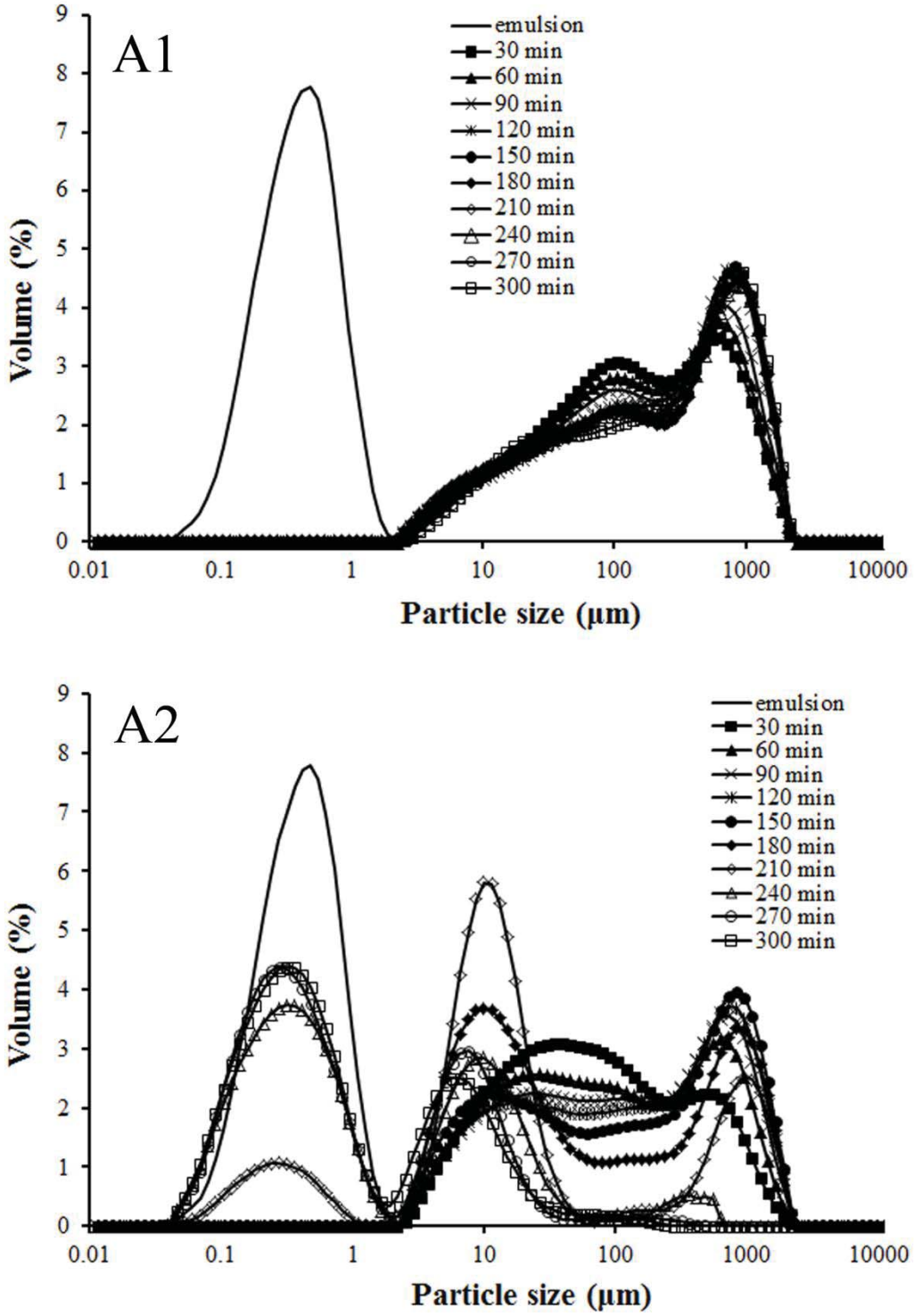

(**Fig 5-6** continued)

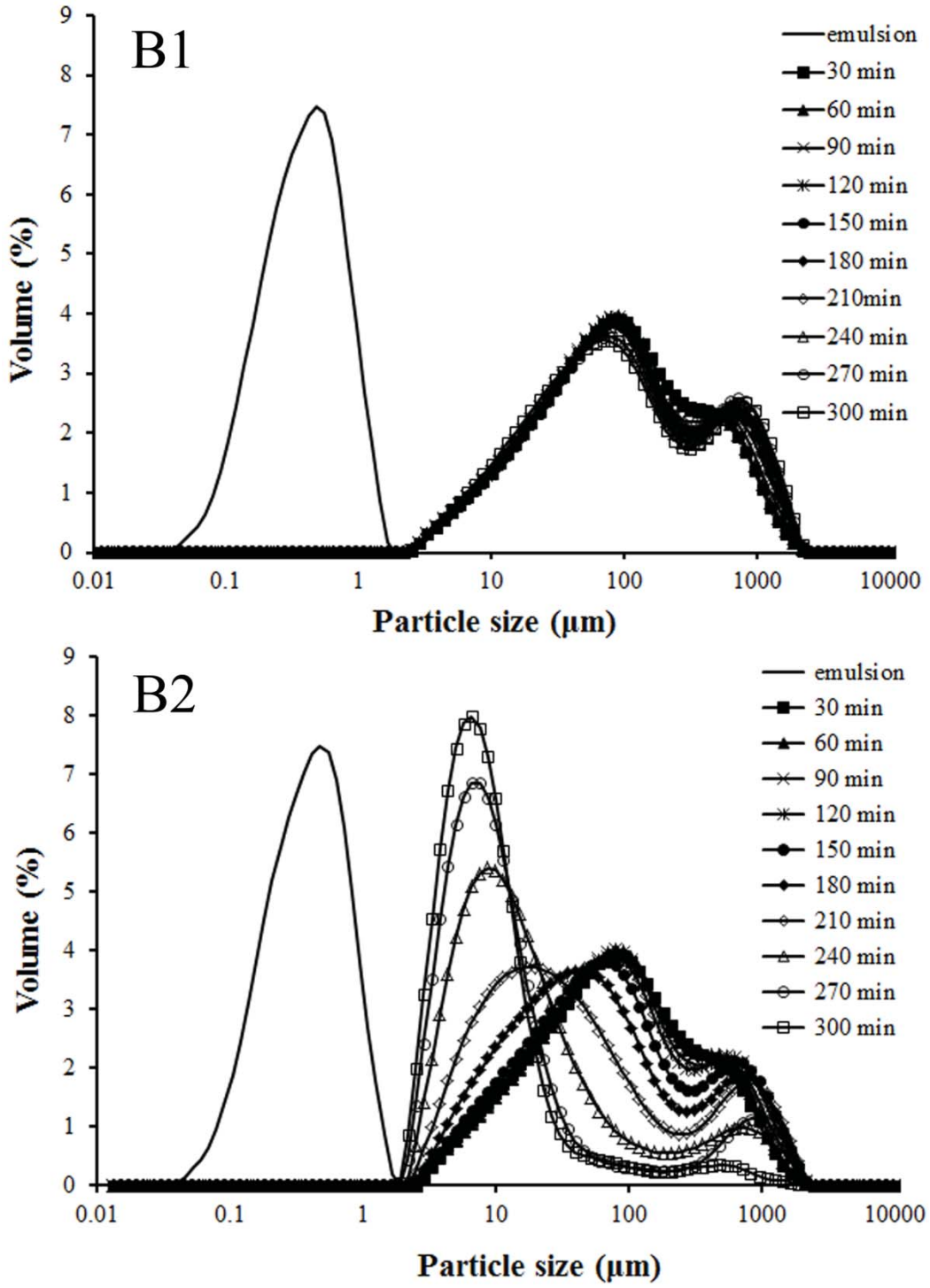

Figure 5-6 Particle size distributions of emptied digesta: A1, soft gel without pepsin; A2, soft gel with pepsin; B1, hard gel without pepsin; B2, hard gel with pepsin.

5.3.3.4 Stability of oil droplets

To examine coalescence of oil droplets, the size of the oil droplets was determined by dissolving the emptied digesta in a SDS and 2-mercaptoethanol solution, which can liberate and stabilize oil droplets (Fig. 5-7). For the soft gel, both without and with the addition of pepsin, the $D_{4,3}$ of the oil droplets within the emptied digesta showed no significant changes during the first 60 min and then increased to a maximum value at around 150−180 min; with further digestion, the $D_{4,3}$ decreased gradually, with that for the soft gel with added pepsin showing a greater decrease. For the hard gel, the $D_{4,3}$ of the oil droplets within the emptied digesta showed no change throughout the 300 min of digestion.

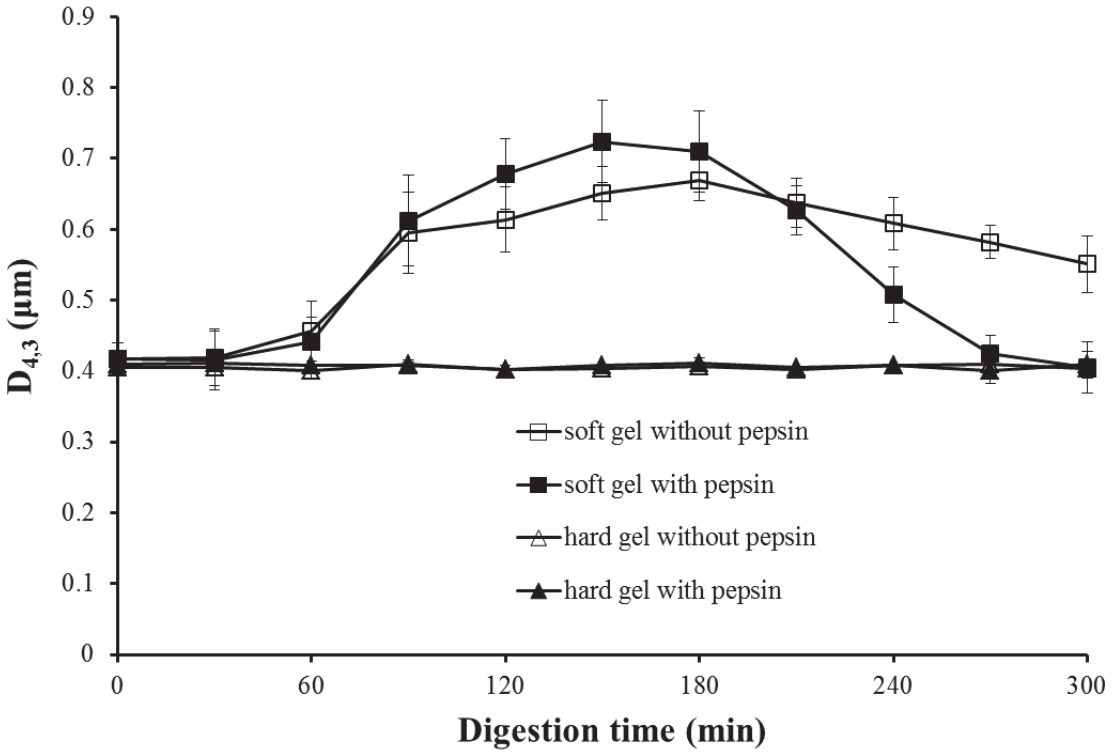

Figure 5-7 Volume-weighted average diameter ($D_{4,3}$) of oil droplets in emptied digesta as a function of time.

Particle size distributions of the oil droplets within the emptied digesta are presented in Fig. 5-8. For the soft gel, with and without the addition of pepsin, an obvious peak appeared at ~ 2−10 μm after 90 min of digestion, indicating possible coalescence of the oil droplets (Figs. 5-8A1 and A2). The areas of this peak were greatest at 180 and 150 min for digestion without and with pepsin respectively and then decreased with further digestion, especially in the presence of pepsin (Figs. 5-8A1 and A2). For the hard gel, with and without the addition of pepsin, the particle size distributions showed no change (Figs. 5-8B1 and B2), indicating that there was no coalescence of the oil droplets during gastric digestion.

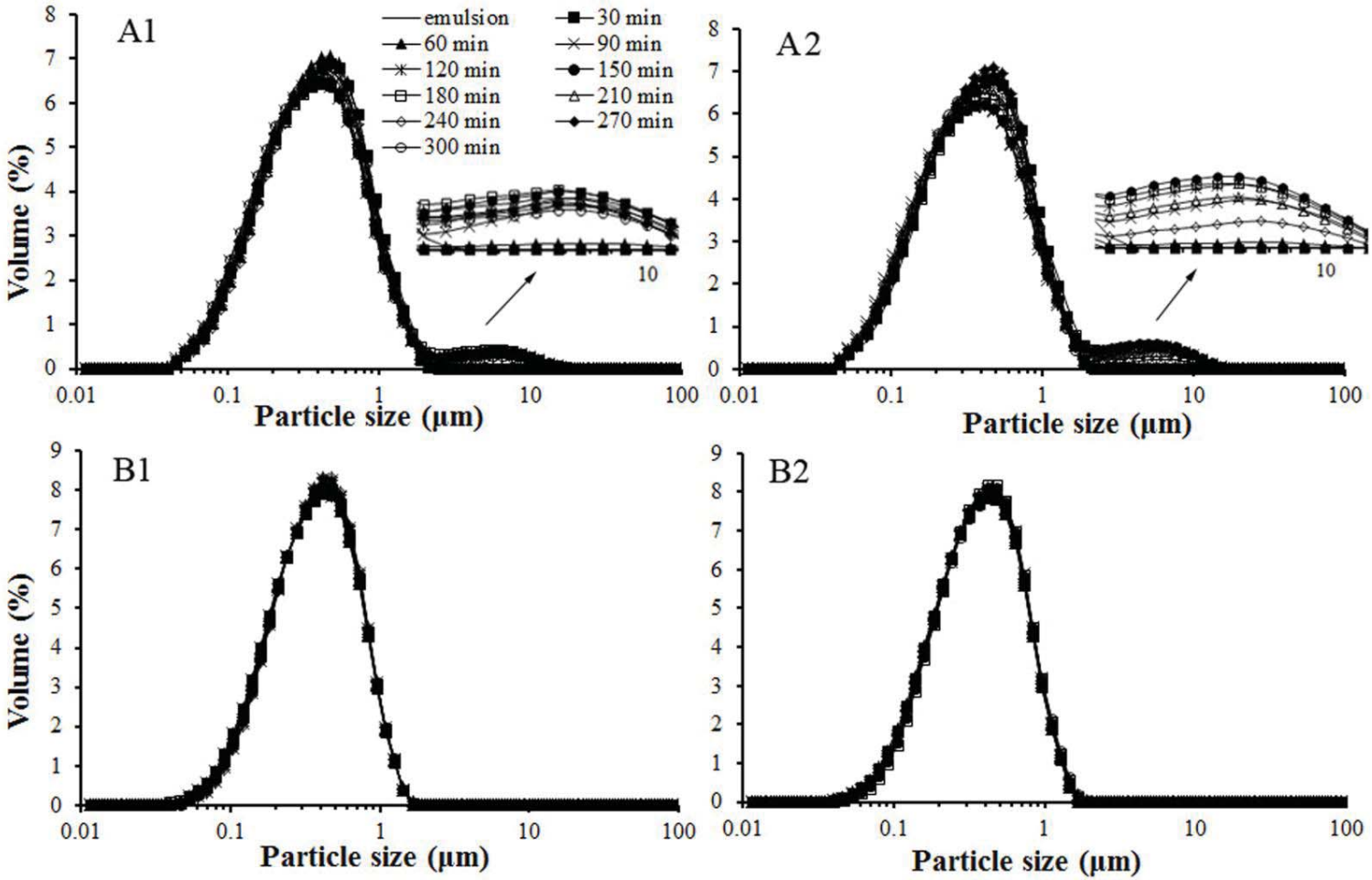

Figure 5-8 Particle size distributions of oil droplets in emptied digesta: A1, soft gel without pepsin; A2, soft gel with pepsin; B1, hard gel without pepsin; B2, hard gel with pepsin.

5.3.3.5 Microstructure of emptied digesta

The original soft and hard gels showed distinctly different structures (Fig. 5-9). At the micron scale, the soft gel appeared to have a continuous protein network (green) with the flocculation of oil droplets whereas the hard gel showed a more particulate structure with oil droplets evenly distributed.

In the emptied digesta of the soft gel, large oil droplets (around 2−10 μm) were observed at 120, 180 and 240 min whereas there were few large oil droplets at 60 and 300 min (Fig. 5-9A, ×400), which is consistent with the laser diffraction results (Figs. 5-7 and 8). During the first 180 min, the large gel particles gradually disintegrated into small particles (several to a few tens of microns), but still retained their structure (Fig. 5-9A, x3000), and released a small portion of oil droplets. However, at 240 and 300 min, the protein matrix appeared to be dissolved (the intensity of the green colour, which represents the protein concentration of the protein matrix, decreased sharply) and the gel particles were almost totally broken down, which explains the increase in the solid content of the emptied digesta after 180 min. Large quantities of oil droplets were released from the dissociated protein matrix, which is also consistent with the laser diffraction results. At 300 min, the emptied gastric digesta had an appearance similar to that of a typical liquid oil-in-water emulsion.

The hard gel showed a different behaviour. No large oil droplets were observed, no oil droplets were released from the protein matrix during the digestion process and large particles were gradually broken down into small particles (~ 10 μm) (Fig. 5-9B, ×400). The dissolution of the protein matrix appeared to be slow (the intensity of the green colour did not change significantly) and all oil droplets appeared to be connected firmly with the ~ 10 μm particles of the protein matrix, even after 300 min of digestion

(Fig. 5-9B, ×3000), which explains the slight increase in the solid content of the emptied digesta after 180 min.

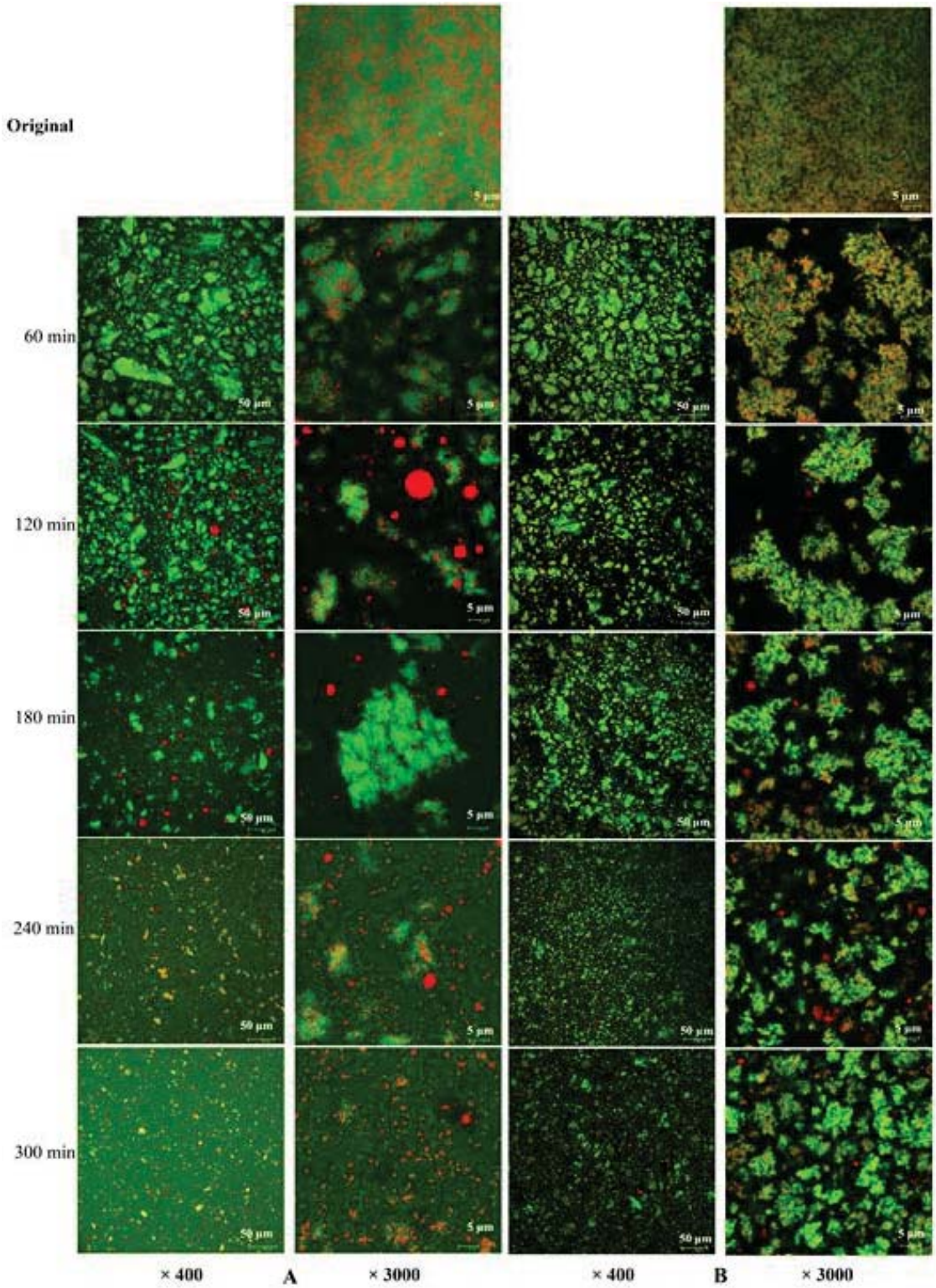

Figure 5-9 Microstructure of emptied digesta as a function of time: A (soft gel) and B (hard gel). x400 and x3000 represent the low and high magnification respectively. Green colour represents protein, red colour represents the oil phase, and black colour represents air or water.

5.3.3.6 SDS-PAGE of protein patterns in emptied digesta

SDS-PAGE patterns of emptied gastric digesta in the absence of pepsin are presented in Fig. 5-10. The lane of 0 min described the protein patterns in whey protein emulsion gels which mainly contain β-Lg and α-La for both gels. For the soft gel, the whey proteins were not affected during the first 180 min. After that time, the protein hydrolysis occurred slightly with the appearance of peptides of 10 kDa. For the hard gel, the proteins remained intact during the first 150 min. After that time, the slight protein hydrolysis occurred. This may be attributed to the acid hydrolysis of proteins (Synge, 1945; Harris et al., 1956; Zhong et al., 2005). The amounts of protein reduced with time because of the decrease of solid content in the emptied gastric digesta with time (30 to 300 min).

SDS-PAGE patterns of emptied gastric digesta in the presence of pepsin are presented in Fig. 5-11. In both the soft and hard gels, β-Lg and α-La were gradually digested by pepsin, with no intact whey proteins remaining after 240 min. The molecular weights of the main peptides released during digestion was below 10 kDa. Both protein appeared to be hydrolysed slightly faster in the soft gel than in the hard gel, particularly during the first 60 min (see the bands at 30 and 60 min in Figs. 5-10A and B), which is consistent with the previous study on the digestion of fine-strand (soft) and particulate (hard) whey protein gels under the simulated gastrointestinal conditions (Liang et al., 2010).

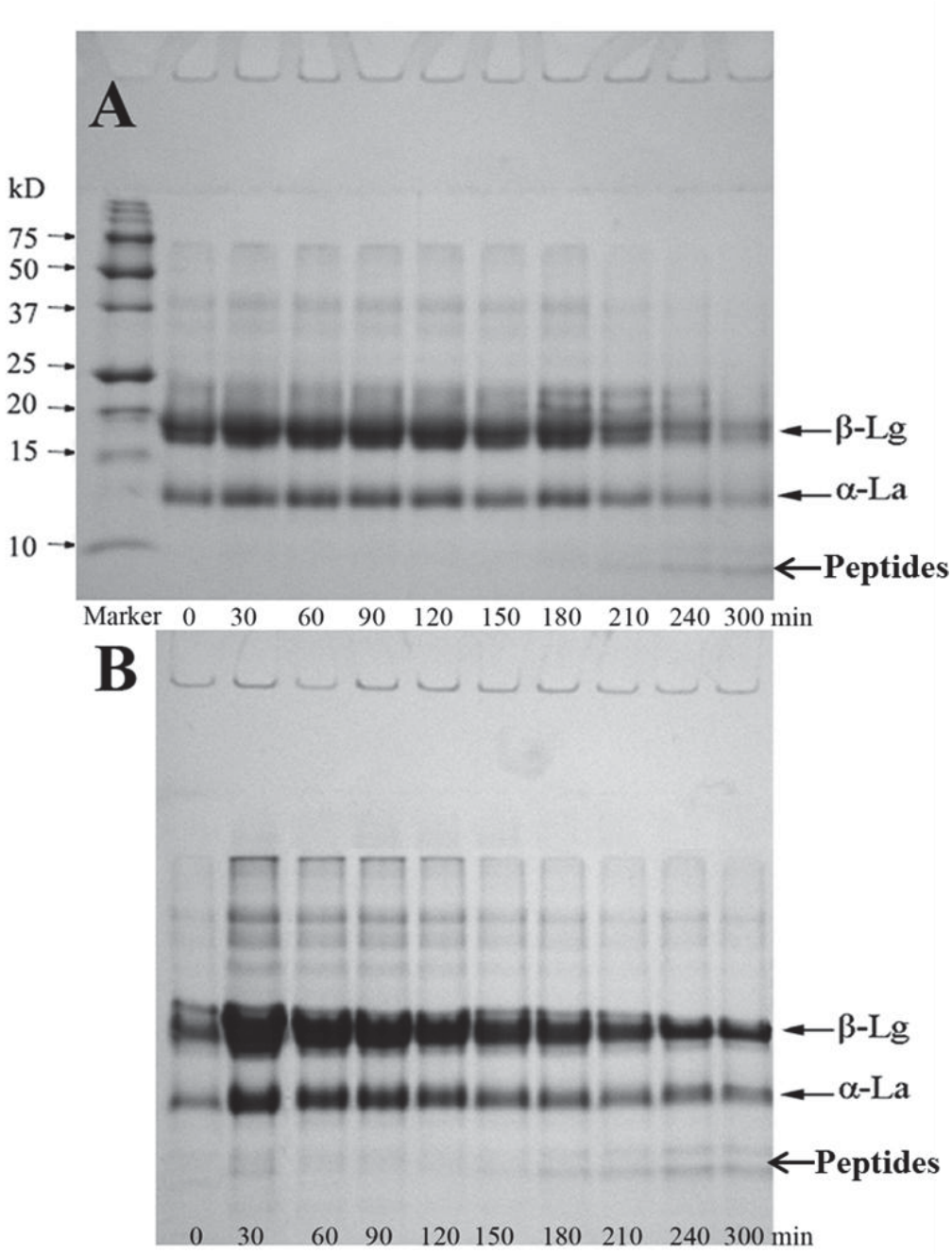

Figure 5-10 Tricine SDS-PAGE patterns under reducing conditions of proteins in emptied digesta in the absence of pepsin: A, soft gel; B, hard gel.

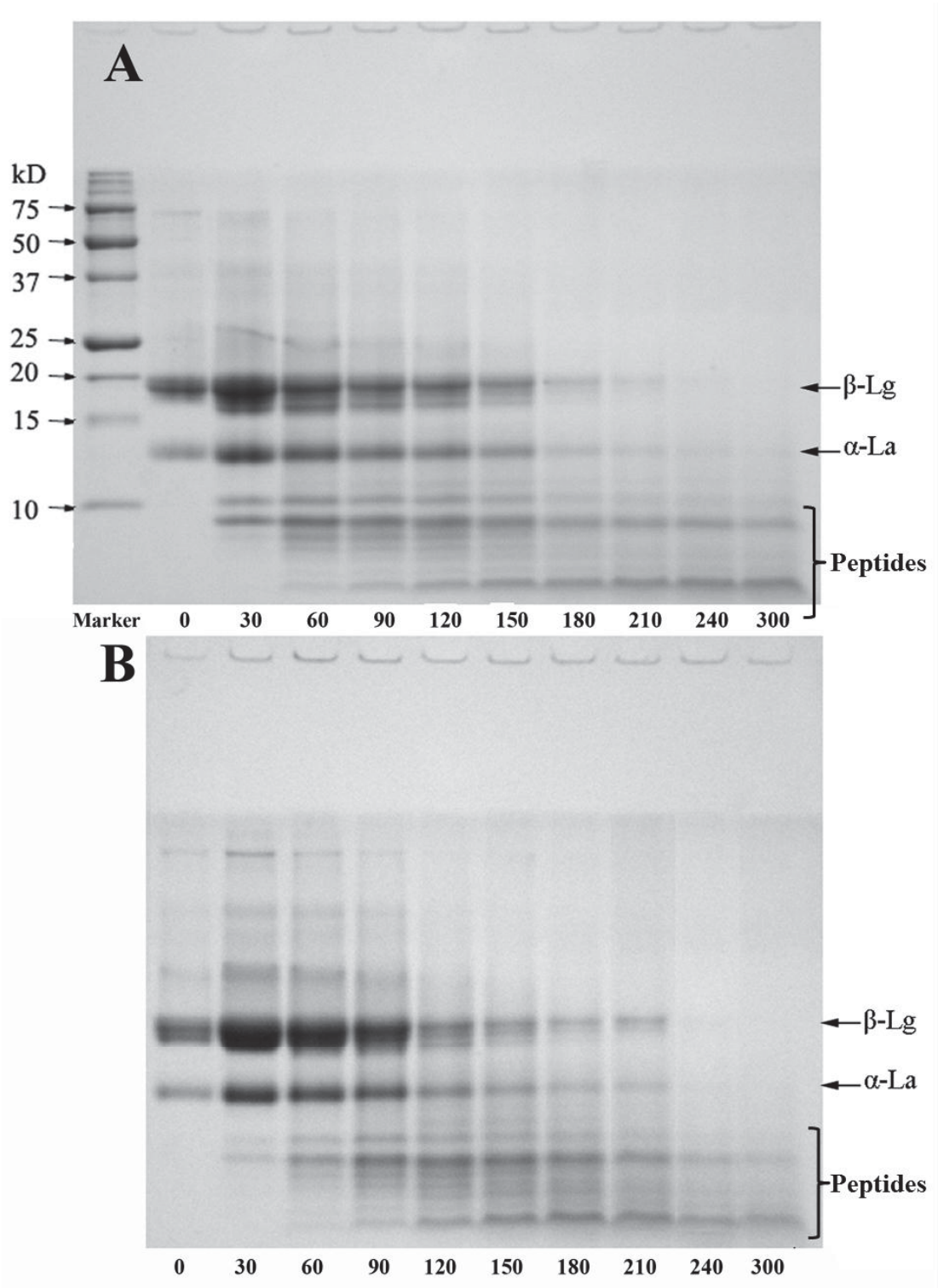

Figure 5-11 Tricine SDS-PAGE patterns under reducing conditions of proteins in emptied digesta in the presence of pepsin: A, soft gel; B, hard gel.

5.3.4 Gastric digestion of gels at the low level of pepsin

5.3.4.1 Particle size distributions of emptied digesta

Gastric digestion of gels at a lower level of pepsin provides a good comparison to that at a higher level and can better explain the role of pepsin during gastric digestion. Fig. 5-12 presents the temporal evolution of particle size distributions of emptied digesta of the soft gel during gastric digestion at a low level of pepsin (1 g/L). The changes in particle size distributions showed a similar trend to those at a high level of pepsin (3 g/L) as shown in Fig. 5-6A2. The volume of the peak at ~ 1000 μm increased to the highest value at 180 min and had a significant decrease at 240 min. The peak at ~ 100 μm shifted to the smaller size (~ 10 μm) with the digestion time. A new peak between 0.1 to 1 μm (individual oil droplets) appeared at 240 min with the volume of the peak at ~ 10 μm reaching the maximum value, which was about 30 min later than that at a high level of pepsin. This indicates that higher pepsin level promoted the digestion of gels.

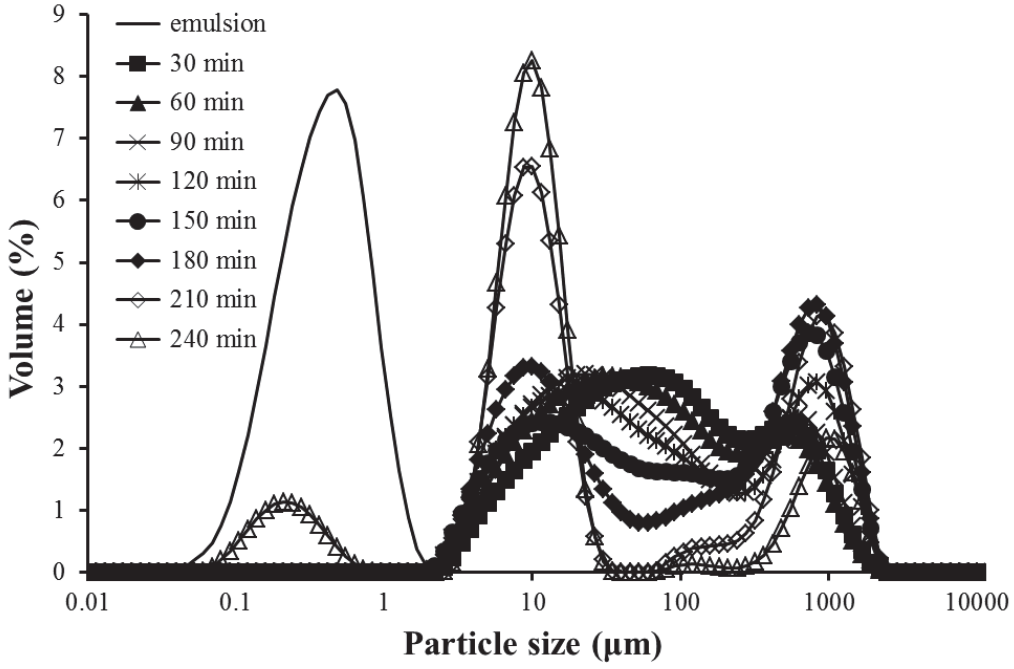

Figure 5-12 Evolution of particle size distributions of emptied digesta during gastric digestion at the low level of pepsin.

The changes in $D_{4,3}$ during gastric digestion of the soft gel are presented in Fig. 5-13. During the first 180 min, the $D_{4,3}$ of the emptied gastric digesta of the soft gel significantly increased from ~ 178 to ~ 363 μm. After that time (180 min), the $D_{4,3}$ had a sharp decrease because of pepsin digestion (pepsin activity is very high at the pH below 3). These changes of $D_{4,3}$ of the emptied digesta at a low level of pepsin was also similar to those observed at the high level of pepsin (Fig.5-5). The main difference were that at the low level of pepsin the sharp decrease of $D_{4,3}$ occurred 30 min later than that at the high level of pepsin.

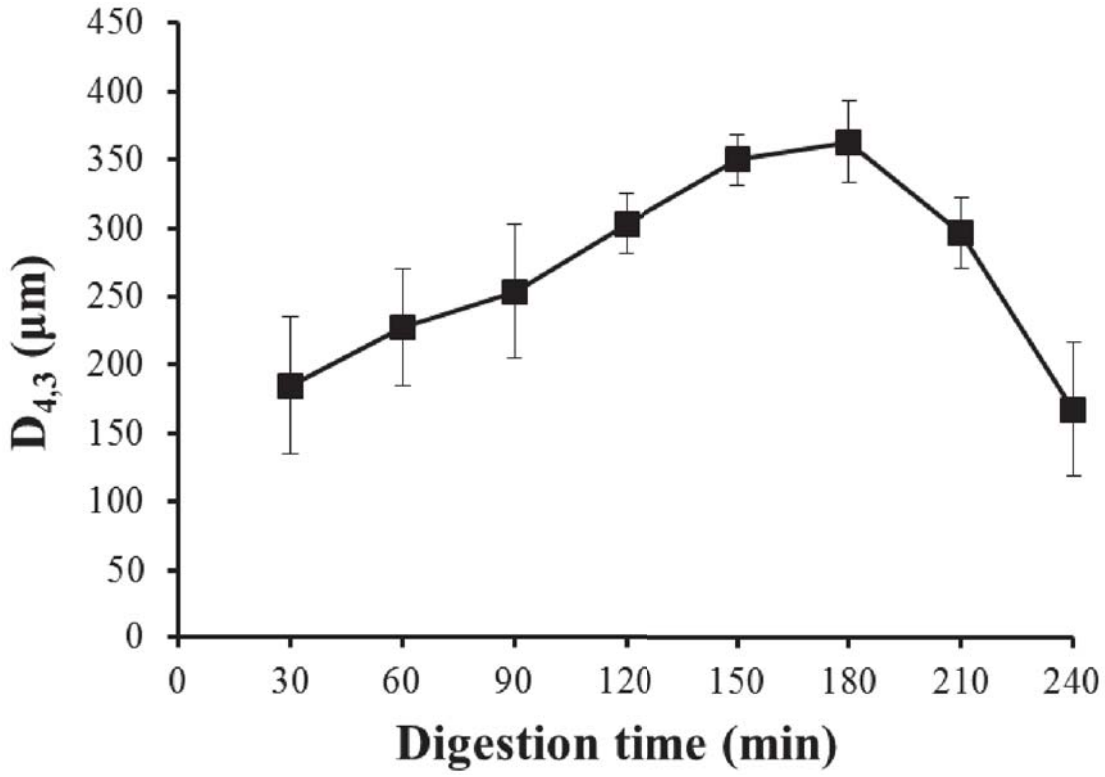

Figure 5-13 $D_{4,3}$ of emptied gastric digesta of the soft gel as a function of time at the low level of pepsin.

5.3.4.2 Stability of oil droplets

The particle size distributions of oil droplets in the emptied gastric digesta of the soft gel are presented in Fig. 5-14. At 30 min, there was only one peak in the particle size distribution of emptied digesta, which was similar to that of original emulsion.

With further digestion, a small peak between ~1 to ~ 10 μm appeared which indicates that the coalescence of oil droplets occurred during gastric digestion. This small peak gradually increased with the digestion time reaching to the maximum at 120 min. After 120 min, the area of this peak gradually decreased. In general, the degree of coalescence of oil droplets incorporated in the gels during the gastric digestion was low.

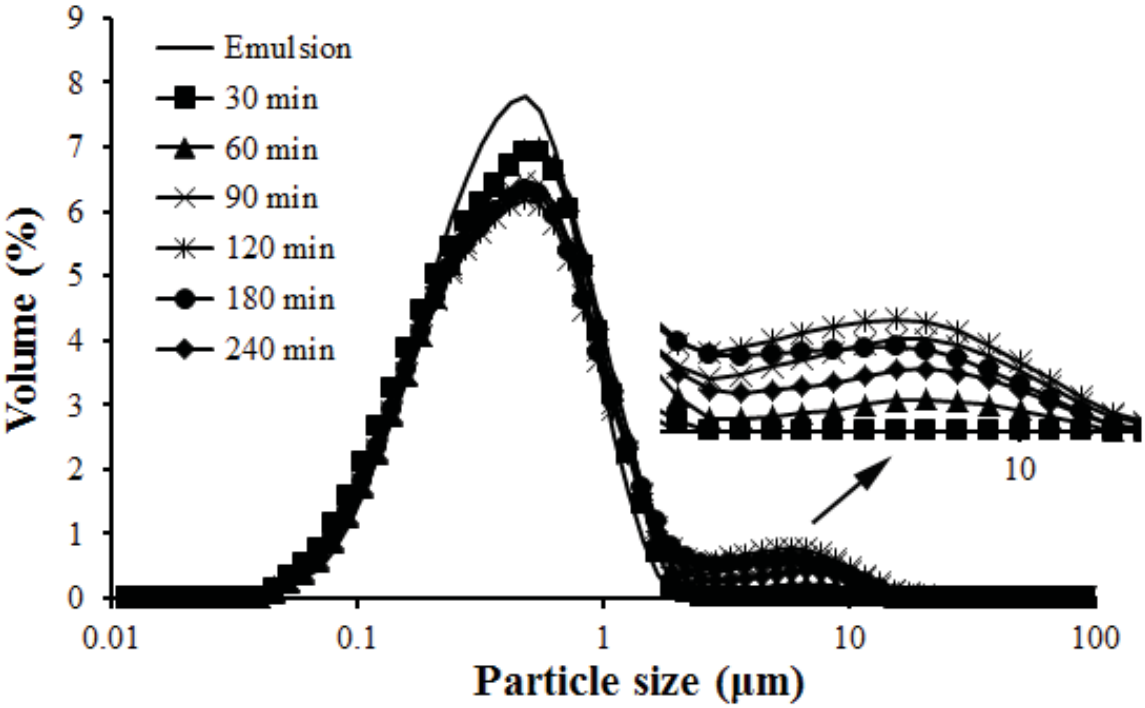

Figure 5-14 Evolution of size distribution of oil droplets in the emptied gastric digesta of the soft gel as a function of time at the low level of pepsin.

The evolution of $D_{4,3}$ of oil droplets in the emptied gastric digesta of the soft gel with time is presented in Fig. 5-15. During the first 30 min, the oil droplets in the emptied digesta were stable (i.e. the $D_{4,3}$ had no changes). With increasing time from 30 to 120 min, the value of $D_{4,3}$ significantly increased from ~ 0.425 to ~ 0.924 μm. After that time (120 min), the $D_{4,3}$ gradually decreased with time indicating the decreasing degree of coalescence of oil droplets.

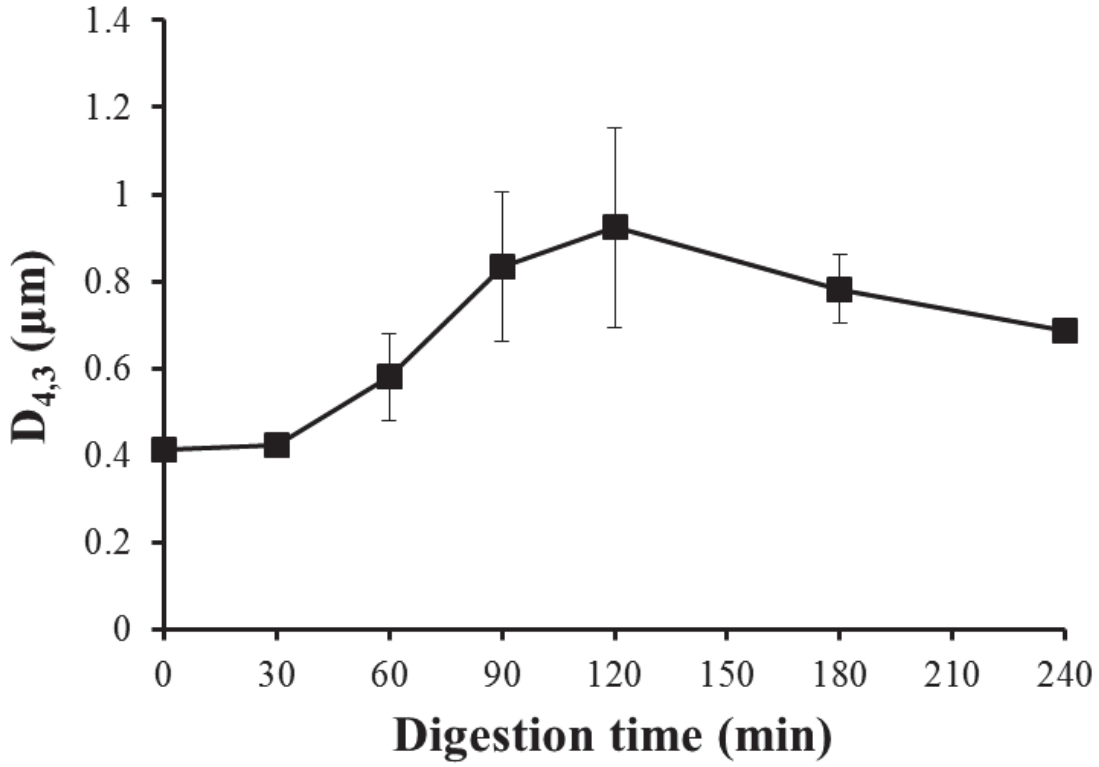

Figure 5-15 $D_{4,3}$ of oil droplets in the emptied gastric digesta of the soft gel as a function of time at the low level of pepsin.

5.3.4.3 Microstructure

The microphotographs (Fig. 5-16) revealed that the gel particles of the soft gel were gradually disrupted during gastric digestion. During this process, a small portion of oil droplets were released from the gel particles and the low degree of coalescence of oil droplets occurred. With digestion time, the size of small particles in the emptied gastric digesta decreased because of pepsin digestion, which is consistent with the results of laser diffraction. At 180 and 240 min, the gel particles were disintegrated into the particles of ~ 10 μm. However, unlike the behaviour of the soft gel at the high level of pepsin (Fig.5-9), less oil droplets (~ 0.45 μm) appeared to release from the gel particles at 240 min, which is also consistent with results of laser diffraction. This indicates that a lower pepsin concentration slowed down the gel disintegration during gastric digestion especially after 180 min compared with the digestion at a high pepsin concentration.

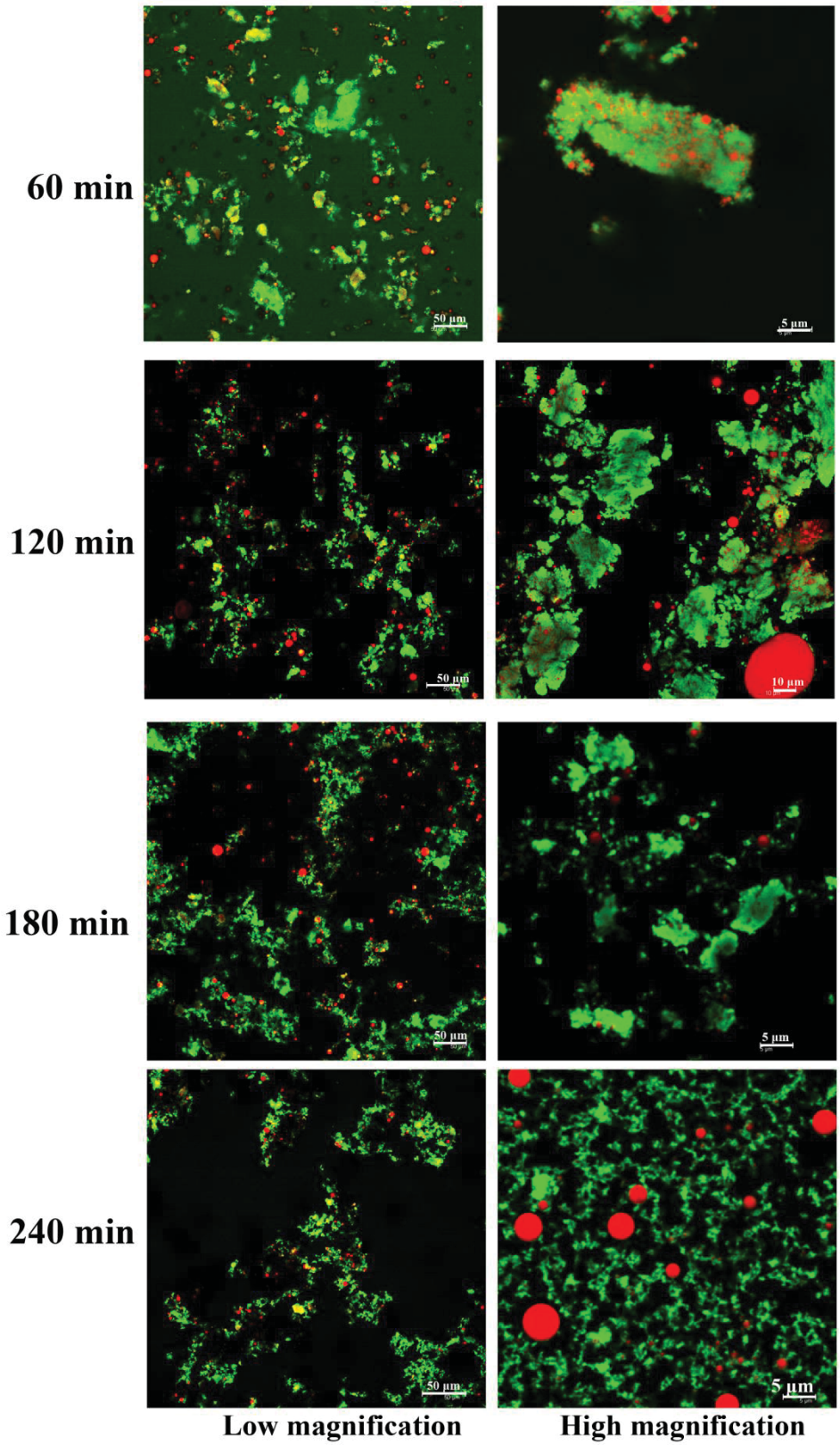

Figure 5-16 Microstructure of emptied gastric digesta of the soft gel as a function of time at the low level of pepsin. Green colour represents protein, red colour represents the oil phase, and black colour represents air or water.

5.3.4.4 Protein hydrolysis

The hydrolysis patterns of whey proteins during gastric digestion at a low level of pepsin are presented in Fig. 5-17. The 0 min lane showed the proteins in the original gel bolus, which mainly included two bands; one at 18 kDa (β-Lg) and the other one at 14 kDa (α-La). At 30 min, peptides with molecular weight of ~ 10 kDa were generated. With further digestion, β-Lg and α-La were gradually hydrolysed with generation of more peptides of ~ 10 kDa and peptides smaller than 10 kDa. At 240 min, some intact β-Lg and α-La still remained. The rate of protein hydrolysis in the emptied gastric digesta at the low level of pepsin was lower than that at the high level of pepsin. This explains the slower breakdown of gel particles and release of oil droplets from the gel particles during gastric digestion.

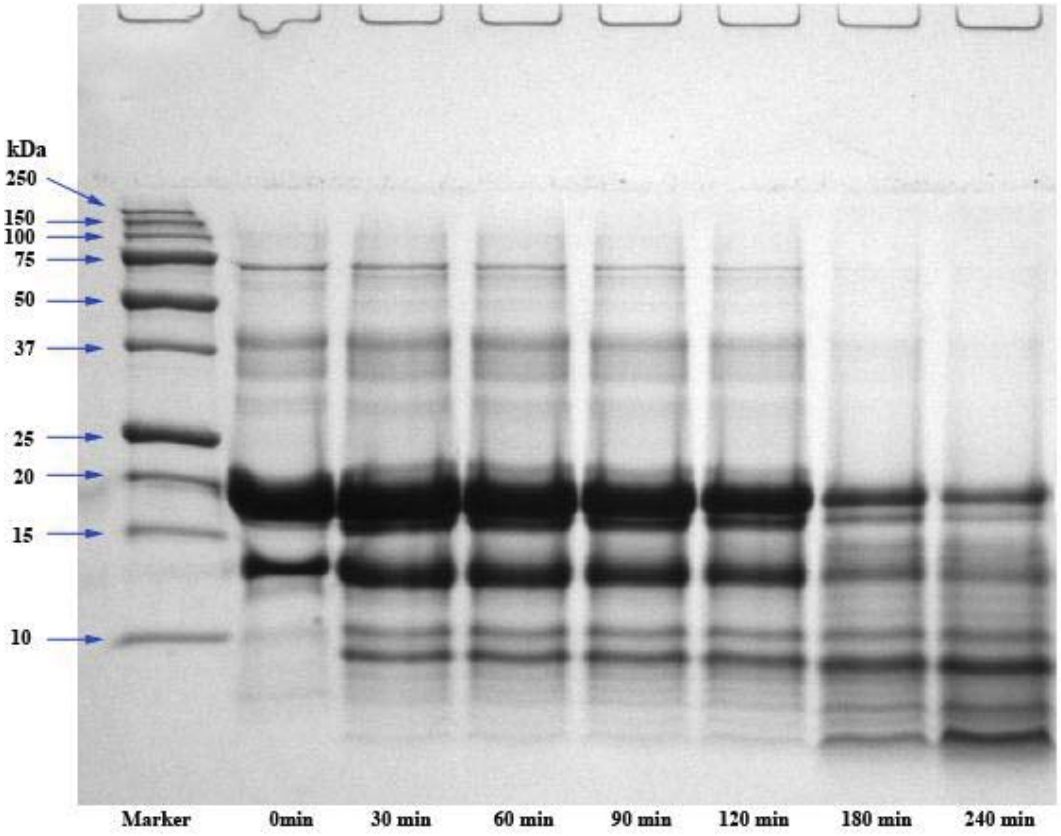

Figure 5-17 Tricine SDS-PAGE patterns under reducing conditions of proteins in emptied digesta of the soft gel at the low level of pepsin.

5.4 Discussion

In both the soft gels and the hard gels, a peak at ~100 μm appeared in the particle size distributions of the emptied digesta without added pepsin (Figs.5-6A1 and 6B1) even though these two gels had different structures. With an increase in the digestion time, this peak did not move towards a smaller size, indicating that the limit of mechanical fragmentation for the forces applied in the HGS had been reached. In the presence of pepsin, the hydrolysis of whey proteins into peptides led to further breakdown of the gel particles. The swelling behaviour of the whey protein emulsion gels (Fig. 5-1) suggested that pepsin could more easily permeate both gels, and this may aid the disintegration process. As observed from SDS-PAGE under reducing conditions, the hydrolysis rate of the whey proteins in emptied digesta was similar for both gels (Fig. 5-10). However, the effect of pepsin digestion on the breakdown of the soft gel was more prominent (Figs. 5-3, 4, 5, 6 and 9). Furthermore, in the presence of pepsin, the large particles of both the soft gels and the hard gels gradually disintegrated to ~10 μm particles (Figs. 5-6A2 and 6B2). With further digestion of the soft gel, the 10 μm particles were broken down into emulsion droplets (Figs. 5-6A2 and 9A); this was not observed in the hard gel (Figs. 5-6B2 and 9B). These differences were related to the structure of heat-set whey protein emulsion gels which influenced the type of peptides generated and subsequent migration to SGF (solvent).

The structure of a protein-stabilized emulsion gel can be understood as a combination of the structure of protein matrix, oil droplet size distribution and the extent of oil droplet-protein matrix interactions. The heat-induced gelation of whey proteins at neutral pH involves their aggregation into so-called primary aggregates, with a size of a few tens of nanometres, mainly via hydrophobic interactions and sulfhydryl−disulfide exchange (Dalgleish et al., 1997; Havea et al., 2001; Ikeda, 2003).

At low ionic strength, the primary aggregates associate into larger aggregates through 'head to tail' association because of the high intermolecular repulsion, resulting in the formation of a fine-stranded gel above a critical protein concentration (C_g). At high ionic strength (> 150 mM NaCl), the primary aggregates randomly associate into larger aggregates (because of a decreased intermolecular repulsion), which separate into compact and dense protein-rich domains (phase separation) with a radius of several microns. Subsequently, these domains randomly associate into a particulate gel at protein concentrations above the C_g (Ikeda et al., 2002; Ako et al., 2009b; Phan-Xuan et al., 2013).

During the formation of the emulsion gels, the situation is rendered more complex because the oil droplets are stabilized by adsorbed whey proteins, which will participate in the gelling reaction, but it is known that the gel structures are different (Ako et al., 2009b). The differences in gel structures caused by the different salt concentrations are shown in the confocal microscopy images shown in Fig. 5-9. The soft gel appeared to have undergone flocculation during the gelation process, so that there were distinct regions of protein and oil droplets. In contrast, the hard gel had a particulate structure and distinct regions of oil droplets and protein were not discernable; there were also indications of pores within the gel that were absent from the soft gel (Fig. 5-9). These results suggested that the oil droplets were more intimately involved in the gel structure of the hard gel. Moreover, the increase of salt level will promote the cross-links between whey proteins through both disulfide bridges and hydrophobic interactions (Verheul et al., 1998; Vardhanabhuti et al., 2001; Macierzanka et al., 2012) and will change the aggregation process of whey proteins, leading to changes in the interactions between adsorbed whey proteins and those in the gelling solution. There

will be increased interactions between oil droplets and protein matrix in the hard gel, compared to the soft gel.

As a result of the particulate structure and these strong cross-links between the whey proteins, some cleavage sites of the whey proteins are likely to be changed and/or made more difficult to access by pepsin in the hard gel. Thus, although the original proteins are broken down by pepsin at much the same rate in the two gels, the breakdown of the secondary peptides may be different. So, large peptides will be formed, cross-linked mainly by disulfide bridges and hydrophobic interactions during the gastric digestion of the hard gel (Peram et al., 2013). The large peptides generated from interfacial layers or protein matrix that is adsorbed at the oil-water interface (Persaud et al., 2000) will allow continued bridging between the oil droplets by sharing peptides or interacting with other peptides or proteins (Creusot et al., 2006). Therefore, although the proteins may be broken down by pepsin, the increased cross-linking (especially disulphides) of the peptides in the hard gel leads to the slow breakdown or the resistance to breakdown of the hard gel particles during the gastric digestion (Figs. 5-5 and 9B). By contrast, the proteins of the soft gel are more weakly cross-linked (Liang et al., 2010) and contain fewer disulphide bridges so that the matrix of the gel (fine-stranded structure) falls apart more readily than that of the hard gel. Thus the protein matrix is more rapidly dispersed, leading to the rapid disintegration of gel particles, especially after 180 min (Fig. 5-5 and 9A). The lack of crosslinks between matrix and adsorbed proteins at the surfaces of the oil droplets allows the release of individual fat droplets. Thus the disintegration patterns of the two gels depend on the crosslinking originally present in the gel structures.

In addition, the mechanical instability of gel particles induced by the gel swelling may be another important factor influencing the disintegration of gel particles

during gastric digestion. The gel swelling weakens and disrupts the elastic gel network that lead to the mechanical instability of gel particles (Tanaka et al., 1987). The gel swelling probably has a greater effect on the disintegration of the soft gel because of a greater swelling ability than the hard gel.

During digestion, the pH in the HGS slowly passes through the iso-electric point of the denatured whey proteins (~ pH4−5), which is likely to be the cause of the flocculation of liberated oil droplets (Helbig et al., 2012; Shani-Levi et al., 2013). In the soft gel, coalescence of the oil droplets can be attributed to flocculation of the released oil droplets and mechanical shearing. Pepsin hydrolysis of interfacial layers of released oil droplets may also contribute to coalescence of released oil droplets in this gel (Sarkar et al., 2009b). For the hard gel, no coalescence of oil droplets was observed as none were released during digestion due to the strong interactions between oil droplets and protein matrix.

In the experiments conducted at a low level of pepsin (1 g/L), the gels had a similar behaviour to those conducted a high level of pepsin (3 g/L) (Figs. 5-12, 13, 14, 15 ,16 and 17). The digestion of the gels was slower at a lower pepsin concentration. However, the increase of pepsin concentration by 3 times did not greatly accelerate the gastric digestion of the gels.

During gastric digestion, the food must be disintegrated into particles small enough to pass through pylorus. Therefore, a schematic diagram of the breakdown of soft and hard gel particles in the HGS is presented in Fig. 5-18. Large particles in both the soft and hard gel boluses with so-called fine-stranded and particulate structure respectively are disintegrated into ~ 10 μm particles. With further digestion, ~ 10 μm particles with fine-stranded structure are disrupted into free oil droplets in the soft gel whereas those with particulate structure resist the breakdown in the hard gel.

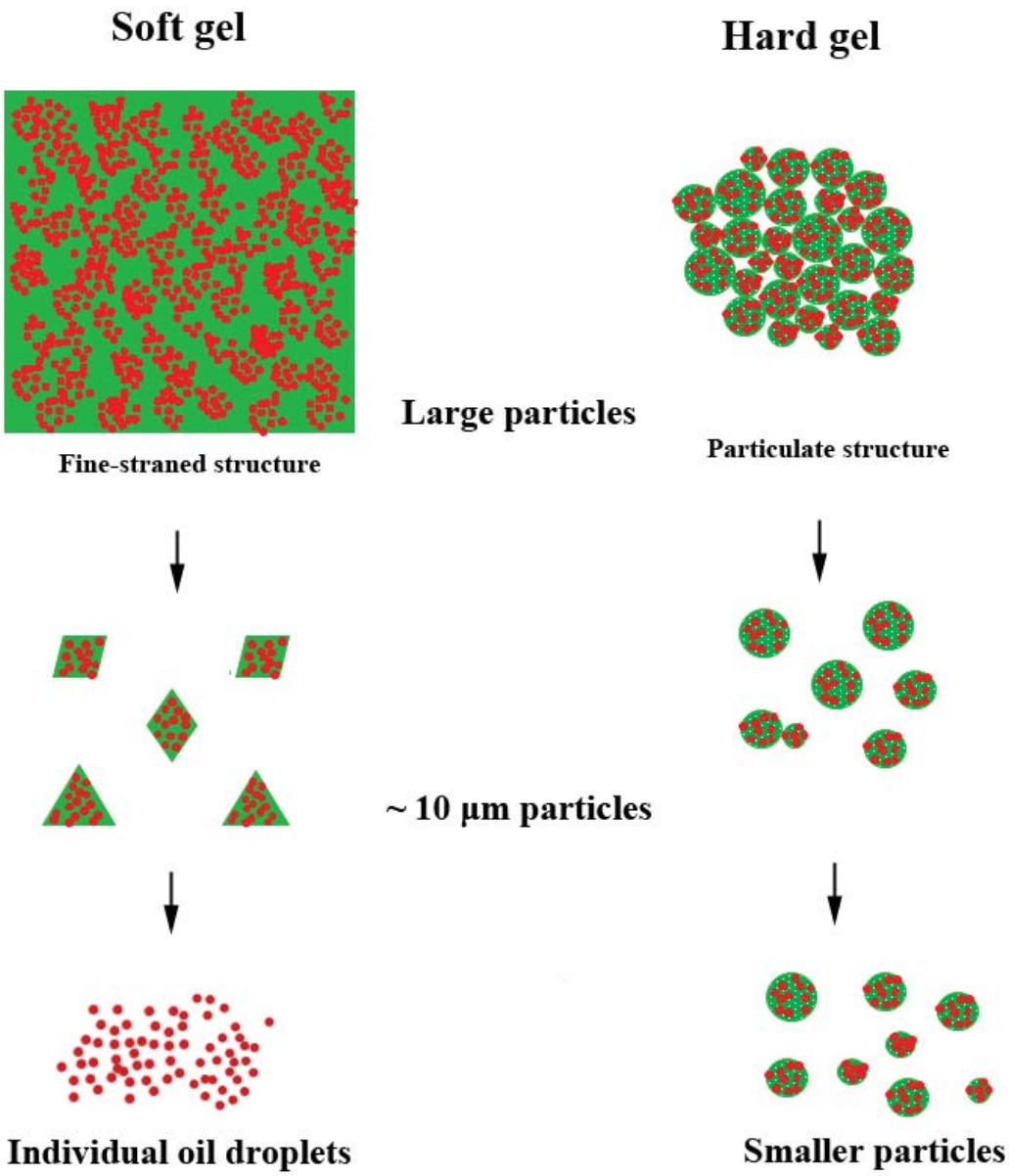

Figure 5-18 Schematic diagram of the breakdown of soft and hard gel particles during gastric digestion. Green colour represents the protein matrix; red colour represents oil droplets.

5.5 Conclusions

This study presented an overview of the digestion behaviour of simulated gel boluses of heat-set whey protein emulsion gels in an HGS, in which both proteolysis of the gel structure by pepsin and mechanical shearing of the stomach played a key role in their disintegration in the gastric environment. The gastric digestion of gels was greatly

influenced by the gel structure. The soft gel had a fine-stranded continuous protein matrix filled with oil droplets. The hard gel had a porous structure. Most proteins adsorbed and coated at the surfaces of oil droplets; the hard gel appeared to be formed by the aggregation or cross-linking of protein coated oil droplets. A 'hard' gel structure can slow down disintegration of the protein matrix and the subsequent gel particles (~ 10 μm) were still retained in the structure with no oil droplet release after 5 h of digestion, whereas a 'soft' gel structure can be totally broken down after 4 h of digestion, with the protein dissolving and oil droplets being released. In addition, a low pepsin level in SGF during *in vitro* gastric digestion led to slower gel disintegration.

Chapter 6 Disintegration Kinetics of Food Gels During Gastric Digestion and its Role on Gastric Emptying[3]

6.1 Abstract

In this study, a dynamic stomach model (human gastric simulator, HGS) was employed to investigate the disintegration and subsequent emptying of two differently structured whey protein emulsion gels (soft and hard gels). The gels were mechanically ground into fragments to reproduce the particle size distribution of an in vivo gel bolus. The simulated gel bolus was prepared by mixing gel fragments and artificial saliva, and exposed to 5 hours of simulated gastric digestion in the presence and absence of pepsin. Results showed that regardless of pepsin, the soft gel always disintegrated faster than the hard gel. The presence of pepsin significantly accelerated the disintegration of both gels. The emptying of the gels was influenced by the combined effects of the original particle size of the gel boluses and their disintegration kinetics in the HGS. In the presence or absence of pepsin, the larger particles of the soft gel emptied slower than those of the hard one during the first 120 min of process. However, in the presence of pepsin, the soft gel emptied faster than the hard one after 120 min because of a higher level of disintegration. These findings highlight the role of food structure, bolus properties and biochemical effects on the disintegration and gastric emptying patterns of gels during gastric digestion.

[3]Part of contents presented in this chapter has been published in a peer-reviewed paper: Guo, Q., Ye, A., Lad, M., Ferrua, M., Dalgleish, D., & Singh, H. (2015). Disintegration Kinetics of Food Gels During Gastric Digestion and its Role on Gastric Emptying: an in vitro Analysis. *Food and Function, 6*(3), 756-764.

6.2 Introduction

As the first step in the digestion of food by the human body, mastication breaks down food into small particles and mixes it with saliva to form a cohesive bolus ready for swallowing (Chen, 2009). Human subjects appear to select different patterns of food oral processing (e.g. number of chewing cycles, masticatory force and jaw activity) based on the properties of the foods (Agrawal et al., 1998; Kohyama et al., 2004; Foster et al., 2006; Mishellany et al., 2006). The fragmentation degree of foods during oral processing increases linearly with gel hardness, with the soft foods reaching a larger threshold size for swallowing than the hard foods (Peyron et al., 2004; Jalabert-Malbos et al., 2007). The fragmentation and lubrication experienced in the mouth permanently change the physical and chemical form of food and influence its digestion in the stomach (Urbain et al., 1989; Bornhorst et al., 2013).

Following the mouth, the stomach is the main site for the food disintegration (Moore et al., 1986). The most important function of the stomach is mixing and disintegrating the meal into a semi-solid mixture that is continuously delivered into the intestine for further digestion and absorption. Peristaltic movements of the stomach wall (known as antral contraction waves, ACWs) mix, shear, and force food towards the pylorus (Ferrua et al., 2010). The emptying of the gastric chyme into the small intestine is modulated by the periodic opening of the pylorus sphincter in coordination with the ACW activity. As the antral contraction approaches the pylorus, the ACWs propel the chyme forward toward the pyloric sphincter, the sphincter closes and the indentation of ACWs deepens, resulting in mechanical shearing and grinding (Ehrlein & Schemann, 2005). The repeated shearing and grinding of gastric contents by the ACW together with the biochemical degradation of acids and enzymes facilitate the progressive digestion of solid food until it is suitable for further digestion in the intestine.

For solid foods, the disintegration kinetics in the stomach is an important factor influencing the gastric emptying as the pyloric sphincter is selective, retaining particles > 1-2 mm in size (Malagelada et al., 2010). Knowledge of the disintegration of solid food in the mouth and stomach will improve our understanding of the form in which foods pass into the small intestine and help in the development of novel foods for the targeted and controlled delivery of nutrients (Norton et al., 2007; Golding et al., 2010). A few studies have examined the influence of the properties of original food on its gastric digestion. *In vivo* studies have shown that soft agar gels swallowed without chewing are emptied faster than rigid ones, suggesting that the soft food is disintegrated faster than the hard one, and that meal viscosity significantly affects the food disintegration in the stomach (Marciani et al., 2001a; Marciani et al., 2001b). In addition, the food structure and moisture content have been reported to be the key factors controlling the breakdown rate of food bolus during *in vitro* gastric digestion (Bornhorst et al., 2013).

In this chapter, the simulated gel boluses were created from two differently structured whey protein emulsion gels (soft and hard) which are similar to gel boluses produced by chewing in human subjects. The HGS was employed to investigate: (1) the disintegration kinetics of soft and hard gel boluses under simulated gastric conditions in the presence and absence of biochemical degradation by pepsin and (2) the emptying pattern of the boluses from the HGS and its possible relationship with disintegration kinetics. Different disintegration mechanisms are proposed for the soft and hard gels, respectively.

6.3 Results and Discussion

6.3.1 Physical characteristics of initial gel bolus

As shown in Table 6-1, the D_{50} of the hard gel bolus was ~ 4 times smaller than that of the soft gel bolus (0.97±0.1 *vs.* 3.84±0.5 mm). This difference in the D_{50} was attributed to the gel hardness, i.e. the higher the gel hardness, the greater the extent of gel fragmentation within the mouth (Gwartney et al., 2004). Fig. 6-2 shows the photographs of simulated gel boluses before the *in vitro* gastric digestion step. The cohesive force of the gel bolus reflects the attraction forces by which the gel particles are held together (Foegeding et al., 2011). The cohesiveness of the hard gel bolus was ~ 2.8 times higher than that of the soft gel (Table 6-1). The possible explanations are: (1) a higher total surface area of particles within the hard gel; (2) stronger interactions between the hard gel particles because of the strong shielding of charges by the higher concentration of NaCl.

Table 6-1 Cohesive force of simulated gel bolus

Gel type	D_{50} (mm)	Cohesive force (N•s)
Soft gel	3.84±0.5	4.0±0.5
Hard gel	0.97±0.1	11.2±0.6

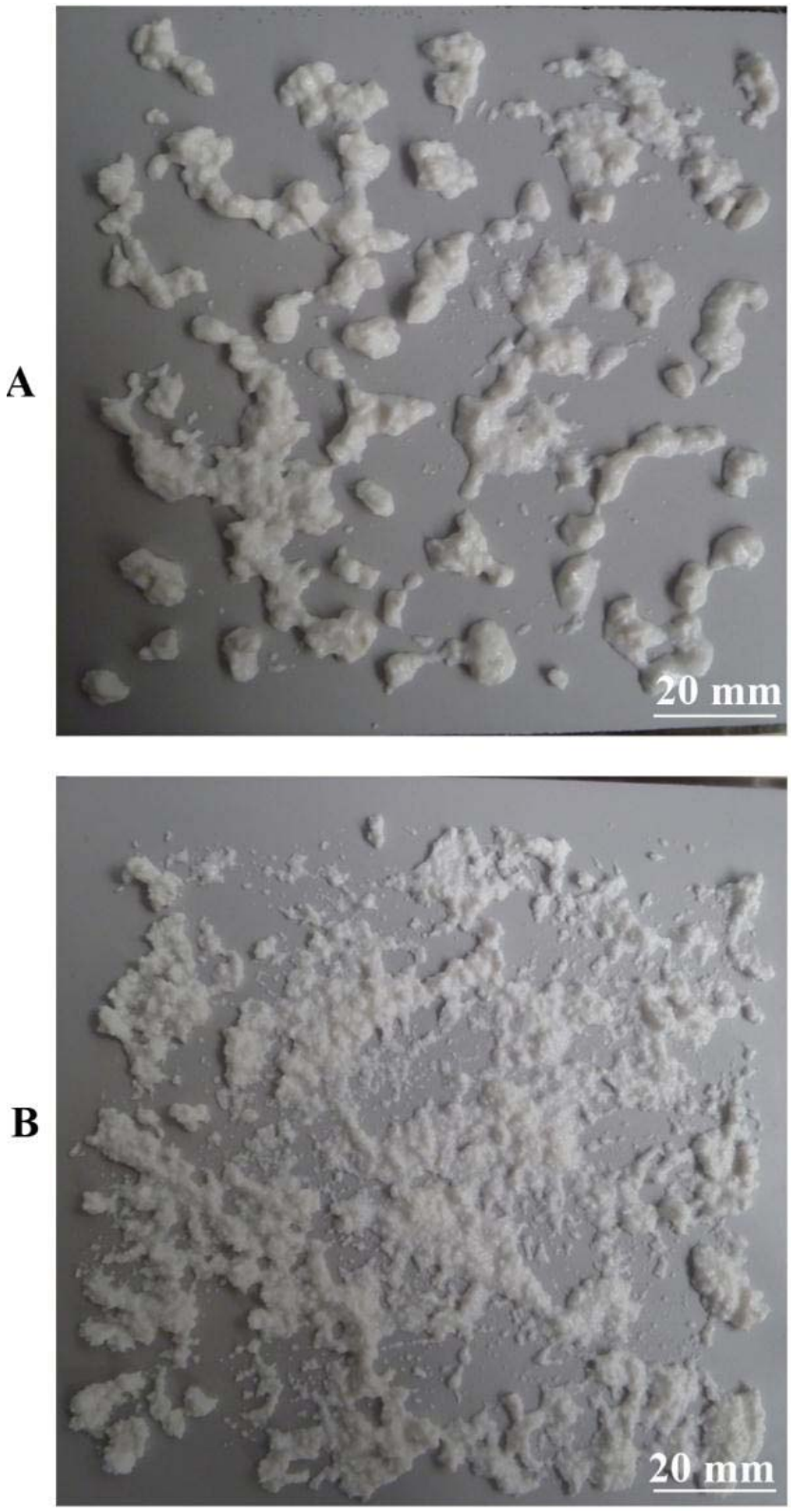

Figure 6-1 Photographs of gel bolus. A and B represent the soft and hard gels, respectively.

6.3.2 Disintegration kinetics

The disintegration profiles of both gel boluses by the peristaltic activity of the HGS in the presence and absence of pepsin are illustrated in Fig. 6-2.

In the presence of pepsin, the weight percentage of large particles (> 2.00 mm) of the soft gel decreased sharply from ~ 78% to ~ 42% during the first 30 min, with the percentage of fine particles (< 0.425 mm) increasing the most (~ 3% to ~ 24%) (Fig. 6-2-A1). This pattern kept repeating with further digestion, with the percentage of large particles gradually decreasing down to ~ 6% and the percentage of fine particles up to ~ 80%. In the absence of pepsin, the disintegration of the soft gel initially followed a similar trend (Fig. 6-2-A2). Particles larger than 2 mm were the ones experiencing the largest reduction, with fine particles showing the largest increase. However, the sharp increase in the percentage of fine particles observed in the presence of pepsin after 180 min was not observed (significant at $P<0.05$). By contrast, the hard gel always showed a slower disintegration (Figs. 6-2-B1 and B2). In the presence of pepsin, the percentage of large particles (>2 mm) decreased markedly slower especially during the first 60 min. After that time (60 min), the disintegration was accelerated leading to a rapid increase on the amount of fine particles (< 0.425 mm). In the absence of pepsin, the large particles (>2 mm) disintegrated slowly over the whole process of 300 min (the percentage decreasing from ~ 27% to ~ 19%). A similar phenomenon has been observed in the disintegration of soft and rigid agar beads in a dynamic gastric model (DGM) (Vardakou et al., 2011; Faulks & Wickham, 2012), which was also verified by the human studies using the same samples (Marciani et al., 2001a).

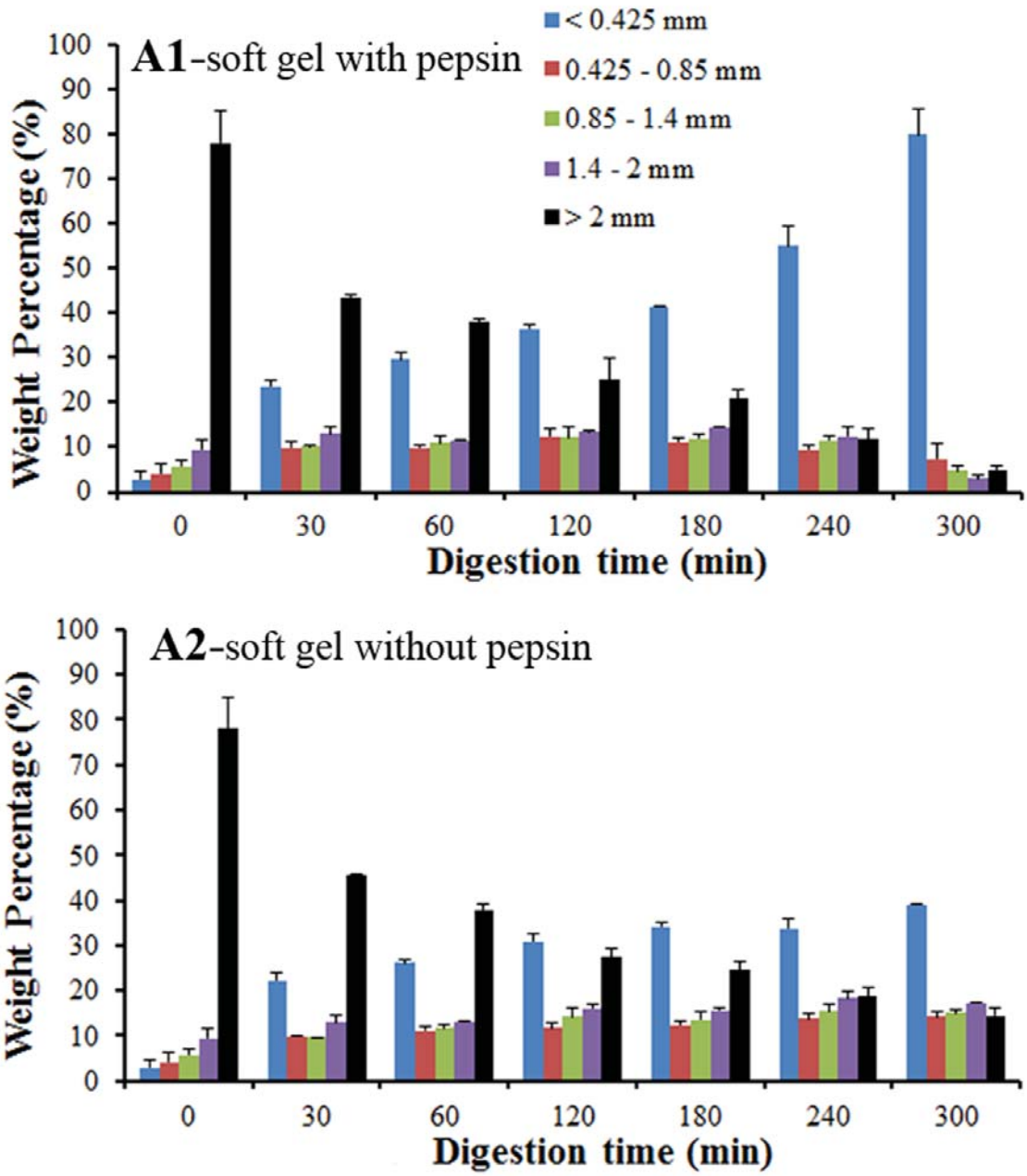

Figure 6-2 continued

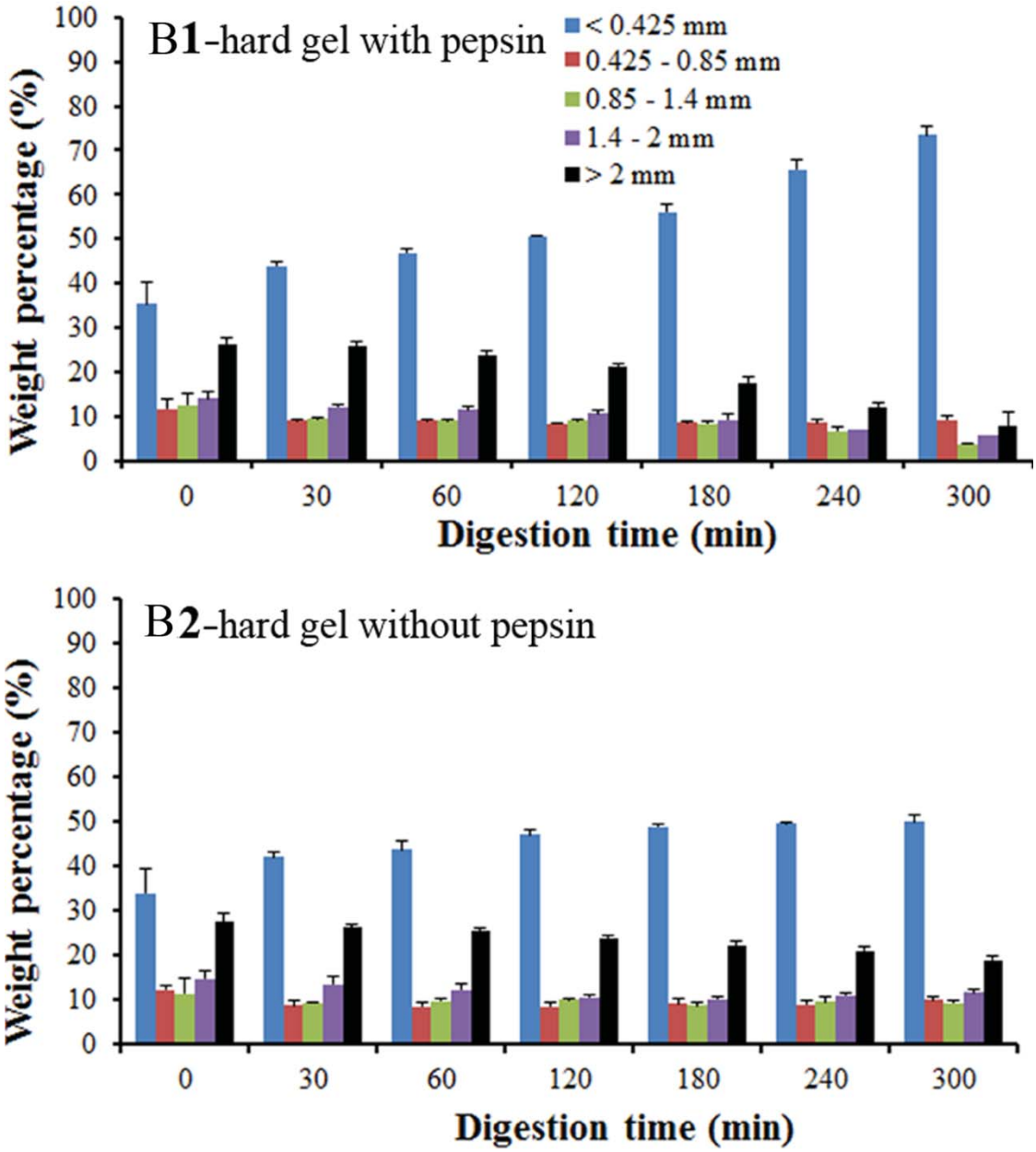

Figure 6-2 Comparison of the amount of gel particles of different sizes in the combined digesta at different digestion times. A1 and A2 represent the soft gels with and without pepsin, respectively. B1 and B2 represent the hard gels with and without pepsin.

As described above, the disintegration of large particles was largely associated with the formation of fine particles, proving abrasion (i.e. small bits being worn away) was one of disintegration mechanisms, regardless of gel structure and enzymatic hydrolysis. However, in the absence of pepsin the medium particles (0.425 to 2 mm) increased significantly with the digestion time, suggesting that the fragmentation of large particles into medium ones also played an important role in the gel disintegration

(Fig. 6-2-A2). And the absence of pepsin seemed to significantly decrease the susceptibility of the soft gel to abrasion, especially after 180 min (Figs. 6-2-A1 and A2). As a result, both effects of abrasion and fragmentation led to a rapid disintegration of the soft gel. On the other hand, the percentage of medium particles (0.425 to 2 mm) of the hard gel decreased over the entire process, proving that abrasion was the predominant mechanism for the hard gel disintegration regardless of pepsin level (Figs. 6-2-B1 and B2).

The disintegration mechanism of the gels in the HGS can be explained based on their initial gel hardness and the level of forces applied on the food particles by the stomach. Unlike the mouth where jaw muscles can exert a bite force of ~ 400 N (Helkimo et al., 1977; Jalabert-Malbos et al., 2007), the maximum destructive force from the human stomach is ~ 1.9 N (Kamba et al., 2000). Therefore it is difficult for the stomach to fragment hard food particles into smaller pieces. For example, agar gel beads (diameter: 1.27 cm) with low fracture strength (0.15-0.65 N) are broken down quickly in the human stomach whereas the beads with high fracture strength (> 0.65 N) are broken down into smaller particles much slowly (Marciani et al., 2001a). The relatively large fracture force of the hard (17.2 N) and soft (3.9 N) gels (16×16×25 mm) measured using a pair of fracture wedges might explain the relevance of abrasive mechanism in their disintegration and the particular low impact of fracture effect in the case of the hard one (Chapter 4). It should also be noted that the particles in the hard gel bolus were considerable smaller than the particles in the soft gel bolus so that the mechanical effects of the peristalsis in the stomach would be smaller.

Enzymatic hydrolysis of whey proteins by pepsin accelerated the disintegration of both gels especially after 180 min (Figs. 6-2), which could be explained by the ability of pepsin to disrupt and dissolve the protein matrix. As described in Chapter 5 that

investigated the changes of gel structure with time at the microscopic scale, the pepsin had a greater effect on the weakening of the flexible fine-stranded structure of the soft gel than the particulate structure of the hard gel.

The temporal evolution of the particle size distributions of gel boluses is shown in Fig. 6-3. As expected, the longer the digestion time, the higher the cumulative percentage of smaller particles. The temporal evolution of D_{50} extracted from the curves is shown in Fig. 6-4. The D_{50} values for the soft gel boluses decreased rapidly during the first 30 min of the process, whether or not pepsin was present. After that a slow decay was observed particularly in the absence of pepsin. On the other hand, the D_{50} of hard gel boluses experienced a much slower and uniform decay, with the absence of pepsin having a detrimental effect on the decay.

In order to quantify the difference of decay of D_{50} of both gel boluses during gastric digestion, a Weibull distribution function: $D_{50}(t) = D_{50}(0)e^{-(\lambda t)^{\theta}}$ was fitted to the data (see materials and methods: 3.2.10.5). The fitted curves are shown in Fig. 6-4 and the fitting parameters are shown in Table 6-2. In the presence or absence of pepsin, the λ value of the soft gel was significantly higher than that of the hard gel ($P<0.05$) indicating the soft gel has a higher disintegration rate. The λ values of both gels in the absence of pepsin were lower than those in the presence of pepsin although the difference was not statistically significant. These calculations confirm that the presence of pepsin accelerates the gel disintegration. The values of θ being lower than 1 showed that there was a decrease in the disintegration rate of both gels with time, i.e. the disintegration process could be regarded as a first rapid stage followed by a slower stage. As expected, T_{50} significantly increased with the gel hardness and the absence of pepsin ($P<0.05$).

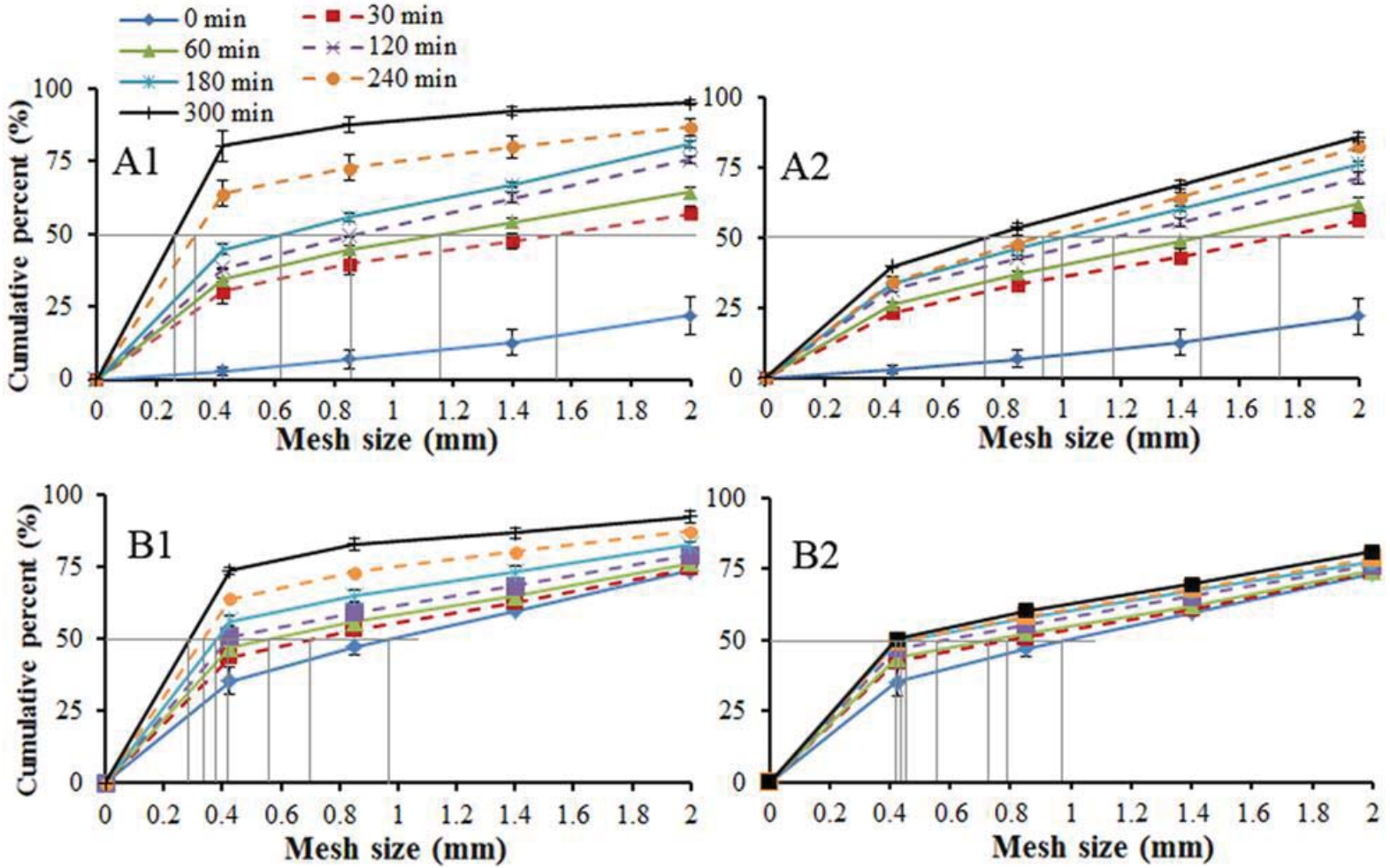

Figure 6-3 Mean particles size distributions of the combined digesta at different digestion times. A1 and A2 represent the soft gels with and without pepsin respectively and B1 and B2 represent the hard gels with and without pepsin

Table 6-2 Parameters of fitted curves of gel disintegration in the HGS.

Parameter	Soft gel		Hard gel	
	with pepsin	without pepsin	with pepsin	without pepsin
λ(1/min)	0.029±0.016	0.017±0.007	0.005±0.001	0.003±0.013
θ	0.446±0.08	0.303±0.05	0.557±0.03	0.790±0.44
R^2	0.993±0.03	0.996±0.03	0.992±0.04	0.958±0.04
T_{50}(min)	19.0±10.7	20.9±13.7	105.8±17.8	182.6±71.8

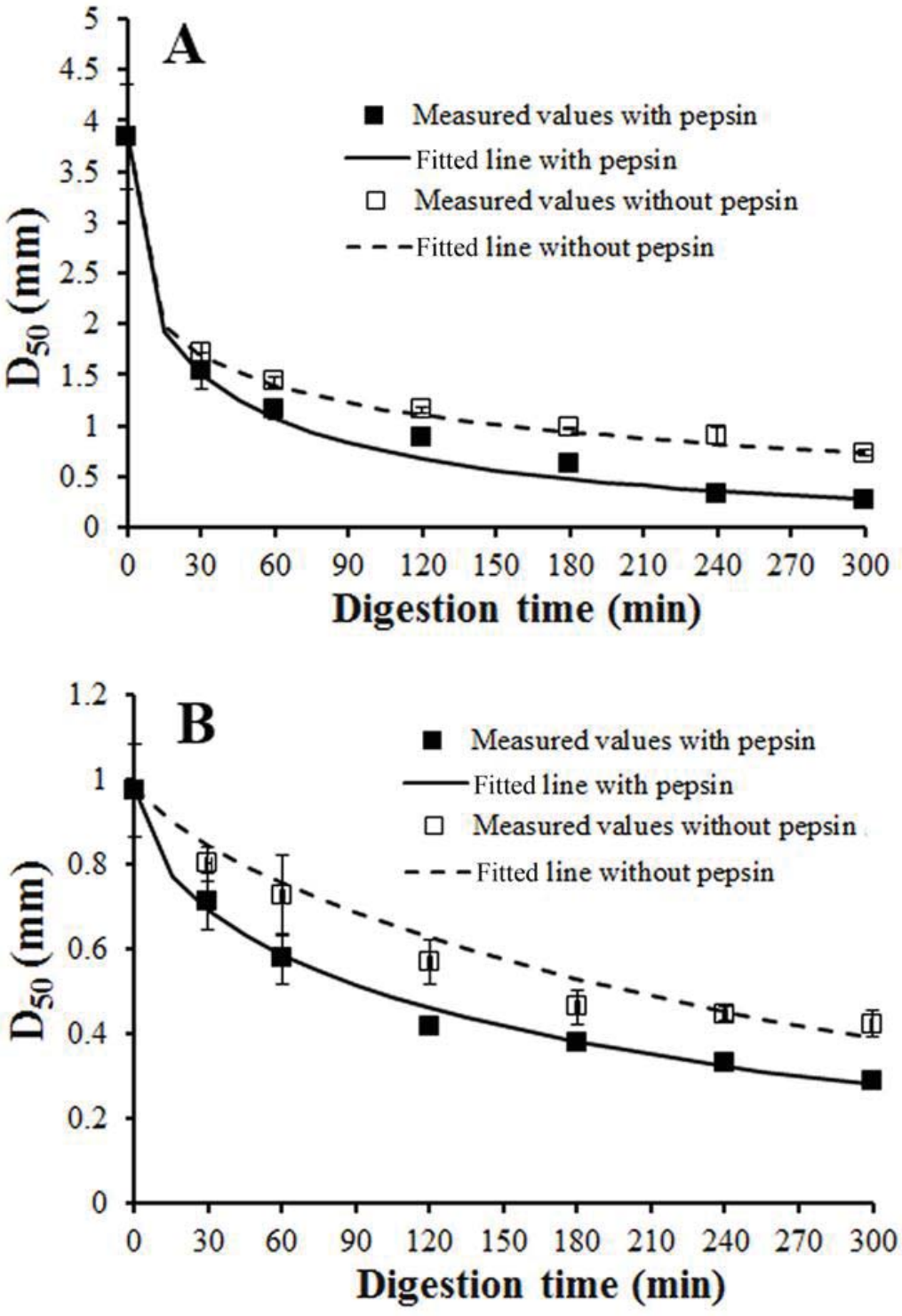

Figure 6-4 Disintegration profiles of whey protein emulsion gels in the HGS. Data dots are experimentally measured values and the lines represent the fitting of the data according to the Weibull model (see text and Table 6-2). A and B represent the soft and hard gels, respectively.

6.3.3 Assessment of emptying from HGS

The profiles of gel retention *vs.* time of both gel boluses in the HGS are illustrated in Fig.6-5. The presence of pepsin had a significant impact on the emptying of gel particles from the HGS particularly after 60 min of process. About 49% and 37% of gel particles from soft and hard gels respectively were still retained in the HGS at the end of the process when pepsin was absent. Pepsin accelerated the emptying rate of gel particles as a result of the proteolysis of whey proteins, with only ~ 26% of gels retained in the HGS at the end of process for both gels. A similar phenomenon has been found previously showing that pepsin digestion can accelerates gastric emptying in dogs by reducing large food particles into an emulsion size (Ohashi & Meyer, 1980). Comparing the emptying profiles in the presence or absence of pepsin for both gels, the effect of pepsin was greater in the emptying of the soft gel. This was attributed to a faster disruption and dissolution of the soft gel particles into the emulsion especially after 180 min as shown in Chapter 5.

In the presence of pepsin, the retention of the soft gel in the HGS was higher than that of the hard gel until 120 min of digestion, which can be explained by the initial large particle size of the soft gel. This indicates the large particle size of original gel bolus slows down the emptying of gel particles from the HGS which is consistent with the previous studies (Urbain et al., 1989; Pera et al., 2002). However, as time evolved, the relative emptying of gel particles was affected by the level of disintegration of the gels because the gels with different structures had different disintegration kinetics (i.e. slow or fast). The faster disintegration of the soft gel led to a higher level of emptying after the first 120 min of digestion when it exceeded the effect of original large particle size. Meyer et al. (1985) found that gastric emptying of spheres was promoted greatly

with decrease of sphere size from 5 to 1 mm, with feeding dogs with a standard test meal to which they added indigestible spheres of different sizes.

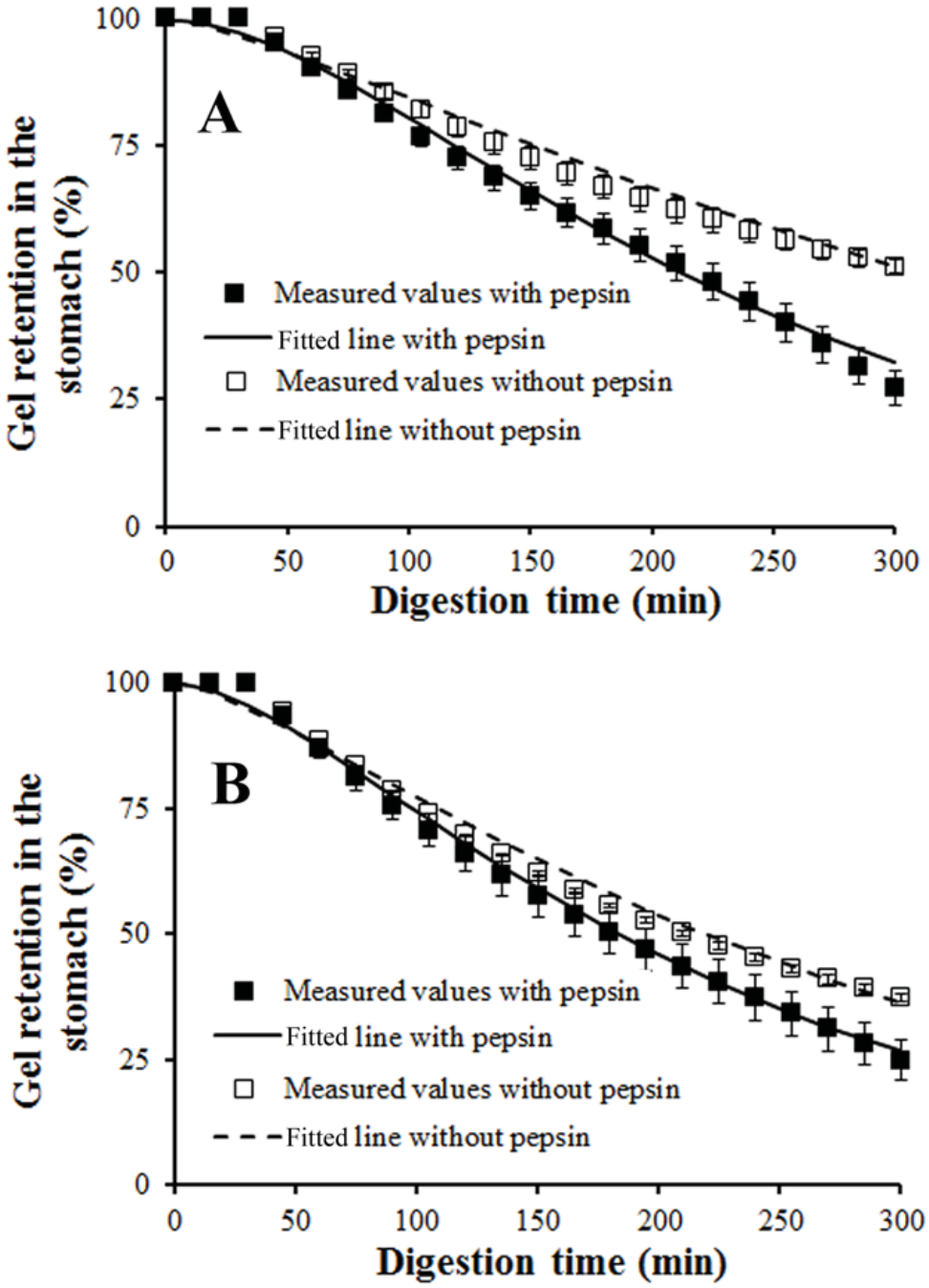

Figure 6-5 Gel retention in the HGS over the digestion time of 300 min. A and B represent the soft and hard gels, respectively. Lines represent the fitting of the data to the Siegel's model using the parameters in Table 6-3.

The Siegel's power exponential model was fitted to the emptying profiles. The fitted curves are shown in Fig. 6-5 and the parameters examined from Siegel's model are shown in Table 6-3 (see materials and methods: 3.2.10.2). For both gels, the emptying rate (κ) in the presence of pepsin was significantly higher than that in the absence of pepsin ($P<0.05$). In the absence of pepsin, the value of κ of the hard gel was markedly higher than that of the soft gel ($P<0.05$). However, the value of κ was almost same for both gels in the presence of pepsin ($P=0.545$), indicating the combined effect of different original particle size of boluses (large or small) and different kinetic disintegration (fast or slow) on the emptying of solids from the HGS. The values of β of both gels were higher than 1 indicating there was a lag phase in the gastric emptying of solids. In the presence of pepsin, T_{half} of the soft gel was significantly higher than that of the hard gel ($P<0.05$), indicating the significant effect of large particle size of the original gel bolus on the emptying of gels from the HGS (i.e. slowing down emptying). The addition of pepsin caused a significant decrease of T_{half} in both gels. The values of T_{lag} of the soft gel with or without added pepsin were significantly higher than those of the hard gel ($P<0.05$). The values of T_{lag} of both gels in the presence of pepsin were similar to those obtained from *in vivo* studies (chicken liver: 62 min; egg meal: 31 min; low fat meal: 21 min; a hamburger with 150 ml 10 wt% dextrose: 37 min) (Collins et al., 1983; Siegel et al., 1988; Tougas et al., 2000).

Table 6-3 Parameters of fitted model of gastric emptying.

Parameter	Soft gel		Hard gel	
	with pepsin	without pepsin	with pepsin	without pepsin
κ (1/min)	0.006±0.0006	0.003±0.0	0.006±0.001	0.004±0.0006
β	1.963±0.18	1.381±0.06	1.713±0.03	1.414±0.03
R^2	0.994±0.001	0.993±0.003	0.997±0.001	0.992±0.001
T_{half} (min)	214.0±8.7	309.5±11.4	186.6±30.1	220.8±24.3
T_{lag} (min)	43.1±2.6	40.5±3.9	32.4±4.8	29.8±2.6

6.3.4 Relationship between disintegration kinetics and emptying from the HGS

The relationships between the emptying and the kinetics of disintegration of whey protein emulsion gels (represented by D_{50}) are shown in Fig. 6-6. The relationships between 30-300 min are shown because the emptying began at 30 min in consideration of the lag phase of gastric emptying of food (Fig. 6-6). A linear correlation was exhibited between gel retention in the HGS and the disintegration kinetics for both gels, which strongly supports that the food disintegration kinetics in the stomach is a key factor influencing the gastric emptying. The soft gel exhibiting a linear correlation between gel retention and the disintegration kinetics as the hard gel can be explained by the rapid disintegration of the soft gel during the first 30 min. Compared with ~ 58% of particles (<1 mm) of the hard gel, the soft gel was disintegrated rapidly during the first 30 min of process (i.e. lag phase) with the generation of ~ 47% of particles <1 mm (Figs. 6-3 and 4). The slope of the equations of relationships of both gels was different. This was due to the varying disintegration rates (i.e. a faster disintegration had a smaller slope).The gastrointestinal response to a meal in the human body can be recognized as two periods: (1) lag phase (quiescence) for preparing a meal for transport into the duodenum and (2) plateau phase for regular activity (e.g. gastric emptying) (Azpiroz & Malagelada, 1987). Therefore, this linear correlation may reveals the relationship between gastric emptying and disintegration of foods in the plateau stage of postprandial gastric activity.

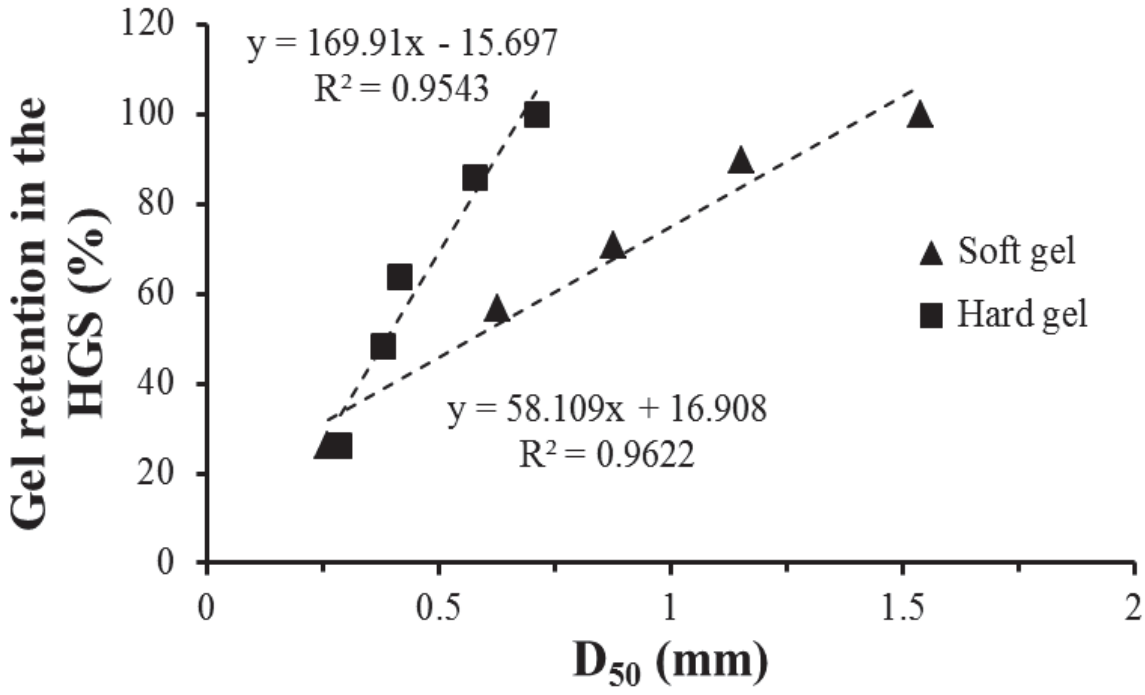

Figure 6-6 Linear relationship between the emptying from the HGS and disintegration kinetics of whey protein emulsion gels in the presence of pepsin (30 – 300 min).

Moreover, to illustrate the relationship between emptying and disintegration of gels over the whole digestion process, gel retention *vs.* $D_{50}(t)/D_{50}(0)$ was plotted in Fig. 6-7. The curves of both soft and hard gels had similar shape with an initial plateau followed by a linear decrease. Empirically, this relationship can be described by the cumulative distribution function for Weibull distribution because the change rate of Weibull distribution can be controlled by the shape parameter:

$$y(t) = 1 - e^{-(\lambda \frac{D_{50}(t)}{D_{50}(0)})^{\theta}} \quad \cdots\cdots\cdots\cdots \text{Eqn 6-4}$$

where $y(t)$ is the gel retention in the HGS, λ is the scale parameter, θ is the shape parameter and $D_{50}(t)$ and $D_{50}(0)$ are D_{50} at time of 0 and t respectively (the timescale is not included in this equation). The R^2 of fitted curves of both soft and hard gels was higher than 0.97 indicating the relationship between gastric emptying and D_{50} was well described by Weibull function. $\theta>1$ of both soft and hard gels indicates the fitted curves have the similar shape. However, λ of the soft gel was much higher than that of the hard

gel, which reflects difference in gel characteristics (i.e. a much higher decrease in $D_{50}(t)/D_{50}(0)$ in the soft gel during the same period).

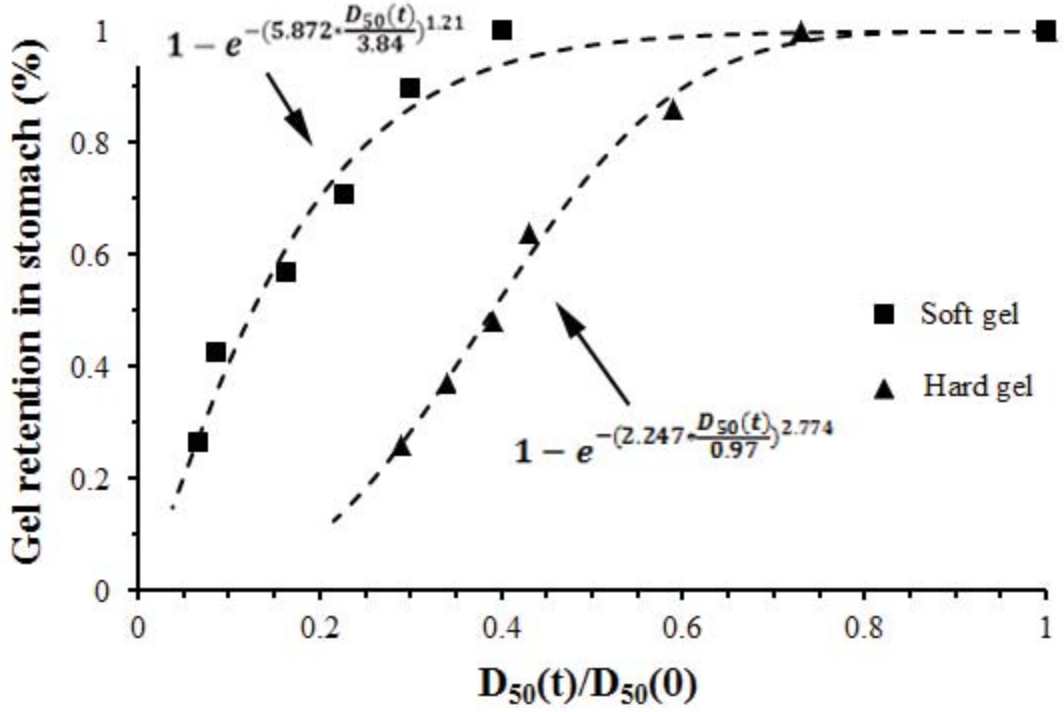

Figure 6-7 Relationship between emptying of gels from the HGS and gel disintegration (0-300 min).

6.4 Disintegration mechanisms of gels during gastric digestion

The schematic diagram of the disintegration mechanisms of the soft and hard gels is presented in Fig. 6-8. The soft and hard gels had different disintegration mechanisms. For the hard gel, the surface abrasion (i.e. the wearing away of the surface of food particles) was the predominant mechanism for the gel disintegration during gastric digestion because of the higher gel hardness. However, both the fragmentation (i.e. the breakdown of large food particles into several small pieces) and surface abrasion played an important role during gastric digestion of the soft gel because of the

low gel strength. The disintegration mechanisms for the gels with different gel hardness may help understand the disintegration of various real foods in the stomach.

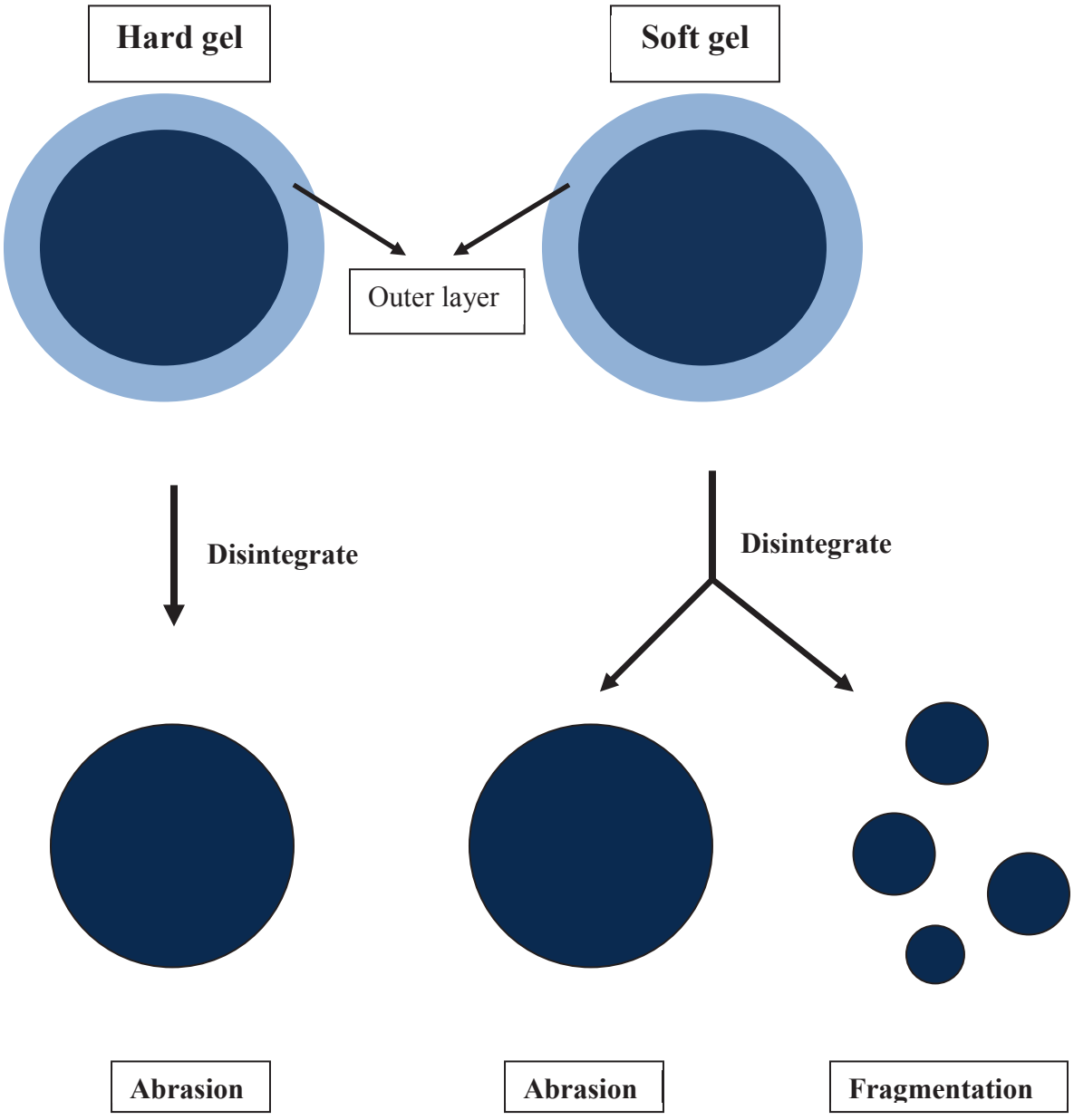

Figure 6-8 Disintegration mechanisms of the soft and hard gels during gastric digestion.

6.5 Conclusions

Disintegration of solid gel boluses in the HGS is a complex process. The key factor determining the disintegration mechanics is the gel strength or fracture force. The soft gel had a faster disintegration in the HGS, which involved abrasion and to some extent fragmentation. The hard gel had a much slower disintegration largely governed by abrasion. The model of $D_{50}(t) = D_{50}(0)e^{-(\lambda t)^{\theta}}$ can describe well the disintegration process of gels with different strengths. Emptying of gels from the HGS was affected by the original particle size of gel boluses in the HGS and its disintegration kinetics. The larger particle size of original soft gel bolus slowed down the emptying process regardless of the lower gel strength. The disintegration of gels facilitated the emptying of both gels. Enzymatic digestion of pepsin had a greater effect on both the gel disintegration and emptying. In addition, the disintegration kinetics exhibited a linear relationship with the emptying of gels.

Chapter 7 Behaviour of Whey Protein Emulsion Gels during Oral and Gastric Digestion: Effect of Droplet Size[4]

7.1 Abstract

A set of whey protein stabilized-emulsion gels with different droplet size distributions ($D_{4,3}$ = ~ 1, 6 and 12 μm) was produced by heating and adding salt (100 mM NaCl). The mechanical properties of the gels in the linear viscoelastic region and at large deformation were measured, along with the physicochemical and structural changes of the gels during oral mastication and gastric digestion. The gels containing 1 μm oil droplets had an aggregated particle structure with proteins coating at oil droplets whereas the gels containing 12 μm oil droplets had a particle-filled structure with spatially continuous matrix. During oral processing, the release of oil droplets from the gels increased as the droplet size increased, with coalescence being seen in gels containing oil droplets of 6 and 12 μm diameter. Under gastric digestion, high degrees of coalescence and phase separation of oil droplets occurred in the gels containing 6 and 12 μm oil droplets because of oil droplet release from the gel matrix; this led to slow gastric emptying. The gels, containing 1 μm oil droplets disintegrated into various particles of several microns to several tens of microns with a low degree of oil droplet release and coalescence. Protein breakdown was slower in these gels, suggesting that the protein structures of the gel matrices were affected by the sizes of the incorporated oil droplets.

[4]Part of contents presented in this chapter has been published in a peer-reviewed paper: Guo, Q., Ye, A., Lad, M., Dalgleish, D., & Singh, H. (2014). Behaviour of whey protein emulsion gel during oral and gastric digestion: effect of droplet size. *Soft Matter, 10*(23), 4173-4183.

7.2 Introduction

The digestion of lipids is an interfacial process which is controlled by interfacial properties of emulsified oil droplets (Maldonado-Valderrama et al., 2011; Singh et al., 2013). Thus, the states of oil/fat in solid food (e.g. released or trapped within the food matrix) during oral and gastric processing are important to the lipid digestion which mainly occurs in the human intestine (Singh et al., 2009). Emulsion gels are semi-solid materials containing dispersed oil droplets whose formation and mechanical properties have been a subject of study over several decades (Dickinson, 2012). The structure of an emulsion gel can be understood as a combination of the structure of the matrix, the size distribution of oil droplets, the crystallinity of the oil and the extent of oil droplet-matrix interactions. Because the structures of emulsion gels can be precisely manipulated by changing protein/oil ratios, oil droplet sizes and salt content, the emulsion gel model represents an ideal food material for investigating the mechanistic relationships between food structure and food digestion (especially the digestion of emulsified lipid in solid foods with varying structures).

The initial droplet size distribution is an important factor, which strongly influences both the structure and sensory characteristics of food emulsions (McClements et al., 2005). In the present study, heat-set whey protein emulsion gels with different structures were formed by varying oil droplet size distributions. The behavior of emulsion gels during oral and gastric processing was investigated. The main objective was to examine the effect of gel structure varied by oil droplet size on the disintegration of gels during oral and gastric processing with a focus on the behavior of oil droplets bound to the gel matrix during digestion. This study may help to develop a rational means of controlling lipid digestion and target release of oil-soluble nutrients in the human body.

7.3 Results and discussion

7.3.1 Gel structure and mechanical properties

As shown in Fig 7-1-LM, oil droplets appeared to be homogeneously distributed within the protein networks in the gels containing 1 and 6 μm oil droplets. For the gels containing oil droplets of 12 μm, the droplets did not appear as evenly distributed or as firmly bound to the protein network as did the smaller droplets. CLSM image of the gels containing 1 μm oil droplets with high magnification shows the porous network structure (Fig. 7-1-HM). Proteins adsorbed and surrounded the oil droplets to form a thick layer and the gel appeared to be formed by the aggregation of protein-coated oil droplets via surface-surface cross-links or interactions. However, in the gel containing 12 μm oil droplets, large oil droplets were just embedded or bound to a typical heat-induced whey protein network formed at high ionic strength (i.e. syneresis and spatially continuous protein matrix) (Fig. 7-1-HM) (Ako et al., 2010). The structure of protein matrix in the gels containing 1 μm droplets was totally modified by the adsorption and surrounding of whey protein strands or aggregates at oil-water interfaces during gel formation because of a much larger surface area of the oil phase (Dalgleish, 1997; Phan-Xuan et al., 2013; Guo et al., 2014b). Whey protein strands (l tens of nanometres) assembled from whey protein molecules are the primary structural units for protein gelation (heating) (Ikeda et al., 2002). At high ionic strength, these strands randomly aggregate into larger dense aggregates (several microns) which are cross-linked into the 3D gel network (Ikeda, 2003). Moreover, for an oil content of 20%, and even distribution of droplets, it can be calculated that each droplet resides inside a cube with a side 2.75R, where R is the radius of the droplet (i.e. $\frac{Droplet\ volume}{Cube\ volume} = \frac{n\frac{4}{3}\pi R^3}{n(2.75R)^3} \approx 20\%$, n is the number of droplets). The distance between the droplets' surfaces is 0.75 R (i.e. ~

0.38, 2.25 and 4.50 μm for the gels containing 1, 6 and 12 μm oil droplets respectively). Therefore, the gels containing 1 μm oil droplets can be regarded as a type of aggregated particle gel whereas the gels containing 12 μm oil droplets can be regarded as a type of particle-filled gel with spatially continuous protein matrix as shown in Fig. 7-2 (Dickinson, 2012). The structure of the gels containing 6 μm oil droplets was in between these two gel types.

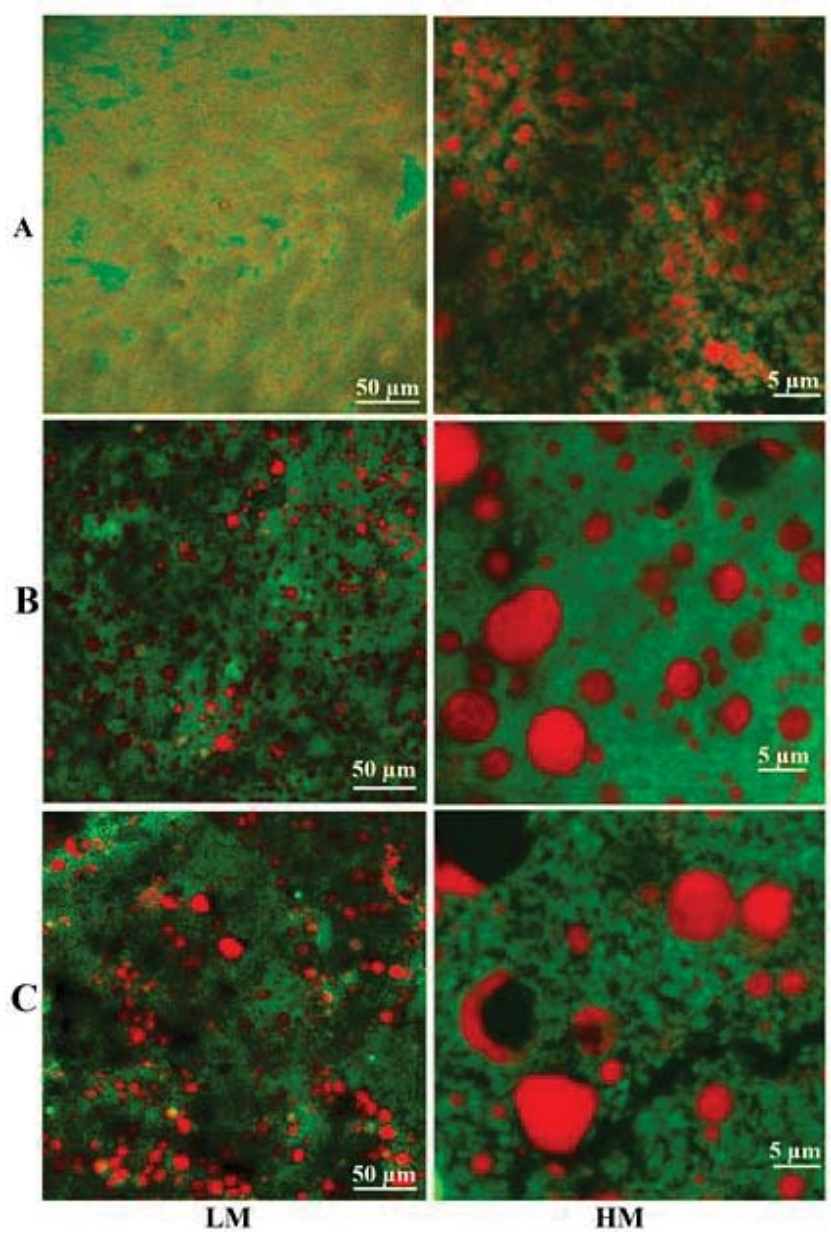

Figure 7-1 CLSM images of whey protein emulsion gels (A, B and C: gels containing 1, 6 and 12 μm oil droplets respectively). Green colour represents protein, red colour represents the oil phase, and black colour represents air or water. LM and HM represent the low and high magnification respectively. All gels contain 100 mM NaCl.

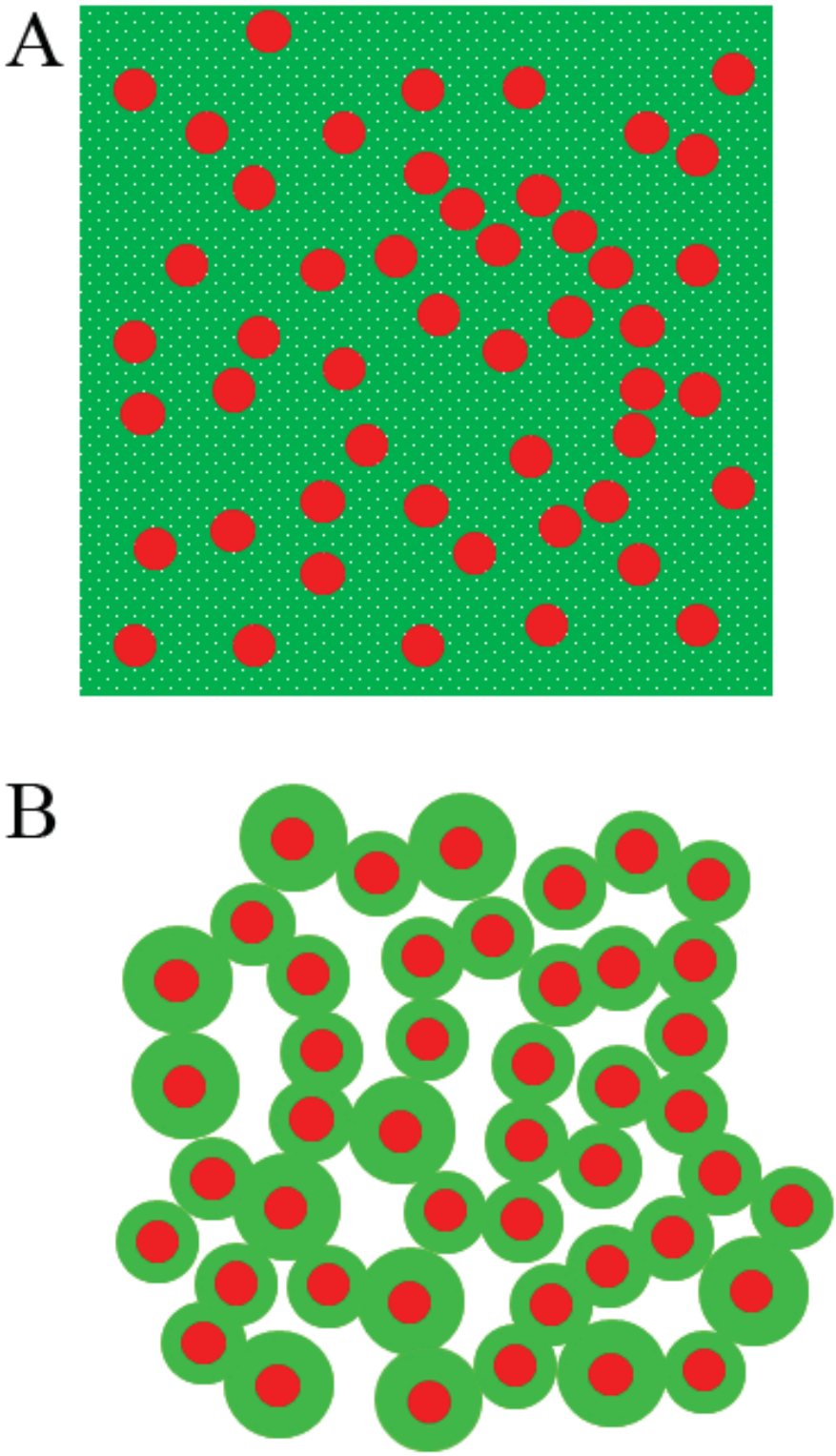

Figure 7-2 Schematic diagram of the emulsion-filled gel (A) and the particle aggregated gel (B). Green colour and red colour represent protein and oil, respectively. All gels contain 100 mM NaCl.

The mechanical properties of whey protein emulsion gels containing ~ 1, 6 and 12 μm oil droplets are presented in Table 7-1. The shear storage modulus (i.e. mechanical property in the linear viscoelastic region) of the emulsion gels decreased significantly with increasing droplet size which is in accordance with the study of Ye et al. (2009). Effective stress transfer is the most important factor which contributes to the strength of two-phase composite gels (Fu et al., 2008). For a given oil content, smaller oil droplets induce strong bonding between oil droplets and protein matrix because of the higher interfacial surface area to which protein is adsorbed compared to large oil droplets. This strong bonding can effectively transfer the applied stress to the emulsion droplets from the protein matrix and improve gel strength (Qian et al., 2000), which explains the decrease of storage modulus with increasing oil droplet size. Similarly, the fracture force and strain significantly decreased with the increase of droplet size, indicating that large oil droplets may act as defects in the fracture test (McClements et al., 1993).

Table 7-1 Mechanical properties of whey protein emulsion gels

Gel type	Storage modulus (kPa)	Fracture force (N)	Fracture strain (%)
A	84.0±3.5*	12.0±2.7*	50.6±4.8*
B	71.4±1.7**	7.5±1.2**	46.2±5.7**
C	63.7±3.9***	4.0±0.2***	31.3±2.4***

A, B and C represent the gel with oil droplet size ($D_{4,3}$) of ~ 1, 6 and 12 μm respectively. All gels contain 100 mM NaCl. * to *** represent significant difference between different gels ($P<0.05$).

To visualize the differences in breakdown pattern of whey protein emulsion gels after the fracture point, force versus time curves were normalized by their fracture force and fracture time (Fig. 7-3). The slope of the normalized curves, which indicates the crack propagation speed within the material, showed major differences among different gels. As shown in Fig. 7-3, gel A had the highest slope followed by gels B and C, which implied that the crack propagation speed decreased with increasing oil droplet size.

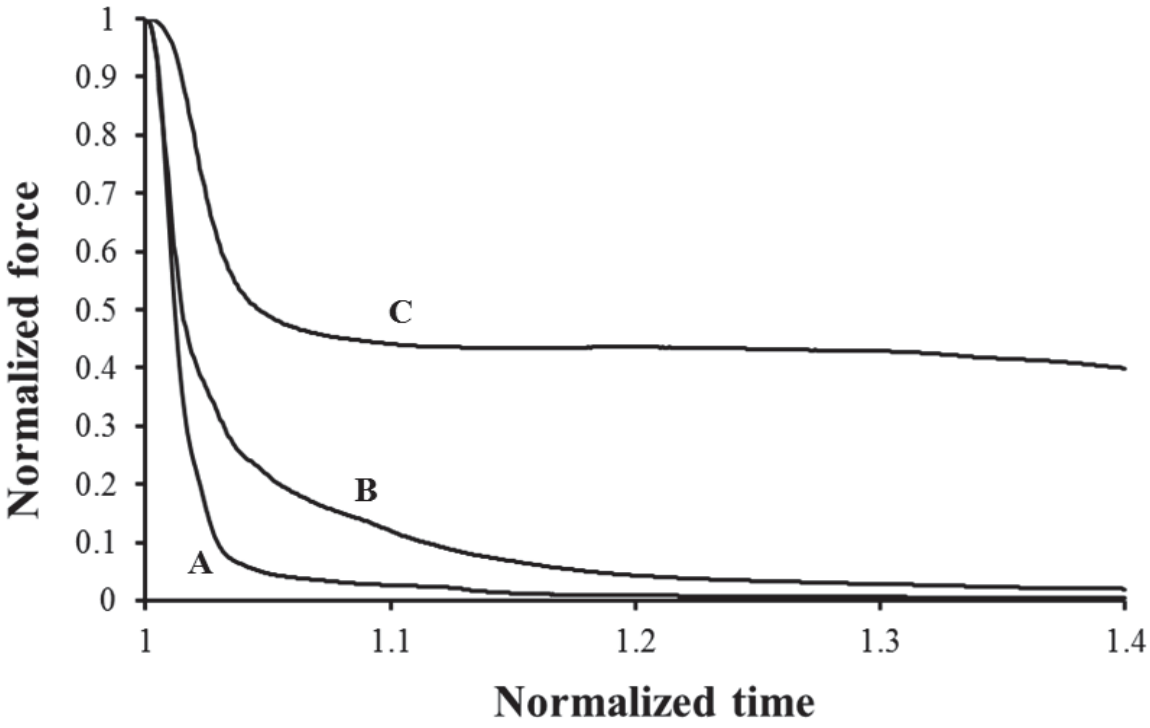

Figure 7-3 Normalized force versus normalized time curves after fracture point of whey protein emulsion gels. A, B and C represent the gels containing 1, 6 and 12 μm oil droplets, respectively. All gels contain 100 mM NaCl.

7.3.2 Breakdown properties of gels in the human mouth

Mean mastication parameters of eight human subjects are presented in Table 7-2. The droplet size significantly affected the mastication of gels containing oil droplets of different sizes. With increasing droplet size, both the number of chewing cycles and chew duration decreased markedly. That is to say that the number of chewing cycles and chew duration increased with the gel hardness. However, the chew frequency showed no significant difference between gels. Jalabert-Malbos et al. (2007) found that there were no differences in masticatory frequency among various natural foods with a large range of hardness.

Table 7-2 Mastication parameters of whey protein emulsion gels with different oil droplet sizes.

Gel type	Number of chews	Chew duration (s)	Chew frequency (1/s)
A	26.4±4.2*	14.5±3.4*	1.86±0.29*
B	22.7±3.3**	12.4±2.5*	1.87±0.29*
C	17.8±3.2***	10.1±2.7**	1.82±0.30*

A, B and C represent the gel with oil droplet size ($D_{4,3}$) of ~ 1, 6 and 12 μm respectively. All gels contain 100 mM NaCl. * to *** represent significant difference between different gels ($P<0.05$).

CLSM images of gel boluses are presented in Fig. 7-4. After mastication, only a few oil droplets were released from the gels containing smaller oil droplets (1 μm) whereas large quantities of oil droplets were released from the protein matrices of gels

containing the larger oil droplets. The difference in oil droplet release was attributed to the differences in gel structure caused by the oil droplet size. Oil droplet release was difficult in the oral processing of aggregated particle gel because of the protection of thick protein coating around them and strong interactions between protein-coated oil droplets. However, for the particle-filled gel, the oil droplets released easily upon the deformation or cutting because of the low stress transfer capacity across oil-protein interface thereby leading to cracking of the interface, which was supported by the decrease of the fracture force and strain with increasing oil droplet size. In the CLSM images, there appeared to be larger oil droplets in the bolus of the gels containing 12 μm oil droplets than in the original gel, suggesting that coalescence occurred during mastication (Fig. 7-4). The $D_{4,3}$ values of oil droplets in the original gels were 1.03, 6.01 and 11.84 μm, respectively. After mastication, droplet size distributions showed no significant changes with those before mastication for the first two gels (Fig. 7-4). The value of $D_{4,3}$ of oil droplets in the bolus showed only a slight increase in the gels containing 12 μm oil droplets. A similar phenomenon has also been observed in the oral behaviour of liquid emulsions (Dresselhuis et al., 2008a). This could be explained by the limitation of particle size measuring technique (i.e. large oil droplets and free oil are difficult to disperse in water) and creaming or phase separation of large oil droplets before or duing particle size measurement.

The mean particle size distributions of the gel boluses are presented in Fig. 7-5. The shapes of the curves of three gels were similar. The approximate median size D_{50} extracted from these curves was around 1 mm for the gels containing ~ 1, 6 and 12 μm oil droplets, and there was not much difference between the gels. This does not mean the gels containing ~ 1, 6 and 12 μm oil droplets had the same fragmentation degree because of the release of oil droplets in the gels containing ~ 6 and 12 μm oil droplets.

However, the D_{50} of gel bolus obtained from *in vivo* oral processing can be used to create the simulated gel bolus as shown in the next section.

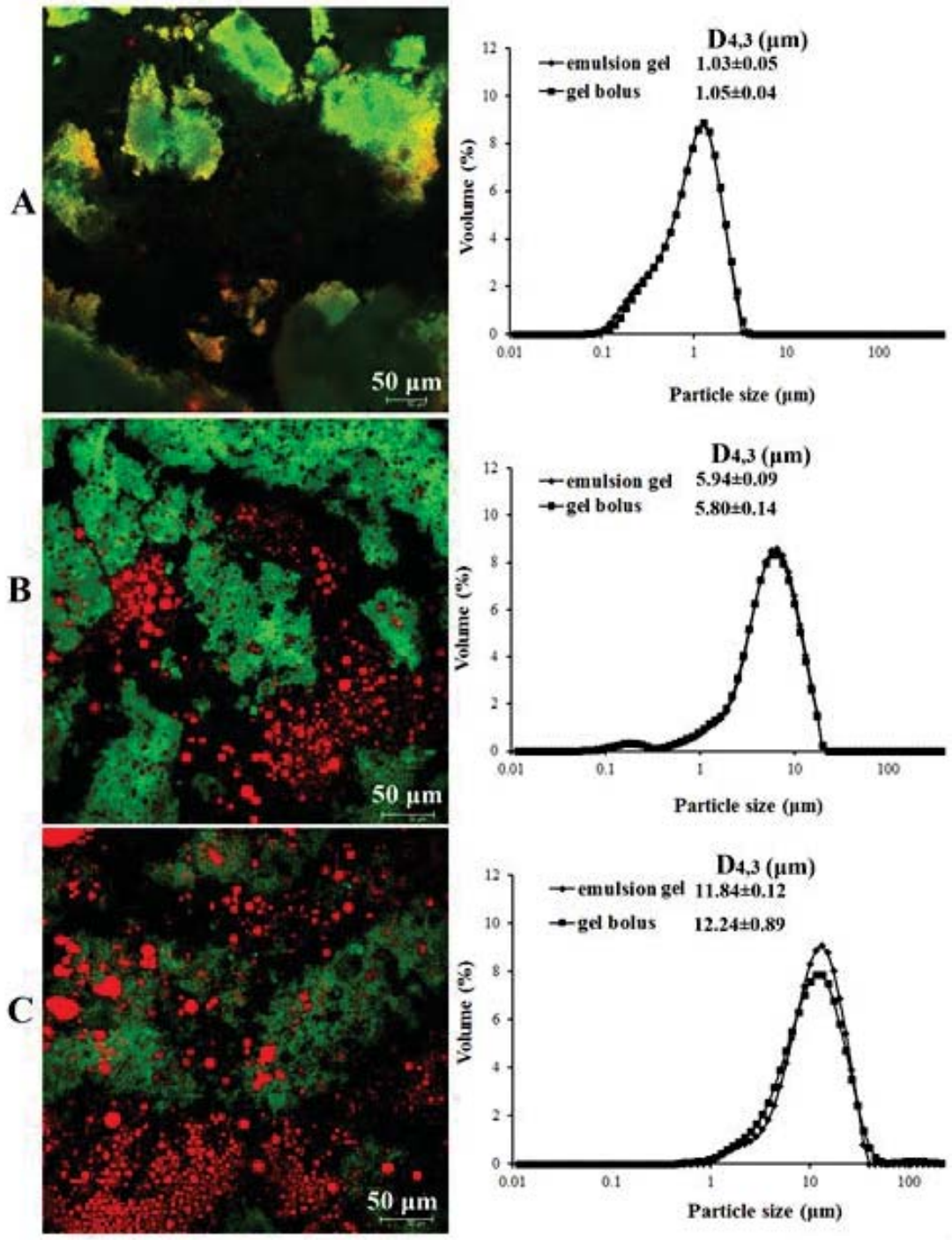

Figure 7-4 CLSM images of boluses of whey protein emulsion gels after human mastication and oil droplet distributions in the gel boluses (A, B and C: gels containing 1, 6 and 12 μm oil droplets respectively). Green colour represents protein, red colour represents the oil phase, and black colour represents air or water. All gels contain 100 mM NaCl.

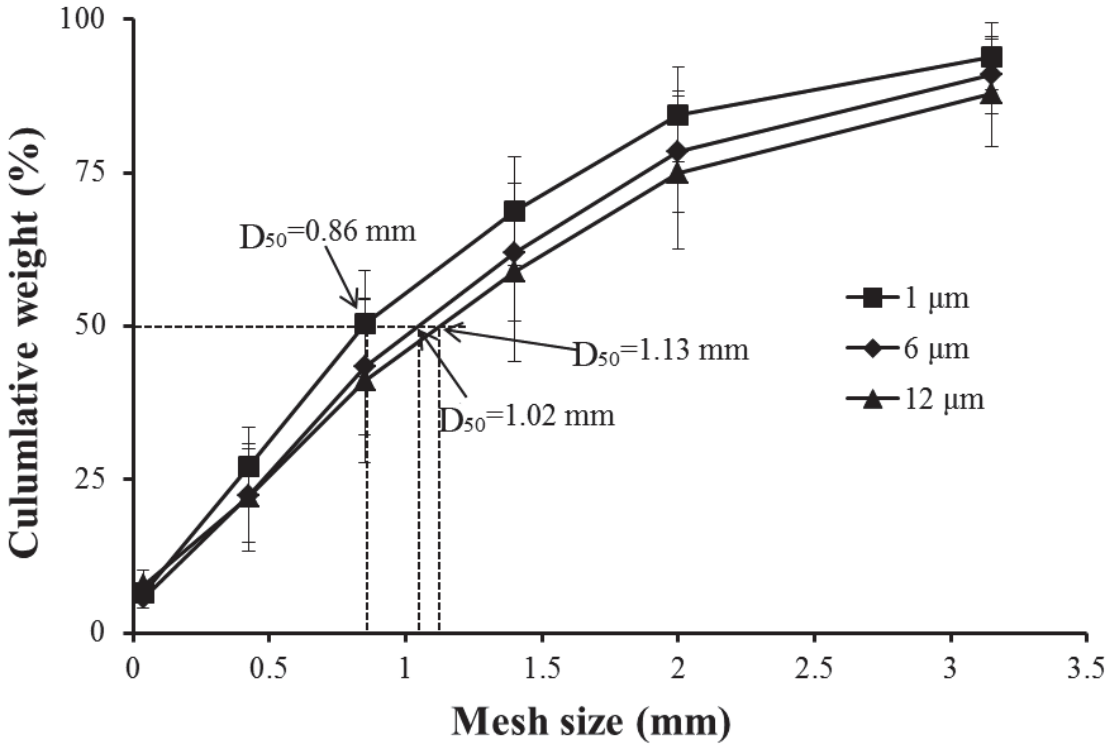

Figure 7-5 Mean particle size distribution of fragments of whey protein emulsion gels containing oil droplets of different sizes after chewing (obtained from 8 human subjects). All gels contain 100 mM NaCl.

7.3.3 Characterization of the simulated gel bolus

The simulated gel boluses which were created for the gastric digestion experiments in the HGS had similar particle size distributions (~ 1 mm) with those of human subjects (Fig. 7-6). The behaviour of oil droplets in gels during the creation of simulated gel boluses is presented in Fig. 7-7. During *in vitro* oral processing, the gels containing 1 μm oil droplets showed similar behaviour to that by *in vivo* oral processing. By contrast, the value of $D_{4,3}$ of oil droplets significantly increased from 5.94 and 11.84 to 7.74 and 24.92 μm for the gels containing 6 and 12 μm oil droplets, respectively (Fig. 7-7A) indicating that significant coalescence of oil droplets occurred during the creation of simulated boluses of the gels containing 6 and 12 μm oil droplets. In addition, the oil droplet release during both *in vivo* and *in vitro* oral processing increased with increasing droplet size (Fig. 7-7B). Oil droplet release from the simulated bolus of gels containing

6 and 12 μm oil droplets was higher than that from the gel bolus produced by human subjects. The different behaviour between the *in vitro* and *in vivo* oral processing for the gels containing large oil droplets was attributed to a higher retention of coalesced oil droplets in *in vivo* processing. Dresslhuis et al. (2008b) found that over 15% WPI-stabilized emulsion (0.3 wt% protein and 7 wt% oil) was retained in the mouth after the oral processing (i.e. processing 10 ml emulsion by moving the tongue against the palate for 15 s and rinsing the mouth with water using the same procedure as for the emulsion immediately after expectoration). In these studies, the fat retention increased with the increase of droplet size, which explains a higher oil droplet release during the *in vitro* oral processing. Furthermore, *ex vivo* oral processing (tribology measurement using pig's tongue) of WPI-stabilized emulsions showed that coalescence of emulsion droplets occurred due to the surface friction (Dresselhuis et al., 2008a). Therefore, the retention of coalesced oil droplets in the mouth during oral processing is likely to be the key factor leading to a lower apparent coalescence of oil droplets in the gels containing large oil droplets (6 and 12 μm) as shown in the CLSM images of gel boluses of human subjects.

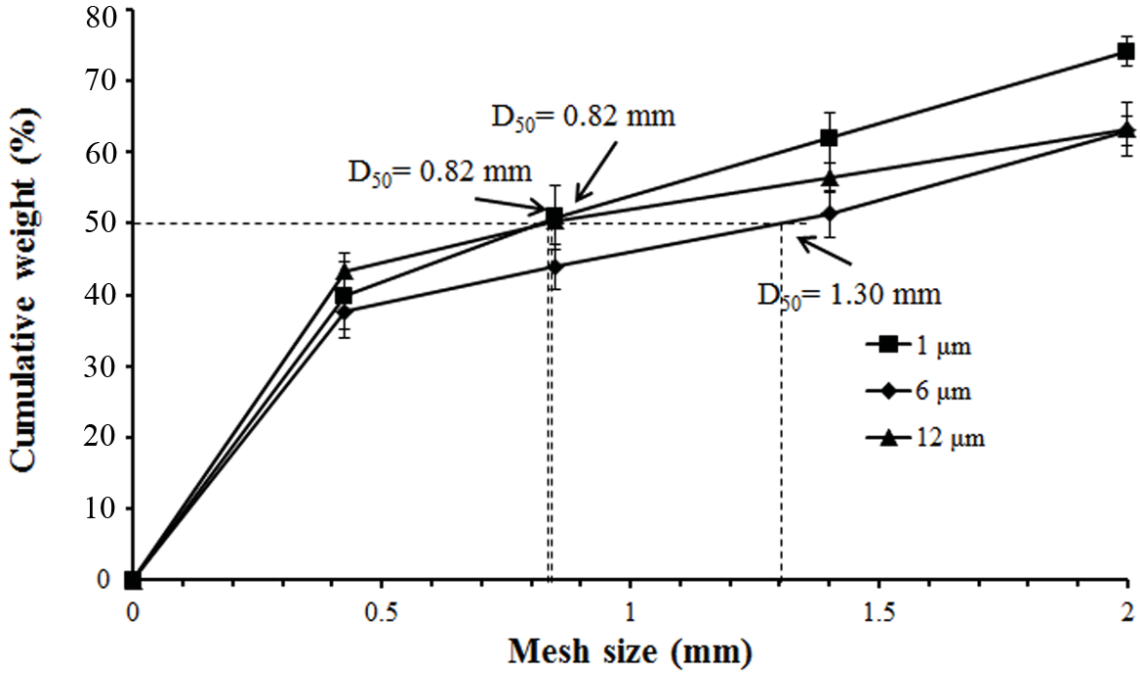

Figure 7-6 Mean particle size distributions of simulated gel bolus produced from whey protein emulsion gels containing oil droplets of different sizes. All gels contain 100 mM NaCl.

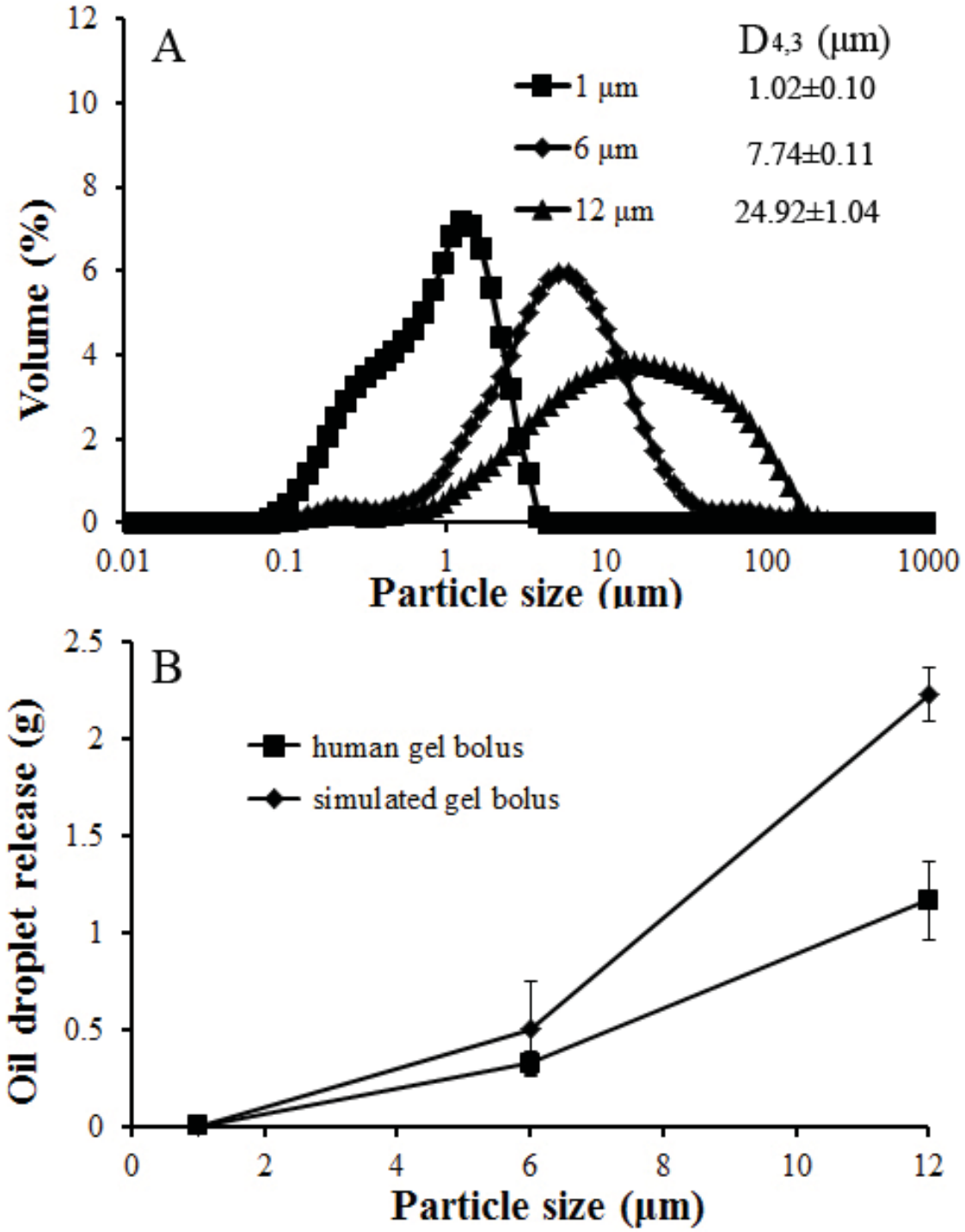

Figure 7-7 Particle size distributions of oil droplets in the simulated gel bolus produced from whey protein emulsion gels containing oil droplets of different sizes (A) and their oil droplet release during the oral processing (B). All gels contain 100 mM NaCl.

7.3.4 *In vitro* gastric digestion

7.3.4.1 pH

The changes of pH over 300 min digestion of whey protein emulsion gels containing 1, 6 and 12 μm oil droplets are shown in Fig.7-8. The pH gradually decreased from ~ 5.8 to ~ 1.7 for three gels with no significant differences between them.

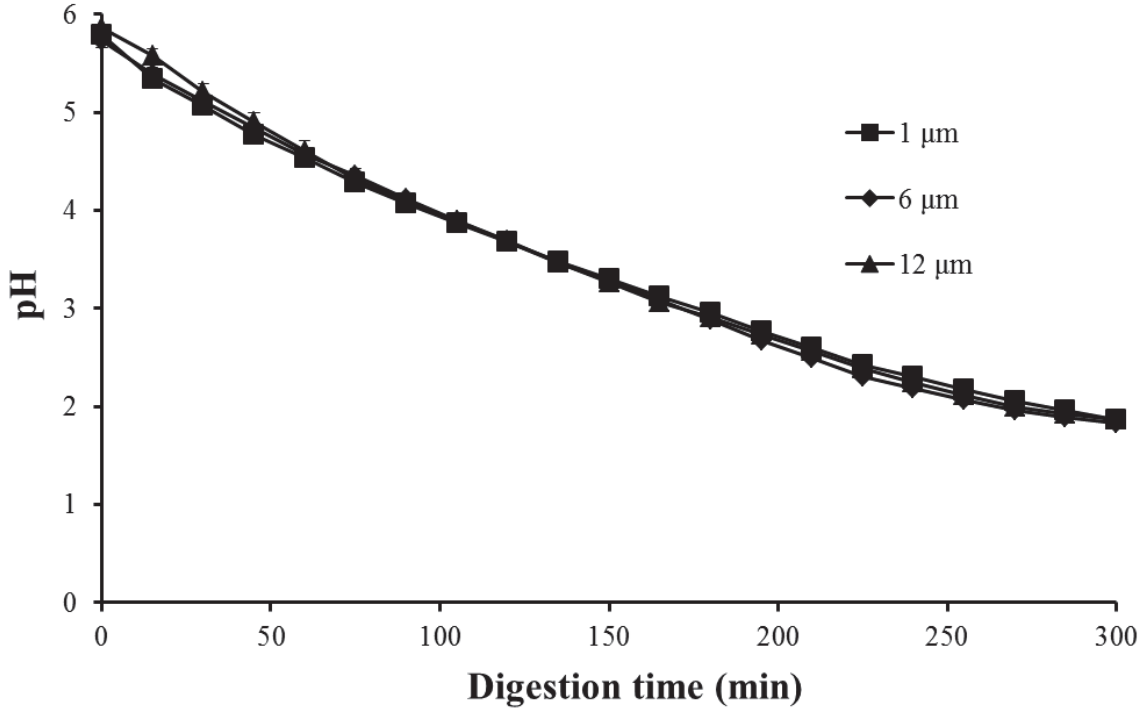

Figure 7-8 Profiles of pH of whey protein emulsion gels during *in vitro* gastric digestion (A, B and C: gels containing 1, 6 and 12 μm oil droplets, respectively). All gels contain 100 mM NaCl.

7.3.4.2 Gastric emptying

The acidic environment, pepsin-digestion and mechanical shearing led to further disintegration of emulsion gels in the HGS. The gastric emptying profiles of emulsion gels, which are represented by the retention of solids in the HGS as a function of time, are illustrated in Fig. 7-9. The gastric emptying curve of the gels containing 1 μm oil droplets was more rapid than those of the gels containing larger oil droplets and there

were ~ 20.1, 27.9 and 33.6 % of total gel particles retained in the HGS for the gels containing 1, 6 and 12 μm oil droplets respectively after 300 min digestion. This indicates the emptying rate of the gels decreased with the increase of oil droplet size, which can be attributed to the creaming of large oil droplets during gastric digestion. After 300 min digestion, a free oil layer was observed in the gels containing 6 and 12 μm oil droplets because of the creaming of coalesced oil droplets (Fig. 7-10). This is consistent with previous studies showing that acid-unstable emulsions rapidly separated into lipid-depleted 'aqueous' and lipid layers in the human stomach, as observed by magnetic resonance imaging (Marciani et al., 2006) and whey protein stabilized-emulsions showed distinct creamed layers during *in vitro* gastric digestion (van Aken et al., 2011). However, creaming of emulsion droplets was not observed in the gels containing small oil droplets (1 μm).

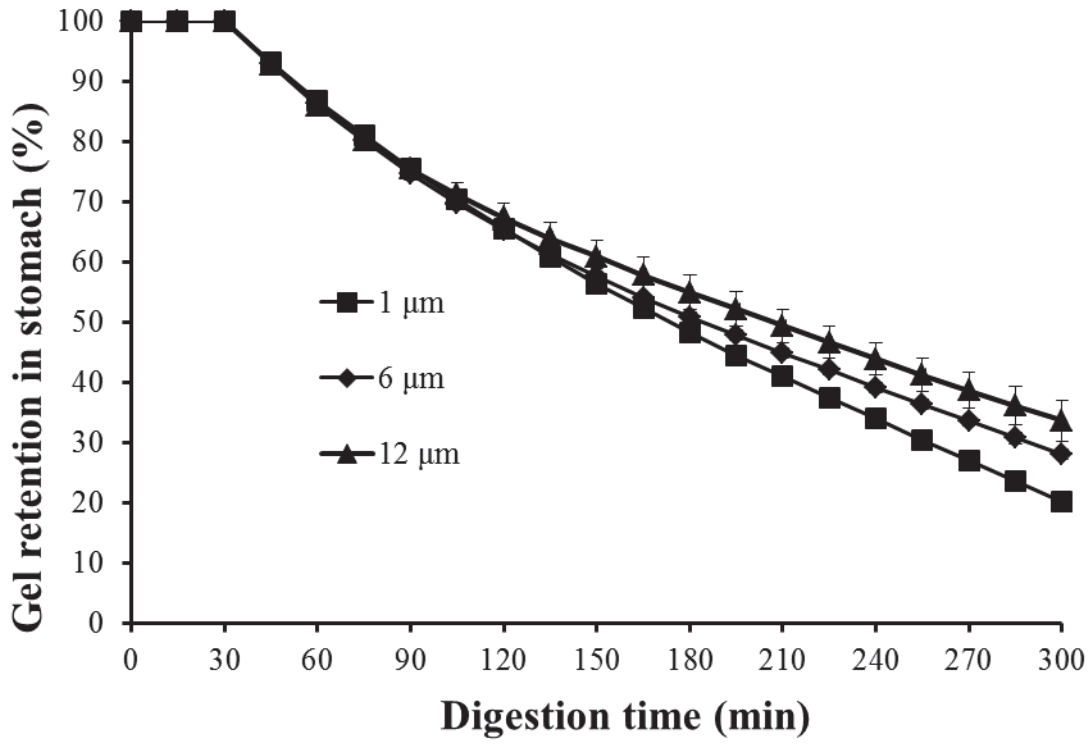

Figure 7-9 Gastric emptying profiles of whey protein emulsion gels with varied droplet size distributions in the HGS. All gels contain 100 mM NaCl.

Figure 7-10 Images of top oil layer after 300 min of *in vitro* gastric digestion (A, B and C: gels containing 1, 6 and 12 μm oil droplets respectively). All gels contain 100 mM NaCl.

7.3.4.3 Protein hydrolysis

The gastric proteolysis of whey proteins within the emptied digesta was followed by tricine-SDS-PAGE in reducing conditions (Fig. 7-11). BSA disappeared rapidly during digestion; α-La and β-Lg were gradually hydrolysed with digestion time. For all three emulsion gels, the whey proteins were gradually hydrolysed into peptides < ~ 10 kD as the digestion proceeded. Although all three gels had the same protein and oil contents, the intensity of α-La and β-Lg bands decreased more rapidly in the samples with larger oil droplets and especially these bands disappeared at an early time in the digestion of gels containing 12 μm oil droplets (i.e. the hydrolysis rate of whey proteins increases with increasing droplet size). This may be attributed to the effect of droplet size on the protein network. In the gels with the smallest oil droplets, the droplets themselves had a strong effect on the gel structure (Figs. 7-1, 2 and Table 7-1). This strong effect of the oil droplets on the protein matrix is likely to modify the cleavage sites of the whey proteins or to restrict the access of pepsin to the cleavage sites, which will hinder the whey protein hydrolysis. The protein in the gels containing the largest oil droplets was easily hydrolysed because of the limited effect of oil droplets on the protein matrix structure (i.e. small effects of the oil droplets on the protein matrix). The protein hydrolysis rate in the gels containing 6 μm oil droplets was between those two gels (i.e. aggregated particle and particle-filled gels).

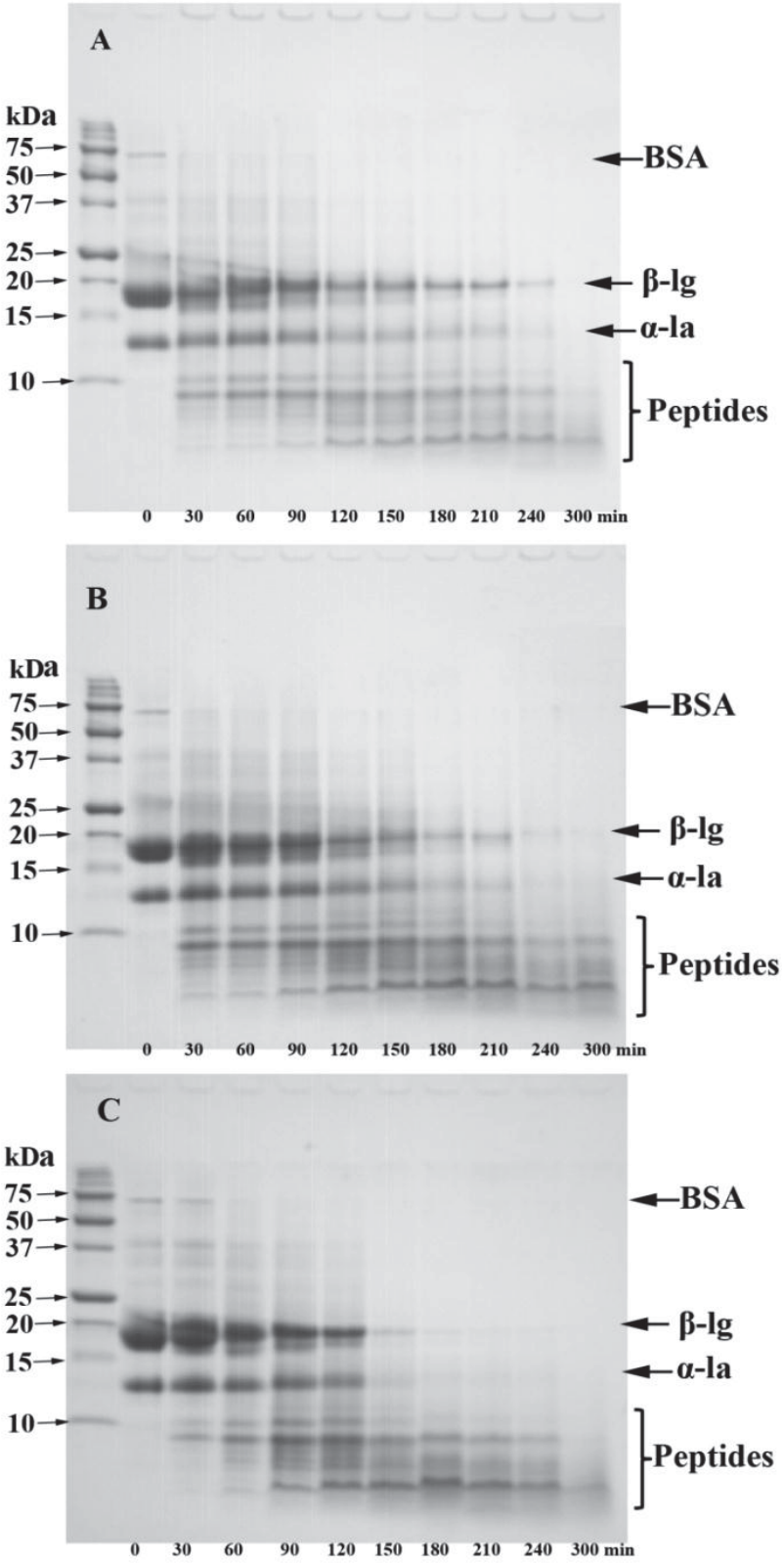

Figure 7-11 Tricine SDS-PAGE patterns under reducing conditions of proteins in emptied digesta (A, B and C: gels containing 1, 6 and 12 μm oil droplets respectively). All gels contain 100 mM NaCl.

7.3.4.4 Breakdown of gel particles and behaviour of oil droplets

The evolution of particle size of the gel fragments in emptied digesta during gastric digestion was followed by light scattering (Fig. 7-12). For the gels containing 1 μm oil droplets, the value of $D_{4,3}$ gradually increased followed by a rapid decrease (Fig. 12-A1). At 30 min, the particle size distribution was bimodal, with peaks at about 100 and 1000 μm. With further digestion, the area of the peak at 1000 μm increased to a maximum at 180 min because of the breakdown of large gel particles and then decreased because of protein digestion by pepsin. The peak at 100 μm gradually shifted towards smaller size (~10 μm) (Fig. 12-A2). The gels containing 6 μm oil droplets showed a similar trend to the gels containing 1 μm oil droplets (Fig. 12-B). For the gels containing 12 μm oil droplets, the value of $D_{4,3}$ gradually decreased from 219.3 to 79.6 μm after 300 min digestion (Fig. 12-C1). At 30 min, the particle size distribution was monomodal (Fig. 12-C2), and this pattern remained over the first 120 min. With further digestion, a bimodal pattern appeared, and the peak slowly shifted to a smaller size.

Coalescence of oil droplets was observed in all three gels during gastric digestion (Fig. 7-13). Coalescence of emulsion droplets during gastric digestion could be induced by the decreased electrostatic repulsion at isoelectric point, mechanical shearing and pepsin-digestion of the adsorbed protein layer (Sarkar et al., 2009b; Golding et al., 2011; Guo et al., 2014b). The degree of coalescence of oil droplets in the gels containing 1 μm oil droplets was low because of limited oil droplet release, as shown by the appearance of only small amounts of material above 5μm diameter (Fig. 7-13A). Van Aken et al. (2011) found that WPI-stabilized emulsions (oil droplet size: ~ 1 μm) had a significant coalescence during gastric digestion, suggesting that the gel matrix in our experiments provided a good protection for oil droplets in the gel containing 1 μm oil droplets. In contrast, a high degree of coalescence occurred in the

gels containing 6 and 12 μm oil droplets during gastric digestion because of oil droplet release and large droplet size (Figs. 7-13B, C). However, the value of $D_{4,3}$ of oil droplets decreased quickly after 60-90 min due to the creaming of large coalesced oil droplets. Compared with Fig. 7-12, a small overlap of particle size distributions between emptied digesta and oil droplets in the emptied digesta at different times in the gels containing 1 μm oil droplets suggested most oil droplets were still retained in the gel particles during gastric digestion. However, the overlaps of the gels containing larger oil droplets (6 and 12 μm) were high suggesting large quantities of oil droplets released from the gel particles.

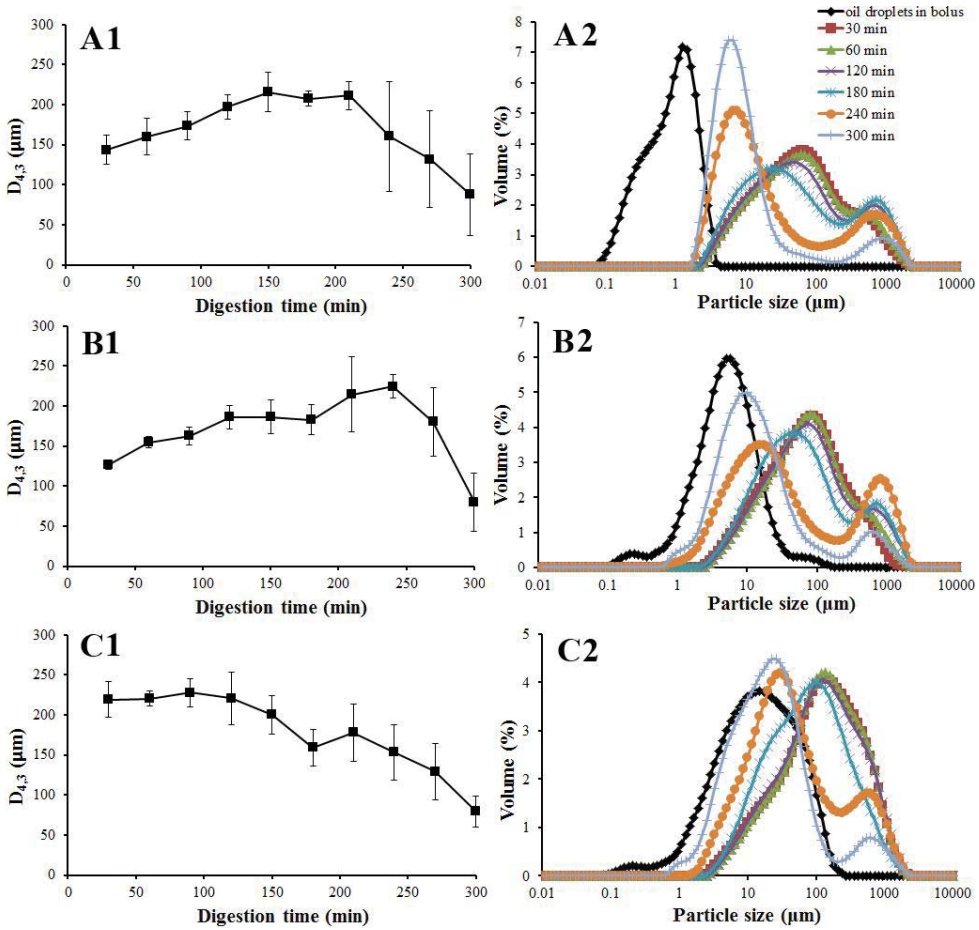

Figure 7-12 Evolution of the volume-weighted diameter ($D_{4,3}$) (-1) and size distributions (-2) of emptied digesta (i.e. gel fragments) of gels with varied droplet size (A, B and C: gels containing 1, 6 and 12 μm oil droplets respectively). All gels contain 100 mM NaCl.

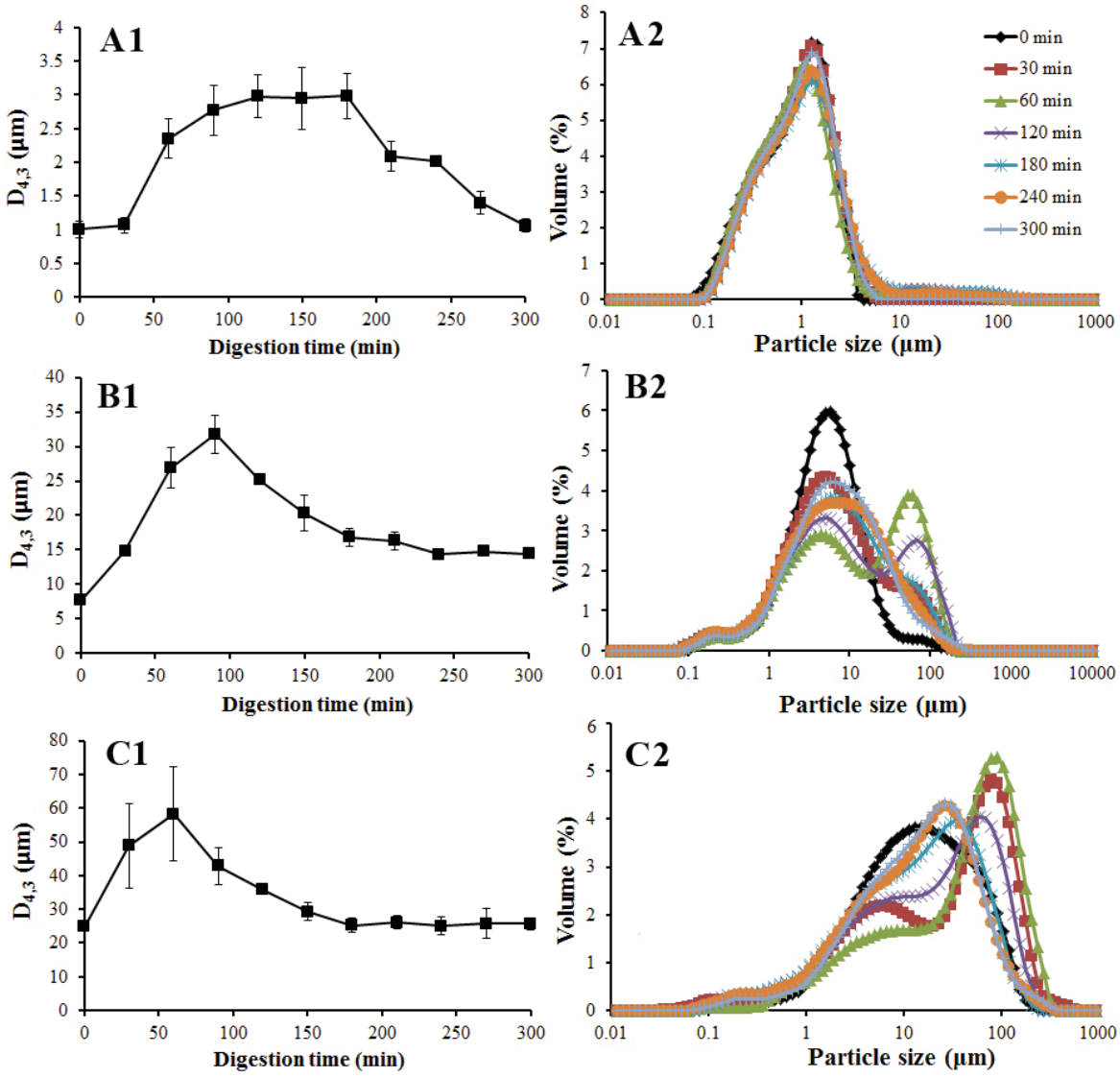

Figure 7-13 Evolution of the volume-weighted diameter ($D_{4,3}$) (-1) and size distributions (-2) of oil droplets in emptied digesta of gels with varied droplet size during gastric digestion (A, B and C: gels containing 1, 6 and 12 μm oil droplets respectively). All gels contain 100 mM NaCl.

Microstructure of emptied digesta at different times is shown in Figs. 14 and 15 which is consistent with the results of light scattering. A few coalesced oil droplets were observed in the gels containing 1 μm oil droplets (Fig. 7-14A). ~ 10 μm gel particles were still retained after 300 min digestion and oil droplets were within the protein matrix (Fig. 7-15A). By contrast, significant oil droplet release and coalescence of oil droplets at 60 and 120 min was observed for the gels containing 6 and 12 μm oil droplets (Figs. 7-14 and 15B, C). A few oil droplets appeared to be still linked by

proteins after the 300 min digestion for the gels containing 6 μm oil droplets, whereas the gel particles were broken down into free oil droplets and peptide aggregates in the gels containing 12 μm oil droplets. The microphotographs of the gels containing 12 μm oil droplets at 240 and 300 min looked more uniform than those at 60 and 120 min and the average droplet size was smaller. This was probably because the large coalesced oil droplets creamed at the early stage of digestion.

The gel structure plays a key role in the breakdown of gel particles during gastric digestion. Slow protein hydrolysis hindered the breakdown of gel particles of the gel containing small oil droplets (1 μm). Although very few intact whey proteins survived after 300 min digestion, the peptide aggregates formed mainly via disulfide bridges and hydrophobic interactions can link oil droplets together because of the aggregated particle structure (Dalgleish et al., 1997; Creusot et al., 2006; Peram et al., 2013; Guo et al., 2014b). However, for the gels containing large oil droplets (12 μm), the protein hydrolysis was much higher, which accelerated the breakdown of gel particles. The continuous protein matrix of particle filled gel was easily disintegrated by pepsin-digestion, mechanical shearing and acidic effect and peptide aggregates did not link large oil droplets over long distances (Figs. 7-1, 14 and 15).

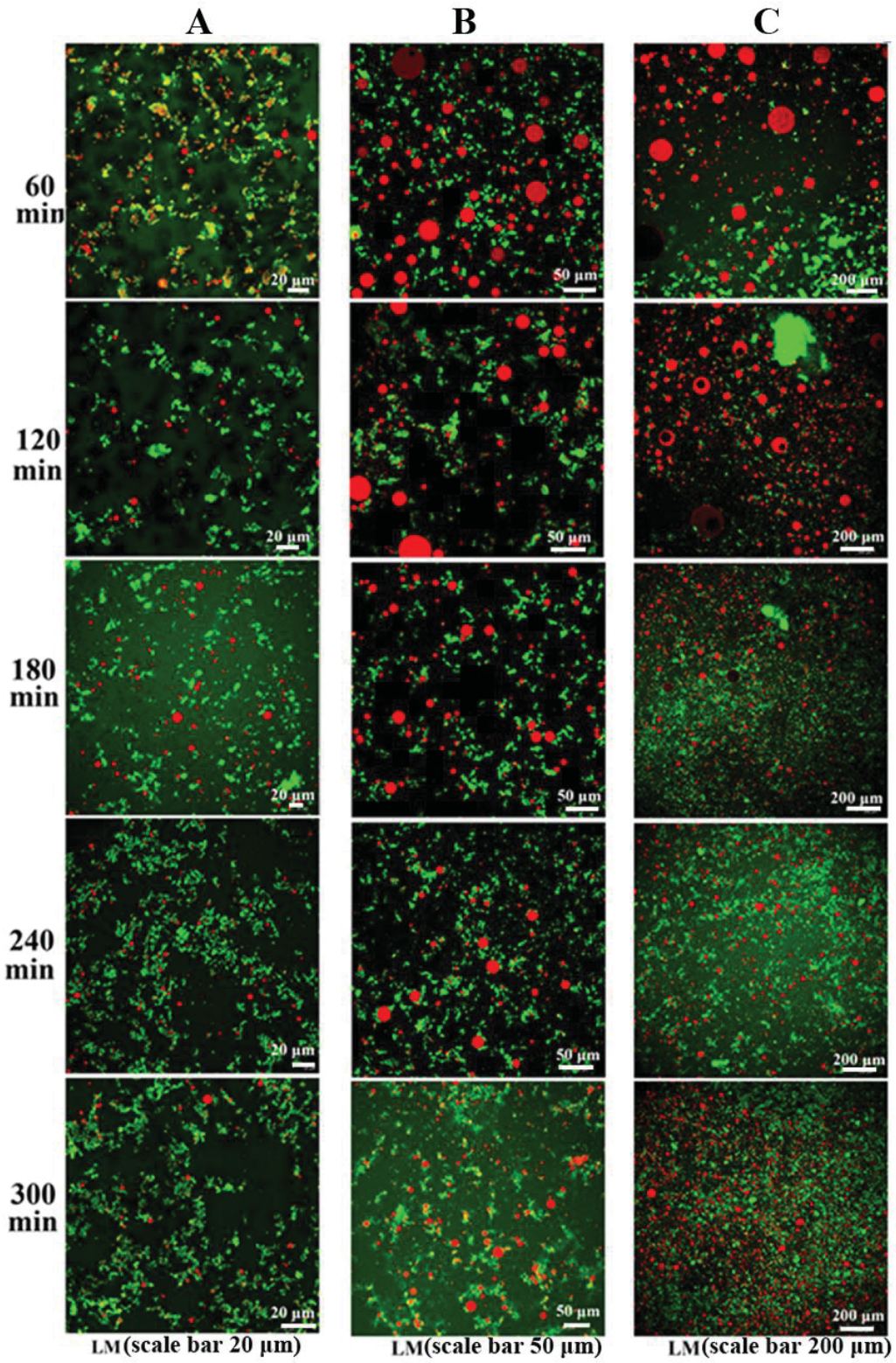

Figure 7-14 Microstructure of emptied gastric digesta at low magnification (LM). A, B and C represent gels containing 1, 6 and 12 µm oil droplets, respectively. Green colour represents protein, red colour represents the oil phase, and black colour represents air or water. All gels contain 100 mM NaCl.

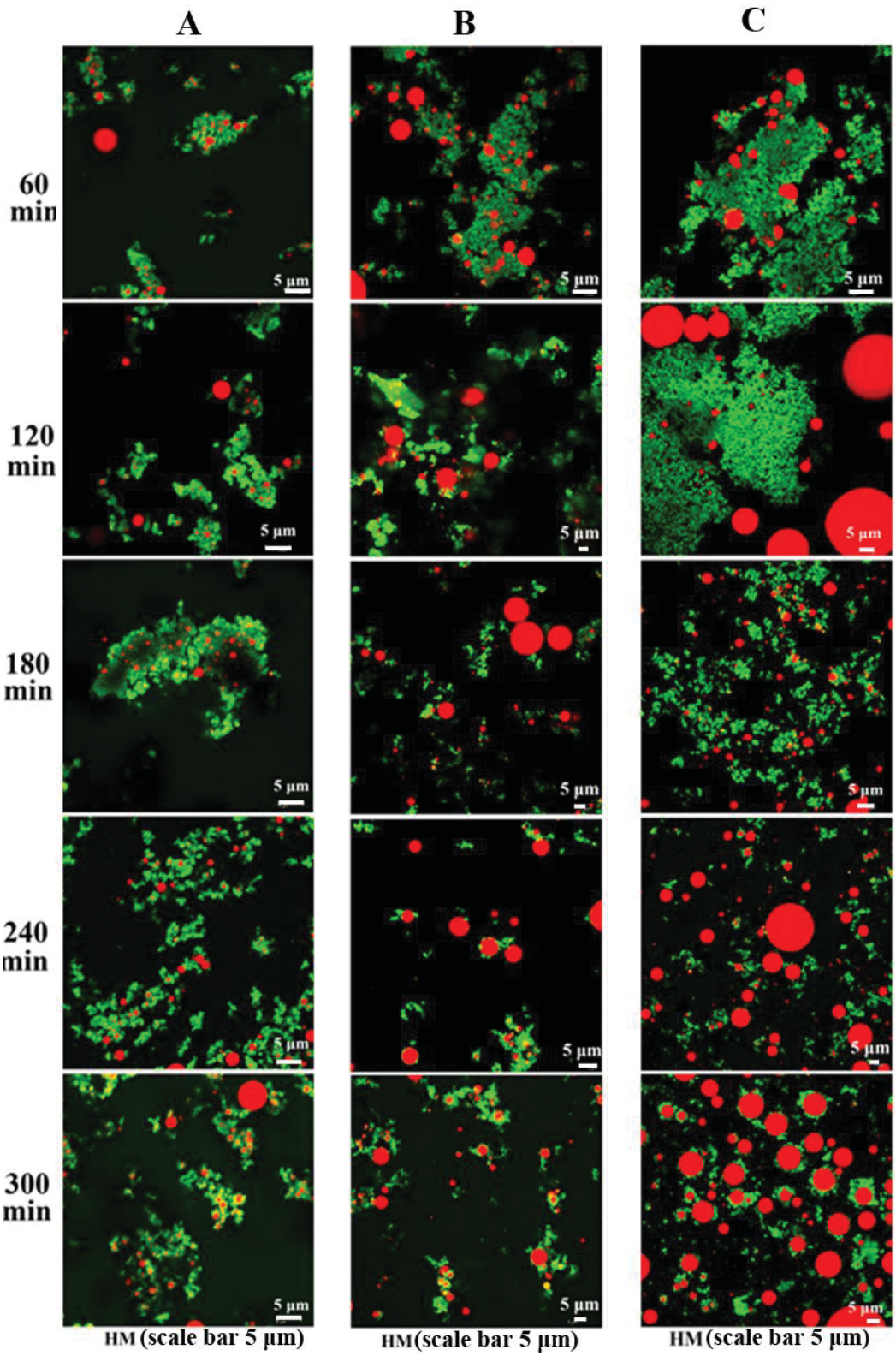

Figure 7-15 Microstructure of emptied gastric digesta at high magnification (HM). A, B and C represent gels containing 1, 6 and 12 µm oil droplets, respectively. Green colour represents protein, red colour represents the oil phase, and black colour represents air or water. All gels contain 100 mM NaCl.

7.4 Mechanisms of disintegration of emulsion gels containing ~ 1 and 12 μm oil droplets

The disintegration of differently structured whey protein emulsion gels varied with the oil droplet size, as presented in Fig. 7-16. Particle-filled gel and aggregated particle gel had different disintegration mechanisms. For the aggregated particle gel containing 1 μm oil droplets, the solid gel was fragmented into small pieces during mastication without the release of oil droplets. With subsequent gastric digestion, the gel pieces were disintegrated into smaller gel particles but oil droplets were still retained in the gel structure. By contrast, the particle-filled gel containing 12 μm oil droplets was fragmented into small pieces during oral processing with the release of oil droplets and consequent coalescence of oil droplets. During gastric digestion, the particle-filled gel containing 12 μm oil droplets were disintegrated into individual oil droplets with the high degree of coalescence of oil droplets and phase separation of emulsions.

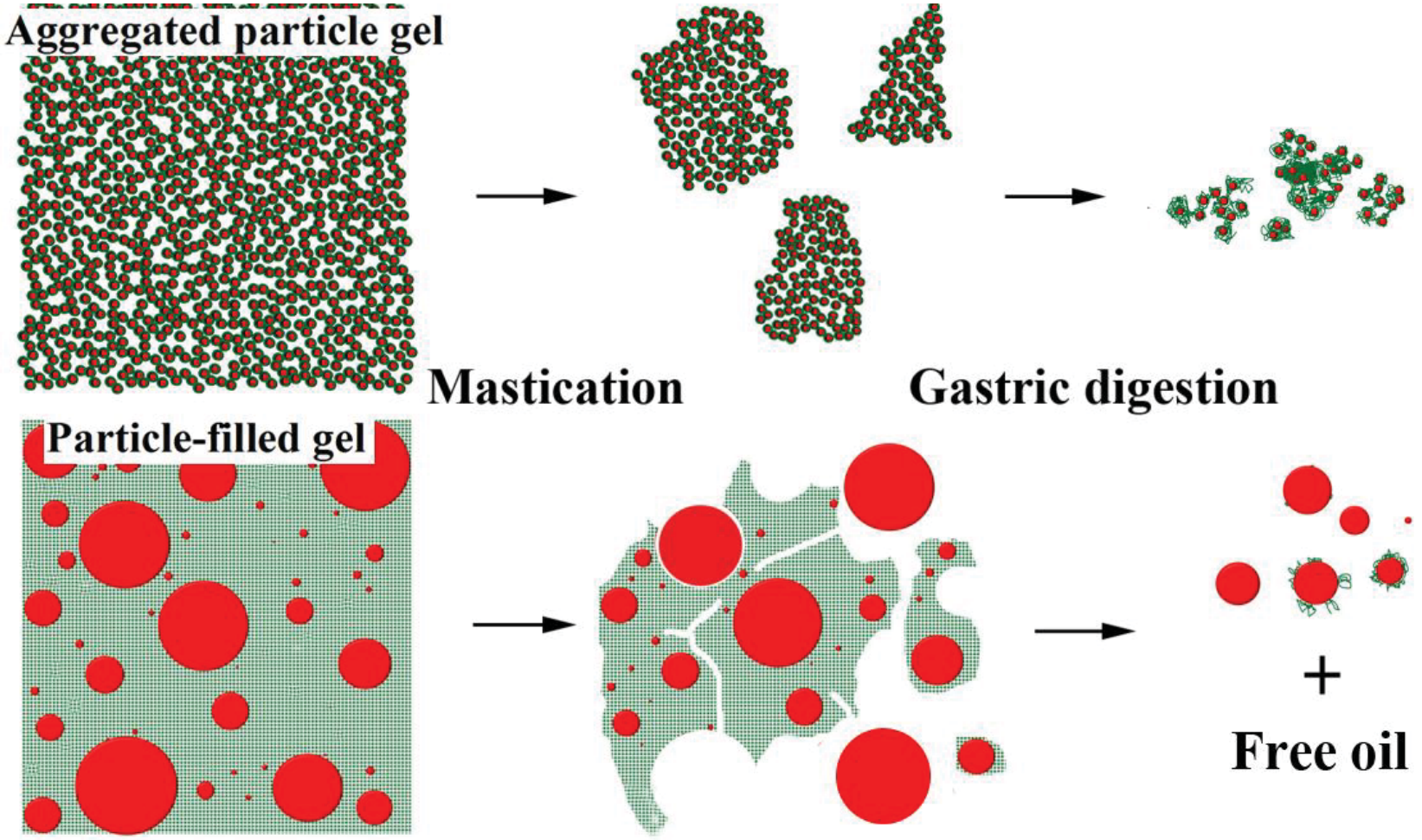

Figure 7-16 Schematic diagram of disintegration of gels containing ~ 1 and 12 μm oil droplets in the human mouth and human gastric simulator. The aggregated gel is the gel containing ~ 1 μm oil droplets; the particle-filled gel is the gel containing ~ 12 μm oil droplets.

7.5 Conclusions

In summary, the structure of whey protein emulsion gels was determined by the oil droplet distribution. The solid protein matrix of the gels containing large oil droplets (6 and 12 μm) cannot protect oil droplets during the oral and gastric digestion because of the particle-filled structure (low interactions between protein matrix and oil droplets). When the oil droplets were released from the gel matrix, they behaved similarly to a protein-stabilized oil-in-water emulsion (i.e. destabilization of oil droplets will occur). Meanwhile, small well-bonded oil droplets (1 μm) can pass the mouth and stomach with limited destruction because of the aggregated particle structure with thick coating at oil droplets. Moreover, the aggregated particle structure can hinder the hydrolysis of whey proteins.

Chapter 8 Impact of Colloidal Structure of Gastric Digesta on *in vitro* Intestinal Digestion of Whey Protein Emulsion Gels

8.1 Abstract

In this chapter, two whey protein emulsion gels containing 10 (soft gel) and 200 mM (hard gel) NaCl were formed, which had distinct structures as described in Chapter 4. A sequential digestion model including *in vitro* gastric model and *in vitro* intestinal model was used to investigate the effect of colloidal structure of gastric digesta on intestinal digestion of whey protein emulsion gels. The breakdown of gel particles, stability of oil droplets, microstructure and release of free fatty acids during the intestinal digestion were examined. The results showed that after 60 and 240 min gastric digestion the digesta of both gels had different physicochemical forms. The 60 min gastric digesta of both gels was mainly composed of gel particles ranging from ~ 1 to ~ 1000 μm. The 240 min gastric digesta of the soft gel mainly consisted of individual oil droplets and small gel particles (~ 10 μm) while that of the hard gel mainly consisted of small gel particles (~ 10 μm). The remaining gel network of hard gel particles hindered their breakdown especially in the 60 min emptied gastric digesta during the intestinal digestion. This delayed the lipid digestion significantly. During the intestinal digestion, the breakup and coalescence of oil droplets occurred simultaneously. In addition, a layer was formed around the undigested oil droplets which probably negatively affected the lipid hydrolysis.

8.2 Introduction

The intestine is the major place for lipid digestion, although a lingual lipase (secreted by salivary glands) and gastric lipase in the stomach can digest as much as 30% of dietary triglyceride (Ganong et al., 2005). The lipid is mainly hydrolysed by pancreatic lipase in the intestine, which is an interface-active enzyme with a maximum activity at around pH 6.5 (Carriere et al., 1993). Pancreatic lipase prefers to hydrolyse the Sn1 and Sn3 positions of triglycerides to give monoglycerides and the corresponding fatty acids. Lipid digestion is a dynamic and complex process. Lipolytic products can precipitate at the surface of undigested oil droplets (e.g. fatty acids, diglycerides and monoglycerides) and can inhibit pancreatic lipase accessing the surfaces of oil droplets (Reis et al., 2008a; Reis et al., 2008b). Bile salts, as bio-surfactants, play an important role in release of lipolytic products from oil droplet surfaces and transport of these products to the enterocyte cells that line the gut wall (Maldonado-Valderrama et al., 2011). Bile salts can solubilize the lipolytic products in a form of mixed micelles with phosphatidylcholine, thereby preventing building precipitates of lipolytic products at oil surfaces that limit lipolysis (Carey et al., 1983). It has been found that presence of bile salts in the digestion system lead to a higher amount of free fatty acid release in emulsions prepared by different surfactants (Mun et al., 2007; Sarkar et al., 2010b). However, the real situation of lipolysis of oil droplets is more complicated. During the digestion, the lipid undergoes several changes in phase due to the formation of self-assembled structures (e.g. emulsified microemulsions, and further dispersed micellar cubic, hexagonal and biocontinuous cubic structures).

Monoglycerides as interface-active products of lipid digestion are known to form these structures in combination with oil and water (Qiu et al., 2000). During the lipid digestion, the simple oil droplets containing monoglycerides do not translate into

the complex mixtures of diglycerides, monoglycerides, fatty acids and other polar lipids. Mixing emulsions with monoglycerides-based internally structured particles can lead to equilibration of the internal particle structure according to the composition, due to the entropy of mixing (Moitzi et al., 2007; Salonen et al., 2010; Salentinig et al., 2011). Salentinig et al. (2011) showed the transition from normal oil-in-water emulsions to internally self-assembled oil droplets or particles during *in vitro* digestion of lipids under simulated *in vivo* concentrations of bile salts juice, pancreatin porcine solution and pH as found in the human intestine. The final forms of oil droplets during the intestinal digestion are vesicles and mixed bile salts micelles in the presence of enough bile salts.

In the last decade, the behaviour of oil-in-water emulsion stabilized by different surfactants like proteins and small molecular surfactants during *in vitro* or *in vivo* intestinal digestion has been studied extensively (Golding et al., 2010; Singh et al., 2013). However, behaviour of oil droplets incorporated in solid matrix during intestinal digestion has drawn very limited attention. This may be relevant to the digestion process of many foods containing oil droplets like cheese, tofu, sausages, and dairy desserts. In Chapters 5 and 7, the gastric digestion of whey protein emulsion gels with different structures was investigated with a focus on the physicochemical properties of emptied gastric digesta. The physiochemical properties of the emptied gastric digesta were believed to continue to affect the gel digestion in the intestine.

Thus, in this chapter, *in vitro* oral processing and gastric digestion of whey protein emulsion gels were carried out first for preparing the samples for the intestinal digestion. It is noted that amano lipase A was added into the gastric model to simulate gastric lipase. The behaviour of whey protein emulsion gel in an *in vitro* intestinal model was investigated with a focus on the effect of colloidal structures of gastric

digesta (or chyme) on the intestinal digestion of oil droplets incorporated in gels. This study may help unravel the complex process of lipid digestion in solid foods.

8.3 Results and discussion

8.3.1 Physicochemical properties of emptied gastric digesta

The solid content of the emptied gastric digesta of the soft and hard gels is presented in Table 8-1. The 60 min emptied gastric digesta of the hard gel had the highest solid content because of a high gel fragmentation degree during oral processing. The solid content of the 60 min emptied gastric digesta was significantly higher than that of the 240 min emptied gastric digesta for both gels. The 240 min emptied gastric digesta of the hard gel had the lowest solid content. At 60 min, the pH of emptied gastric digesta was ~ 4.5 for both gels. At 240 min, the pH decreased to ~ 2.3 for both gels.

Table 8-1 Solid content and pH of the emptied gastric digesta.

	Soft gel		Hard gel	
	60 min	240 min	60 min	240 min
Solid content (%)	7.1 ± 0.3^{b}	5.8 ± 0.2^{c}	9.6 ± 0.1^{a}	4.8 ± 0.1^{d}
pH	4.3 ± 0.03^{b}	2.4 ± 0.02^{c}	4.7 ± 0.08^{a}	2.3 ± 0.08^{c}

Different alphabetical characters (a, b, c and d) represent the significant difference in statistics.

Particle size distributions of the emptied gastric digesta are presented in Fig. 8-1. There were two peaks in the particle size distributions of the 60 min digesta of the soft gel, one near ~ 1000 μm and the other one between ~ 10 and 100 μm. At 240 min, the large particles near ~ 1000 μm were almost totally broken down. There were two main peaks in the particle size distribution: one at ~ 10 μm and the other one at ~ 0.1 to 1 μm. This suggested that large quantities of oil droplets were released from the gel particles due to the gel disintegration. For the hard gel, there was one peak at ~ 100 μm at 60 min in the particle size distribution profile. After 240 min digestion, a large peak at ~ 10 μm and a small peak at ~ 1000 μm appeared in the particle size distribution. This means the large particles were disintegrated into smaller particles during the gastric digestion. However, no peak appeared at 0.1 to 1 μm, suggesting no oil droplets were released and the gel particles still remained structured to some extent.

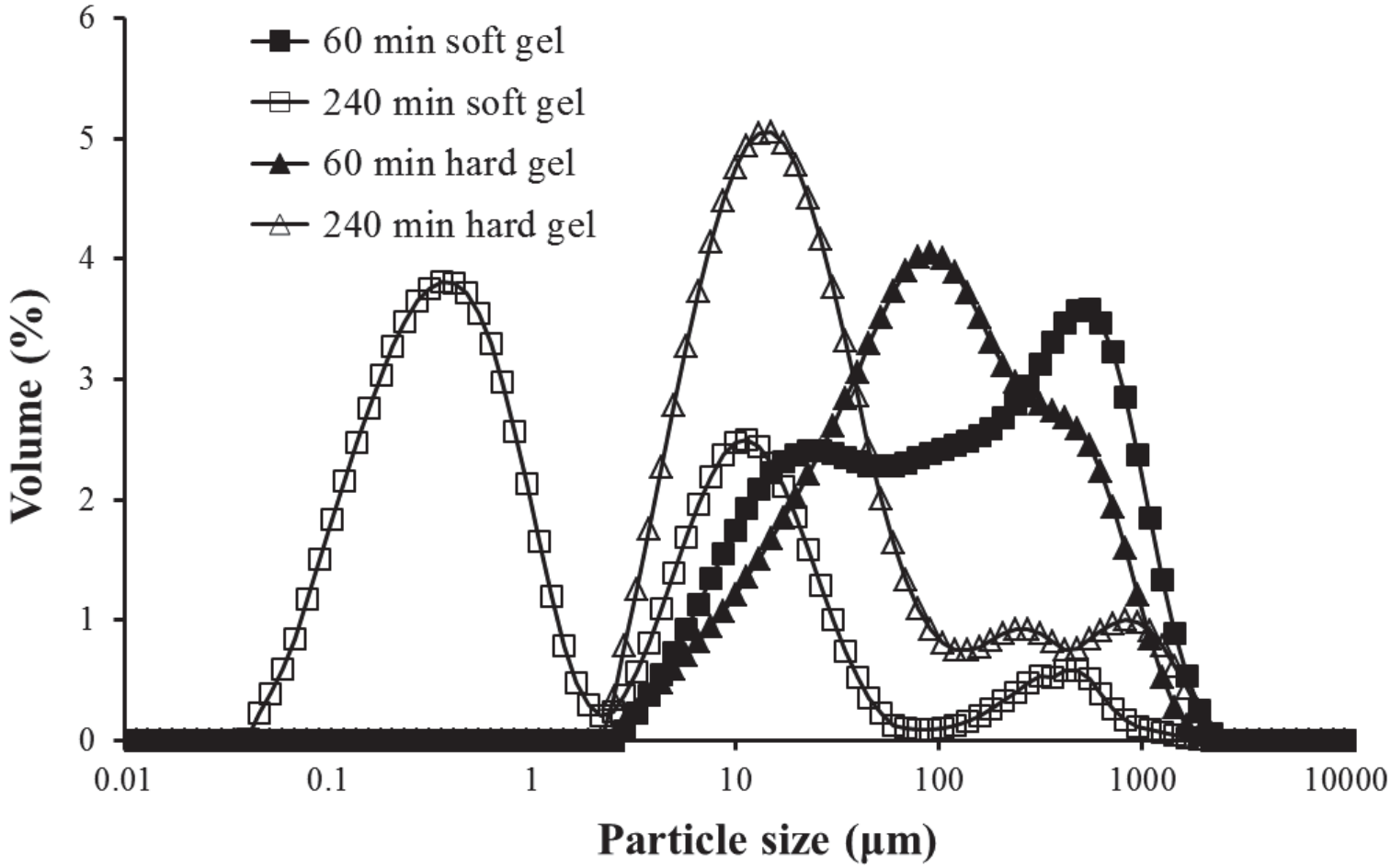

Figure 8-1 Particle size distributions of gastric digesta of the soft and hard gels emptied at 60 and 240 min.

The $D_{4,3}$ and $D_{3,2}$ of the emptied gastric digesta are presented in Table 8-2. $D_{4,3}$ is sensitive to the changes of large particles while $D_{3,2}$ is sensitive to the changes of small particles. According to the $D_{4,3}$ and $D_{3,2}$ values, the gel particles (especially the soft gel particles) were disintegrated significantly from 60 to 240 min.

Table 8-2 Particle size of the emptied gastric digesta.

	Soft gel		Hard gel	
	60 min	240 min	60 min	240 min
$D_{4,3}$ (μm)	263.6 ± 33.6^{a}	28.9 ± 23.3^{cd}	186.4 ± 2.0^{ab}	110.7 ± 55.2^{bc}
$D_{3,2}$ (μm)	32.7 ± 0.03^{b}	0.38 ± 0.1^{d}	35.6 ± 0.5^{a}	12.7 ± 1.9^{c}

Different alphabetical characters (a, b, c and d) represent the significant difference in statistics.

The particle size distributions of oil droplets in the emptied gastric digesta are presented in Fig. 8-2. Oil droplet size distributions and average diameters in all digesta were similar to that of the original emulsions (Table 8-3). This suggested that oil droplets in the emptied gastric digesta were relatively stable after 60 and 240 min gastric digestion.

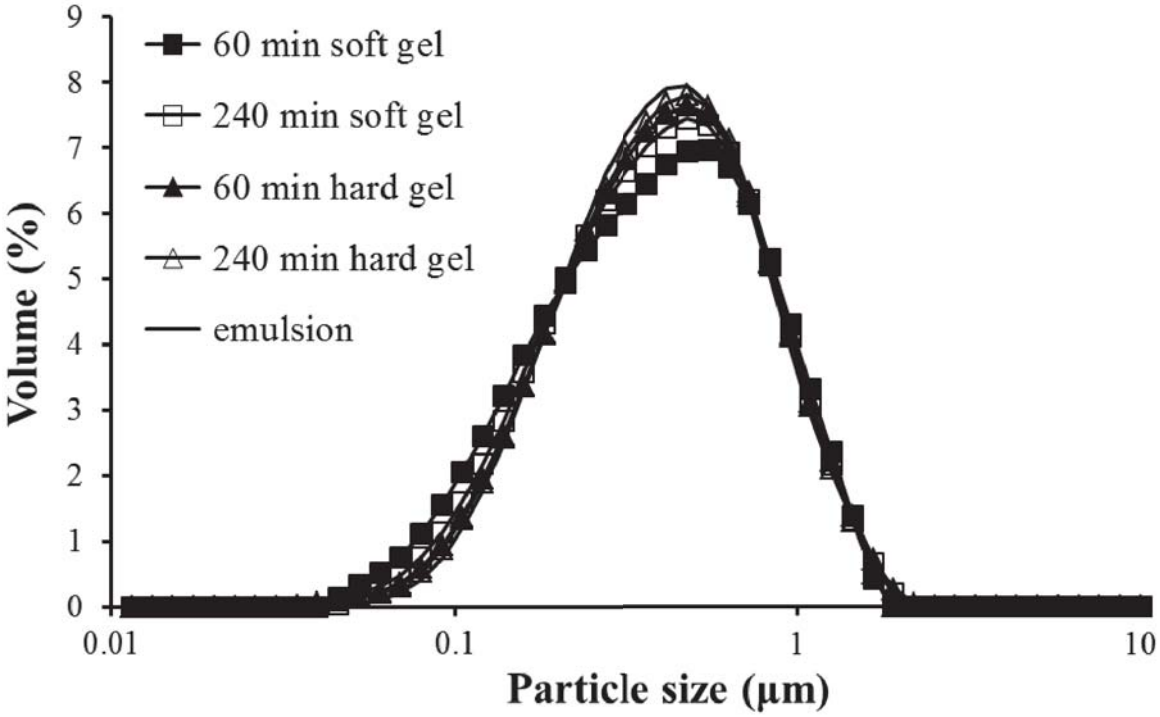

Figure 8-2 Size distributions of oil droplets in gastric digesta of the soft and hard gels emptied at 60 and 240 min.

Table 8-3 Particle size of oil droplets in the emptied gastric digesta.

	Soft gel		Hard gel	
	60 min	240 min	60 min	240 min
$D_{4,3}$ (μm)	0.44±0.01[a]	0.45.±0.01[a]	0.45±0.02[a]	0.45±0.01[a]
$D_{3,2}$ (μm)	0.283±0.003[a]	0.287±0.003[a]	0.292±0.003[a]	0.299±0.013[a]

Different alphabetical characters (a, b, c and d) represent the significant difference in statistics.

The microstructure of the emptied gastric digesta is presented in Fig. 8-3. After 60 min digestion, for both gels, almost all oil droplets were retained in the gel network; the emptied digesta of both gels was composed of gel particles of various sizes. At 240 min, the protein matrix of the soft gel particles was dissolved, and large quantities of individual oil droplets were released from the gel network. For the hard gel, oil droplets were still retained in the gel network after 240 min of digestion. The gel particles of 240 min digesta appeared to become smaller than those of 60 min digesta. In general, the results of CLSM were consistent with those of the particle size results.

Compared with the gastric digestion of gels without the addition of amano lipase A in Chapter 5, the addition of 0.5% g/L amano lipase A seemed not to affect the digestion of whey protein emulsion gels based on the above analysis of physicochemical properties of emptied gastric digesta. Amano lipase A is a lipase used to simulate gastric lipase (see details in Chapter 3-materials). The protection of protein matrix from lipase accessing the surfaces of oil droplets may play the most important role. In addition, amano lipase A was far away from its optimum pH during gastric digestion, which hindered its activity.

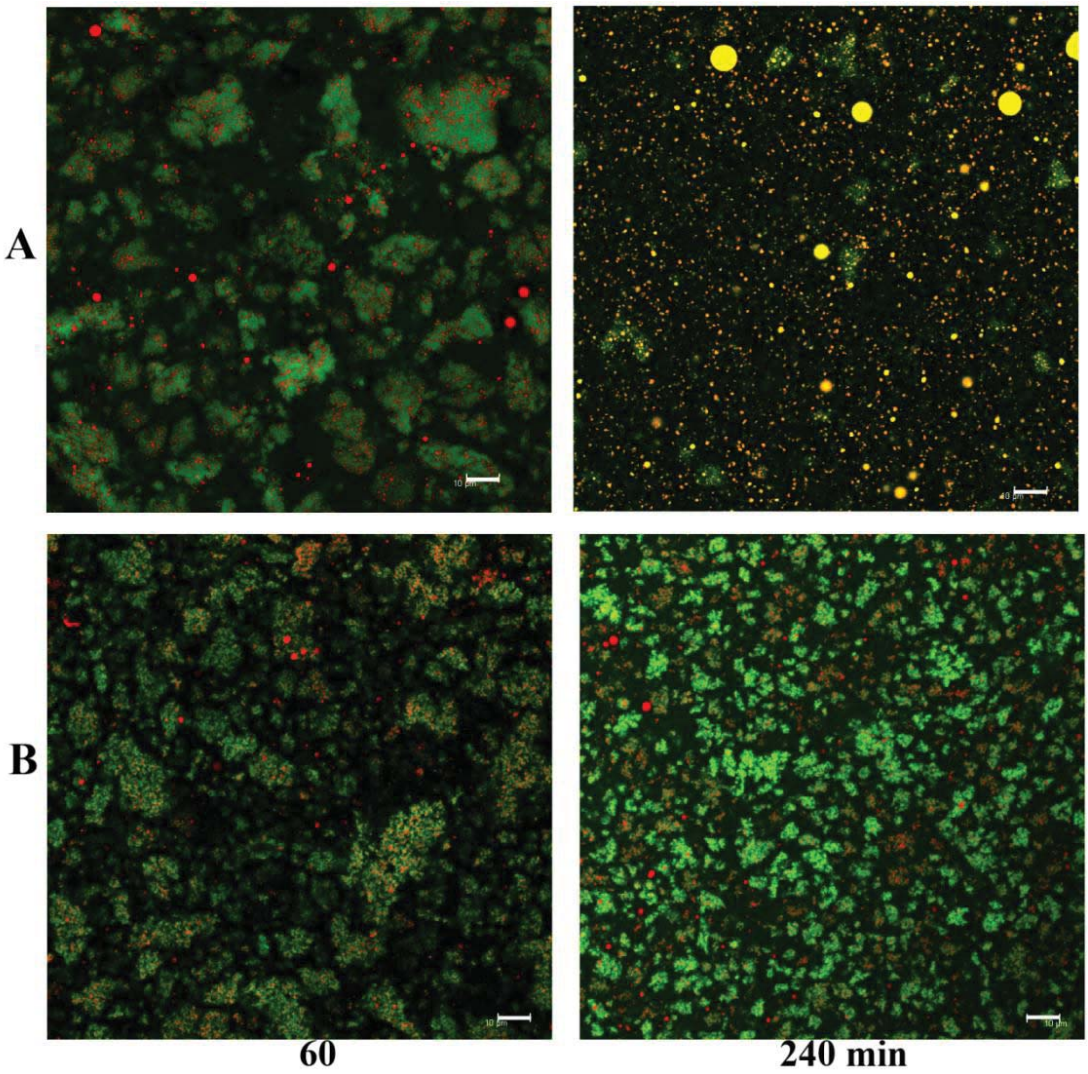

Figure 8-3 CLSM images of gastric digesta of the soft (A) and hard (B) gels emptied at 60 and 240 min. Red colour represents the oil and green colour represents the protein. Scale bar is 5 μm.

8.3.2 Breakdown of gel particles during intestinal digestion

Fig. 8-4A shows that the particle size distributions of the 60 min gastric digesta of the soft gel after intestinal digestion. At 0 min, there were two peaks in the particle size distribution, one between 10 to 100 μm and the other one near ~ 1000 μm. Upon 15 min digestion, the particles between 10 and 100 μm were mostly broken down, and a new large peak between 1 to 10 μm appeared. After 30 min digestion, the large particles of 100 to 1000 μm disappeared while the peak between 1 to 10 μm evolved into

bimodal peaks (a smaller one at 1 μm and a larger one near 10 μm). With further digestion, the peak at 1 μm shifted towards smaller size slightly with the decrease of the volume of the peak; the peak around 10 μm shifted to larger size slowly with a significant decrease of the peak volume at 90 min. The 240 min gastric digesta of the soft gel mainly constituted particles of 0.1 to 1 μm and 10 μm with a small portion of large particles between 100 and 1000 μm (Fig. 8-4B). Upon digestion, the large particles around 100 to 1000 μm were broken down, which is similar to the large particles in the 60 min digesta of the soft gel. This indicates that the protein matrix of soft gel particles was easily disintegrated in the intestinal digestion conditions regardless of gastric digestion time. The area of the peak at ~ 10 μm increased slightly during the first 30 min, increased sharply at 60 min, and then decreased markedly after 90 min. During the first 30 min, the peak between 0.1 and 1 μm, which represents the individual oil droplets, shifted to larger size. After this time (30 min), the peak (0.1 to 1μm) shifted to the smaller size gradually, and the area of the peak decreased to the lowest at 60 min. These changes reflected the lipolysis of oil droplets.

The 60 min gastric digesta of the hard gel had a peak at 100 μm with a size range from ~ 1 to ~ 1000 μm (Fig. 8-4C). During the first 30 min, the peak gradually shifted towards the smaller size. At 60 min, the large particles (100 to 1000 μm) were almost totally broken down into small particles of ~ 10 μm and a new peak between 0.1 and 1 μm appeared indicating oil droplet release from gel matrix. With further digestion, the volume of the peak at ~ 10 μm had a significant increase, but decreased markedly at 150 min; the volume of the peak between 0.1 and 1 μm reached the highest value at 90 min and then deceased. Fig. 8-4D showed that there were two peaks: one at 10 μm and the other at 1000 μm in the particle size distribution of the 240 min gastric digesta of the hard gel. After 15 min digestion, a new peak between 0.1 and 1 μm appeared suggesting

oil droplet release and its area markedly increased with digestion time. For the peak at ~ 10 μm, there were no significant changes during first 90 min and then its area significantly decreased. The large particles (~ 1000 μm) disappeared at 90 min. The vesicles and mixed micelles (most below 50 nm) could not be detected by the Mastersizer (Salentinig et al., 2011).

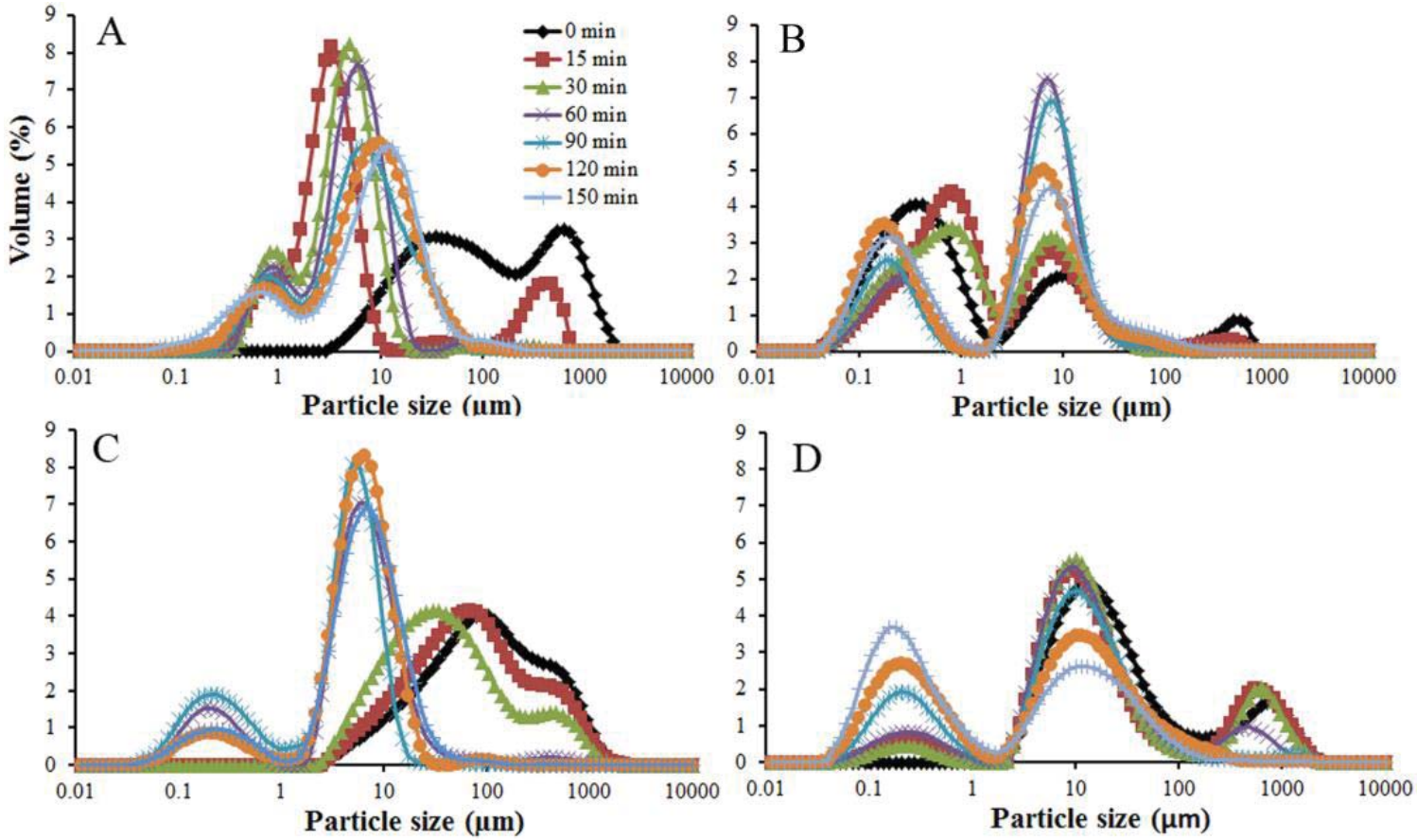

Figure 8-4 Evolution of particle size distributions of emptied gastric digesta after intestinal digestion (0, 15, 30, 60, 90, 120 and 150 min). A: gastric digesta of the soft gel emptied at 60 min, B: gastric digesta of the soft gel emptied at 240 min, C: gastric digesta of the hard gel emptied at 60 min and D: gastric digesta of the hard gel emptied at 240 min.

In the intestinal digestion, both $D_{4,3}$ and $D_{3,2}$ of the 60 min gastric digesta of the soft gel had a sharp decrease during the first 15 min but showed no significant changes after 30 min (Fig. 8-5A). In contrast, the 60 min gastric digesta of the hard gel took 60 min to reach the similar degree of breakdown to that of the soft gel (Fig. 8-5C). For 240 min gastric digesta of the soft gel, $D_{4,3}$ had a marked decrease during the first 30 min but then showed no changes with digestion time. $D_{3,2}$ had a significant increase upon the intestinal digestion and decreased gradually after 60 min. For 240 min gastric digesta of the hard gel (Fig. 8-5D), the $D_{4,3}$ showed no significant changes during the first 15 min and then decreased with digestion time; the $D_{3,2}$ decreased gradually from 0 to 150 min.

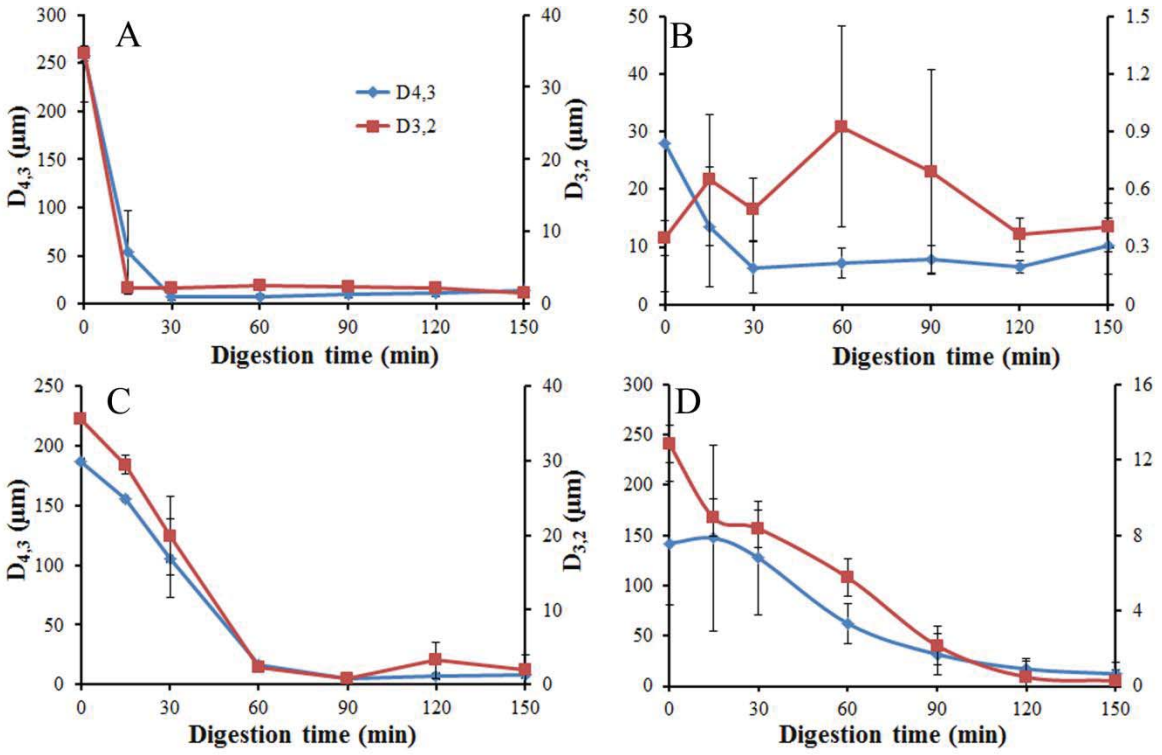

Figure 8-5 Change in $D_{4,3}$ and $D_{3,2}$ of emptied gastric digesta after intestinal digestion as a function of time (min). A: gastric digesta of the soft gel emptied at 60 min, B: gastric digesta of the soft gel emptied at 240 min, C: gastric digesta of the hard gel emptied at 60 min and D: gastric digesta of the hard gel emptied at 240 min.

8.3.3 Stability of oil droplets

Fig. 8-6A shows the oil droplet size distributions of the 60 min gastric digesta of the soft gel after intestinal digestion. At 0 min, there was only one peak in the distribution between 0.1 to 1 μm, confirming there were no free oil droplets in the digesta. After 15 min digestion, the distribution became bimodal (one near to 0.1 μm and the other between 1 and 10 μm). With further digestion, the peak between 1 and 10 μm shifted to larger size and the area of this peak gradually decreased after 60 min. However, the area of the peak at 0.1 μm gradually increased to the highest value at 120 min and then had a slight decrease at 150 min. The shifting of droplet size towards both smaller and larger sizes implies the simultaneous occurrence of coalescence and breakup of oil droplets during intestinal digestion. The coalescence of oil droplets can be explained by the presence of internal structures, such as oil droplets during intestinal digestion. X-ray scattering showed that the initial oil droplets are transformed into droplets that contain a variety of self-assembled internal structures like emulsified microemulsion (EME), micellar cubic, and bicontinuous cubic liquid-crystalline droplets (Salentinig et al., 2011). The internal structures contain up to ~30% water. Coalescence of oil droplets in the gastric digesta during intestinal digestion is consistent with previous studies on liquid protein-stabilized emulsions (Mun et al., 2007; Sarkar et al., 2010a).

The generation of small oil droplets can be explained by the high interfacial activity of 2-monoglycerides that are generated through lipolysis. Thermodynamic-stable EME for 2-monoglycerides in combination with oil and water may be easily formed even under the shaking (95 rev·min^{-1}) (Yaghmur & Glatter, 2009).

Fig. 8-6B shows the oil droplet size distributions of the 240 min gastric digesta of the soft gel after the intestinal digestion. Droplet size distribution was tri-modal

(three peaks at ~ 0.1, 1 and 10 μm, respectively) after 15 min digestion. Although a new peak (~ 0.1 μm) appeared, there was no considerable difference compared to the corresponding particle size distribution of the intestinal digesta. This indicates that the intestinal digesta (15 min) mainly consisted of individual oil droplets or digested oil droplets. With further digestion, the peak at 10 μm gradually disappeared because of lipolysis; the area of the peak at 1 μm increased to the highest value at 30 min and then decreased; the area of the peak at 0.1 μm increased with digestion time. This also confirms that the breakup and coalescence of oil droplets occurred simultaneously.

The 60 min gastric digesta of the hard gel showed different behaviour to that of the soft gel during intestinal digestion (Fig. 8-6C). During the first 30 min, the distributions did not change. After that time, the particle size began to shift to both larger (1 μm) and smaller (0.1 μm) sizes, with a minimal peak at 10 μm. At 120 and 150 min, the distribution became bimodal: one peak at 0.1 μm and the other one at 1 μm. Generally, oil droplet size distributions did not change significantly during 150 min of intestinal digestion. The degree of coalescence and breakup of oil droplets were low, because the particulate structure of the hard gel limited oil droplet release from inside the gel particles.

Fig. 8-6D shows oil droplet size distributions of the 240 min gastric digesta of the hard gel after intestinal digestion. At 0 min, there was only one peak in the distribution between 0.1 and 1 μm. After 15 min digestion, the area of the peak between 0.1 and 1 μm significantly decreased and large coalesced oil droplets (10 and 100 μm) appeared. The peak between 0.1 and 1 μm did not show a bimodal peak, as obvious as that of digesta of the soft gel, indicating colloidal structure of the 240 min gastric digesta also significantly affected the lipolysis of digesta. With further digestion, the

peak between 0.1 and 1 μm shifted to smaller size and the large oil droplets (~ 10 to 100 μm) gradually disappeared.

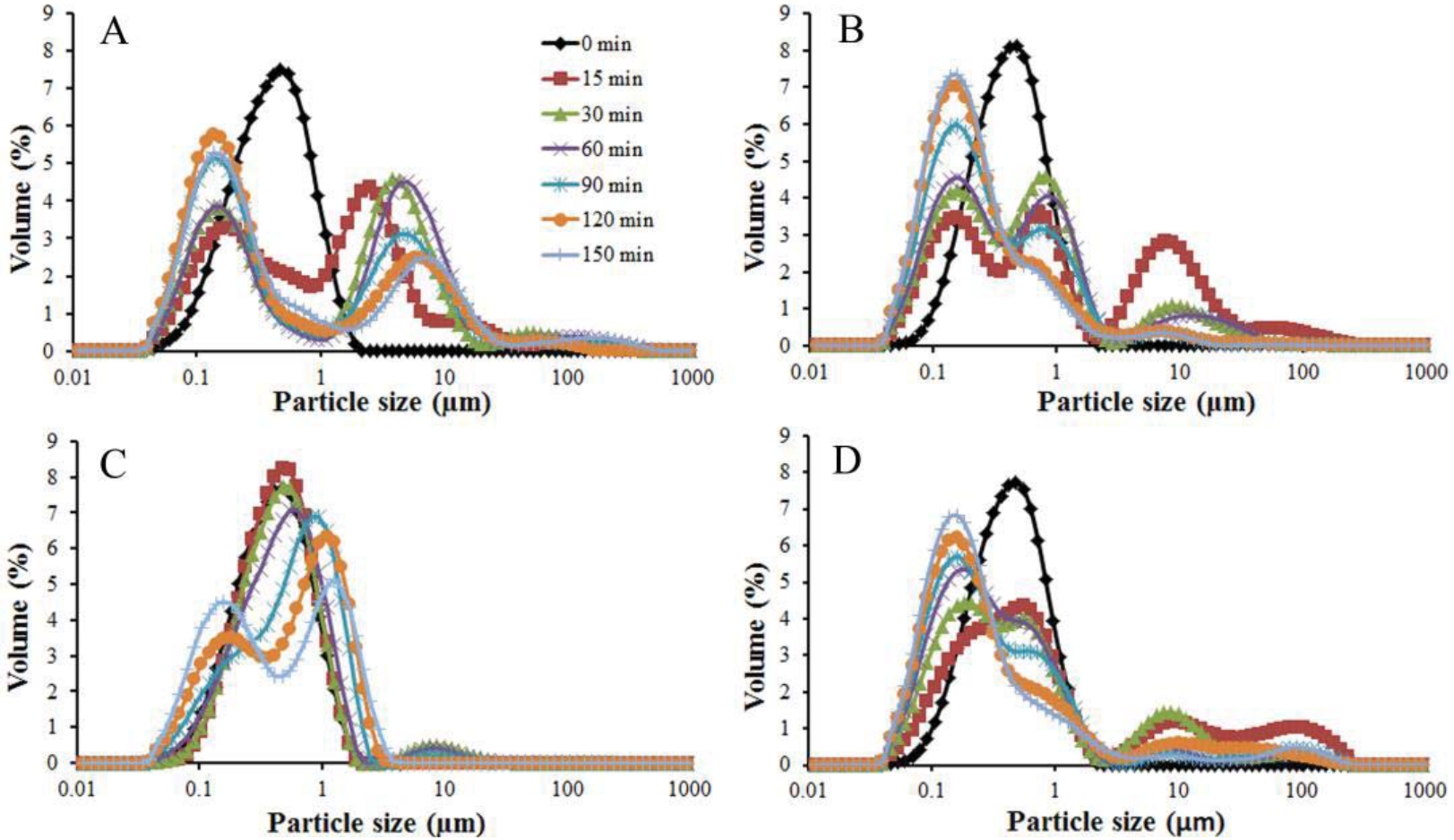

Figure 8-6 Evolution of oil droplet size distributions of emptied gastric digesta after intestinal digestion at different times (0, 15, 30, 60, 90, 120 and 150 min). A: gastric digesta of the soft gel emptied at 60 min, B: gastric digesta of the soft gel emptied at 240 min, C: gastric digesta of the hard gel emptied at 60 min and D: gastric digesta of the hard gel emptied at 240 min.

Fig. 8-7 illustrates the changes in $D_{4,3}$ and $D_{3,2}$ of oil droplets in the gastric digesta after intestinal digestion. In general, the $D_{4,3}$ of oil droplets in the 60 min gastric digesta of the soft gel had a large increase after intestinal digestion, because of coalescence of oil droplets. However, the $D_{3,2}$ gradually decreased from ~ 0.3 to 0.2 μm which is explained by the breakup of oil droplets. For the 240 min gastric digesta of the soft gel, the $D_{4,3}$ increased sharply to the highest value during the first 15 min, rapidly decreased in the following 15 min and gradually decreased after 30 min; the $D_{3,2}$ showed a similar trend. The $D_{4,3}$ of the 60 min gastric digesta of the hard gel increased from 0.43 to 1.0 μm during the first 60 min and then gradually decreased to ~ 0.7 μm; $D_{3,2}$ increased from 0.28 to 0.32 μm during the first 30 min and then decreased to 0.22 μm with further digestion. For the 240 min gastric digesta of the soft and hard gels, the $D_{4,3}$ increased sharply from 0.43 to 7-13 μm during the first 15 min and rapidly decreased from 15 to 30 min and gradually decreased after that time; the $D_{3,2}$ showed a similar trend.

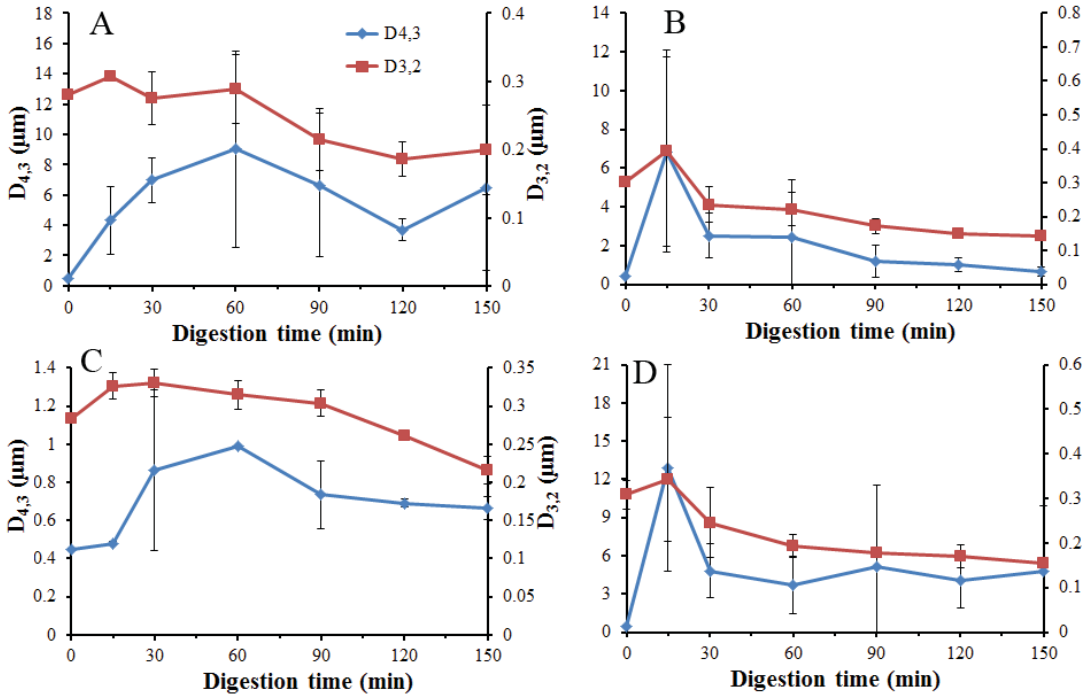

Figure 8-7 Change in $D_{4,3}$ and $D_{3,2}$ of oil droplets in emptied gastric digesta after intestinal digestion as a function of time (min). A: gastric digesta of the soft gel emptied at 60 min, B: gastric digesta of the soft gel emptied at 240 min, C: gastric digesta of the hard gel emptied at 60 min and D: gastric digesta of the hard gel emptied at 240 min.

8.3.4 Microstructure

The CLSM results were consistent with those of particle size. Fig. 8-8A shows that the 60 min gastric digesta of the soft gel at 0 min mainly consisted of large gel fragments. A high magnification image clearly showed that oil droplets were incorporated in the gel particles (Fig. 8-9A). After 30 min intestinal digestion, the large gel particles of the 60 min gastric digesta of the soft gel were totally broken down with protein matrix disruption, release of individual oil droplets and coalescence of oil droplets (Figs.8-8A and 8-9A). With further digestion, the oil droplets gradually disappeared due to the lipolysis.

Figs. 8-8B and 8-9B show that the 240 min gastric digesta of the soft gel at 0 min mainly consisted of individual oil droplets and a few of small gel particles. With intestinal digestion, oil droplets were rapidly hydrolysed and complex aggregates

appeared. These complex aggregates may be composed of peptides, fatty acids, bile salts and oil droplets.

Figs. 8-8C and 8-9C present the evolution of microstructure of the 60 min gastric digesta of the hard gel during intestinal digestion. Although the particle size appeared to decrease gradually with time, the gel particles retained some structure even at 150 min. It is interesting to note that coalescence appeared to occur between the adjacent oil droplets inside the gel fragments. This can be explained by the protein network or colloidal network of gel particles restricting the motions of oil droplets. Therefore, coalescence of oil droplets was likely to occur only between neighbouring oil droplets. The short distance between oil droplets (0.75 R, Chapter 7) and interfacial instability caused by internal structure and displacement of proteins or peptides by bile salts facilitated coalescence of oil droplets.

Figs. 8-8D and 9D show that the 240 min gastric digestion was mainly composed of gel particles, with the size smaller than the 60 min gastric digesta. No intact whey proteins remained in the gel particles, as described in Chapter 5. With 30 min intestinal digestion, most gel particles were broken down with a portion of gel particles remaining. This indicates that the colloidal structure of the 240 min gastric digesta of the hard gel inhibited the digestion more significantly than that of the soft gel. With further digestion, the gel particles disappeared and oil droplets became fewer because of lipolysis. The aggregated material, which was similar to that in the 60 min gastric digesta of the soft gel, appeared. It is noted that the resolution limit of the CLSM is about 150 nm. Therefore the oil droplets of nanometres, mixed micelles and vesicles could not be observed.

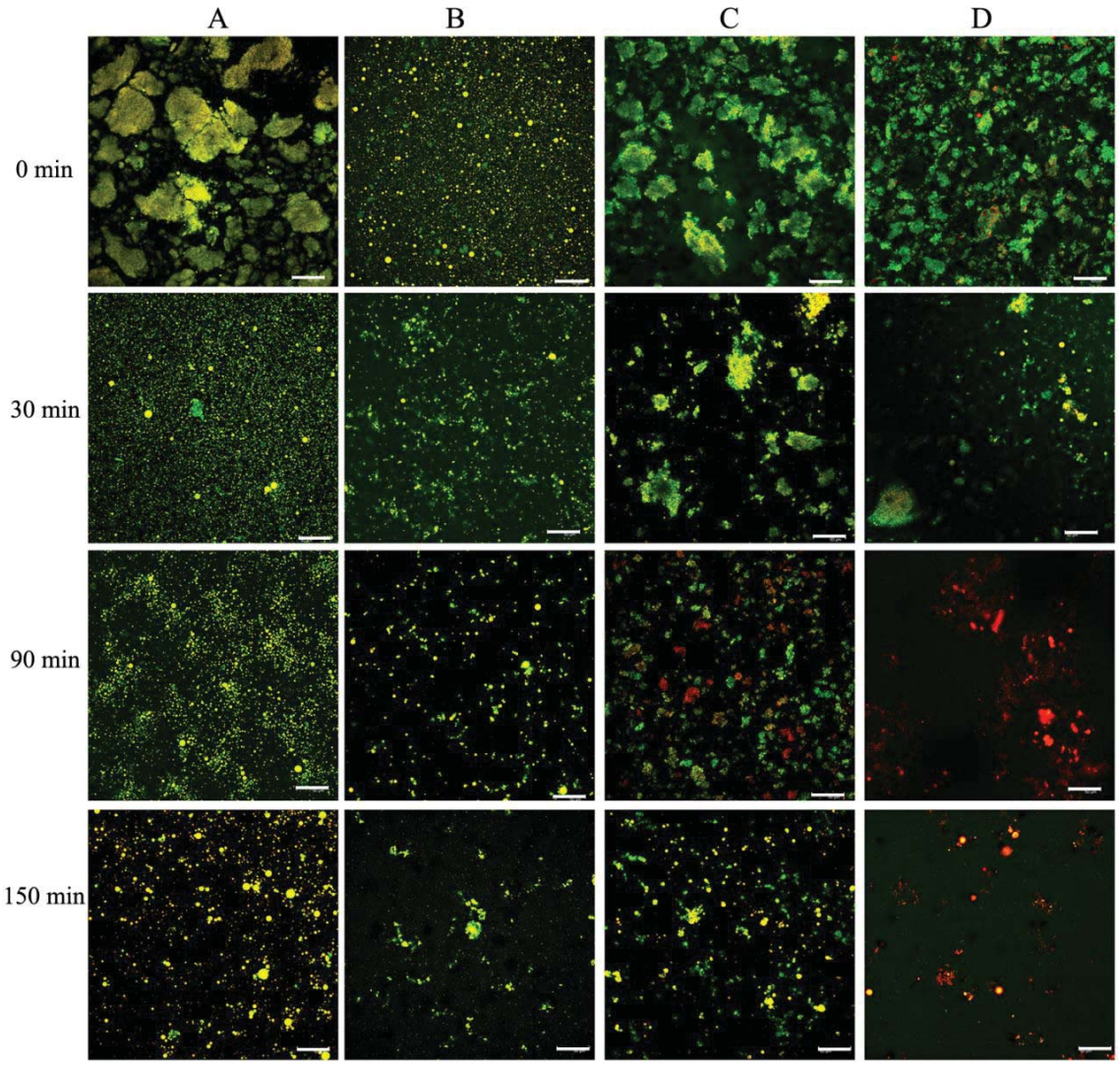

Figure 8-8 CLSM images of emptied gastric digesta after intestinal digestion at different times (0, 30, 90 and 150 min) at low magnification (scale bar is 50 μm).). A: gastric digesta of the soft gel emptied at 60 min, B: gastric digesta of the soft gel emptied at 240 min, C: gastric digesta of the hard gel emptied at 60 min and D: gastric digesta of the hard gel emptied at 240 min.

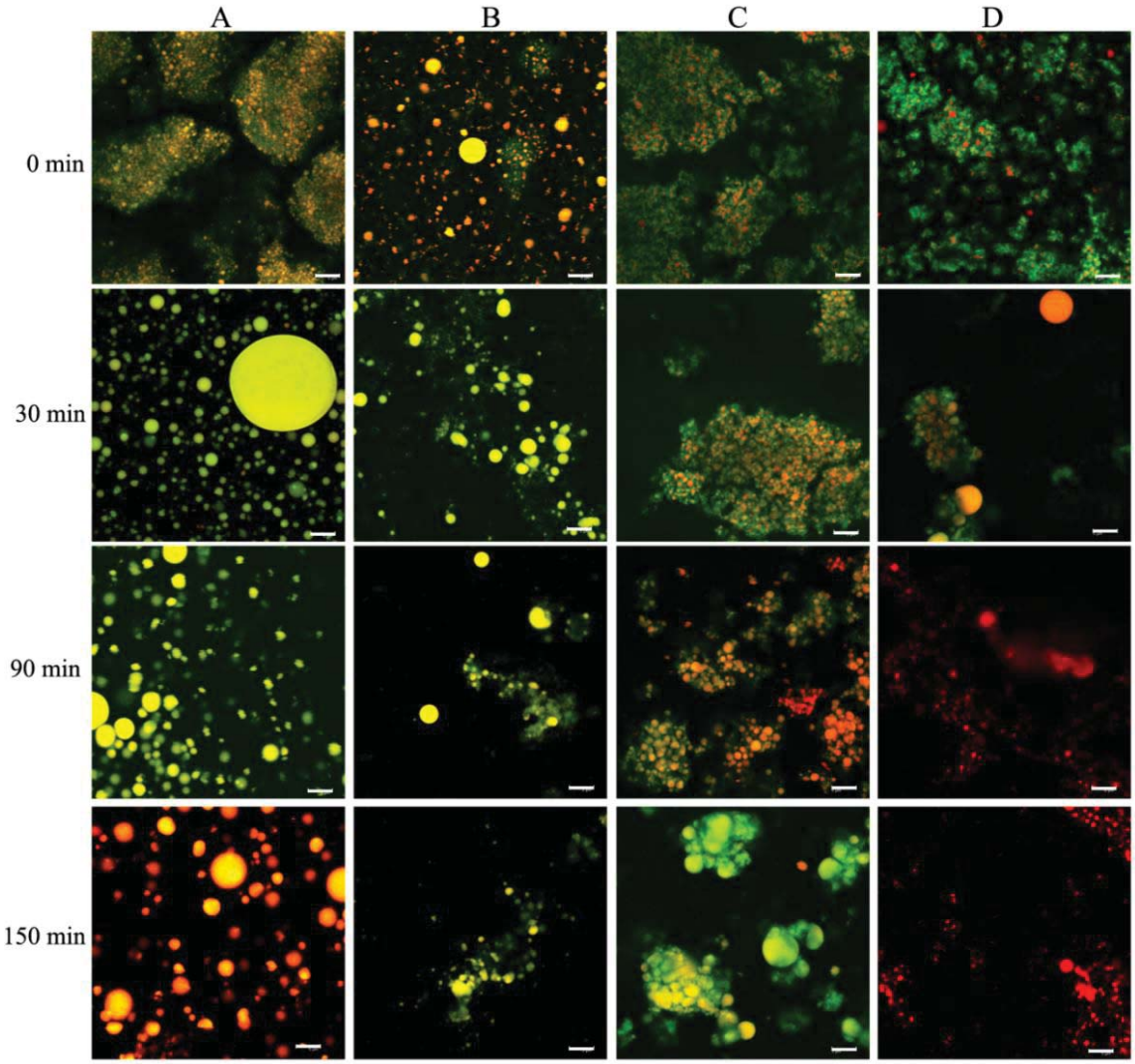

Figure 8-9 CLSM images of emptied gastric digesta after intestinal digestion at different times (0, 30, 90 and 150 min) at high magnification (scale bar is 5 μm).). A: gastric digesta of the soft gel emptied at 60 min, B: gastric digesta of the soft gel emptied at 240 min, C: gastric digesta of the hard gel emptied at 60 min and D: gastric digesta of the hard gel emptied at 240 min.

Fig. 8-10 presents the microphotographs of intestinal digesta (150 min) using transmission light (488 nm) in bright field. The surfaces of undigested oil droplets were covered by distinct layers (black colour). These non-transparent layers may be formed by lipolytic products (e.g. monoglycerides and long chain fatty acids), bile salts and peptides. This is in agreement with the previous studies of intestinal digestion of oil droplets, with the generation of liquid-crystalline lamellae or precipitates surrounding the oil droplets (Rigler et al., 1986; Hernell et al., 1990; Day et al., 2010; Gallier et al., 2013). Needle-shaped crystals of ~10 μm in size were observed in all samples (crystals were also present in samples of the 240 min gastric digesta of the soft gel which are not shown in Fig. 8-10B). Fatty acids with < 12 carbon atoms (e.g. lauric acid and capric acid) have a pKa of ~4.5 and are water soluble when protonated and ionized; long-chain fatty acids with > 12 carbons (e.g. palmitic acid and stearic acid) are less soluble and are totally ionized only at very high pH (Small, 1991; Bracco, 1994). Some long-chain fatty acids like palmitic and stearic acids do not melt in the body temperature. Therefore, long-chain fatty acids likely form into crystals at pH 6-7, which has been observed in human subjects and rats (Knutson et al., 2010; Gallier et al., 2013).

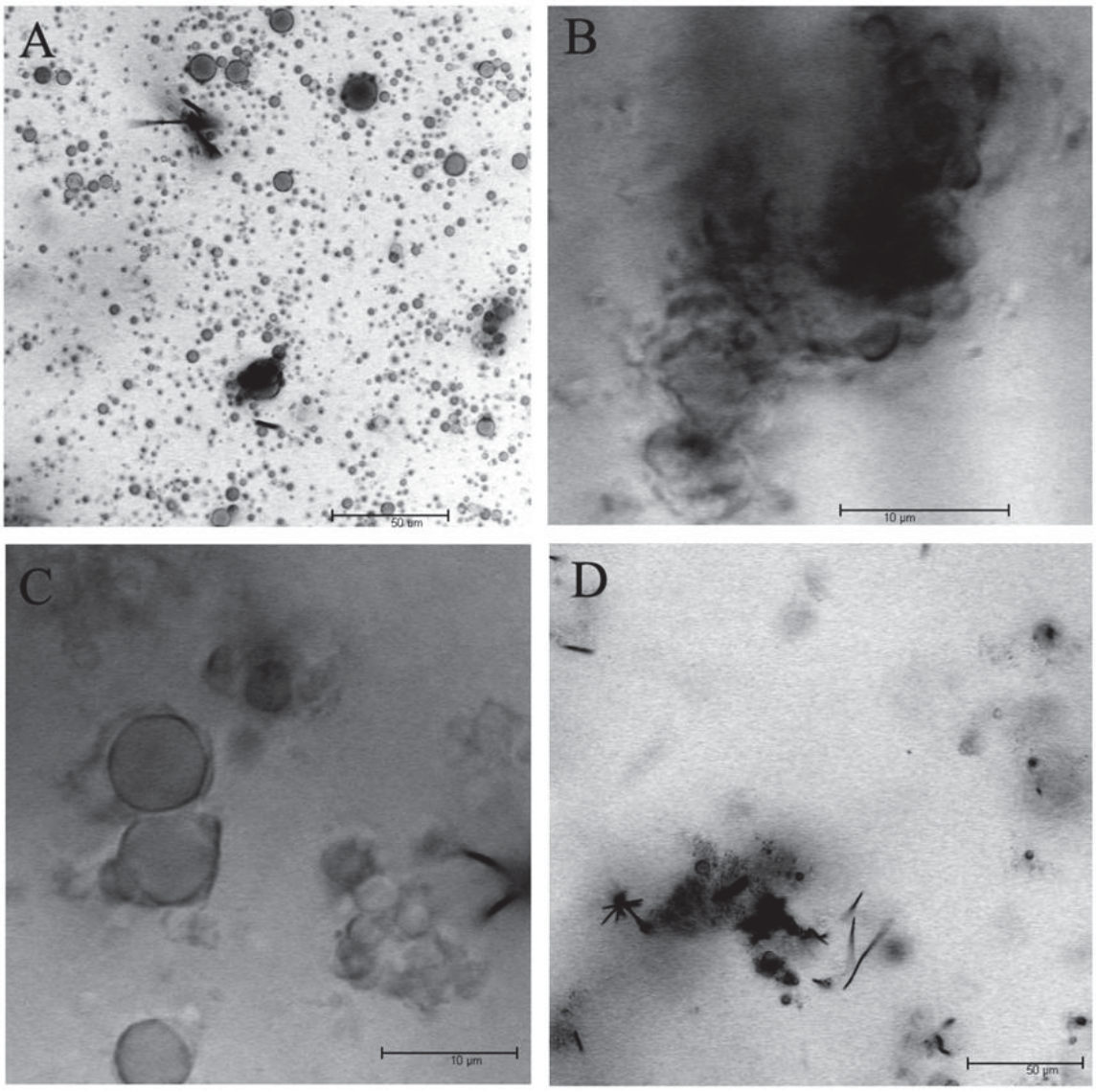

Figure 8-10 Microphotographs (transmission light) of intestinal digesta of whey protein emulsion gels. A, B, C and D represent the 60 min gastric digesta of the soft gel, 240 min gastric digesta of the soft gel, 60 min gastric digesta of the hard gel and 240 min gastric digesta of the hard gel, respectively.

8.3.5 Lipolysis

Initial lipolysis rate, which is calculated from Fig. 8-11A, is presented in Table 8-4. According to Michaelis-Menten equation, the rate of enzyme reaction increases with substrate concentration until reaching the maximum rate. It is noted that the solid content (representing oil content) of the 60 min gastric digesta of the soft gel was significantly lower than that of the hard gel (Table 8-1). However, the initial lipolysis

rate of the 60 min gastric digesta of the soft gel was significantly higher than that of the hard gel during intestinal digestion, indicating the colloidal structure of gel particles generated from the original gel structure dramatically impacts the hydrolysis of oil droplets incorporated in whey protein emulsion gel. Initial lipolysis rate of the 240 min gastric digesta of both gels was higher than that of the 60 min gastric digesta. This indicates that gastric digestion (i.e. colloidal structure modification with digestion time) had a great effect on the intestinal digestion.

After the early stage, the reaction rate of the 60 min gastric digesta of the soft gel decreased gradually due to oil hydrolysis whereas that of the hard gel rapidly decreased and kept at a constant rate for at least 30 min and then decreased (Fig. 8-11A). These differences were also attributed to the gel structure (or colloidal structure of gel particles). For the 60 min digesta of the soft gel, the gel particles were broken down rapidly into individual oil droplets (Figs. 8-4A, 8A and 9A) leading to the free access of pancreatic lipase to the surfaces of oil droplets. The lipolysis rate gradually decreased due to decreasing ratio of enzyme and oil. However, the degradation of gel particles of the hard gel was slow. As shown in Figs. 8-4C 8C and 9C, the particle size of the 60 min gastric digesta of the hard gel, almost linearly decreased during the first 60 min (Fig. 8-5C). As a result, oil droplets were exposed to pancreatic lipase gradually and the ratio of oil and enzyme remained constant for a relatively long time, which explained a constant lipolysis rate. The fatty acid release of the hard gel exceeded that of the soft gel at the final point because of a much higher solid content of the 60 min gastric digesta of the hard gel (i.e. a higher oil content) (Table 8-4). After initial stage, the 240 min digesta of both gels showed a similar lipolysis rate (Fig. 8-11A). . The fatty acid release of the soft gel exceeded that of the hard gel at the final point because of a much higher solid content of the 240 min gastric digesta of the hard gel (Table 8-4).

The fatty acid release per gram gel as a function of time is presented in Fig. 8-11B. The fatty acids liberation of the 60 min gastric digesta of the hard gel was markedly lower than that of the soft gel over 150 min intestinal digestion, especially in the early stage. Although the lipolysis rate of the 240 min gastric digesta of the hard gel in the early stage was lower than that of the soft gel, the fatty acid release profiles of both gels were similar. For the effect of colloidal structure altered due to gastric digestion (different times), the 240 min gastric digesta of both gels had a much higher lipolysis rate than the 60 min gastric digesta.

Table 8-4 Initial lipolysis rate of emptied gastric digesta during intestinal digestion

	Soft gel		Hard gel	
	60 min	240 min	60 min	240 min
Initial reaction rate ($\mu mol \cdot mL^{-1} \cdot min^{-1}$)	1.4 ± 0.2^{b}	2.2 ± 0.5^{a}	0.9 ± 0.1^{c}	1.2 ± 0.6^{bc}

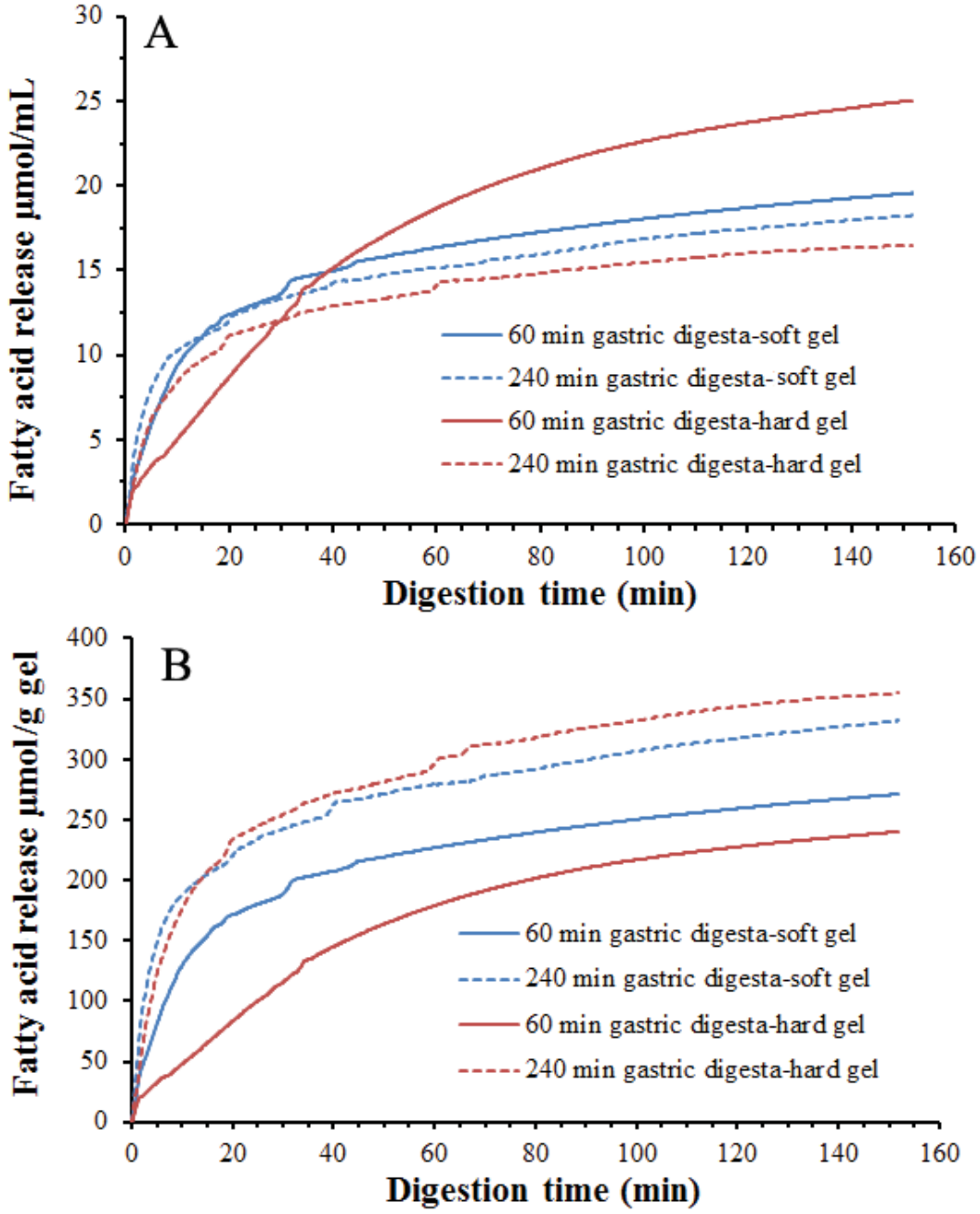

Figure 8-11 Free fatty acid release of gastric digesta emptied at 60 and 240 minduring intestinal digestion. The unit of fatty acid release of A is µmol per mL digesta; the unit of fatty acid release of B is µmol per gram gel.

8.4 Possible mechanisms of lipolysis of oil droplets incorporated in the hard gel

Based on the analysis of intestinal digestion of the 60 min gastric digesta of the hard gel, most oil droplets were restricted in the colloidal structure of the gel particles during the digestion of 150 min. A schematic diagram describes this process as show in Fig. 8-12. During this process, the breakup of free oil droplets by shearing, removal of lipolytic products from the oil droplet surfaces and droplet coalescence occurred simultaneously. However, the amount of small oil droplets (~ 0.1 μm) and degree of coalescence was low, which is attributed to the protection of colloidal structure of gel particles. In this situation, the breakup of oil droplets hardly occurred because of the low oil droplet release from the gel network; the coalescence of oil droplets was difficult because the remaining gel network hindered the collision of oil droplets; the limited access to oil droplet surfaces by pancreatic lipase lowered the rate of removal of lipolytic products from the oil droplet surfaces. This also indicates that the lipid digestion can be modulated by designing the gel structure around the oil droplets.

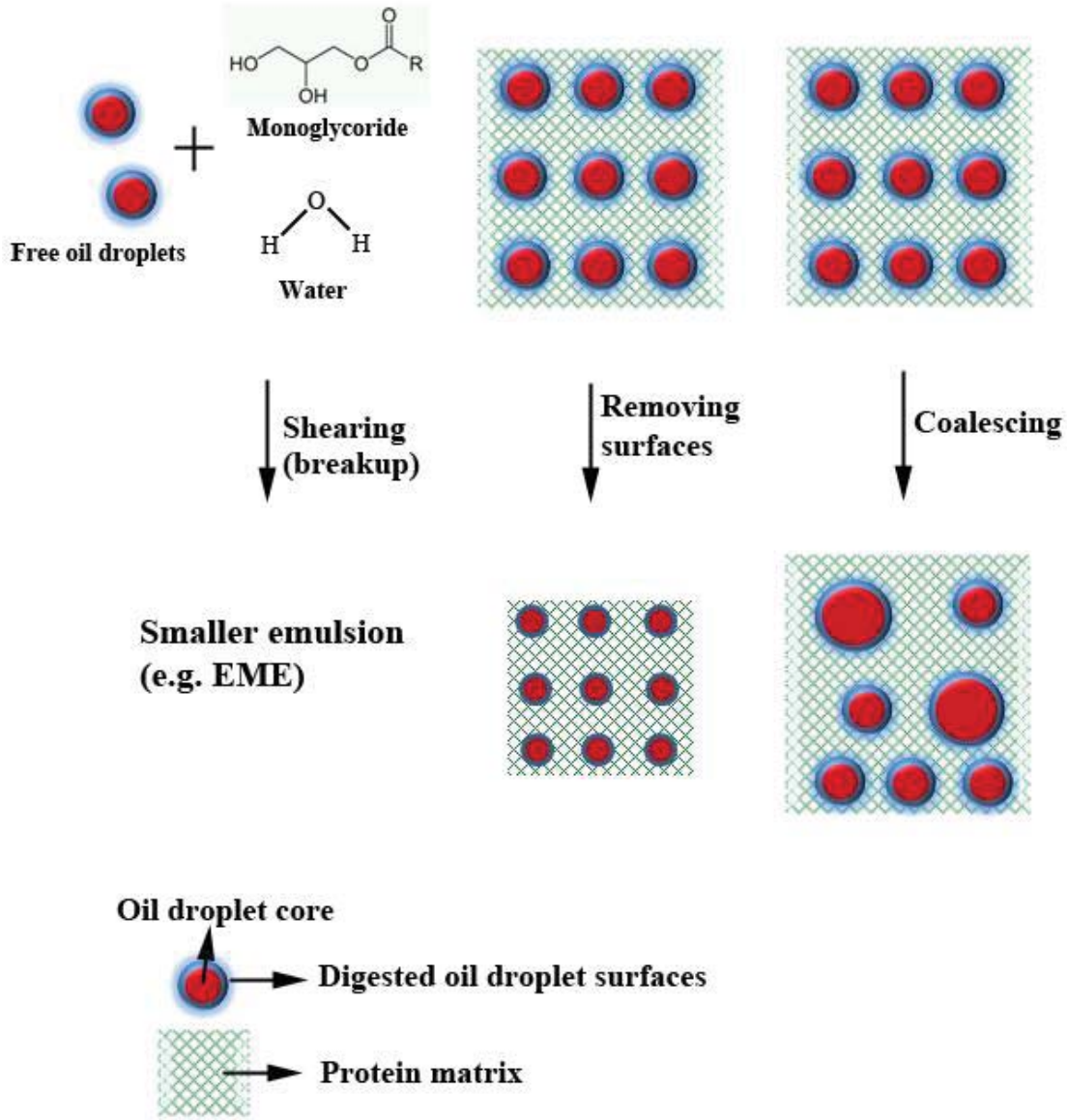

Figure 8-12 Mechanisms of lipolysis of oil droplets of the 60 min gastric digesta of whey protein emulsion gel (hard gel) during intestinal digestion.

8.5 Conclusions

This chapter investigated the fate of the gastric digesta emptied from a dynamic gastric model at different times during *in vitro* intestinal digestion. Compared with gastric digestion of gels in Chapter 5, the addition of amano A lipase did not markedly affect the digestion of whey protein emulsion gels. During intestinal digestion, the oil droplets evolved into both smaller size and larger size because of removal of lipolytic products from oil droplet surfaces, breakup of oil droplets and coalescence of oil droplets. Colloidal structures of gastric digesta which were generated from the structure of original gels significantly affected the oil digestion. The remaining protein network of the 60 min gastric digesta of the hard gel hindered the breakdown of gel particles. In general, the gastric digesta of the hard gel had a slower lipolysis rate than that of the soft gel because of the protection of gel network. The lipolytic products accumulated around the undigested oil droplets that may gain the difficulties of access to oil droplet by pancreatic lipase. It is interesting to note that the coalescence of oil droplets appeared to occur between neighbouring ones in the 60 min gastric digesta of the hard gel. Whey protein emulsion gels with different structures showed a potential to control lipid digestion. *In vivo* studies are expected to be done to validate the effect of gel structure on the regulation of lipid digestion.

Chapter 9 Overall Conclusions, Discussion and Recommendations for Future Work

9.1 Overall conclusions and discussion

A series of studies involving *in vivo* oral processing, *in vitro* oral processing, *in vitro* gastric digestion and *in vitro* intestinal digestion revealed the complex digestion process of whey protein emulsion gels. The gel structure was the key factor influencing the digestion of gels. Although the physicochemical properties of the gels were permanently changed at each stage of digestion, the gel structure played an important role in the whole process of the digestion.

Gel structure is the organization of structural elements and their interactions. By varying the ionic strength and oil droplet size, a series of whey protein emulsion gels with different structures were formed. The gel containing 10 mM NaCl and small oil droplets (~ 0.45 μm) had a fine-stranded continuous protein matrix with filled oil droplets. This structure can be referred to the emulsion-filled structure. With increasing NaCl concentration, the protein matrix of the gels gradually became porous especially at NaCl concentration of 200 mM which appeared to be formed by the links or interactions of thick protein-coated oil droplets. This structure can be referred to aggregated particle structure. On the other hand, the gel containing 100 mM NaCl and ~ 12 μm oil droplets had a continuous protein matrix with filled large oil droplets (i.e. emulsion-filled gel). With decreasing droplet size from 12 to 1 μm, the gel structure became more porous, which can also be regarded as the aggregated particle gel. It should be noted the mechanisms for the formation of emulsion-filled and aggregated particles gels by varying NaCl concentration and oil droplet size are different. The change of gel structure with increasing NaCl concentration can be explained by the formation of dense

and compact protein aggregates at high NaCl concentration, which were adsorbed at oil droplet surfaces. The change of gel structure with decreasing oil droplet is because of the increase of surface area of oil phase leading to large protein adsorption and coating at oil droplets (Chapters 4 and 7).

The viscoelasticity in the linear region, large deformation properties before fracture and fracture properties were used to describe mechanical properties of whey protein emulsion gels. Mechanical properties reflect the gel structure which can explain structure-function relationships and may correlate to the breakdown properties of food in the human body. The shear storage modulus (0.5% strain) and gel hardness (50% strain) increased with NaCl concentration. This indicates that the magnitude of interactions per unit of gel between structural elements increased with NaCl concentration to 100 mM. However, with further increase of NaCl concentration to 200 mM, the shear storage modulus and gel hardness showed a significant decrease. This does not mean that the magnitude of interactions between structural elements decreased. At this condition (200 mM NaCl), the gel had a porous structure at the micro scale. The gel pores dissipated applied energy and the energy could not be stored in the gel network as effectively as the gel containing 100 mM NaCl during the small and large deformation. This led to the significant decrease of shear storage modulus and gel hardness. In the fracture test, the fracture force significantly increased with increasing NaCl from 10 to 200 mM (i.e. the magnitude of interactions between structural elements increased with NaCl concentration). And, the gel containing 200 mM NaCl had a higher fracture strain than that containing 100 mM NaCl. These differences suggest that the pattern of organization of gel elements was one of key factors influencing the mechanical properties of the gels. The gel structure was determined by both magnitude of interactions per unit gel between structural elements and arrangement of structural

elements. Based on analysis of mechanical properties of gels from small strain to fracture, the gel strength or hardness increased with the increase of NaCl concentration in general. The structure of gels containing 1, 6 and 12 μm oil droplets were also determined by the interactions between structural elements and the organization of gel elements. The shear storage modulus, gel hardness (50% strain) and fracture force increased with the decrease of oil droplet size. This can be explained by the increase of interactions between oil droplets and protein matrix with decreasing droplet size, i.e. the energy can be stored more effectively via strong stress transfer ability from protein matrix to oil droplets (Chapters 4 and 7).

For the digestion of solid foods, the fragmentation of foods in the mouth greatly impacts the following digestion in the stomach and intestine. In the human mouth, the gel hardness was the key factor determining the threshold particle size of bolus for swallowing. In general, the fragmentation degree of gels containing different NaCl concentrations in the mouth linearly increased with the gel hardness. The fracture speed of gels increased with the fracture force measured by the texture analyzer. The small oil droplets (~ 0.45 μm) were incorporated in the protein matrix as an integral part, because of the strong bonding between small oil droplets and protein matrix. After mastication, there were few oil droplets released from the gels. However, the situation changed for the gels containing large oil droplets. Considerable quantities of large oil droplets released during the oral processing in the gels containing 6 and 12 μm oil droplets. This can be explained by the weak ability of stress transfer between large oil droplets and protein matrix (Chapters 4 and 7).

It appeared that the human subjects selected different oral processing patterns based on gel hardness (i.e. a higher food hardness, the greater fragmentation degree). From the point of view of the whole process of food digestion in the human body, a

higher fragmentation of hard food in the mouth will aid its digestion in the stomach. The mechanical force generated by the stomach is much lower than that by the teeth. For the gels containing 1, 6 and 12 μm oil droplets, the gel fragmentation after mastication did not show major differences. This does not mean that the gels containing oil droplets of different sizes did not follow the strategy of oral processing based on the gel hardness. Actually, the oil droplet release during oral processing of the gels containing 6 and 12 μm oil droplets decreased the fragmentation degree in the calculation because the sieves could not retain the oil droplets (Chapters 4 and 7).

Food disintegration in the stomach is an important step for food digestion in the human body. This study showed that mechanical shearing, enzymatic hydrolysis, gel swelling and gel structure played an important role in the gel disintegration in the HGS. During gastric digestion, the mechanical shearing was crucial factor leading to the gel breakdown, which played a major role in the gel disintegration. The bolus of the gel containing 10 mM NaCl (soft gel) disintegrated much faster than that of the gel containing 200 mM NaCl (hard gel) during gastric digestion. The disintegration mechanisms of the soft gel during gastric digestion were abrasion and fragmentation because of the low gel strength. However, abrasion is the predominant disintegration mechanism for the hard gel due to its high gel strength. The disintegration of gels could be described well by the Weibull distribution function: $D_{50}(t) = D_{50}(0)e^{-(\lambda t)^{\theta}}$. For both gels, the disintegration showed an initially rapid process followed by a slower process. The gel disintegration during gastric digestion was facilitated by pepsin digestion, as it was able to disrupt the molecular structure of the gels. Pepsin digestion had a greater effect on the disintegration of the soft gel especially after 180 min when the pH decreased below ~ 3. The swelling of gels and diffusion of pepsin and ions (e.g. Na^+, Cl^- and H^+) into the gel can lead to the mechanical instability of inner structure of

gel particles thereby accelerating gel disintegration (Chapters 5 and 6).

In the real digestion, the properties of food bolus greatly affect the food digestion in the stomach. This study showed that the larger particle size of gel bolus slowed down the emptying of gels from the HGS regardless of gel strength. As the gastric digestion progressed, the gel disintegration began to affect the emptying of gels from the HGS (i.e. a faster gel disintegration led to a faster gel emptying). The situation became complicated when the components of the gel were unstable. For example, the instability (i.e. coalescence and creaming into the top layer) of large oil droplets (6 and 12 μm oil droplets) slowed down the emptying of gels from the HGS (Chapters 5 and 7).

The gastric digestion is a continuous and dynamic process. The chyme is regularly delivered into the duodenum. Thus, the physicochemical properties of chyme change with time. The present study monitored this dynamic process by simulating the human gastric digestion. Interestingly, in the early and middle stage of gastric digestion, the particle size of the emptied gastric digesta of the hard gel was lower than that of the soft gel. This is because the gel fragmentation degree during oral processing was relatively high for the hard gel and the abrasion dominated the gel disintegration during gastric digestion. In the late stage, the particle size of emptied gastric digesta of the soft gel was lower than that of the hard gel, because the pepsin digestion had a greater effect on the disruption of the gel network of the soft gel. These findings highlight the effect of food material properties on the gastric digestion of foods (Chapters 5 and 6). However, the situation was different for the gels containing larger oil droplets (6 and 12 μm) because of unstable gel structure (i.e. coalescence and creaming of oil droplets) (Chapter 7).

The physicochemical properties of emptied gastric digesta greatly influenced the

gel digestion in the intestine. The protein matrix of gel particles of both the soft and hard gels was gradually disrupted. With *in vitro* gastric digestion for 4 hours, no intact whey proteins survived in the emptied gastric digesta of both the soft and hard gels. At this time, almost all soft gel particles in the emptied digesta were disrupted into individual oil droplets with the protein matrix dissolved. However, the hard gel particles in the emptied digesta retained much of gel structure without oil droplet release. These differences were attributed to the different network structures of the soft (emulsion-filled structure with fine-stranded protein matrix) and hard (aggregated particle structure) gels. During gastric digestion, the fine-stranded protein matrix was susceptible to pepsin digestion and mechanical shearing. However, the aggregation of thick protein-coated oil droplets at low electrostatic repulsion (200 mM NaCl) was difficult to disrupt. The high degree of cross-linking of whey proteins during gel formation at high NaCl concentration was the key factor hindering the breakdown of particles of the hard gel. Generally, the oil droplets of both gels during gastric digestion were stable. However, for the gels containing larger oil droplets, the coalescence of oil droplets occurred because of large quantities of the oil droplet release, which led to the creaming and phase separation of oil droplets. The protein matrix of the gels containing 12 μm oil droplets was hydrolyzed much faster than that of the gels containing small oil droplets because of the low magnitude of interaction between oil droplets and protein matrix (Chapters 5, 6 and 7).

Small intestine is the main site for food digestion and absorption. The 60 and 240 min emptied gastric digesta of the soft and hard gels was selected for intestinal digestion. These digesta had totally different physicochemical properties. The 60 min gastric digesta of both gels retained most of network structure. However, their particles had different gel strength. The 240 min emptied gastric digesta looked like a typical

liquid oil-in-water emulsion stabilized by peptides. The 240 min emptied gastric digesta of the hard gel was composed of gel particles (~ 10 μm) formed by oil droplets and peptides, which retained the gel structure to some extent. The breakdown of oil droplets in the emptied gastric digesta during *in vitro* intestinal digestion was complicated. The removal of lipolytic products from the oil droplet surfaces, breakup of oil droplets and coalescence of oil droplets occurred simultaneously. In general, the colloidal structure of emptied digesta of the hard gel (especially 60 min digesta) hindered the hydrolysis of oil droplets more significantly than that of the soft gel. This is explained by the protection produced remaining gel structure (i.e. limit the access to oil droplet surfaces by lipase). In the 60 min digesta of the hard gel, the remained protein matrix limited the motion of oil droplets and their release. And the undigested part of the digesta mainly consisted of "gel particles" at 150 min intestinal digestion. The coalescence of oil droplets was likely to occur between neighboring oil droplets. The restricted free motion of oil droplets led to a lower degree of breakup and coalescence of oil droplets. These findings convey that lipid digestion can be modulated by designing the properties of surrounding matrix and in the real digestion process the small intestine may response differently to the gastric digesta emptied at different times.

Moreover, it has been shown that exposure of the distal portion of jejunum and ileum to fat produces a strong inhibition of gastrointestinal motility and gastric and pancreatic secretion, and leads to a reduction in hunger and in food intake (Welch, Saunders, & Read, 1985; Welch, Sepple, & Read, 1988; Meyer, Tabrizi, DiMaso, Hlinka, & Raybould, 1998; Maljaars, Peters, Mela, & Masclee, 2008; Samra, 2010). These are called "jejunal brake" and "ileal brake", respectively. The reduction in food or energy intake is larger when the exposed surface of small intestine is larger. Oil droplets incorporated in the hard gel may reach the distal part of small intestine in the

human body according to above analysis; this may activate jejunal and ileal brakes. Thus, the hard gel may be a potential food ingredient for the functional food targeted at sustainable reduction in food intake (Chapter 8).

Overall, the gel structure played an important role in all three main stages of food digestion including oral processing, gastric digestion and intestinal digestion. Through controlling the gel structure, the digestion of whey protein stabilized oil-in-water emulsion gel can be modulated. This project provided a potential tool or strategy to modulate the lipid digestion in the human body, which would benefit the human health and innovation in new functional foods. In addition, this project showed the relationships between oral digestion and gastric digestion, gastric digestion and intestinal digestion. During *in vitro* studies, each stage of the food digestion affected the next stage of the digestion in a non-reversible manner. The nature of food digestion is the interactions between food material properties and the digestive system (e.g. strategy of food oral processing, how the stomach processing different foods and how nutrients being absorbed by the intestine). These interactions are the very important attributes of the foods, which should be considered in the assessment of nutritional values of foods and food design in the future.

9.2 Recommendations

- *In vivo* studies

The human gastric simulator and *in vitro* intestinal model only simulate several aspects of the real physiological conditions of the human body. Actually, the food digestion process in the human body, which is modulated by hormonal and neural responses, is much more complex than that during *in vitro* digestion. In addition, each stage of the food digestion interacts with each other. To validate *in vitro* studies carried

out in the present project, *in vivo* studies are necessary.

- Mapping the peptides generated during gastric and intestinal digestion

The peptides generated from protein hydrolysis of heat-set whey protein gel (e.g. fine-stranded and particulate gel) during gastric and intestinal digestion should be mapped by HPLC-MS/MS. The nature of peptides generated from the digestion of pure protein gel and emulsion gel should be compared to find out the influence of oil droplet on the formation and digestion of whey protein gel.

- Understanding of the role of nano and molecular-structures in the digestion of protein network

The research evidence of this project suggests that the nano and molecular-structures of protein network determines the digestion of whey protein emulsion gels. Therefore, the fundamental research at nano and molecular-scales should be carried out. First, the structure of whey protein emulsion gels at the nano and molecular scales is investigated. Subsequently, the relationship between nano and molecular-structures and the digestion of whey protein emulsion gels (e.g. gel disintegration and peptides generated by protein hydrolysis) is evaluated.

- Exploring the effect of lipid crystallinity on the digestion of whey protein emulsion gels

Dietary lipids come from various sources such as milks, meats and vegetables. The melting temperature (or crystallinity) of lipids from different sources varies (e.g. animal or plant origin) largely because of their complex compositions and structures. The composition and structure of lipids may have a major effect on the digestion of whey protein emulsion gels, which requires further research. In addition, it is necessary to understand the digestion of lipids from different sources.

- Behaviour of differently structured whey protein emulsion gels induced by calcium, acid and transglutaminase during *in vitro* digestion

The types of whey protein emulsion gels include heat-set gel containing calcium chloride, heat-set gel containing sodium chloride prepared at pH 2, cold-set gel induced by acid and cold-set gel induced by transglutaminase. The breakdown of differently structured whey protein emulsion gels at the macro, micro and nano-scales is worth investigating for mechanistic understanding of the effect of gel structure on the gel disintegration, protein hydrolysis and lipid digestion during the digestion.

- Application of emulsion gel in delivering health benefits

The aggregated particle gel formed by crosslinking thick protein-coated oil droplets may be a good tool for delivering hydrophobic drugs or nutrients. By designing the coating around the oil droplets, the gel can be designed into an effective delivery tool, which can release the nutrients or drugs at a targeted site of the human intestine. Another advantage of the aggregated particle gel is that it may protect the nutrients or drugs against severe environment in the stomach by the protein matrix.

- Disintegration of solid foods during gastric digestion

Solid foods (e.g. breads, rice, meats, vegetables, fruits and cheeses) are the main type of the human diet. Understanding the disintegration of solid foods during gastric digestion is a very important aspect for gaining insights of the whole digestion process of food in the human body. Thus, the disintegration behaviour and mechanism of various solid foods with different structures and hardness is required to investigate further.

Bibliography

Agrawal, K. R., Lucas, P. W., Prinz, J. F., & Bruce, I. C. (1997). Mechanical properties of foods responsible for resisting food breakdown in the human mouth. *Archives of Oral Biology, 42*(1), 1-9.

Agrawal, K. R., Lucas, P. W., Bruce, I. C., & Prinz, J. F. (1998). Food Properties that Influence Neuromuscular Activity During Human Mastication. *Journal of Dental research, 77*(11), 1931-1938.

Aguilera, J. M. (1995). Gelation of whey proteins. *Food Technology, 49*, 83-89.

Ahrens Jr, E., Blankenhorn, D., & Hirsch, J. (1956). Measurement of the human intestinal length in vivo and some causes of variation. *Gastroenterology, 31*(3), 274.

Ako, K., Durand, D., Nicolai, T., & Becu, L. (2009a). Quantitative analysis of confocal laser scanning microscopy images of heat-set globular protein gels. *Food Hydrocolloids, 23*(4), 1111-1119.

Ako, K., Nicolai, T., Durand, D., & Brotons, G. (2009b). Micro-phase separation explains the abrupt structural change of denatured globular protein gels on varying the ionic strength or the pH. *Soft Matter, 5*(20), 4033-4041.

Ako, K., Nicolai, T., & Durand, D. (2010). Salt-induced gelation of globular protein aggregates: structure and kinetics. *Biomacromolecules, 11*(4), 864-871.

Alting, A. C., van der Meulena, E. T., Hugenholtz, J., & Visschers, R. W. (2004). Control of texture of cold-set gels through programmed bacterial acidification. *International Dairy Journal, 14*(4), 323-329.

Anderson, D. J. (1956). Measurement of stress in mastication. *Journal of Dental Research, 35*(5), 664-670.

Arai, A., & Yamada, Y. (1993). Effect of the texture of food on the masticatory process.

Japanese Journal of Oral Biology, 35, 312-322.

Arora, S., Ali, J., Ahuja, A., Khar, R., & Baboota, S. (2005). Floating drug delivery systems: A review. *AAPS PharmSciTech, 6*(3), E372-E390.

Azpiroz, F., & Malagelada, J.-R. (1987). Gastric tone measured by an electronic barostat in health and postsurgical gastroparesis. *Gastroenterology, 92*(4), 934-943.

Barbé, F., Ménard, O., Le Gouar, Y., Buffière, C., Famelart, M.-H., Laroche, B., et al. (2013). The heat treatment and the gelation are strong determinants of the kinetics of milk proteins digestion and of the peripheral availability of amino acids. *Food Chemistry, 136*(3–4), 1203-1212.

Barbut, S., & Foegeding, E. A. (1993). Ca^{2+}-induced gelation of pre-heated whey protein isolate. *Journal of Food Science, 58*(4), 867-871.

Barbut, S., & Drake, D. (1997). Effect of reheating on sodium-induced cold gelation of whey proteins. *Food Research International, 30*(2), 153-157.

Barnes, H. A. (2000). *A handbook of elementary rheology*. Aberystwyth: University of Wales.

Bear, M. F., Connors, B. W., & Paradiso, M. A. (2001). *Neuroscience: Exploring the Brain*. Baltimore: Williams and Wilkins.

Benini, L., Castellani, G., Brighenti, F., Heaton, K. W., Brentegani, M. T., Casiraghi, M. C., et al. (1995). Gastric emptying of a solid meal is accelerated by the removal of dietary fibre naturally present in food. *Gut, 36*(6), 825-830.

Benmoussa, M., Suhendra, B., Aboubacar, A., & Hamaker, B. R. (2006). Distinctive sorghum starch granule morphologies appear to improve raw starch digestibility. *Starch, 58*(2), 92-99.

Bilecen, D., Scheffler, K., Seifritz, E., Bongartz, G., & Steinbrich, W. (2000). Hydro-

MRI for the visualization of gastric wall motility using RARE magnetic resonance imaging sequences. *Abdominal Imaging, 25*(1), 30-34.

Bird, R. B., Armstrong, R. C., & Hassager, O. (1987). *Dynamics of polymeric liquids. Vol. 1: Fluid mechanics* (2 ed. Vol. 1). New York: John Wiley & SONS.

Bordoni, A., Laghi, L., Babini, E., Di Nunzio, M., Picone, G., Ciampa, A., et al. (2014). The foodomics approach for the evaluation of protein bioaccessibility in processed meat upon *in vitro* digestion. *Electrophoresis., 35*(11), 1607-1614.

Bornhorst, G., & Singh, R. P. (2013). Kinetics of *in vitro* bread bolus digestion with varying oral and gastric digestion parameters. *Food Biophysics, 8*(1), 50-59.

Bornhorst, G., Rutherfurd, S., Roman, M., Burri, B., Moughan, P., & Singh, R. P. (2014). Gastric pH distribution and mixing of soft and rigid food particles in the stomach using a dual-marker technique. *Food Biophysics, 9*(3), 292-300.

Bourne, M. C. (1978). Texture profile analysis. *Food Technology, 32*(7), 62-66, 72.

Bourne, M. C. (2002). Relationship between rheology and food texture. In *Engineering and Food for the 21st Century.* New York: CRC Press.

Bourne, M. C. (2004). Relation between texture and mastication. *Journal of Texture Studies, 35*(2), 125-143.

Boutin, C., Giroux, H. J., Paquin, P., & Britten, M. (2007). Characterization and acid-induced gelation of butter oil emulsions produced from heated whey protein dispersions. *International Dairy Journal, 17*(6), 696-703.

Bracco, U. (1994). Effect of triglyceride structure on fat absorption. *The American Journal of Clinical Nutrition, 60*(6), 1002S-1009S.

Bray, G., & Popkin, B. (1998). Dietary fat intake does affect obesity! *The American Journal of Clinical Nutrition, 68*(6), 1157-1173.

Brener, W., Hendrix, T. R., & McHugh, P. R. (1983). Regulation of the gastric emptying

of glucose. *Gastroenterology, 85*(1), 76-82.

Breuil, P., & Meullenet, J.-F. (2001). A comparison of three instrumental tests for predicting sensory texture profiles of cheese. *Journal of Texture Studies, 32*(1), 41-55.

Brew, K. (2003). α-Lactalbumin. In P. F. M. Fox, P. L. H. (Ed.), *Advanced dairy chemistry* (3rd ed., Vol. 1, pp. 387-419). New York: Kluwer Academic/Plenum Publishers.

Brownlow, S., Morais Cabral, J. H., Cooper, R., Flower, D. R., Yewdall, S. J., Polikarpov, I., et al. (1997). Bovine β-lactoglobulin at 1.8 Å resolution - still an enigmatic lipocalin. *Structure, 5*(4), 481-495.

Bryant, C. M., & McClements, D. J. (1998). Molecular basis of protein functionality with special consideration of cold-set gels derived from heat-denatured whey. *Trends in Food Science & Technology, 9*(4), 143-151.

Bryant, C. M., & McClements, D. J. (2000). Influence of NaCl and $CaCl_2$ on cold-set gelation of heat-denatured whey protein. *Journal of Food Science, 65*(5), 801-804.

Bujacz, A. (2012). Structures of bovine, equine and leporine serum albumin. Acta Crystallographica section D: biological crystallography*, 68*(10), 1278-1289.

Burton-Freeman, B. (2000). Dietary fiber and energy regulation. *The Journal of Nutrition, 130*(2), 272S-275S.

Çakir, E., Daubert, C. R., Drake, M. A., Vinyard, C. J., Essick, G., & Foegeding, E. A. (2012). The effect of microstructure on the sensory perception and textural characteristics of whey protein/κ-carrageenan mixed gels. *Food Hydrocolloids, 26*(1), 33-43.

Calbet, J., & MacLean, D. (1997). Role of caloric content on gastric emptying in

humans. *The Journal of Physiology, 498*(Pt 2), 553-559.

Calvo, M. M., Leaver, J., & Banks, J. M. (1993). Influence of other whey proteins on the heat-induced aggregation of α-lactalbumin. *International Dairy Journal, 3*(8), 719-727.

Camilleri, M., & Prather, C. M. (1994). Axial forces during gastric emptying in health and models of disease. *Digestive Diseases and Sciences, 39*(12), 14S-17S.

Carey, M. C., Small, D. M., & Bliss, C. M. (1983). Lipid digestion and absorption. *Annual Review of Physiology, 45*(1), 651-677.

Carriere, F., Barrowman, J., Verger, R., & Laugier, R. (1993). Secretion and contribution to lipolysis of gastric and pancreatic lipases during a test meal in humans. *Gastroenterology, 105*(3), 876-888.

Cecil, J. E., Francis, J., & Read, N. W. (1999). Comparison of the effects of a high-fat and high-carbohydrate soup delivered orally and intragastrically on gastric emptying, Appetite, and Eating Behaviour. *Physiology & Behavior, 67*(2), 299-306.

Chaplin, L. C., & Lyster, R. L. J. (1986). Irreversible heat denaturation of bovine α-lactalbumin. *Journal of Dairy Research, 53*(02), 249-258.

Chen, J., & Dickinson, E. (1998). Viscoelastic properties of heat-set whey protein isolate gels. *Journal of Texture Studies, 29*(3), 285-304.

Chen, J., & Dickinson, E. (1999a). Effect of surface character of filler particles on rheology of heat-set whey protein emulsion gels. *Colloids and Surfaces B: Biointerfaces, 12*(3-6), 373-381.

Chen, J., Dickinson, E., & Edwards, M. (1999b). Rheology of acid-induced sodium caseinate stabilized emulsion gels. *Journal of Texture Studies, 30*(4), 377-396.

Chen, J., Dickinson, E., Langton, M., & Hermansson, A.-M. (2000). Mechanical

properties and microstructure of heat-set whey protein emulsion Gels: effect of emulsifiers. *LWT - Food Science and Technology, 33*(4), 299-307.

Chen, J. (2009). Food oral processing--A review. *Food Hydrocolloids, 23*(1), 1-25.

Chen, J., Gaikwad, V., Holmes, M., Murray, B., Povey, M., Wang, Y., et al. (2011). Development of a simple model device for in vitro gastric digestion investigation. *Food & Function, 2*(3-4), 174-182.

Chu, B.-S., Gunning, A. P., Rich, G. T., Ridout, M. J., Faulks, R. M., Wickham, M. S. J., et al. (2010). Adsorption of bile Salts and pancreatic colipase and lipase onto digalactosyldiacylglycerol and dipalmitoylphosphatidylcholine monolayers. *Langmuir, 26*(12), 9782-9793.

Cistola, D. P., Atkinson, D., Hamilton, J. A., & Small, D. M. (1986). Phase behavior and bilayer properties of fatty acids: hydrated 1:1 acid-soaps. *Biochemistry, 25*(10), 2804-2812.

Collins, L. M. C., & Dawes, C. (1987). The surface area of the adult human mouth and thickness of the salivary film covering the teeth and oral mucosa. *Journal of Dental Research, 66*(8), 1300-1302.

Collins, P. J., Horowitz, M., Cook, D. J., Harding, P. E., & Shearman, D. J. (1983). Gastric emptying in normal subjects--a reproducible technique using a single scintillation camera and computer system. *Gut, 24*(12), 1117-1125.

Costa, P., & Sousa Lobo, J. M. (2001). Modeling and comparison of dissolution profiles. *European Journal of Pharmaceutical Sciences, 13*(2), 123-133.

Creamer, L. K., Parry, D. A. D., & Malcolm, G. N. (1983). Secondary structure of bovine β-lactoglobulin B. *Archives of Biochemistry and Biophysics, 227*(1), 98-105.

Creusot, N., Gruppen, H., van Koningsveld, G. A., de Kruif, C. G., & Voragen, A. G. J.

(2006). Peptide–peptide and protein–peptide interactions in mixtures of whey protein isolate and whey protein isolate hydrolysates. *International Dairy Journal, 16*(8), 840-849.

Curtis, H., & Barnes, N. S. (1994). *Invitation to biology*. New York: Macmillan.

Dalgleish, D. G. (1997). Adsorption of protein and the stability of emulsions. *Trends in Food Science & Technology, 8*(1), 1-6.

Dalgleish, D. G., Senaratne, V., & Francois, S. (1997). Interactions between α-lactalbumin and β-lactoglobulin in the early stages of heat denaturation. *Journal of Agricultural and Food Chemistry, 45*(9), 3459-3464.

Danielsson, I., & Lindman, B. (1981). The definition of microemulsion. *Colloids and Surfaces, 3*(4), 391-392.

Danov, K. D., Denkov, N. D., Petsev, D. N., Ivanov, I. B., & Borwankar, R. (1993). Coalescence dynamics of deformable Brownian emulsion droplets. *Langmuir, 9*(7), 1731-1740.

Darwiche, G., Björgell, O., & Almér, L.-o. (2003). The addition of locust bean gum but not water delayed the gastric emptying rate of a nutrient semisolid meal in healthy subjects. *BMC Gastroenterology, 3*(1), 12.

Dave, A. C., Loveday, S. M., Anema, S. G., Loo, T. S., Norris, G. E., Jameson, G. B., et al. (2013). β-Lactoglobulin self-assembly: structural changes in early stages and disulfide bonding in fibrils. *Journal of Agricultural and Food Chemistry, 61*(32), 7817-7828.

Davenport, H. W. (2010). Gastrointestinal Physiology, 1895–1975: Motility. In *Comprehensive Physiology*. New York: John Wiley & Sons, Inc.

Day, J. P. R., Rago, G., Domke, K. F., Velikov, K. P., & Bonn, M. (2010). Label-free imaging of lipophilic bioactive molecules during lipid digestion by multiplex

coherent anti-Stokes raman scattering microspectroscopy. *Journal of American Chemical Society, 132*(24), 8433-8439.

Decker, E. A., & McClements, D. J. (2007). lipids. In S. Damodarin, K. Parkin & O. R. Fennema (Eds.), *Food Chemistry* (4 ed.). New York: New York: Marcel Dekker.

Desroches, M. J., Castillo, I. A., & Munz, R. J. (2005). Determination of particle size distribution by laser diffraction of doped-CeO_2 powder suspensions: effect of suspension stability and sonication. *Particle & Particle Systems Characterization, 22*(5), 310-319.

Devraj, R., Williams, H. D., Warren, D. B., Mullertz, A., Porter, C. J. H., & Pouton, C. W. (2013). *In vitro* digestion testing of lipid-based delivery systems: Calcium ions combine with fatty acids liberated from triglyceride rich lipid solutions to form soaps and reduce the solubilization capacity of colloidal digestion products. *International Journal of Pharmaceutics, 441*(1–2), 323-333.

deWit, J. N., & Klarenbeek, G. (1984). Effects of various heat treatments on structure and solubility of whey proteins. *Journal of Dairy Science, 67*(11), 2701-2710.

Di Lorenzo, C., Williams, C. M., Hajnal, F., & Valenzuela, J. E. (1985). Pectin delays gastric emptying and increases satiety in obese subjects. *Gastroenterology, 95*(5), 1211-1215.

Di Monaco, R., Cavella, S., & Masi, P. (2008). Predicting sensory cohesivness, hardness and springiness of solid foods from instrumental measurements. *Journal of Texture Studies, 39*(2), 129-149.

Dickinson, E., & Yamamoto, Y. (1996). Rheology of milk protein gels and protein-stabilized emulsion gels cross-linked with transglutaminase. *Journal of Agricultural and Food Chemistry, 44*(6), 1371-1377.

Dickinson, E., & Chen, J. (1999). Heat-set whey protein emulsion gels: role of active

and inactive filler particles. *Journal of Dispersion Science and Technology, 20*(1-2), 197-213.

Dickinson, E. (2012). Emulsion gels: The structuring of soft solids with protein-stabilized oil droplets. *Food Hydrocolloids, 28*(1), 224-241.

Dickinson, E., & Stainsby, G. (1988). Emulsion stability, in advances in food emulsion and foams. In E. Dickinson & G. Stainsby (Eds.). London, UK: Elsevier.

Dokoumetzidis, A., Papadopoulou, V., & Macheras, P. (2006). Analysis of dissolution data using modified versions of Noyes–Whitney equation and the Weibull function. *Pharmaceutical Research, 23*(2), 256-261.

Donnan, F. G. (1924). The theory of membrane equilibria. *Chemical Reviews, 1*(1), 73-90.

Drake, M. A., Gerard, P. D., Truong, V. D., & Daubert, C. R. (1999). Relationship between instrumemtal and sensory measurement of cheese texture. *Journal of Texture Studies, 30*(4), 451-476.

Dresselhuis, D. M., de Hoog, E. H. A., Cohen Stuart, M. A., Vingerhoeds, M. H., & van Aken, G. A. (2008a). The occurrence of in-mouth coalescence of emulsion droplets in relation to perception of fat. *Food Hydrocolloids, 22*(6), 1170-1183.

Dresselhuis, D. M., Stuart, M. A. C., van Aken, G. A., Schipper, R. G., & de Hoog, E. H. A. (2008b). Fat retention at the tongue and the role of saliva: adhesion and spreading of ‘protein-poor’ versus ‘protein-rich’ emulsions. *Journal of Colloid and Interface Science, 321*(1), 21-29.

Ehrlein, H., & Schemann, M. (2005). Gastrointestinal Motility. In: Technische Universität München: Munich.

Engelen, L., Fontijn-Tekamp, A., & Bilt, A. v. d. (2005). The influence of product and oral characteristics on swallowing. *Archives of Oral Biology, 50*(8), 739-746.

Englyst, H. N., Kingman, S., & Cummings, J. (1992). Classification and measurement of nutritionally important starch fractions. *European Journal of Clinical Nutrition, 46*, S33-50.

Evans, D. F., & Wennerstrom, H. (1994). *The colloidal domain: where physics, chemistry, biology and technology meet*. New York, NY: VCH Publisher.

Faisant, N., Buleon, A., Colonna, P., Molis, C., Lartigue, S., Galmiche, J., et al. (1995). Digestion of raw banana starch in the small intestine of healthy humans: structural features of resistant starch. *British Journal of Nutrition, 73*(01), 111-123.

Faulks, R., & Wickham, M. (2012). Dynamic gastric model. In: Google Patents.

Feldman, M., Cryer, B., McArthur, K. E., Huet, B. A., & Lee, E. (1996). Effects of aging and gastritis on gastric acid and pepsin secretion in humans: A prospective study. *Gastroenterology, 110*(4), 1043-1052.

Ferrua, M. J., & Singh, R. P. (2010). Modeling the fluid dynamics in a human stomach to gain insight of food digestion. *Journal of Food Science, 75*(7), R151-R162.

Flory, P. J. (1953). *Principles of Polymer Chemistry.*London: Cornell University Press.

Foegeding, E. A. (2007). Rheology and sensory texture of biopolymer gels. *Current Opinion in Colloid & Interface Science, 12*(4–5), 242-250.

Foegeding, E. A., & Drake, M. A. (2007). Invited review: sensory and mechanical properties of cheese texture. *Journal of Dairy Science, 90*(4), 1611-1624.

Foegeding, E. A., Daubert, C. R., Drake, M. A., Essick, G., Trulsson, M., Vinyard, C. J., et al. (2011). A comprehensive approach to understanding textural properties of semi- and soft-solid foods. *Journal of Texture Studies, 42*(2), 103-129.

Fordtran, J. S., & Walsh, J. H. (1973). Gastric acid secretion rate and buffer content of the stomach after eating. Results in normal subjects and in patients with

duodenal ulcer. *Journal of Clinical Investigation, 52*(3), 645.

Foster, K. D., Woda, A., & Peyron, M. A. (2006). Effect of texture of plastic and elastic model foods on the parameters of mastication. *Journal of Neurophysiology, 95*(6), 3469-3479.

Fox, P. F. M., P. L. H. (2003). Advanced dairy chemistry. In (3 ed., Vol. 1, pp. 18). New York: Kluwer Academic / Plenum Publishers.

French, S. J., & Read, N. W. (1994). Effect of guar gum on hunger and satiety after meals of differing fat content: relationship with gastric emptying. *The American Journal of Clinical Nutrition, 59*(1), 87-91.

Fu, S. Y., Feng, X. Q., Lauke, B., & Mai, Y. W. (2008). Effects of particle size, particle/matrix interface adhesion and particle loading on mechanical properties of particulate–polymer composites. *Composites Part B: Engineering, 39*(6), 933-961.

Fullard, L., Lammers, W., Wake, G. C., & Ferrua, M. J. (2014). Propagating longitudinal contractions in the ileum of the rabbit - Efficiency of advective mixing. *Food & Function, 5(11), 2731-2742.*

Gallier, S., Cui, J., Olson, T. D., Rutherfurd, S. M., Ye, A., Moughan, P. J., et al. (2013). In vivo digestion of bovine milk fat globules: effect of processing and interfacial structural changes. I. Gastric digestion. *Food Chemistry, 141*(3), 3273-3281.

Ganong, W. F., & Barrett, K. E. (2005). *Review of medical physiology* (Vol. 22). New York: McGraw-Hill Medical.

Gavião, M. B. D., Engelen, L., & Van Der Bilt, A. (2004). Chewing behavior and salivary secretion. *European Journal of Oral Sciences, 112*(1), 19-24.

Gérard, C., Colonna, P., Buléon, A., & Planchot, V. (2002). Order in maize mutant starches revealed by mild acid hydrolysis. *Carbohydrate Polymer, 48*(2), 131-

141.

Gezimati, J., Singh, H., & Creamer, L. K. (1996). Heat-induced interactions and gelation of mixtures of bovine β-lactoglobulin and serum albumin. *Journal of Agricultural and Food Chemistry, 44*(3), 804-810.

Gibbs, C. H., Mahan, P. E., Lundeen, H. C., Brehnan, K., Walsh, E. K., & Holbrook, W. B. (1981). Occlusal forces during chewing and swallowing as measured by sound transmission. *The Journal of prosthetic dentistry, 46*(4), 443-449.

Golding, M., & Wooster, T. J. (2010). The influence of emulsion structure and stability on lipid digestion. *Current Opinion in Colloid & Interface Science, 15*(1-2), 90-101.

Golding, M., Wooster, T. J., Day, L., Xu, M., Lundin, L., Keogh, J., et al. (2011). Impact of gastric structuring on the lipolysis of emulsified lipids. *Soft Matter, 7*(7), 3513-3523.

Gottschalk, M., Nilsson, H., Roos, H., & Halle, B. (2003). Protein self-association in solution: The bovine β -lactoglobulin dimer and octamer. *Protein Science, 12*(11), 2404-2411.

Gu, X., Campbell, L. J., & Euston, S. R. (2009). Effects of different oils on the properties of soy protein isolate emulsions and gels. *Food Research International, 42*(8), 925-932.

Guerra, A., Etienne-Mesmin, L., Livrelli, V., Denis, S., Blanquet-Diot, S., & Alric, M. (2012). Relevance and challenges in modeling human gastric and small intestinal digestion. *Trends in Biotechnology, 30*(11), 591-600.

Guo, Q., Ye, A., Lad, M., Dalgleish, D., & Singh, H. (2013). The breakdown properties of heat-set whey protein emulsion gels in the human mouth. *Food Hydrocolloids, 33*(2), 215-224.

Guo, Q., Ye, A., Lad, M., Dalgleish, D., & Singh, H. (2014a). Behaviour of whey protein emulsion gel during oral and gastric digestion: effect of droplet size. *Soft Matter, 10*(23), 4173-4183.

Guo, Q., Ye, A., Lad, M., Dalgleish, D., & Singh, H. (2014b). Effect of gel structure on the gastric digestion of whey protein emulsion gels. *Soft Matter, 10*(8), 1214-1223.

Guo, Q., Ye, A., Lad, M., Ferrua, M., Dalgleish, D., & Singh, H. (2015). Disintegration kinetics of food gels during gastric digestion and its role on gastric emptying: an in vitro analysis. *Food & Function, 6*(3), 756-764.

Gwartney, E. A., Larick, D. K., & Foegeding, E. A. (2004). Sensory texture and mechanical properties of stranded and particulate whey protein emulsion gels. *Journal of Food Science, 69*(9), S333-S339.

Hambling, S. G., MacAlpine, A. S., & Sawyer, L. (1992). β-lactoglobulin. In P. F. M. Fox, P. L. H. (Ed.), *Advanced dairy chemistry*. New York: Springer US

Harris, J., Cole, R., & Pon, N. (1956). The kinetics of acid hydrolysis of dipeptides. *Biochemical Journal, 62*(1), 154.

Havea, P., Singh, H., & Creamer, L. K. (2001). Characterization of heat-induced aggregates of β-lactoglobulin, α-lactalbumin and bovine serum albumin in a whey protein concentrate environment. *Journal of Dairy Research, 68*(03), 483-497.

Helbig, A., Silletti, E., Aken, G., Oosterveld, A., Minekus, M., Hamer, R., et al. (2012). Lipid digestion of protein stabilized emulsions investigated in a dynamic in vitro gastro-intestinal model system. *Food Digestion*, 1-11.

Helkimo, E., Carlsson, G. E., & Helkimo, M. (1977). Bite force and state of dentition. *Acta Odontologica Scandinavica, 35*(6), 297-303.

Hernell, O., Staggers, J. E., & Carey, M. C. (1990). Physical-chemical behavior of dietary and biliary lipids during intestinal digestion and absorption. 2. Phase analysis and aggregation states of luminal lipids during duodenal fat digestion in healthy adult human beings. *Biochemistry, 29*(8), 2041-2056.

Hiiemae, K., Heath, M. R., Heath, G., Kazazoglu, E., Murray, J., Sapper, D., et al. (1996). Natural bites, food consistency and feeding behaviour in man. *Archives of Oral Biology, 41*(2), 175-189.

Hiiemae, K. M., & Palmer, J. B. (1999). Food transport and bolus formation during complete feeding sequences on foods of different initial consistency. *Dysphagia, 14*(1), 31-42.

Hines, M. E., & Foegeding, E. A. (1993). Interactions of α-lactalbumin and bovine serum albumin with β-lactoglobulin in thermally induced gelation. *Journal of Agricultural and Food Chemistry, 41*(3), 341-346.

Hofmann, A. F., & Roda, A. (1984). Physicochemical properties of bile acids and their relationship to biological properties: an overview of the problem. *Journal of Lipid Research,* 1477-1489.

Holt, S., Reid, J., Taylor, T., Tothill, P., & Heading, R. (1982). Gastric emptying of solids in man. *Gut, 23*(4), 292-296.

Hongsprabhas, P., & Barbut, S. (1997). Protein and Salt Effects on Ca^{2+}-induced cold gelation of whey protein isolate. *Journal of Food Science, 62*(2), 382-385.

Hongsprabhas, P., Barbut, S., & Marangoni, A. G. (1999). The structure of cold-set whey protein isolate gels prepared with Ca^{2+}. *LWT - Food Science and Technology, 32*(4), 196-202.

Hoover, R. (2000). Acid-treated starches. *Food Reviews International, 16*(3), 369-392.

Hoover, R., & Zhou, Y. (2003). *In vitro* and *in vivo* hydrolysis of legume starches by α-

amylase and resistant starch formation in legumes—a review. *Carbohydrate Polymers, 54*(4), 401-417.

Horio, T., & Kawamura, Y. (1989). Effects of texture of food on chewing patterns in the human subject. *Journal of Oral Rehabilitation, 16*(2), 177-183.

Huang, B., Babcock, H., & Zhuang, X. (2010). Breaking the diffraction barrier: super-resolution imaging of cells. *Cell, 143*(7), 1047-1058.

Humphrey, S. P., & Williamson, R. T. (2001). A review of saliva: Normal composition, flow, and function. *Journal of Prosthetic Dentistry, 85*(2), 162-169.

Hunt, J., Smith, J., & Jiang, C. (1985). Effect of meal volume and energy density on the gastric emptying of carbohydrates. *Gastroenterology, 89*(6), 1326-1330.

Hunt, J. A., & Dalgleish, D. G. (1995). Heat Stability of Oil-in-Water Emulsions Containing Milk Proteins: Effect of Ionic Strength and pH. *Journal of Food Science, 60*(5), 1120-1123.

Hunt, J. N., & Stubbs, D. F. (1975). The volume and energy content of meals as determinants of gastric emptying. *The Journal of Physiology, 245*(1), 209-225.

Hur, S. J., Lim, B. O., Decker, E. A., & McClements, D. J. (2011). *In vitro* human digestion models for food applications. *Food Chemistry, 125*(1), 1-12.

Hutchings, J. B., & Lillford, P. J. (1988). The perception of food texture - the philosophy of the breakdown path. *Journal of Texture Studies, 19*(2), 103-115.

Hutchings, S. C., Foster, K. D., Xu, J. E., Lentle, R. G., Jones, J. R., & Morgenstern, M. P. (2011). Mastication of heterogeneous foods: peanuts inside two different food matrices. *Food Quality and Preference, 22*(4), 332-339.

Iametti, S., Cairoli, S., De Gregori, B., & Bonomi, F. (1995). Modifications of high-order structures upon heating of β-lactoglobulin: dependence on the protein concentration. *Journal of Agricultural and Food Chemistry, 43*(1), 53-58.

Ibekwe, V., Fadda, H., McConnell, E., Khela, M., Evans, D., & Basit, A. (2008). Interplay between intestinal pH, transit Time and feed status on the *in vivo* performance of pH responsive ileo-colonic release systems. *Pharmaceutical Research, 25*(8), 1828-1835.

Ikeda, S., & Foegeding, E. A. (1999a). Dynamic viscoelastic properties of thermally induced whey protein isolate gels with added lecithin. *Food Hydrocolloids, 13*(3), 245-254.

Ikeda, S., Foegeding, E. A., & Hagiwara, T. (1999b). Rheological study on the fractal nature of the protein gel structure. *Langmuir, 15*(25), 8584-8589.

Ikeda, S., & Morris, V. J. (2002). Fine-stranded and particulate aggregates of heat-denatured whey proteins visualized by atomic force microscopy. *Biomacromolecules, 3*(2), 382-389.

Ikeda, S. (2003). Heat-induced gelation of whey proteins observed by rheology, atomic force microscopy, and Raman scattering spectroscopy. *Food Hydrocolloids, 17*(4), 399-406.

Ilker, R., & Szczesniak, A. S. (1990). Structural and chemical bases for texture of plant food stuffs. *Journal of Texture Studies, 21*(1), 1-36.

Ishihara, S., Nakao, S., Nakauma, M., Funami, T., Hori, K., Ono, T., et al. (2012). Compression test of food gels on artificial tongue and its comparison with human test. *Journal of Texture Studies*, *44(2), 104-114.*

Israelachvili, J. (1992). *Intermolecular and Surface Forces* (2 ed.). London: Academic Press.

Jalabert-Malbos, M. L., Mishellany-Dutour, A., Woda, A., & Peyron, M. A. (2007). Particle size distribution in the food bolus after mastication of natural foods. *Food Quality and Preference, 18*(5), 803-812.

James, P. T., Leach, R., Kalamara, E., & Shayeghi, M. (2001). The worldwide obesity epidemic. *Obesity, 9*(11S), 228S-233S.

Jenkins, G. N. (1978). *The physiology and biochemistry of the mouth* (4 ed.). Oxford: Blackwell.

Ju, Z., & Kilara, A. (1998a). Properties of gels induced by heat, protease, calcium salt, and acidulant from calcium ion-aggregated whey protein isolate. *Journal of Dairy Science, 81*(5), 1236-1243.

Ju, Z. Y., & Kilara, A. (1998b). Gelation of pH-aggregated whey protein isolate solution induced by heat, protease, calcium salt, and acidulant. *Journal of Agricultural and Food Chemistry, 46*(5), 1830-1835.

Jung, J. M., Savin, G., Pouzot, M., Schmitt, C., & Mezzenga, R. (2008). Structure of heat-induced β-lactoglobulin aggregates and their complexes with sodium-dodecyl sulfate. *Biomacromolecules, 9*(9), 2477-2486.

Kalantzi, L., Goumas, K., Kalioras, V., Abrahamsson, B., Dressman, J., & Reppas, C. (2006). Characterization of the human upper gastrointestinal contents under conditions simulating bioavailability/bioequivalence studies. *Pharmaceutical Research, 23*(1), 165-176.

Kamba, M., Seta, Y., Kusai, A., Ikeda, M., & Nishimura, K. (2000). A unique dosage form to evaluate the mechanical destructive force in the gastrointestinal tract. *International Journal of Pharmaceutics, 208*(1), 61-70.

Kim, K. H., Gohtani, S., & Yamano, Y. (1996). Effects of oil droplets on physical and sensory properties of O/W emulsion agar gel. *Journal of Texture Studies, 27*(6), 655-670.

Kinsella, J. E., & Whitehead, D. M. (1989). Proteins in whey: chemical, physical, and functional properties. *Advances in food and nutrition research:33, 343-438.*

Kirby, B. J. (2010). *Micro-and nanoscale fluid mechanics: transport in microfluidic devices*. Cambridge: Cambridge University Press.

Knutson, L., Koenders, D. J., Fridblom, H., Viberg, A., Sein, A., & Lennernäs, H. (2010). Gastrointestinal metabolism of a vegetable-oil emulsion in healthy subjects. *The American Journal of Clinical Nutrition, 92*(3), 515-524.

Kohyama, K., Hatakeyama, E., Sasaki, T., Dan, H., Azuma, T., & Karita, K. (2004). Effects of sample hardness on human chewing force: a model study using silicone rubber. *Archives of Oral Biology, 49*(10), 805-816.

Kong, F., & Singh, R. P. (2008). Disintegration of solid foods in human stomach. *Journal of Food Science, 73*(5), R67-R80.

Kong, F., & Singh, R. P. (2009). Modes of disintegration of solid foods in simulated gastric environment. *Food Biophysics, 4*(3), 180-190.

Kong, F., & Singh, R. P. (2010). A human gastric simulator (HGS) to study food digestion in human stomach. *Journal of Food Science, 75*(9), E627-E635.

Kong, F., & Singh, R. P. (2011). Solid loss of carrots during simulated gastric digestion. *Food Biophysics, 6*(1), 84-93.

Kong, F., Oztop, M. H., Paul Singh, R., & McCarthy, M. J. (2013). Effect of boiling, roasting and frying on disintegration of peanuts in simulated gastric environment. *LWT - Food Science and Technology, 50*(1), 32-38.

Kuhn, P. R., & Foegeding, E. A. (1991). Mineral salt effects on whey protein gelation. *Journal of Agricultural and Food Chemistry, 39*(6), 1013-1016.

Kuwata, K., Hoshino, M., Era, S., Batt, C. A., & Goto, Y. (1998). α → β transition of β-lactoglobulin as evidenced by heteronuclear NMR. *Journal of Molecular Biology, 283*(4), 731-739.

Langenbucher, F. (1972). Letters to the Editor: Linearization of dissolution rate curves

by the Weibull distribution. *Journal of Pharmacy and Pharmacology, 24*(12), 979-981.

Le Bon, C., Nicolai, T., & Durand, D. (1999a). Growth and structure of aggregates of heat-denatured β-lactoglobulin. *International Journal of Food Science & Technology, 34*(5-6), 451-465.

Le Bon, C., Nicolai, T., & Durand, D. (1999b). Kinetics of aggregation and gelation of globular proteins after heat-induced denaturation. *Macromolecules, 32*(19), 6120-6127.

Leclère, C., Champ, M., Boillot, J., Guille, G., Lecannu, G., Molis, C., et al. (1994). Role of viscous guar gums in lowering the glycemic response after a solid meal. *The American Journal of Clinical Nutrition, 59*(4), 914-921.

Leidy, H. J., Apolzan, J. W., Mattes, R. D., & Campbell, W. W. (2010). Food form and portion size affect postprandial appetite sensations and hormonal responses in healthy, nonobese, older adults. *Obesity, 18*(2), 293-299.

Li, Y., Hu, X., Song, Y., Lu, Z., Ning, T., Cai, H., et al. (2011). Identification of novel alternative splicing variants of interferon regulatory factor 3. *Biochimica et Biophysica Acta (BBA) - Gene Regulatory Mechanisms, 1809*(3), 166-175.

Liang, L., Leung Sok Line, V., Remondetto, G. E., & Subirade, M. (2010). *In vitro* release of α-tocopherol from emulsion-loaded β-lactoglobulin gels. *International Dairy Journal, 20*(3), 176-181.

Liao, D., Gregersen, H., Hausken, T., Gilja, O. H., Mundt, M., & Kassab, G. (2004). Analysis of surface geometry of the human stomach using real-time 3-D ultrasonography *in vivo*. *Neurogastroenterology & Motility, 16*(3), 315-324.

Liddle, R. A., Morita, E. T., Conrad, C. K., & Williams, J. A. (1986). Regulation of gastric emptying in humans by cholecystokinin. *Journal of Clinical*

Investigation, 77(3), 992.

Lucas, P. W., & Pereira, B. (1990). Estimation of the fracture toughness of leaves. *Functional Ecology, 4*(6), 819-822.

Lucas, P. W., Prinz, J. F., Agrawal, K. R., & Bruce, I. C. (2002). Food physics and oral physiology. *Food Quality and Preference, 13*(4), 203-213.

Lund, J. (1991). Mastication and its control by the brain stem. *Lund, JP, 2*(1), 33-64.

Macierzanka, A., Böttger, F., Lansonneur, L., Groizard, R., Jean, A.-S., Rigby, N. M., et al. (2012). The effect of gel structure on the kinetics of simulated gastrointestinal digestion of bovine β-lactoglobulin. *Food Chemistry, 134*(4), 2156-2163.

Madenci, D., & Egelhaaf, S. U. (2010). Self-assembly in aqueous bile salt solutions. *Current Opinion in Colloid & Interface Science, 15*(1–2), 109-115.

Malagelada, J.-R., Longstreth, G. F., Summerskill, W. H. J., & Go, V. L. W. (1976). Measurement of gastric functions during digestion of ordinary solid meals in man. *Gastroenterology, 70*(2), 203-210.

Malagelada, J.-R., Go, V. W., & Summerskill, W. H. J. (1979). Different gastric, pancreatic, and biliary responses to solid-liquid or homogenized meals. *Digestive Diseases and Sciences, 24*(2), 101-110.

Malagelada, J. & Azpiroz, F. Determinants of gastric emptying and transit in the small intestine (2011). *Comprehensive Physiology*, Supplement 16: *Handbook of Physiology, The Gastrointestinal System, Motility and Circulation*: 909-937.

Malaki Nik, A., Wright, A. J., & Corredig, M. (2010). Surface adsorption alters the susceptibility of whey proteins to pepsin-digestion. *Journal of Colloid and Interface Science, 344*(2), 372-381.

Malaki Nik, A., Wright, A. J., & Corredig, M. (2011). Impact of interfacial composition on emulsion digestion and rate of lipid hydrolysis using different *in vitro*

digestion models. *Colloids and Surfaces B: Biointerfaces, 83*(2), 321-330.

Maldonado-Valderrama, J., Woodward, N. C., Gunning, A. P., Ridout, M. J., Husband, F. A., Mackie, A. R., et al. (2008). Interfacial characterization of β-lactoglobulin networks: displacement by bile salts. *Langmuir, 24*(13), 6759-6767.

Maldonado-Valderrama, J., Wilde, P., Macierzanka, A., & Mackie, A. (2011). The role of bile salts in digestion. *Advances in Colloid and Interface Science, 165*(1), 36-46.

Maljaars, P. W. J., Peters, H. P. F., Mela, D. J., & Masclee, A. A. M. (2008). Ileal brake: A sensible food target for appetite control. A review. *Physiology & Behavior, 95*(3), 271-281.

Marangoni, A. G., Barbut, S., McGauley, S. E., Marcone, M., & Narine, S. S. (2000). On the structure of particulate gels—the case of salt-induced cold gelation of heat-denatured whey protein isolate. *Food Hydrocolloids, 14*(1), 61-74.

Marciani, L., Gowland, P. A., Fillery-Travis, A., Manoj, P., Wright, J., Smith, A., et al. (2001a). Assessment of antral grinding of a model solid meal with echo-planar imaging. *American Journal of Physiology - Gastrointestinal and Liver Physiology, 280*(5), G844-G849.

Marciani, L., Gowland, P. A., Spiller, R. C., Manoj, P., Moore, R. J., Young, P., et al. (2001b). Effect of meal viscosity and nutrients on satiety, intragastric dilution, and emptying assessed by MRI. *American Journal of Physiology-Gastrointestinal and Liver Physiology, 280*(6), G1227-G1233.

Marciani, L., Young, P., Wright, J., Moore, R., Coleman, N., Gowland, P. A., et al. (2001c). Antral motility measurements by magnetic resonance imaging. *Neurogastroenterology & Motility, 13*(5), 511-518.

Marciani, L., Wickham, M. S. J., Bush, D., Faulks, R., Wright, J., Fillery-Travis, A. J.,

et al. (2006). Magnetic resonance imaging of the behaviour of oil-in-water emulsions in the gastric lumen of man. *British Journal of Nutrition, 95*(02), 331-339.

Matsudomi, N., Oshita, T., Kobayashi, K., & Kinsella, J. E. (1993). .α-lactalbumin enhances the gelation properties of bovine serum albumin. *Journal of Agricultural and Food Chemistry, 41*(7), 1053-1057.

Mattes, R. D., & Campbell, W. W. (2009). Effects of food form and timing of ingestion on appetite and energy intake in lean young adults and in young adults with obesity. *Journal of the American Dietetic Association, 109*(3), 430-437.

McClements, D. J., Monahan, F. J., & Kinsella, J. E. (1993). Effect of emulsion droplets on the rheology of whey protein isolate gels. *Journal of Texture Studies, 24*(4), 411-422.

McClements, D. J., & Keogh, M. K. (1995). Physical properties of cold-setting gels formed from heat-denatured whey protein isolate. *Journal of the Science of Food and Agriculture, 69*(1), 7-14.

McClements, D. J., & Decker, E. A. (2000). Lipid oxidation in oil-in-water emulsions: impact of molecular environment on chemical reactions in heterogeneous food systems. *Journal of Food Science, 65*(8), 1270-1282.

McClements, D. J. (2005). *Food Emulsions: Principles, Practices, and Techniques* (2 ed.). New York: CRC Press.

McClements, D. J., & Weiss, J. (2005). Lipid Emulsions. In *Bailey's Industrial Oil and Fat Products.* New York: John Wiley & Sons, Inc.

McClements, D. J. (2009). Chapter 4 - Biopolymers in Food Emulsions. In Kasapis, S., Norton, I & Ubbink, J. (Eds.), *Modern Biopolymer Science* (pp. 129-166). San Diego: Academic Press.

McClements, D. J. (2012). Nanoemulsions versus microemulsions: terminology, differences, and similarities. *Soft Matter, 8*(6), 1719-1729.

McKenzie, H. A., & Sawyer, W. H. (1967). Effect of pH on β-lactoglobulins. *Nature, 214*(5093), 1101-1104.

Mehalebi, S., Nicolai, T., & Durand, D. (2008a). The influence of electrostatic interaction on the structure and the shear modulus of heat-set globular protein gels. *Soft Matter, 4*(4), 893-900.

Mehalebi, S., Nicolai, T., & Durand, D. (2008b). Light scattering study of heat-denatured globular protein aggregates. *International Journal of Biological Macromolecules, 43*(2), 129-135.

Meyer, J. H., MacGregor, I. L., Gueller, R., Martin, P., & Cavalieri, R. (1976). Tc-Tagged chicken liver asa marker of solid food in the human stomach. *The American Journal of Digestive Diseases, 21*(4), 296-304.

Meyer, J. H., Thomson, J. B., Cohen, M. B., Shadchehr, A., & Mandiola, S. A. (1979). Sieving of solid food by the canine stomach and sieving after gastric surgery. *Gastroenterology, 76*, 804-813.

Meyer, J. H., Ohashi, H., Jehn, D., & Thomson, J. B. (1981). Size of liver particles emptied from the human stomach. *Gastroenterology, 80*(6), 1489-1496.

Meyer, J. H., Dressman, J., Fink, A., & Amidon, G. (1985). Effect of size and density on canine gastric emptying of nondigestible solids. *Gastroenterology, 89*, 805-813.

Meyer, J. H., Tabrizi, Y., DiMaso, N., Hlinka, M., & Raybould, H. E. (1998). Length of intestinal contact on nutrient-driven satiety. *American Journal of Physiology - Regulatory, Integrative and Comparative Physiology: 275(4): 1308-1319.*

Mishellany, A., Woda, A., Labas, R., & Peyron, M.-A. (2006). The Challenge of Mastication: Preparing a Bolus Suitable for Deglutition. *Dysphagia, 21*(2), 87-

94.

Moitzi, C., Guillot, S., Fritz, G., Salentinig, S., & Glatter, O. (2007). Phase reorganization in self-assembled systems through interparticle material transfer. *Advanced materials, 19*(10), 1352-1358.

Moore, J. G., Dubois, A., Christian, P. E., Elgin, D., & Alazraki, N. (1986). Evidence for a midgastric transverse band in humans. *Gastroenterology, 91*(3), 540-545.

Moran, T. H., & McHugh, P. R. (1982). Cholecystokinin suppresses food intake by inhibiting gastric emptying. *American Journal of Physiology, 242*(5), R491-R497.

Morr, C., & Ha, E. (1993). Whey protein concentrates and isolates: processing and functional properties. *Critical Reviews in Food Science and Nutrition, 33*(6), 431-476.

Mukhopadhyay, S., & Maitra, U. (2004). Chemistry and biology of bile acids. *Current Science, 87*(12), 1666-1683.

Mun, S.-H., & Shin, M. (2006). Mild hydrolysis of resistant starch from maize. *Food Chemistry, 96*(1), 115-121.

Mun, S., Decker, E. A., & McClements, D. J. (2007). Influence of emulsifier type on in vitro digestibility of lipid droplets by pancreatic lipase. *Food Research International, 40*(6), 770-781.

Neyraud, E., Prinz, J., & Dransfield, E. (2003). NaCl and sugar release, salivation and taste during mastication of salted chewing gum. *Physiology & Behavior, 79*(4–5), 731-737.

Nicolai, T., Britten, M., & Schmitt, C. (2011). β-lactoglobulin and WPI aggregates: formation, structure and applications. *Food Hydrocolloids, 25*(8), 1945-1962.

Norton, I., Moore, S., & Fryer, P. (2007). Understanding food structuring and

breakdown: engineering approaches to obesity. *Obesity Reviews, 8*, 83-88.

Nyemb, K., Guérin-Dubiard, C., Dupont, D., Jardin, J., Rutherfurd, S. M., & Nau, F. (2014). The extent of ovalbumin in vitro digestion and the nature of generated peptides are modulated by the morphology of protein aggregates. *Food Chemistry, 157*(0), 429-438.

Ohashi, H., & Meyer, J. H. (1980). Effect of peptic digestion on emptying of cooked liver in dogs. *Gastroenterology, 79*(2), 305-310.

Okada, A., Honma, M., Nomura, S., & Yamada, Y. (2007). Oral behavior from food intake until terminal swallow. *Physiology & Behavior, 90*(1), 172-179.

Øktedalen, O., Nesland, A., Opstad, P., & Berstad, A. (1988). The influence of prolonged physical stress on gastric juice components in healthy man. *Øktedalen, O, 23*(9), 1132-1136.

Olausson, E. A., Alpsten, M., Larsson, A., Mattsson, H., Andersson, H., & Attvall, S. (2008). Small particle size of a solid meal increases gastric emptying and late postprandial glycaemic response in diabetic subjects with gastroparesis. *Diabetes Research and Clinical Practice, 80*(2), 231-237.

Onuki, A. (1989). Theory of pattern formation in gels: surface folding in highly compressible elastic bodies. *Physical Review A, 39*(11), 5932.

Papadopoulou, V., Kosmidis, K., Vlachou, M., & Macheras, P. (2006). On the use of the Weibull function for the discernment of drug release mechanisms. *International Journal of Pharmaceutics, 309*(1–2), 44-50.

Paphangkorakit, J., & Osborn, J. W. (1997). The effect of pressure on a maximum incisal bite force in man. *Archives of Oral Biology, 42*(1), 11-17.

Patton, J. S., & Carey, M. C. (1981). Inhibition of human pancreatic lipase-colipase activity by mixed bile salt-phospholipid micelles. *American Journal of*

Physiology - Gastrointestinal and Liver Physiology, 4(4), 328-336.

Pera, P., Bucca, C., Borro, P., Bernocco, C., De Lillo, A., & Carossa, S. (2002). Influence of mastication on gastric emptying. *Journal of dental research, 81*(3), 179-181.

Peram, M. R., Loveday, S. M., Ye, A., & Singh, H. (2013). *In vitro* gastric digestion of heat-induced aggregates of β-lactoglobulin. *Journal of Dairy Science, 96*(1), 63-74.

Pereira, L. J., de Wijk, R. A., Gavião, M. B. D., & van der Bilt, A. (2006). Effects of added fluids on the perception of solid food. *Physiology & Behavior, 88*(4–5), 538-544.

Permyakov, E. A., & Berliner, L. J. (2000). α-lactalbumin: structure and function. *FEBS Letters, 473*(3), 269-274.

Persaud, D. R., Dalgleish, D. G., Nadeau, L., & Gauthier, S. (2000). Isolation and purification of serum and interfacial peptides of a trypsinolyzed β-lactoglobulin oil-in-water emulsion. *Journal of Chromatography B: Biomedical Sciences and Applications, 744*(2), 389-397.

Peyron, M. A., Mishellany, A., & Woda, A. (2004). Particle size distribution of food boluses after mastication of six natural foods. *Journal of dental research, 83*(7), 578-582.

Peyron, M. P., Lassauzay, C. L., & Woda, A. W. (2002). Effects of increased hardness on jaw movement and muscle activity during chewing of visco-elastic model foods. *Experimental Brain Research, 142*(1), 41-51.

Phan-Xuan, T., Durand, D., Nicolai, T., Donato, L., Schmitt, C., & Bovetto, L. (2013). Tuning the structure of protein particles and gels with calcium or sodium ions. *Biomacromolecules, 14*(6), 1980-1989.

Phillips, L. G., Whitehead, D. M., & Kinsella, J. E. (1994). Structure-function properties of food proteins. Boston: Academic Press.

Pinheiro, A. C., Lad, M., Silva, H. D., Coimbra, M. A., Boland, M., & Vicente, A. A. (2013). Unravelling the behaviour of curcumin nanoemulsions during in vitro digestion: effect of the surface charge. *Soft Matter, 9*(11), 3147-3154.

Pionnier, E., Chabanet, C., Mioche, L., Taylor, A. J., Le Quéré, J.-L., & Salles, C. (2004). 2. *In Vivo* Nonvolatile Release during Eating of a Model Cheese: Relationships with Oral Parameters. *Journal of Agricultural and Food Chemistry, 52*(3), 565-571.

Pouzot, M., Durand, D., & Nicolai, T. (2004). Influence of the ionic strength on the structure of heat-set globular protein gels at pH 7. β-lactoglobulin. *Macromolecules, 37*(23), 8703-8708.

Pouzot, M., Nicolai, T., Visschers, R. W., & Weijers, M. (2005). X-ray and light scattering study of the structure of large protein aggregates at neutral pH. *Food Hydrocolloids, 19*(2), 231-238.

Prinz, J. F., & Lucas, P. W. (1995). Swallow thresholds in human mastication. *Archives of Oral Biology, 40*(5), 401-403.

Qian, D., Dickey, E. C., Andrews, R., & Rantell, T. (2000). Load transfer and deformation mechanisms in carbon nanotube-polystyrene composites. *Applied Physics Letters, 76*(20), 2868-2870.

Qin, B. Y., Bewley, M. C., Creamer, L. K., Baker, H. M., Baker, E. N., & Jameson, G. B. (1998). Structural basis of the tanford transition of bovine β-lactoglobulin. *Biochemistry, 37*(40), 14014-14023.

Qiu, H., & Caffrey, M. (2000). The phase diagram of the monoolein/water system: metastability and equilibrium aspects. *Biomaterials, 21*(3), 223-234.

Quesada-Perez, M., Maroto-Centeno, J. A., Forcada, J., & Hidalgo-Alvarez, R. (2011). Gel swelling theories: the classical formalism and recent approaches. *Soft Matter, 7*(22), 10536-10547.

Rabiey, L., & Britten, M. (2009). Effect of protein composition on the rheological properties of acid-induced whey protein gels. *Food Hydrocolloids, 23*(3), 973-979.

Reis, P., Holmberg, K., Miller, R., Krägel, J., Grigoriev, D. O., Leser, M. E., et al. (2008a). Competition between lipases and monoglycerides at interfaces. *Langmuir, 24*(14), 7400-7407.

Reis, P., Miller, R., Leser, M., Watzke, H., Fainerman, V. B., & Holmberg, K. (2008b). Adsorption of polar lipids at the water−oil interface. *Langmuir, 24*(11), 5781-5786.

Relkin, P. (1998). Reversibility of heat-induced conformational changes and surface exposed hydrophobic clusters of β-lactoglobulin: their role in heat-induced sol–gel state transition. *International Journal of Biological Macromolecules, 22*(1), 59-66.

Remondetto, G. E., Beyssac, E., & Subirade, M. (2004). Iron availability from whey protein hydrogels: an in vitro study. *Journal of Agricultural and Food Chemistry, 52*(26), 8137-8143.

Rigler, M. W., Honkanen, R. E., & Patton, J. S. (1986). Visualization by freeze fracture, *in vitro* and *in vivo*, of the products of fat digestion. *Journal of Lipid Research, 27*(8), 836-857.

Sakurai, K., & Goto, Y. (2002). Manipulating monomer-dimer equilibrium of bovine β-lactoglobulin by amino acid substitution. *Journal of Biological Chemistry, 277*(28), 25735-25740.

Sala, G., van de Velde, F., Cohen Stuart, M. A., & van Aken, G. A. (2007). Oil droplet release from emulsion-filled gels in relation to sensory perception. *Food Hydrocolloids, 21*(5-6), 977-985.

Sala, G., van Vliet, T., Cohen Stuart, M., van de Velde, F., & van Aken, G. A. (2009). Deformation and fracture of emulsion-filled gels: effect of gelling agent concentration and oil droplet size. *Food Hydrocolloids, 23*(7), 1853-1863.

Salentinig, S., Sagalowicz, L., Leser, M. E., Tedeschi, C., & Glatter, O. (2011). Transitions in the internal structure of lipid droplets during fat digestion. *Soft Matter, 7*(2), 650-661.

Salonen, A., Moitzi, C., Salentinig, S., & Glatter, O. (2010). Material transfer in cubosome−emulsion mixtures: effect of alkane chain length. *Langmuir, 26*(13), 10670-10676.

Samra, R. A. (2010). *Fats and Satiety*. Boca Raton: CRC Press.

Sandra, S., Decker, E. A., & McClements, D. J. (2008). Effect of interfacial protein cross-linking on the *in vitro* digestibility of emulsified corn oil by pancreatic lipase. *Journal of Agricultural and Food Chemistry, 56*(16), 7488-7494.

Sarkar, A., Goh, K. K. T., & Singh, H. (2009a). Colloidal stability and interactions of milk-protein-stabilized emulsions in an artificial saliva. *Food Hydrocolloids, 23*(5), 1270-1278.

Sarkar, A., Goh, K. K. T., Singh, R. P., & Singh, H. (2009b). Behaviour of an oil-in-water emulsion stabilized by β-lactoglobulin in an in vitro gastric model. *Food Hydrocolloids, 23*(6), 1563-1569.

Sarkar, A., Horne, D. S., & Singh, H. (2010a). Pancreatin-induced coalescence of oil-in-water emulsions in an *in vitro* duodenal model. *International Dairy Journal, 20*(9), 589-597.

Sarkar, A., Horne, D. S., & Singh, H. (2010b). Interactions of milk protein-stabilized oil-in-water emulsions with bile salts in a simulated upper intestinal model. *Food Hydrocolloids, 24*(2–3), 142-151.

Sawyer, L., & Kontopidis, G. (2000). The core lipocalin, bovine β-lactoglobulin. *Biochimica et Biophysica Acta (BBA) - Protein Structure and Molecular Enzymology, 1482*(1–2), 136-148.

Schägger, H., & von Jagow, G. (1987). Tricine-sodium dodecyl sulfate-polyacrylamide gel electrophoresis for the separation of proteins in the range from 1 to 100 kDa. *Analytical biochemisty, 166*(2), 368-379.

Schmidt, R. H. (1981). Gelation and coagulation. In J. P. Cherry (Ed.), *Protein functionality in foods* (pp. 131-147). Washington, DC: American Chemical Society.

Schokker, E. P., Singh, H., Pinder, D. N., Norris, G. E., & Creamer, L. K. (1999). Characterization of intermediates formed during heat-induced aggregation of β-lactoglobulin AB at neutral pH. *International Dairy Journal, 9*(11), 791-800.

Schreiber, G., & Urban, J. (1978). The synthesis and secretion of albumin. *Reviews of Physiology, Biochemistry and Pharmacology, 82*, 27-95.

Schulze, K. (2006). Imaging and modelling of digestion in the stomach and the duodenum. *Neurogastroenterology & Motility, 18*(3), 172-183.

Shafer, R., Levine, A., Marlette, J., & Morley, J. (1985). Do calories, osmolality, or calcium determine gastric emptying? *American Journal of Physiology, 248*(4), R479-R483.

Shani-Levi, C., Levi-Tal, S., & Lesmes, U. (2013). Comparative performance of milk proteins and their emulsions under dynamic *in vitro* adult and infant gastric digestion. *Food Hydrocolloids, 32*(2), 349-357.

Shimoyama, Y., Kusano, M., Kawamura, O., Zai, H., Kuribayashi, S., Higuchi, T., et al. (2007). High-viscosity liquid meal accelerates gastric emptying. *Neurogastroenterology & Motility, 19*(11), 879-886.

Siegel, J. A., Urbain, J. L., Adler, L. P., Charkes, N. D., Maurer, A. H., Krevsky, B., et al. (1988). Biphasic nature of gastric emptying. *Gut, 29*(1), 85-89.

Simonian, H., Vo, L., Doma, S., Fisher, R., & Parkman, H. (2005). Regional postprandial differences in pH within the stomach and gastroesophageal junction. *Digestive Diseases and Sciences, 50*(12), 2276-2285.

Simopoulos, A. P. (1999). Essential fatty acids in health and chronic disease. *American Journal of Clinical Nutrition, 70*(3 SUPPL.), 560S-569S.

Singh, H., & Havea, P. (2003). Thermal denaturation, aggregation and gelation of whey proteins. *Advanced dairy chemistry, 1*, 1257-1283.

Singh, H., Ye, A., & Horne, D. (2009). Structuring food emulsions in the gastrointestinal tract to modify lipid digestion. *Progress in Lipid Research, 48*(2), 92-100.

Singh, H., & Sarkar, A. (2011). Behaviour of protein-stabilised emulsions under various physiological conditions. *Advances in Colloid and Interface Science, 165*(1), 47-57.

Singh, H., & Ye, A. (2013). Structural and biochemical factors affecting the digestion of protein-stabilized emulsions. *Current Opinion in Colloid and Interface Science, 18*(4), 360-370.

Small, D. M. (1991). The effects of glyceride structure on absorption and metabolism. *Small, D M, 11*(1), 413-434.

Smith, B. J. (1984). SDS polyacrylamide gel electrophoresis of proteins. In J. Walker (Ed.), *Proteins* (Vol. 1, pp. 41-55). New York: Humana Press.

Snow, P., & O'Dea, K. (1981). Factors affecting the rate of hydrolysis of starch in food.

The American Journal of Clinical Nutrition, 34(12), 2721-2727.

Sok Line, V. L., Remondetto, G. E., & Subirade, M. (2005). Cold gelation of β-lactoglobulin oil-in-water emulsions. *Food Hydrocolloids, 19*(2), 269-278.

Stull, A. J., Apolzan, J. W., Thalacker-Mercer, A. E., Iglay, H. B., & Campbell, W. W. (2008). Liquid and solid meal replacement products differentially affect postprandial appetite and food intake in older adults. *Journal of the American Dietetic Association, 108*(7), 1226-1230.

Synge, R. L. M. (1945). The kinetics of low temperature acid hydrolysis of gramicidin and of some related dipeptides. *Biochemical Journal, 39*(4), 351.

Szczesniak, A. S. (1963). Classification of textural characteristicsa. *Journal of Food Science, 28*(4), 385-389.

Szczesniak, A. S., Brandt, M. A., & Friedman, H. H. (1963). Development of standard rating scales for mechanical parameters of texture and correlation between the objective and the sensory methods of texture evaluation. *Journal of Food Science, 28*(4), 397-403.

Szczesniak, A. S. (2002). Texture is a sensory property. *Food Quality and Preference, 13*(4), 215-225.

Tadros, T. F., & Vincent, B. (1983). Emulsion stability. In P. Becher (Ed.), *Encyclopedia of emulsion technology* (Vol. 1). New York: Marcel Dekker.

Tanaka, H., Tomita, H., Takasu, A., Hayashi, T., & Nishi, T. (1992). Morphological and kinetic evolution of surface patterns in gels during the swelling process: Evidence of dynamic pattern ordering. *Physical review letters, 68*(18), 2794.

Tanaka, H., & Sigehuzi, T. (1994). Surface-pattern evolution in a swelling gel under a geometrical constraint: Direct observation of fold structure and its coarsening dynamics. *Tanaka, Hajime, 49*(1), R39.

Tanaka, T., Sun, S.-T., Hirokawa, Y., Katayama, S., Kucera, J., Hirose, Y., et al. (1987). Mechanical instability of gels at the phase transition. *Nature, 325*(6107), 796-798.

Tang, J., Wolf, S., Caputto, R., & Trucco, R. E. (1959). Isolation and crystallization of gastricsin from human gastric juice. *Journal of Biological Chemistry, 234*(5), 1174-1178.

Tolstoguzov, V. B., & Braudo, E. E. (1983). Fabricated foodstuffs as multicomponent gels. *Journal of Texture Studies, 14*(3), 183-212.

Tortora, G. J., & Derrickson, B. H. (2008). *Principles of anatomy and physiology* (12 ed.). Hoboken: John Wiley & Sons.

Tougas, G., Eaker, E. Y., Abell, T. L., Abrahamsson, H., Boivin, M., Chen, J., et al. (2000). Assessment of gastric emptying using a low fat meal: establishment of international control values. *American Journal of Gastroenterology, 95*(6), 1456-1462.

Tydeman, E. A., Parker, M. L., Faulks, R. M., Cross, K. L., Fillery-Travis, A., Gidley, M. J., et al. (2010). Effect of carrot (Daucus carota) microstructure on carotene bioaccessibility in the upper gastrointestinal tract. 2. *In Vivo* Digestions. *Journal of Agricultural and Food Chemistry, 58*(17), 9855-9860.

Uhrínová, S., Smith, M. H., Jameson, G. B., Uhrín, D., Sawyer, L., & Barlow, P. N. (2000). Structural changes accompanying pH-induced dissociation of the β-lactoglobulin dimer. *Biochemistry, 39*(13), 3565-3574.

Ulleberg, E., Comi, I., Holm, H., Herud, E., Jacobsen, M., & Vegarud, G. (2011). Human gastrointestinal juices intended for use in *in vitro* digestion models. *Food Digestion, 2*(1-3), 52-61.

Urbain, J. L., Siegel, J., Charkes, N. D., Maurer, A., Malmud, L., & Fisher, R. (1989).

The two-component stomach: effects of meal particle size on fundal and antral emptying. *European Journal of Nuclear Medicine, 15*(5), 254-259.

van Aken, G. A., Blijdenstein, T. B. J., & Hotrum, N. E. (2003). Colloidal destabilisation mechanisms in protein-stabilised emulsions. *Current Opinion in Colloid & Interface Science, 8*(4–5), 371-379.

van Aken, G. A., Vingerhoeds, M. H., & de Hoog, E. H. A. (2007). Food colloids under oral conditions. *Current Opinion in Colloid & Interface Science, 12*(4–5), 251-262.

van Aken, G. A., Bomhof, E., Zoet, F. D., Verbeek, M., & Oosterveld, A. (2011). Differences in *in vitro* gastric behaviour between homogenized milk and emulsions stabilised by Tween 80, whey protein, or whey protein and caseinate. *Food Hydrocolloids, 25*(4), 781-788.

van der Bilt, A., Engelen, L., Abbink, J., & Pereira, L. J. (2007). Effects of adding fluids to solid foods on muscle activity and number of chewing cycles. *European Journal of Oral Sciences, 115*(3), 198-205.

van der Bilt, A. (2012). Oral Management of Food. In J. S. Chen (Eds), *Food Oral Processing* (1 ed., pp. 61-93). Oxford: Wiley-Blackwell.

van Nieuw Amerongen, A., Bolscher, J. G. M., & Veerman, E. C. I. (2004). Salivary proteins: Protective and diagnostic value in cariology? *Caries Research, 38*(3), 247-253.

van Vliet, T., van Aken, G. A., de Jongh, H. H. J., & Hamer, R. J. (2009). Colloidal aspects of texture perception. *Advances in Colloid and Interface Science, 150*(1), 27-40.

van Vliet, T., Luyten, H., & Walstra, P. (1993). Time dependent fracture behavior of food. In E. Dickinson & P. Walstra (Eds.), *Food colloids and polymer, stability*

and mechanical properties (Vol. 113, pp. 175-199). Cambridge: Royal Society of Chemistry.

Vardakou, M., Mercuri, A., Barker, S. A., Craig, D. Q., Faulks, R. M., & Wickham, M. S. (2011). Achieving antral grinding forces in biorelevant *in vitro* models: comparing the USP dissolution apparatus II and the dynamic gastric model with human *in vivo* data. *APS PharmSciTech, 12*(2), 620-626.

Vardhanabhuti, B., Foegeding, E. A., McGuffey, M. K., Daubert, C. R., & Swaisgood, H. E. (2001). Gelation properties of dispersions containing polymerized and native whey protein isolate. *Food Hydrocolloids, 15*(2), 165-175.

Vardhanabhuti, B., Khayankan, W., & Foegeding, E. A. (2010). Formation of elastic whey protein gels at low pH by acid equilibration. *Journal of Food Science, 75*(5), E305-E313.

Veerman, C., Baptist, H., Sagis, L. M. C., & van der Linden, E. (2003). A new multistep Ca^{2+}-induced cold gelation process for β-lactoglobulin. *Journal of Agricultural and Food Chemistry, 51*(13), 3880-3885.

Velchik, M. G., Reynolds, J. C., & Alavi, A. (1989). The effect of meal energy content on gastric emptying. *Journal of Nuclear Medicine, 30*(6), 1106-1110.

Verde, A. V., & Frenkel, D. (2010). Simulation study of micelle formation by bile salts. *Soft Matter, 6*(16), 3815-3825.

Verheul, M., & Roefs, S. P. F. M. (1998). Structure of particulate whey protein gels: effect of NaCl concentration, pH, heating temperature, and protein composition. *Journal of Agricultural and Food Chemistry, 46*(12), 4909-4916.

Verheul, M., Roefs, S. P. F. M., & de Kruif, K. G. (1998). Kinetics of heat-induced aggregation of β-lactoglobulin. *Journal of Agricultural and Food Chemistry, 46*(3), 896-903.

Versantvoort, C. H. M., Oomen, A. G., Van de Kamp, E., Rompelberg, C. J. M., & Sips, A. J. A. M. (2005). Applicability of an *in vitro* digestion model in assessing the bioaccessibility of mycotoxins from food. *Food and Chemical Toxicology, 43*(1), 31-40.

Vincent, J. (2012). *Structural biomaterials* (3 ed.). Princeton: Princeton University Press.

Wang, Y.-J., Truong, V.-D., & Wang, L. (2003). Structures and rheological properties of corn starch as affected by acid hydrolysis. *Carbohydrate Polymers, 52*(3), 327-333.

Ward, I. M., & Sweeney, J. (2012). *Mechanical properties of solid polymers* (3 ed.). Chichester: John Wiley & Sons.

Welch, I., Saunders, K., & Read, N. (1985). Effect of ileal and intravenous infusions of fat emulsions on feeding and satiety in human volunteers. *Gastroenterology, 89*(6), 1293.

Welch, I., Sepple, C., & Read, N. (1988). Comparisons of the effects on satiety and eating behaviour of infusion of lipid into the different regions of the small intestine. *Gut, 29*(3), 306-311.

Weurding, R. E., Veldman, A., Veen, W. A., van der Aar, P. J., & Verstegen, M. W. (2001). *In vitro* starch digestion correlates well with rate and extent of starch digestion in broiler chickens. *The Journal of Nutrition, 131*(9), 2336-2342.

Wikipedia-contributors. (2014). Zeta potential. In: Wikipedia, The Free Encyclopedia.

Wikipedia-contributors. (2015). Confocal laser scanning microscopy. In: Wikipedia, The Free Encyclopedia.

Wikipedian-contributors. (2014). Small intestine. In: Wikipedia, The Free Encyclopedia. .

Wilde, P. J., & Chu, B. S. (2011). Interfacial & colloidal aspects of lipid digestion. *Advances in Colloid and Interface Science, 165*(1), 14-22.

Wolff, M., & Kleinberg, I. (1998). Oral mucosal wetness in hypo- and normosalivators. *Archives of Oral Biology, 43*(6), 455-462.

Wood, G. D., & Williams, J. E. (1981). Gnathodynamometers: measuring opening and closing forces. *Dental Update, 8*(4), 239-41, 243, 246-7.

Wu, H., Xie, J., & Morbidelli, M. (2005). Kinetics of cold-set diffusion-limited aggregations of denatured whey protein isolate colloids. *Biomacromolecules, 6*(6), 3189-3197.

Xu, W. L., & Bronlund, J. E. (2010). *Mastication Robots* . Berlin: Springer.

Yaghmur, A., & Glatter, O. (2009). Characterization and potential applications of nanostructured aqueous dispersions. *Advances in Colloid and Interface Science, 147–148*, 333-342.

Ye, A., & Taylor, S. (2009). Characterization of cold-set gels produced from heated emulsions stabilized by whey protein. *International Dairy Journal, 19*(12), 721-727.

Ye, A., Cui, J., Zhu, X., & Singh, H. (2013). Effect of calcium on the kinetics of free fatty acid release during *in vitro* lipid digestion in model emulsions. *Food Chemistry, 139*(1–4), 681-688.

Zangenberg, N. H., Müllertz, A., Kristensen, H. G., & Hovgaard, L. (2001). A dynamic in vitro lipolysis model. I. Controlling the rate of lipolysis by continuous addition of calcium. *European Journal of Pharmaceutical Sciences, 14*(2), 115-122.

Zhang, S., & Vardhanabhuti, B. (2014). Effect of initial protein concentration and pH on *in vitro* gastric digestion of heated whey proteins. *Food Chemistry, 145*(0), 473-

480.

Zhong, H., Marcus, S. L., & Li, L. (2005). Microwave-assisted acid hydrolysis of proteins combined with liquid chromatography MALDI MS/MS for protein identification. *Journal of the American Society for Mass Spectrometry, 16*(4), 471-481.

Zhu, Y., Hsu, W. H., & Hollis, J. H. (2013). The impact of food viscosity on eating rate, subjective appetite, glycemic response and gastric emptying rate. *PLoS ONE, 8*(6), e67482.

DRC 16 Forms

DRC 16 form is the statement of contribution to doctoral thesis containing publications.

DRC 16

MASSEY UNIVERSITY
GRADUATE RESEARCH SCHOOL

STATEMENT OF CONTRIBUTION TO DOCTORAL THESIS CONTAINING PUBLICATIONS

(To appear at the end of each thesis chapter/section/appendix submitted as an article/paper or collected as an appendix at the end of the thesis)

We, the candidate and the candidate's Principal Supervisor, certify that all co-authors have consented to their work being included in the thesis and they have accepted the candidate's contribution as indicated below in the *Statement of Originality*.

Name of Candidate: Qing Guo

Name/Title of Principal Supervisor: Dr Aiqian Ye

Name of Published Research Output and full reference:

The breakdown properties of heat-set whey protein emulsion gels in the human mouth

Guo, Q., Ye, A., Lad, M., Dalgleish, D., & Singh, H. (2013). The breakdown properties of heat-set whey protein emulsion gels in the human mouth. Food Hydrocolloids, 33(2), 215-224.

In which Chapter is the Published Work: 4

Please indicate either:

- The percentage of the Published Work that was contributed by the candidate:

  and / or

- Describe the contribution that the candidate has made to the Published Work:

  - Planning and designing experimental studies
  - Standardizing protocols for methodologies by preliminary experiments
  - Conducting experiments including those to resolve comments from the peer-review process
  - Preliminary interpretation of results
  - Preparation of drafts of manuscript

QING GUO Digitally signed by QING GUO DN: cn=QING GUO, o=Massey University, ou=Riddet, email=q.guo@massey.ac.nz, c=NZ Date: 2015.05.01 15:56:41 +12'00'

Candidate's Signature

01/05/2015

Date

Aiqian Ye Digitally signed by Aiqian Ye DN: cn=Aiqian Ye, o=Riddet Institute, Massey University, ou, email=a.m.ye@massey.ac.nz, c=US Date: 2015.05.06 14:16:21 +12'00'

Principal Supervisor's signature

06/05/2015

Date

GRS Version 3– 16 September 2011

DRC 16

MASSEY UNIVERSITY
GRADUATE RESEARCH SCHOOL

STATEMENT OF CONTRIBUTION TO DOCTORAL THESIS CONTAINING PUBLICATIONS

(To appear at the end of each thesis chapter/section/appendix submitted as an article/paper or collected as an appendix at the end of the thesis)

We, the candidate and the candidate's Principal Supervisor, certify that all co-authors have consented to their work being included in the thesis and they have accepted the candidate's contribution as indicated below in the *Statement of Originality*.

Name of Candidate: Qing Guo

Name/Title of Principal Supervisor: Dr Aiqian Ye

Name of Published Research Output and full reference:

Effect of gel structure on the gastric digestion of whey protein emulsion gels

Guo, Q., Ye, A., Lad, M., Dalgleish, D., & Singh, H. (2014). Effect of gel structure on the gastric digestion of whey protein emulsion gels. Soft matter, 10(8), 1214-1223.

In which Chapter is the Published Work: 5

Please indicate either:

- The percentage of the Published Work that was contributed by the candidate:

  and / or

- Describe the contribution that the candidate has made to the Published Work:

  - Planning and designing experimental studies
  - Standardizing protocols for methodologies by preliminary experiments
  - Conducting experiments including those to resolve comments from the peer-review process
  - Preliminary interpretation of results
  - Preparation of drafts of manuscript

QING GUO Digitally signed by QING GUO DN: cn=QING GUO, o=Massey University, ou=Riddet, email=q.guo@massey.ac.nz, c=NZ Date: 2015.05.01 16:00:05 +12'00'

Candidate's Signature

01/05/2015

Date

Aiqian Ye Digitally signed by Aiqian Ye DN: cn=Aiqian Ye, o=Riddet Institute, Massey University, ou, email=a.m.ye@massey.ac.nz, c=US Date: 2015.05.06 14:17:10 +12'00'

Principal Supervisor's signature

06/05/2015

Date

GRS Version 3– 16 September 2011

DRC 16

MASSEY UNIVERSITY
GRADUATE RESEARCH SCHOOL

STATEMENT OF CONTRIBUTION TO DOCTORAL THESIS CONTAINING PUBLICATIONS

(To appear at the end of each thesis chapter/section/appendix submitted as an article/paper or collected as an appendix at the end of the thesis)

We, the candidate and the candidate's Principal Supervisor, certify that all co-authors have consented to their work being included in the thesis and they have accepted the candidate's contribution as indicated below in the *Statement of Originality*.

Name of Candidate: Qing Guo

Name/Title of Principal Supervisor: Dr Aiqian Ye

Name of Published Research Output and full reference:

Disintegration Kinetics of Food Gels During Gastric Digestion and its Role on Gastric Emptying: an in vitro Analysis

Guo, Q., Ye, A., Lad, M., Ferrua, M., Dalgleish, D., & Singh, H. (2015). Disintegration Kinetics of Food Gels During Gastric Digestion and its Role on Gastric Emptying: an in vitro Analysis. Food and Function, 6(3), 756-764.

In which Chapter is the Published Work: 6

Please indicate either:

- The percentage of the Published Work that was contributed by the candidate:

  and / or

- Describe the contribution that the candidate has made to the Published Work:

  - Planning and designing experimental studies
  - Standardizing protocols for methodologies by preliminary experiments
  - Conducting experiments including those to resolve comments from the peer-review process
  - Preliminary interpretation of results
  - Preparation of drafts of manuscript

QING GUO Digitally signed by QING GUO DN: cn=QING GUO, o=Massey University, ou=Riddet, email=q.guo@massey.ac.nz, c=NZ Date: 2015.05.01 16:05:43 +12'00'

Candidate's Signature

01/05/2015

Date

Aiqian Ye Digitally signed by Aiqian Ye DN: cn=Aiqian Ye, o=Riddet Institute, Massey University, ou, email=a.m.ye@massey.ac.nz, c=US Date: 2015.05.06 14:18:24 +12'00'

Principal Supervisor's signature

06/05/2015

Date

GRS Version 3– 16 September 2011

DRC 16

MASSEY UNIVERSITY
GRADUATE RESEARCH SCHOOL

STATEMENT OF CONTRIBUTION TO DOCTORAL THESIS CONTAINING PUBLICATIONS

(To appear at the end of each thesis chapter/section/appendix submitted as an article/paper or collected as an appendix at the end of the thesis)

We, the candidate and the candidate's Principal Supervisor, certify that all co-authors have consented to their work being included in the thesis and they have accepted the candidate's contribution as indicated below in the *Statement of Originality*.

Name of Candidate: Qing Guo

Name/Title of Principal Supervisor: Dr Aiqian Ye

Name of Published Research Output and full reference:

Behaviour of whey protein emulsion gel during oral and gastric digestion: effect of droplet size

Guo, Q., Ye, A., Lad, M., Dalgleish, D., & Singh, H. (2014). Behaviour of whey protein emulsion gel during oral and gastric digestion: effect of droplet size. Soft matter, 10(23), 4173-4183.

In which Chapter is the Published Work: 7

Please indicate either:

- The percentage of the Published Work that was contributed by the candidate:

  and / or

- Describe the contribution that the candidate has made to the Published Work:

  - Planning and designing experimental studies
  - Standardizing protocols for methodologies by preliminary experiments
  - Conducting experiments including those to resolve comments from the peer-review process
  - Preliminary interpretation of results
  - Preparation of drafts of manuscript

QING GUO Digitally signed by QING GUO DN: cn=QING GUO, o=Massey University, ou=Riddet, email=q.guo@massey.ac.nz, c=NZ Date: 2015.05.01 16:03:15 +12'00'

Candidate's Signature

01/05/2015

Date

Aiqian Ye Digitally signed by Aiqian Ye DN: cn=Aiqian Ye, o=Riddet Institute, Massey University, ou, email=a.m.ye@massey.ac.nz, c=US Date: 2015.05.06 14:17:51 +12'00'

Principal Supervisor's signature

06/05/2015

Date

GRS Version 3– 16 September 2011